UNIVERSITÀ DI PARMA

UNIVERSITA' DEGLI STUDI DI PARMA

DOTTORATO DI RICERCA IN SCIENZE DELLA TERRA

CICLO XXXIII

Approcci idrogeologico-metagenomici per l'ottimizzazione dei modelli di flusso e delle soluzioni di bonifica ambientale

Coordinatore:

Chiar.mo Prof. Mario Tribaudino

Tutor:

Chiar.mo Prof. Fulvio Celico

Co-Tutor:

Chiar.ma Prof.ssa Anna Maria Sanangelantoni

Dottorando: Pietro Rizzo

Anni Accademici 2017/2018 – 2019/2020

Indice

1. Introduzione

Nel 2011 l'European Environmental Agency (EEA) ha stimato la presenza di circa 2,5 milioni di potenziali siti contaminati all'interno del territorio dell'Unione Europea; di questi, circa 1,1 milioni sono stati identificati, ma solo il 15% sono stati bonificati [1]. La contaminazione da idrocarburi, in particolare, è un fenomeno che può intaccare la salute dell'uomo ed impattare negativamente sulla qualità dell'ambiente [2]. Le fonti di contaminazione ambientale riconducibili in toto o in gran parte alla presenza di idrocarburi possono essere diverse, come altrettanto diversificate possono essere le modalità di migrazione degli stessi all'interno di acquiferi più o meno eterogenei dal punto di vista idraulico (ad es., [3-8]).

Secondo l'EEA, tra i contaminanti più diffusi all'interno degli acquiferi saturi si possono trovare prodotti derivati dal petrolio come i BTEX (Benzene, Toluene, Etilbenzene, Xilene), gli IPA (Idrocarburi Policiclici Aromatici) e i CHC (Idrocarburi Clorurati).

Negli anni, sono state sviluppate diverse tecnologie per la bonifica di siti contaminati applicabili *in situ*, le quali prevedono il risanamento della matrice contaminata direttamente in loco, o *ex situ*, le quali prevedono il risanamento della matrice contaminata in impianti di trattamento esterni e che richiedono quindi l'escavazione ed il trasporto della matrice. Queste tecnologie possono essere riunite in due macro-gruppi: (i) gli approcci chimico-fisici e (ii) gli approcci biologici.

Le principali tecnologie chimico-fisiche per la bonifica di siti contaminati sono:

- *Soil Washing*: tecnologia *ex situ* che si basa sul lavaggio con acqua, tensioattivi e agenti chelanti utili alla rimozione del contaminante [9];
- *Soil Flushing*: tecnologia *in situ* che prevede il lavaggio con acqua e tensioattivi iniettati nel terreno per favorire la lisciviazione [10];
- *Soil Vapor Extraction* (SVE): tecnologia di trattamento *in situ*, rapida, efficace e relativamente economica per rimuovere, dalla zona insatura dell'acquifero, contaminanti organici volatili e prodotti petroliferi adsorbiti alla matrice solida [11];
- Ossidazione chimica: tecnologia che prevede l'utilizzo di agenti ossidanti come perossido di idrogeno (H_2O_2) e persolfato di sodio ($Na_2S_2O_8$) per convertire gli inquinanti in molecole più stabili e facilmente degradabili [12];
- *Air Sparging*: tecnologia rivolta ad agenti volatili e semivolatili accoppiata spesso alla SVE, che prevede l'insufflazione di aria nella matrice, per agevolare il desorbimento e la volatilizzazione dei contaminanti [13].

Questi sistemi, se correttamente applicati, dovrebbero garantire l'eliminazione della sostanza inquinante, ma allo stesso tempo comportano un maggiore impatto dell'intervento sull'ecosistema ed un elevato costo di realizzazione e gestione. L'approccio alternativo ai trattamenti chimico–fisici per le sostanze organiche è il biorisanamento, cioè un insieme di tecnologie che utilizzano una componente biologica per eliminare sostanze tossiche e pericolose attraverso processi metabolici aerobi e/o anaerobi [14]. Le principali tecnologie di biorisanamento per la bonifica di siti contaminanti sono:

- Bioreattori: tecnica di biorisanamento *ex situ*, che consiste nello sfruttare dispositivi che garantiscono la degradazione con parametri controllati e con un sistema di monitoraggio costante [15];
- *Landfarming*: trattamento biologico *ex situ* che consiste nel preparare un manto impermeabile per isolare il suolo contaminato e disporlo sopra un letto sabbioso; il terreno

viene periodicamente rimescolato per garantire un'efficace miscelazione fra microorganismi naturalmente presenti o inoculati, l'ossigeno, i nutrienti e i contaminanti [16];

- Biopila: tecnica *ex situ* (spesso *on site*) che consiste nella stesura di strati successivi di terreno inquinato sopra un telo impermeabile, successivamente coperti con un ulteriore telo impermeabile o semi-permeabile: tra uno strato e l'altro viene posto un sistema di tubi forati con i quali viene fatta circolare aria all'interno della pila [17];
- *Bioventing*: tecnica *in situ* che è utilizzata principalmente per degradare prodotti petroliferi leggeri, gasolio e cherosene e altri composti volatili come il tricoloroetilene, il tricoloroetano, il dibromuro di etilene e il dicloroetilene; viene applicata una leggera ventilazione al fine di fornire l'ossigeno necessario a sostenere l'attività microbica, ma facendo attenzione ad evitare la volatilizzazione veloce dei contaminanti e la loro dispersione in atmosfera prima che siano biodegradati [18];
- *Monitoring Natural Attenuation* (MNA): tecnica *in situ* che sfrutta i processi naturali fisici, chimici e biologici per ridurre le concentrazioni di contaminanti [19];
- *Biosparging*: tecnica biologica *in situ* che viene utilizzata principalmente per il trattamento di acque di falda, principalmente in siti contaminati da composti che tendono a volatilizzare rapidamente [18];
- *Biostimulation*: tecnica *in situ* che consiste nell'aggiunta di particolari nutrienti a suoli contaminati in modo da stimolare la crescita di microorganismi autoctoni, capaci di degradare in modo efficace i contaminanti dispersi nella zona d'interesse; consente di garantire le condizioni ambientali adatte al fine di accelerare i processi di decontaminazione [20];
- *Bioaugmentation*: tecnica *in situ* che consiste nell'aggiunta di ceppi batterici o consorzi di batteri, sia autoctoni sia alloctoni, nell'acquifero insaturo o saturo, per velocizzare la degradazione [20].

Questi approcci biologici si contrappongono a quelli chimico-fisici soprattutto per quanto riguarda il basso impatto sull'ecosistema ed i minori costi di realizzazione e gestione dell'intervento. In entrambi i casi, soprattutto quando la matrice da bonificare coinvolge un acquifero saturo, i suddetti approcci non possono prescindere da un corretto ed approfondito modello idrogeologico concettuale e, in alcuni casi, anche numerico. Entrambi i modelli idrogeologici sono infatti finalizzati alla corretta progettazione di sistemi di bonifica.

Spesso la propagazione dei contaminanti è mediata attraverso la componente liquida dell'acquifero saturo, per trasporto in sospensione o in soluzione, comportando la necessità di realizzare interventi atti al contenimento della contaminazione entro un areale circoscritto. Uno degli scenari più comuni in questi casi è la progettazione e realizzazione di sistemi di barrieramento idraulico e/o fisico-idraulico che possano fungere, in prima battuta, da opere di messa in sicurezza d'emergenza. Per integrare tali opere con un sistema di bonifica generalmente viene realizzato un sistema denominato *pump and treat* (Fig.1.1). Questo sistema consiste nell'emungimento di acqua di falda contaminata attraverso delle pompe sommerse posizionate all'interno di pozzi barriera, nel suo successivo trattamento, mediante tecniche differenti a seconda del tipo di contaminante presente, presso un centro di Trattamento delle Acque di Falda (TAF), e nella conseguente immissione delle acque trattate in un corpo idrico superficiale, oppure nella re-immissione delle stesse nell'acquifero saturo.

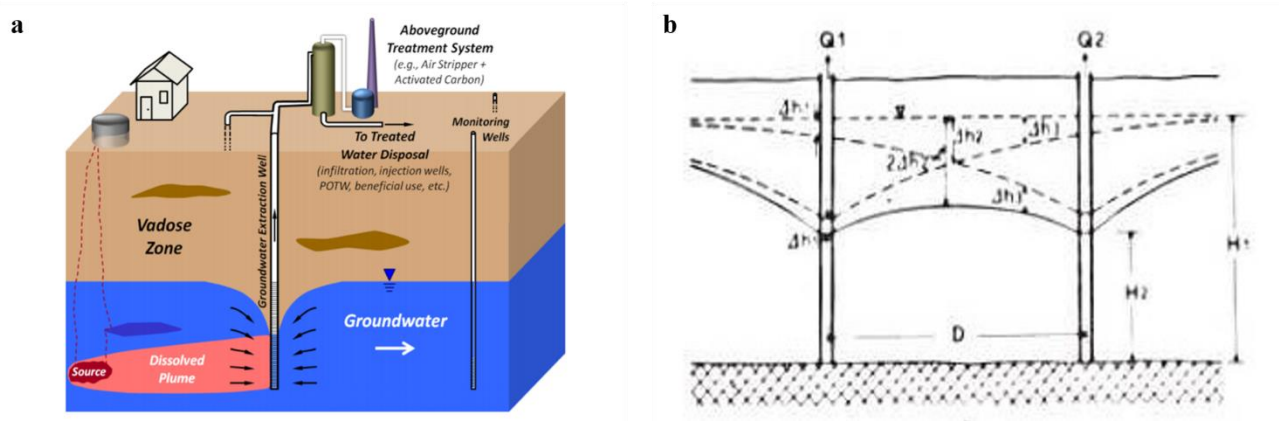

Figura 1.1 [a] Ricostruzione schematizzata di un sistema pump & treat [21]; [b] schematizzazione del funzionamento di un barrieramento idraulico [22]

Uno dei maggiori problemi nella gestione del sistema di bonifica con *pump & treat* è la manutenzione continua che questo sistema richiede; questo sistema è infatti soggetto al cosiddetto fenomeno del *well clogging.* Questo fenomeno comporta la graduale perdita di efficienza dei pozzi-barriera, a causa della formazione di ostruzioni sia lungo i rivestimenti fenestrati dei pozzi, sia sulle fenestrature e all'interno delle pompe di emungimento sommerse (Fig. 1.2). Le cause della formazione di questo fenomeno possono essere legate a fattori fisici (materiale fine presente in sospensione nelle acque emunte), chimici (precipitazioni di carbonato di calcio, gesso o ferro) e biologici (accumulo di alghe, batteri o apparati radicali). In particolare, il fattore biologico legato alla componente batterica è una delle cause più diffuse del manifestarsi di questo problema e viene spesso identificato nella formazione di *biofilm*, una sostanza extracellulare prodotta da alcuni ceppi microbici [23].

Figura 1.2 Formazione di ostruzioni sulle fenestrature e all'interno di pompe sommerse in sistemi di barrieramento idraulico

In tutti gli scenari in cui sia coinvolta, nel processo di bonifica, la componente satura di un acquifero, risulta di particolare importanza (i) identificare l'eventuale presenza di orizzonti a bassa permeabilità (*aquitard*) (ii) testare i caratteri idraulici di questi ultimi e (iii) accertare il ruolo che questi elementi svolgono, non solo sulla distribuzione del carico idraulico all'interno del mezzo saturo (reticolo di flusso) [24-25], ma anche sulla migrazione dei contaminanti idroveicolati (*plume* di contaminazione) (Fig.1.3). In estrema sintesi, risulta di fondamentale importanza determinare tutto quanto ruoti intorno alla cosiddetta "*aquitard integrity*" (*sensu*, [26]). Gli *aquitard* sono infatti generalmente considerati come degli orizzonti a bassissima permeabilità o impermeabili, e vengono

quindi spesso identificati come degli elementi in grado di tutelare la qualità delle acque sotterrane in caso di contaminazione e di confinare porzioni di acquifero. Tuttavia, un *aquitard* con caratteristiche eterogenee potrebbe permettere, in alcuni casi, la migrazione di contaminanti [26-30]. Nel corso degli anni sono stati sviluppati vari metodi per la classificazione dell'eterogeneità degli *aquitard*, su larga scala e a scala di laboratorio, di natura idrogeologica, idrochimica ed isotopica [28, 31-39]. Per un approfondito studio sull'integrità degli *aquitard*, risulta in ogni caso imprescindibile la combinazione della conoscenza dei caratteri geologici (litologici e stratigrafici) e di quelli idraulici (porosità efficace, conducibilità idraulica, ecc.) del mezzo.

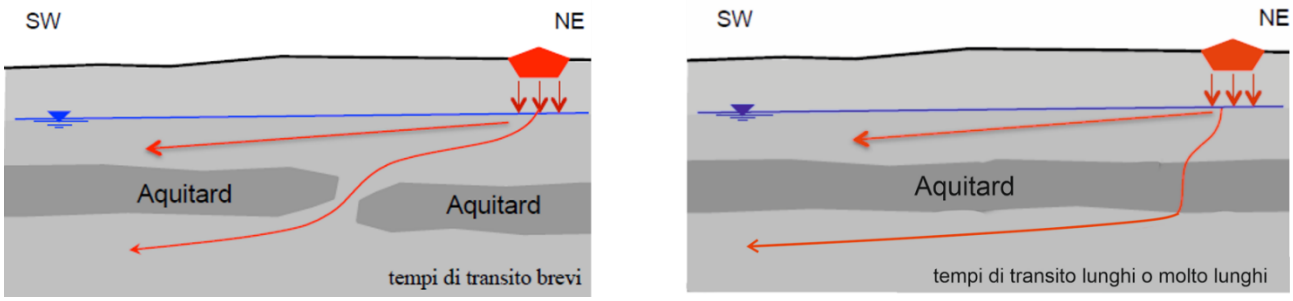

Figura 1.3 Schematizzazione di due possibili scenari di propagazione del contaminante in presenza di un aquitard discontinuo (sx) o continuo (dx).

Tenendo conto di quanto sopra premesso e di quanto ad oggi disponibile in letteratura scientifica, l'attività di ricerca è ruotata intorno a tre obiettivi principali, tra essi strettamente concatenati:

- approfondire le conoscenze relative alla propagazione di contaminanti idroveicolati in mezzi a bassa permeabilità ("*aquitard integrity*"), mediante (i) l'utilizzo delle cellule batteriche [40] o (ii) degli isotopi di ossigeno e idrogeno ($\delta^{18}O$, $\delta^{2}H$, ^{3}H; [41]) quali traccianti naturali dei processi idrodinamici e di trasporto;
- approfondire le conoscenze relative agli approcci di biorisanamento mediante (i) disamina dei processi di attenuazione naturale (approccio metagenomico in un sito contaminato da solventi clorurati; [42] e (ii) selezione di nuovi ceppi microbici degradatori, all'interno di sistemi idrogeologici attivi caratterizzati dalla presenza naturale di idrocarburi [43-44];
- approfondire l'influenza delle comunità microbiche sulla progressiva perdita di efficienza idraulica dei pozzi-barriera (*well clogging*), frequentemente osservata in siti contaminati.

2. Attività di Ricerca

Le attività di ricerca sono state sviluppate in diverse aree di studio idonee al conseguimento degli obiettivi sopracitati, ma non necessariamente ricadenti in siti contaminati. Questa scelta progettuale ha consentito, tra l'altro, di minimizzare il rischio che il segreto industriale andasse a coprire e rendere non divulgabili molti dei risultati delle ricerche effettuate. Al termine del Dottorato, gli unici elementi di conoscenza non pubblicabili attengono al tema del *well clogging*.

Il presente paragrafo è dedicato alla sintesi dei principali risultati conseguiti nel corso del Dottorato, attraverso la successione degli articoli scientifici pubblicati in riviste indicizzate Scopus e Web of Science. Per agevolarne la lettura e la collocazione all'interno dei diversi temi trattati nel corso del triennio, si riportano di seguito le corrispondenze tra i singoli temi e le pubblicazioni:

- approfondire le conoscenze relative alla propagazione di contaminanti idroveicolati in mezzi a bassa permeabilità ("*aquitard integrity*"), mediante (i) l'utilizzo delle cellule batteriche [40] o (ii) degli isotopi di ossigeno e idrogeno ($\delta^{18}O$, $\delta^{2}H$, ^{3}H; [41]) quali traccianti naturali dei processi idrodinamici e di trasporto;
    - Rizzo, P., Petrella, E., Bucci, A., Salvioli Mariani, E., Chelli, A., Sanangelantoni, A.M., Raimondo, M., Quagliarini, A., & Celico, F., (2020a). Studying hydraulic interconnections in low-permeability media by using bacterial communities as natural tracers. Water, doi: 10.3390/w12061795
    - Rizzo, P., Cappadonia, C., Rotigliano, E., Iacumin, P., Sanangelantoni, A.M., Zerbini, G., & Celico, F. (2020b). Hydrogeological behaviour and geochemical features of waters in evaporite-bearing low-permeability successions: A case study in southern Sicily, Italy. https://doi.org/10.3390/app10228177
- approfondire le conoscenze relative agli approcci di biorisanamento mediante (i) disamina dei processi di attenuazione naturale (approccio metagenomico in un sito contaminato da solventi clorurati; [42] e (ii) selezione di nuovi ceppi microbici degradatori, all'interno di sistemi idrogeologici attivi caratterizzati dalla presenza naturale di idrocarburi [43-44];
    - Zanini, A., Petrella, E., Sanangelantoni A.M., Angelo, L., Ventosi, B., Viani, L., Rizzo, P., Remelli, S., Bartoli, M., Bolpagni, R., Chelli, A., Feo, A., Francese, R., Iacumin, P., Menta, C., Racchetti, E., Selmo, E.M., Tanda, M.G., Ghirardi, M., Boggio, P., Pappalardo, F., De Nardo, M.T., Segadelli, S., & Celico, F. (2019). Groundwater characterization from an ecological and human perspective: an interdisciplinary approach in the Functional Urban Area of Parma, Italy. Rendiconti Lincei. Scienze Fisiche e Naturali, 30(1), 93-108. https://doi.org/10.1007/s12210-018-0748-x
    - Rizzo, P., Bucci, A., Sanangelantoni, A.M., Iacumin, P., & Celico, F., (2020c). Coupled microbiological-isotopic approach for studying hydrodynamics in deep reservoirs: the case of the Val d'Agri oilfield (Southern Italy). Water, doi: 10.3390/w12051483
    - Rizzo, P., Malerba, M., Bucci, A., Sanangelantoni, A.M., Remelli, S., & Celico, F., (2020d). Potential enhancement of in-situ bioremediation of contaminated sites through isolation and screening of bacterial strains in natural hydrocarbon springs. Water, 12, 1795, doi: 10.3390/w12061795.
- approfondire l'influenza delle comunità microbiche sulla progressiva perdita di efficienza idraulica dei pozzi-barriera (*well clogging*), frequentemente osservata in siti contaminati;
    - coperto da segreto industriale.

Nell'ambito della presente Tesi di Dottorato non sarà dedicato un paragrafo ai Materiali e Metodi, per i quali si rinvia di volta in volta alle singole pubblicazioni scientifiche riportate in successione logica e non temporale. Analogamente, si rinvia ai medesimi articoli per una disamina più approfondita dello stato dell'arte sui vari temi trattati.

In merito al contributo fornito nell'ambito delle singole pubblicazioni sopra citate, si riportano di seguito i dettagli in forma schematica:

- "Studying hydraulic interconnections in low-permeability media by using bacterial communities as natural tracers":
  - buona parte delle attività sperimentali;
  - analisi integrata dei dati, con particolare riferimento a quelli geologici, idrogeologici, idrochimici e metagenomici;
  - scrittura del testo, incluse tabelle, grafici e figure;
  - lavoro di revisione durante le fasi di referaggio;
- "Hydrogeological behaviour and geochemical features of waters in evaporite-bearing low-permeability successions: A case study in southern Sicily, Italy":
  - buona parte delle attività sperimentali;
  - analisi integrata dei dati, con particolare riferimento a quelli idrogeologici, isotopici e metagenomici;
  - scrittura del testo, incluse tabelle, grafici e figure;
  - lavoro di revisione durante le fasi di referaggio;
- "Groundwater characterization from an ecological and human perspective: an interdisciplinary approach in the Functional Urban Area of Parma, Italy":
  - parte delle attività sperimentali, con particolare riferimento ad aspetti idrogeologici, metagenomici e microbiologici;
- "Coupled microbiological-isotopic approach for studying hydrodynamics in deep reservoirs: the case of the Val d'Agri oilfield (Southern Italy)":
  - buona parte delle attività sperimentali;
  - analisi integrata dei dati, con particolare riferimento a quelli geologici, idrogeologici, idrochimici, isotopici e metagenomici;
  - scrittura del testo, incluse tabelle, grafici e figure;
  - lavoro di revisione durante le fasi di referaggio;
- "Potential enhancement of in-situ bioremediation of contaminated sites through isolation and screening of bacterial strains in natural hydrocarbon springs":
  - buona parte delle attività sperimentali;
  - analisi integrata dei dati, con particolare riferimento a quelli geologici, idrogeologici, microbiologici e metagenomici;
  - scrittura del testo, incluse tabelle, grafici e figure;
  - lavoro di revisione durante le fasi di referaggio.

2.1. Approfondimento delle conoscenze relative alla propagazione di contaminanti idroveicolati in mezzi a bassa permeabilità

water

MDPI

Article

Studying Hydraulic Interconnections in Low-Permeability Media by Using Bacterial Communities as Natural Tracers

Pietro Rizzo [1], Emma Petrella [1], Antonio Bucci [2,*], Emma Salvioli-Mariani [1], Alessandro Chelli [1], Anna Maria Sanangelantoni [1], Melinda Raimondo [1], Andrea Quagliarini [1] and Fulvio Celico [1]

[1] Department of Chemistry, Life Sciences and Environmental Sustainability, University of Parma, Parco Area delle Scienze 157/A, 43124 Parma, Italy; pietro.rizzo2@studenti.unipr.it (P.R.); emma.petrella@unipr.it (E.P.); emma.salviolimariani@unipr.it (E.S.-M.); alessandro.chelli@unipr.it (A.C.); annamaria.sanangelantoni@unipr.it (A.M.S.); melinda.raimondo@studenti.unipr.it (M.R.); andrea.quagliarini15@gmail.com (A.Q.); fulvio.celico@unipr.it (F.C.)

[2] Department of Biosciences and Territory, University of Molise, C. da Fonte Lappone, 86090 Pesche, Italy

* Correspondence: antonio.bucci@unimol.it; Tel.: +39-0874-404156

Received: 2 June 2020; Accepted: 19 June 2020; Published: 23 June 2020

Abstract: Knowledge about the processes governing subsurface microbial dynamics in and to groundwater represents an important tool for the development of robust, evidence-based policies and strategies to assess the potential impact of contamination sources and for the implementation of appropriate land use and management practices. In this research, we assessed the effectiveness of using microorganisms as natural tracers to analyze subsurface dynamics in a low-permeability system of northern Italy. Microbial communities were investigated through next-generation sequencing of 16S rRNA gene both to study hydraulic interconnections in clayey media and to verify the efficacy of outcropping clayey horizons in protecting groundwater against contamination. During the observation period, a rapid water percolation from the ground surface to the saturated medium was observed, and the mixing between lower-salinity fresh-infiltration waters and higher-salinity groundwater determined the formation of a halocline. This rapid percolation was a driver for the transport of microorganisms from the topsoil to the subsurface, as demonstrated by the presence of soil and rhizosphere bacteria in groundwater. Some of the species detected can carry out important processes such as denitrification or nitrate-reduction, whereas some others are known human pathogens (*Legionella pneumophila* and *Legionella feeleii*). These findings could be of utmost importance when studying the evolution of nitrate contamination over space and time in those areas where agricultural, industrial, and civil activities have significantly increased the levels of reactive nitrogen (N) in water bodies but, at the same time, could highlight that groundwater vulnerability of confined or semi-confined aquifers against contamination (both chemical and microbiological) could be higher than expected.

Keywords: groundwater; soil; microbiological investigations; prokaryotes; low-permeability media

1. Introduction

Microorganisms are ubiquitous in the natural environment: in soils, their concentrations can be of approximately 10^8–10^9 cells per gram [1]. While a significant majority of them carry out beneficial processes (e.g., they can play a critical role in subsurface biogeochemical cycling), some bacteria and other microorganisms (e.g., protozoa and viruses) are pathogenic, that is, they are capable of causing disease in humans [2].

Accordingly, studying the transport and retention of microorganisms in soil and in the underlying layers can be of interest for many reasons such as the analysis of water supplies pathogen contamination and pollutants degradation during *in situ* bioremediation. A range of physical, physicochemical, and biological processes may play a role in controlling the fate and transport of a microorganism once it has been introduced into the natural subsurface environment [1]. Among these, various macroscopic processes and mechanisms (e.g., advection, sedimentation, hydrodynamic dispersion, chemotaxis, motility, retention, inactivation, and growth) act on microorganisms in both saturated and unsaturated subsurface zones. Thus, knowledge of the processes governing subsurface microbial dynamics in and to groundwater represents an important tool for the development of robust, evidence-based policies and strategies to assess the potential impact of contamination sources and for the implementation of appropriate land use and management practices to protect groundwater supplies [1].

Many studies have examined physical (size of the microbe and the porous medium, microbe concentration, water velocity, water content, and surface roughness) and chemical (surface chemistry of the microbe and soil, aqueous solution pH, ionic strength (IS), and chemical composition) factors that influence the retention of microorganisms in homogeneous porous media [3–9] through repacked column breakthrough curves (BTCs) and retention profiles (RPs), batch experiments, and complementary micromodel studies allowing direct microscopic observation [10].

In this research, we evaluated the effectiveness of microorganisms as natural tracers of subsurface dynamics in a low-permeability system of northern Italy by using next-generation sequencing (NGS) of the 16S rRNA gene, one of the most widely used applications for the taxonomic and phylogenetic evaluation of microbial community composition [11,12].

Generally, tracing techniques have demonstrated particular usefulness in hydrogeology. They represent powerful investigative tools which allow quantification of transport parameters and measurement of subsurface properties in a way often unmatched by standard physical methods. Furthermore, tracer tests directly measure properties *in situ* and can be used to investigate very specific processes by selecting tracers with appropriate physicochemical properties. Most of the groundwater tracers used for hydrogeological purposes are chemicals and isotopic; they are used to determine the water origin, groundwater directions, velocities of subsurface flow, etc. Nonetheless, these more commonly used tracers can also have some drawbacks. For example, one obstacle to the use of environmental tracers is the potential lack of information on the input function, whereas artificial tracers pose the problem of the introduction of undesirable substances into groundwater resources. On the other hand, the migration of bacterial cells through natural clayey media has been studied mostly at the laboratory scale through column tests [13–16].

Microbial communities, which are greatly influenced by the physicochemical features of the environment in which they live, have been proven to be excellent tracers in some hydrogeological scenarios, allowing the analysis of complex phenomena. The efficacy of using microorganisms for specific hydrogeological purposes has been verified in recent researches [17–19], concerning recharge processes in karst environments, flow processes in compartmentalized aquifer systems [20,21], mixing processes between deep and shallow fluids in hydrothermal systems [22], mixing processes between groundwater and seawater in coastal aquifers [22,23], and mixing processes between brines and groundwater in evaporates bearing low-permeability successions.

2. Materials and Methods

2.1. Test Site

The test site is located within the Taro River valley (Italian northern Apennines; Figure 1). The local geological sequence (belonging to the Ligurian Domain of the northern Apennines [24]), can be described as follows (from top to bottom): (i) Arenarie di Scabiazza (SCB) is made up of thin layers of clay stone alternating with layers of sandstones and marls; (ii) Argillle a Palombini di Monte Rizzone (AMR) is made up of clay stones and limestone; locally, SCB lies directly on the underlying

Ottone tectonic unit that is made of clay stones containing clasts and blocks of limestone (Argille a blocchi, CCVb); and (iii) the latter lies directly (tectonic boundary) on the underlying Flysch of Monte Caio (CAO) made of marly-limestones turbidites and argillites.

At the test site, where groundwater and soil samples were collected for microbial community investigations, a matrix-supported deposit characterized by a clay-silty matrix was detected from the ground surface to about 31 m below ground level (b.g.l.). From 31 m to 34 m b.g.l., the rocks are clast-supported and poorer in the matrix. The top of the bedrock was detected at 35 m b.g.l. [25]. Four falling-head tests were carried out at different depths to estimate the hydraulic conductivity of the clayey medium (1.9×10^{-9} to 3.3×10^{-8} m/s) and confirmed its expected low permeability.

The local land use can be classified as permanent grassland. The soil medium is characterized [25] by pH values ranging from neutral to moderately alkaline and high percentage of Soil Organic Matter (SOM; about 19%). As observed by Remelli et al. [25], high SOM is further confirmed by the presence of arthropods of the order Diptera [26] and the class Symphyla [27]. However, the soil arthropod abundance detected by Remelli et al. [25] was lower than a typical grassland condition [28], therefore suggesting a stressful action that dramatically affected the study site.

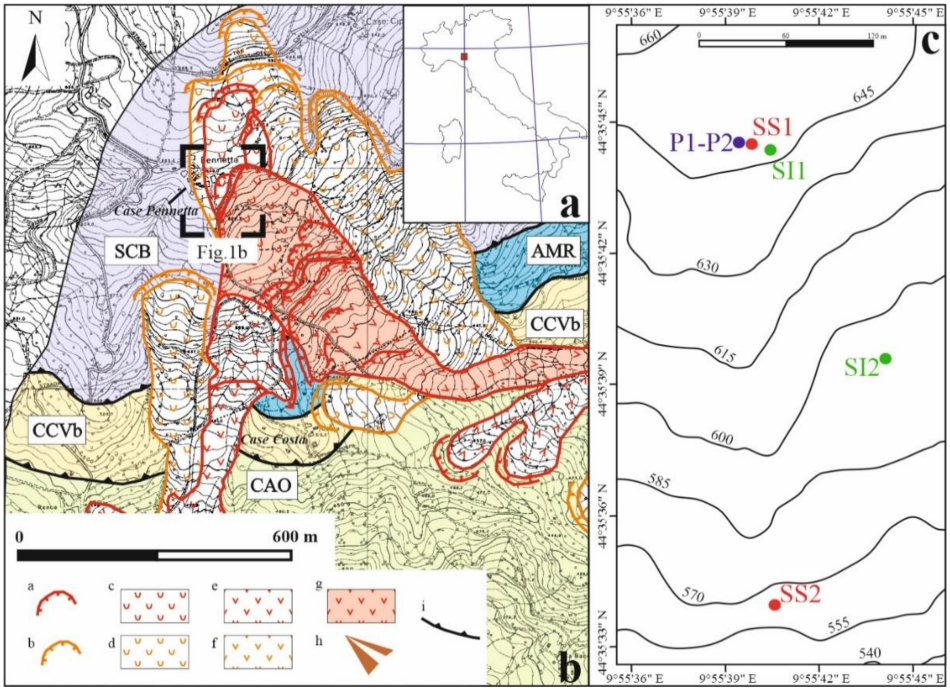

Figure 1. (**a**) Localization of the study area and (**b**) geological and geomorphological sketch map of the study area: (a) scarp of active landslide, (b) scarp of dormant landslide, (c) active landslide, (d) dormant landslide, (e) active earth flow, (f) dormant earth flow, (g) active earth slide/earth flow, (h) debris/earth flows cone with man interventions, and (i) main thrust. SCB: Arenarie di Scabiazza (sandstone); AMR: Argillle a Palombini di Monte Rizzone (clay stone); CCVb: Argille a blocchi (clay stone with blocks); CAO: Flysch of Monte Caio (marly-limestone). Base map: Technical Regional Map 1:5000, Emilia-Romagna Region 1998 (ed.) [29]. (**c**) Detailed topographic map with the location of boreholes (SI1–SI2), piezometers (P1–P2), and soil sample collection sites (SS1–SS2).

2.2. Mineralogical Investigations

Mineralogical analyses were performed on four soil samples collected at two different locations within the study site (SI1 and SI2 in Figure 1) during the drilling operations of two boreholes. The samples, taken at depths of 10.30–10.60 m and 16.50–17.00 m at SI1 and of 6.70–7.30 m and 8.20–8.80 m at SI2, were manually crushed with an agate mortar until the material passed a 230 mesh

sieve. The obtained powder was subjected to sonication in distilled water with an ultrasonic probe to obtain a homogeneous dispersion.

The clay fraction of <2 μm was separated by gravitational settling in a column of water 10 cm high. Oriented preparations (obtained by sedimentation on glass slides) were used for X-ray diffraction under three different states: air-dried, after saturation with ethylene glycol, and heated at 550 °C.

X-ray diffraction was performed by using a Bruker D2 PHASER diffractometer (Billerica, MA, USA) with Cu Kα radiation (λ = 1.5406 Å), under operating conditions of 30 kV and 10 mA, Ni filtered, and angle 2θ in the range 5–60°, with steps of 0.02° and a collecting time for each step of 1 s. The diffractometer has a θ-θ focalizing geometry and a solid-state detector. A sample rotation of 30 rpm was applied to minimize crystal preferential orientation effects. The diffraction patterns were identified using the Bruker software EVA and the Crystallography Open Database.

2.3. Hydrogeological Investigations

The hydraulic head was measured in P1 (see location in Figure 1) in high flow, and head fluctuations were compared with local precipitations. The groundwater Electrical Conductivity (EC) was measured both in P1 and P2 during the same observation period. P1 is a 25-meter-deep piezometer, screened between 1 and 24 meters b.g.l., while the piezometer P2 is 35 meters deep and has been screened between 30 and 34 meters b.g.l. They are part of a multilevel groundwater monitoring system (cluster type).

The hydraulic head was measured on an hourly basis through a pressure transducer with data-logger (STS DL.OCS/N/RS485, Sirnach, Switzerland) from 04/07/2018 to 15/01/2019. The reliability of the measurements was verified monthly by using a water level meter.

EC vertical profiles were obtained on a monthly basis from 15/11/2018 to 15/01/2019 by using a borehole probe (SOLINST TLC, Georgetown, ON, Canada). Measurements were carried out at 1-m-depth intervals. The reliability of EC values was always verified through laboratory analyses. Groundwater EC measurements were carried out in order to verify the presence of haloclines and the chance to use them for the investigation of the hydrogeological behavior of the analyzed system [30–32].

2.4. Next-Generation Sequencing (NGS) for Bacterial Community Analyses

Bacterial community analyses were performed on three groundwater (GWS1, GWS2, and GWS3; 1 L each) and two soil samples (SS1 and SS2; 0.5 g each) collected within the test site.

Groundwater sample collection occurred once in the high-flow period at the two piezometers. GWS1 was taken immediately below the hydraulic head in P1 through sterile bailers, whereas GWS2 was collected at the well bottom through a stainless-steel bailer fitted with a one-way valve at the lower end and attached to 6-mm plastic tubing at the upper end. The upper end of the tubing was attached to a pump. The bailer was pressurized with air before, lowering it to the chosen sampling depth. At the chosen depth, the pressure was released, allowing water to enter the bailer. After the bailer was withdrawn, water was transferred to a sterile bottle. GWS3 was sampled in P2 at the well bottom with the same procedure described above.

One soil sample (SS1) was collected very close to the piezometers P1 and P2, while the other (SS2) was taken at a greater distance (Figure 1). Soils were stored in sterile vials and were transported in refrigerated boxes, together with the water samples, to the laboratory for subsequent biomolecular analyses.

Water samples were filtered through sterile mixed esters of cellulose filters (S-Pak™ Membrane Filters, 47 mm diameter, 0.22 μm pore size, Millipore Corporation, Billerica, MA, USA) within 24 h from the collection. Bacterial DNA extraction from filters was performed using the commercial kit FastDNA SPIN Kit for soil (MP Biomedicals, LLC, Solon, OH, USA) and FastPrep®Instrument (MP Biomedicals, LLC, Solon, OH, USA). After the extraction, DNA integrity and quantity were evaluated by electrophoresis in 0.8% agarose gel containing 1 μg/mL of Gel-Red™ (Biotium, Inc., Fremont, CA, USA). The bacterial community profiles in the samples were generated by NGS technologies at the

Genprobio Srl Laboratory. Partial 16S rRNA gene sequences were obtained from the extracted DNA by Polymerase Chain Reaction (PCR) using the primer pair Probio_Uni and Probio_Rev, targeting the V3 region of the bacterial 16S rRNA gene sequence [33]. Amplifications were carried out using a Veriti Thermal Cycler (Applied Biosystems, Foster City, CA, USA), and PCR products were purified by the magnetic purification step involving the Agencourt AMPure XP DNA purification beads (Beckman Coulter Genomics GmbH, Bernried, Germany) in order to remove primer dimers. Amplicon checks were carried out as previously described [33]. Sequencing was performed using an Illumina MiSeq sequencer (Illumina, Hayward, CA, USA) with MiSeq Reagent Kit v3 chemicals. The .fastq files were processed using a custom script based on the QIIME software suite [34]. Paired-end read pairs were assembled to reconstruct the complete Probio_Uni/Probio_Rev amplicons. Quality control retained sequences with a length between 140 and 400 bp and mean sequence quality score > 20, while sequences with homopolymers >7 bp and mismatched primers were omitted. To calculate downstream diversity measures, operational taxonomic units (OTUs) were defined at 100% sequence homology using DADA2 [35]; OTUs not encompassing at least 2 sequences of the same sample were removed. All reads were classified to the lowest possible taxonomic rank using QIIME2 [34,36] and a reference dataset from the SILVA database v132 [37]. The biodiversity of the samples (alpha-diversity) was calculated with the Shannon index.

3. Results

3.1. Mineralogical Investigations

Mineralogical analyses showed the presence of significant amounts of quartz, discrete quantities of clay minerals, and subordinate plagioclase. The highest content of clay minerals was found in the sample collected at 16.50–17.00 m at SI1. The identified clay minerals were illite, chlorite, and irregular mixed layers illite-smectite and illite-chlorite. Illite was always characterized by a rather large and weak (002) reflection, suggesting disordered illite (1 Md polytype) and the presence of Fe^{3+} in the octahedral sites. Chlorite had a strong (002) reflection and a (001) reflection with very low intensity and was partially hidden by the asymmetry of the peak at about 10 Å of the illite. The behavior of chlorite reflections in ethylene glycol saturated and heated preparations suggested swelling chlorite (Cg). The asymmetry of the illite (001) reflection towards low angular values indicated the presence of irregular mixed layers with smectite (montmorillonite) and chlorite.

In samples collected at SI2 and at the topmost layer at SI1, a shoulder towards the low angular values of the (001) reflection of illite, corresponding to a d value of about 12 Å and a strong increase in the illite (001) reflection in the heated sample, suggested the presence of regular mixed layers illite-montmorillonite or illite-vermiculite or both. Finally, the most superficial horizon analyzed at SI2 showed a doublet related to the (004) reflection of chlorite and the (002) reflection of kaolinite. The shape of the irregular mixed layers illite-montmorillonite suggested the presence of Ca^{2+} as the interlayer cation of montmorillonite.

3.2. Hydrogeological Investigations

The hydraulic head in P1 rapidly fluctuated during infiltration events (Figure 2), confirming the fast percolation of fresh-infiltration waters from the ground surface towards the phreatic zone observed by Remelli et al. [25] at the same site. The rapid arrival of percolation waters from the ground surface was further supported by the sharp decrease of groundwater EC measured below the hydraulic head in P1 (Figure 3), indicating a mixing process between lower-salinity fresh-infiltration waters and higher-salinity groundwater. In detail, during the observation period, a significant difference between values recorded at the bottom (>4700 µS/cm) and the top of the screened interval (682 to 1945 µS/cm) was detected, with a step-like shape of the EC profiles. The step-like shape of the halocline is further emphasized when analyzing on the whole the EC profiles of the piezometers P1 and P2 (Figure 3).

As a matter of fact, hydrogeological investigations suggested that the near-surface medium is characterized by porosity and permeability higher than those expected in clay-rich sediments even though no information is available concerning the possible pore-size of the rock mass within the unsaturated zone at the observation scale.

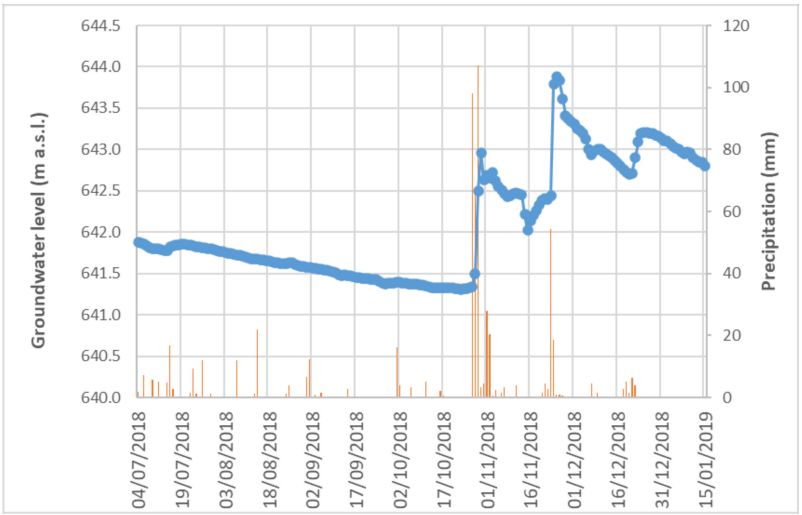

Figure 2. Groundwater level fluctuations vs rainfall in piezometer P1.

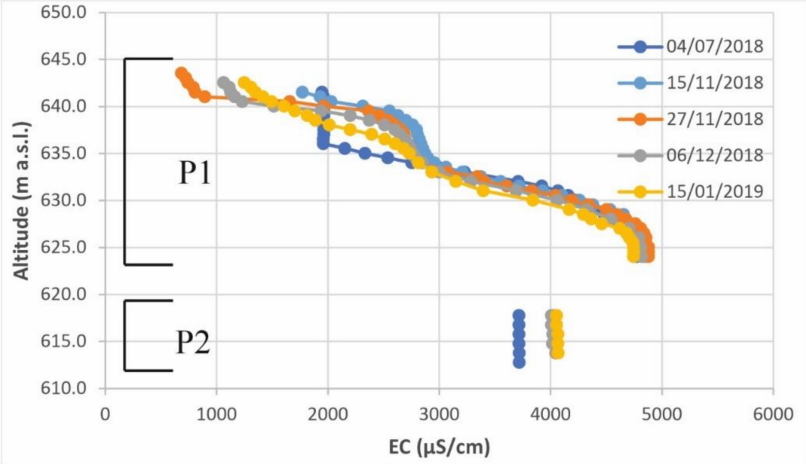

Figure 3. Vertical profile of groundwater Electrical Conductivity (EC) recorded in P1 and P2.

3.3. Groundwater and Soil Microbial Communities

MiSeq runs produced an average of 65,914 and 69,210 reads for groundwater (GWS1-2-3) and soil samples (SS1 and SS2), respectively (Table 1). 16S rRNA gene sequences generated in this study have been deposited in the National Center for Biotechnology Information (NCBI) Sequence Read Archive under the accession number PRJNA630902. The rarefaction analysis (a measure used to estimate the alpha-diversity in samples and to gauge whether sequencing efforts captured the microbial diversity; Figure 4) showed relatively higher biodiversity in soils (SS1 and SS2) and groundwater collected at the well bottom of the piezometer P2.

NGS results allowed to obtain detailed information about the composition of microbial communities.

Proteobacteria, *Patescibacteria*, *Actinobacteria*, and *Bacteroidetes* represented the four major phyla in samples GWS1 and GWS3, accounting for, on average, 57.41%, 15.05%, 7.52%, and 7.11%, respectively (Figure 5). In groundwater collected at the well bottom of the piezometer P1 (GWS2), a dominance of

Proteobacteria (75.57%) was observed while other phyla such as *Spirochaetes* (4.59%), *Nitrospirae* (3.88%), and *Actinobacteria* (3.83%) occurred at lower percentages (Figure 5).

Table 1. Number of 16S rDNA sequences obtained after next-generation sequencing (NGS) analysis for groundwater and soil samples.

Sample	Final Read Number
GWS1	46,615
GWS2	94,558
GWS3	56,571
SS1	76,569
SS2	61,852

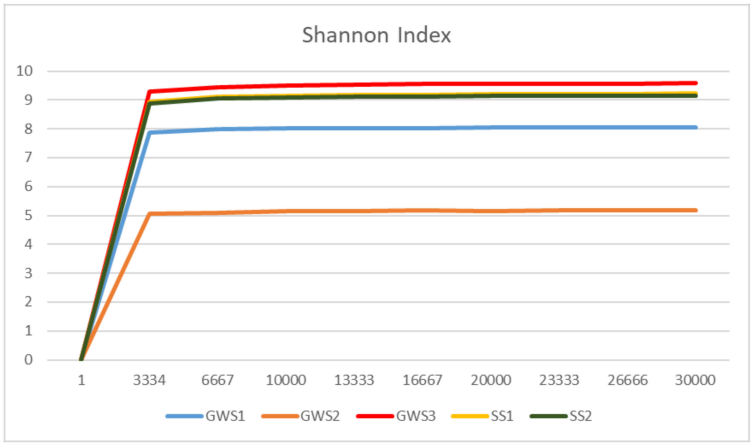

Figure 4. Rarefaction curves of groundwater and soil samples: The alpha-diversity plots were obtained by using the Shannon index.

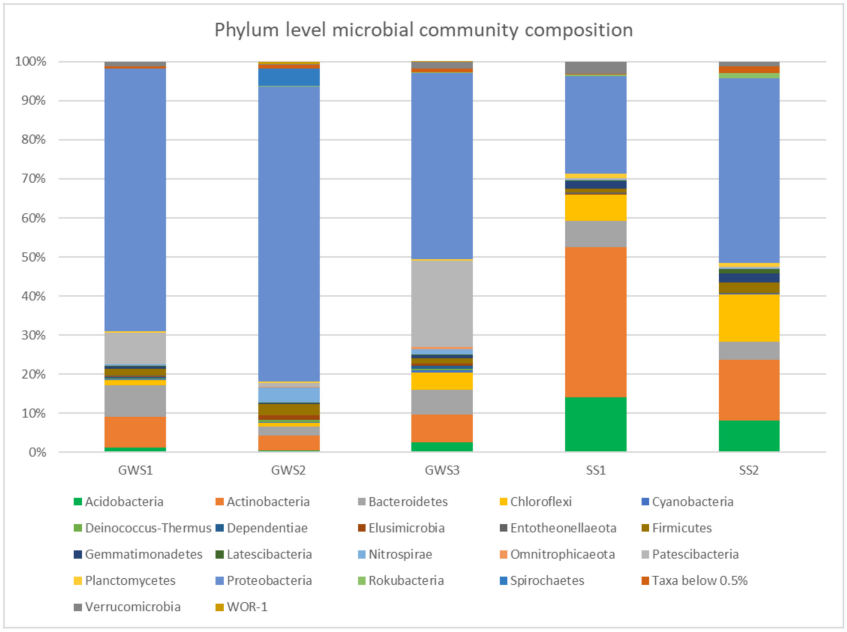

Figure 5. Phylum level microbial community composition in samples collected from groundwater and soil.

Soil bacterial communities were mainly composed of *Proteobacteria*, *Actinobacteria*, *Acidobacteria*, and *Chloroflexi* with mean relative abundance values of 36.01%, 27.05%, 11.08%, and 9.39%, respectively (Figure 5).

The analysis of bacterial community composition at the family level (Figure 6) revealed, in samples GWS1 and GWS2, a predominance of *Pseudomonadaceae* (23.80% and 42.51%, respectively). Among the most abundant families, *Burkholderiaceae* (8.49%), *Sphingomonadaceae* (3.10%), *Micrococcaceae* (3.09%) and unclassified microorganisms belonging to the *Saccharimonadales* order (5.57%) occurred in GWS1 whereas *Desulfobacteraceae* (13.28%), *Leptospiraceae* (4.46%), *Thermodesulfovibrionia* (3.04%), and *Desulfovibrionaceae* (2.68%) were found in GWS2.

In GWS3, unclassified microorganisms of the *Saccharimonadales* order represented the most numerous group (12.37%), followed by *Sphingomonadaceae* (5.21%), *Burkholderiaceae* (3.98%), *Acidiferrobacteraceae* (3.02%), and *Legionellaceae* (2.76%).

Soil samples were characterized by high percentages of unclassified microorganisms (29.73% in SS1 and 23.47% in SS2). Some of these belong to the *Acidobacteria* (subgroup 6 class; 9.28% in SS1 and 3.80% in SS2) and *Chloroflexi* (1.53% in SS1 and 1.92% in SS2) phyla, and *Gaiellales* order (4.21% in SS1 and 1.10% SS2). Other representative families were *Propionibacteriaceae* (4.86%), *Gaiellaceae* (4.66%), *Xanthobacteraceae* (4.29%), *Nocardioidaceae* (3.29%), and *Burkholderiaceae* (3.10%) in SS1 and *Rhodobacteraceae* (8.82%), *Halomonadaceae* (3.27%), *Sphingomonadaceae* (2.84%), and *Nitrosomonadaceae* (2.75%) in SS2.

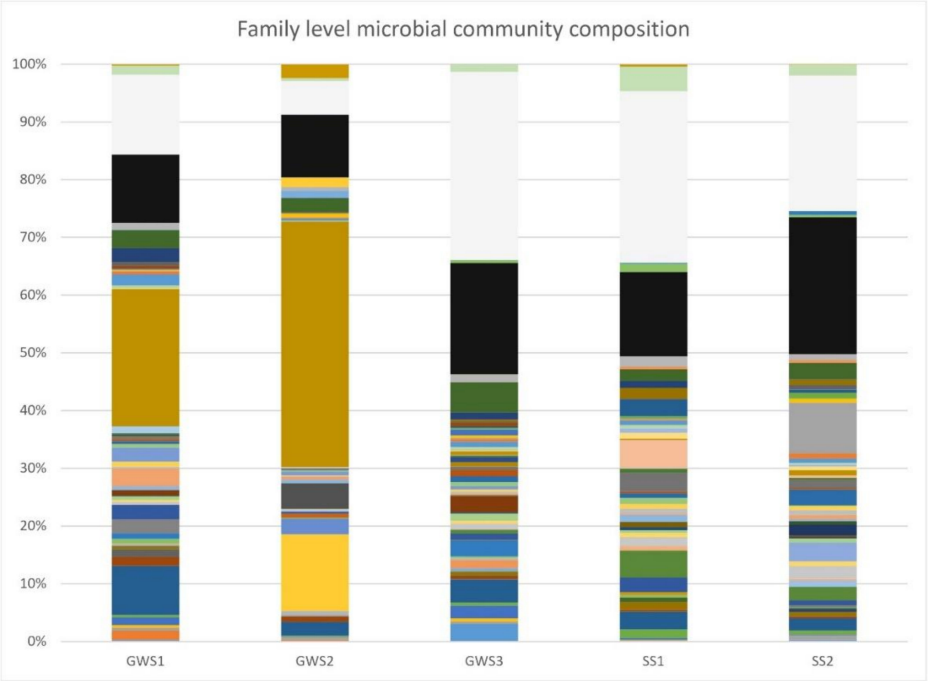

Figure 6. Family level microbial community composition in samples collected from groundwater and soil: Unclassified bacterial families are reported in light grey. Taxa with relative abundance below 0.5% are reported in black. The remaining colours indicate identified bacterial families.

When analyzing the groundwater microbial communities at the genus level (Figure 7), it emerged that *Pseudomonas* reached the highest percentages in GWS1 (23.76%) and GWS2 (42.49%) samples whereas its relative abundance in GWS3 was only 0.58%. The results suggested the existence of different bacterial communities within the saturated zone intercepted by P1, from the hydraulic head (GWS1) to the well bottom (GWS2), in terms of abundance and presence of the various taxa. Most of the genera detected at the highest percentages in GWS1 were also found in GWS2 but with lower values. In addition to *Pseudomonas*, GWS1 microbial community was also characterized by the *Kocuria* [38], *Sphingomonas* [39] *Massilia* [40], *Flavobacterium* [41], and *Rahnella* [42] genera, including aerobic or facultative anaerobic, mainly mesophilic and psychrophilic, species.

On the other hand, other genera detected in GWS2 were *Stenotrophomonas* [43], *Sphingomonas* [39], *Staphylococcus* [44], *Desulfatitalea* [45], and *Desulfovibrio* [46], including mesophilic, psychrotolerant, halophilic or halotolerant, and sulfate-reducing bacteria.

Microbial community of the groundwater sample GWS3 (collected at the well bottom of the piezometer P2) was mainly composed by unclassified microorganisms of the *Saccharimonadales* order (12.28%) and the genera *Sphingomonas* [39], *Sulfurifustis* [47], and *Legionella* [48].

The top four genera in soil samples were *Gaiella* (4.57%), *Microlunatus* (4.14%), unclassified microorganisms of the subgroup 6 class (8.61%) (*Acidobacteria* phylum), and unclassified microorganisms of the *Gaiellales* order (4.13%) in SS1 and *Roseovarius* (5.55%), *Halomonas* (3.21%), *Sphingomonas* (2.69%), and unclassified microorganisms of the subgroup 6 class (3.46%) in SS2.

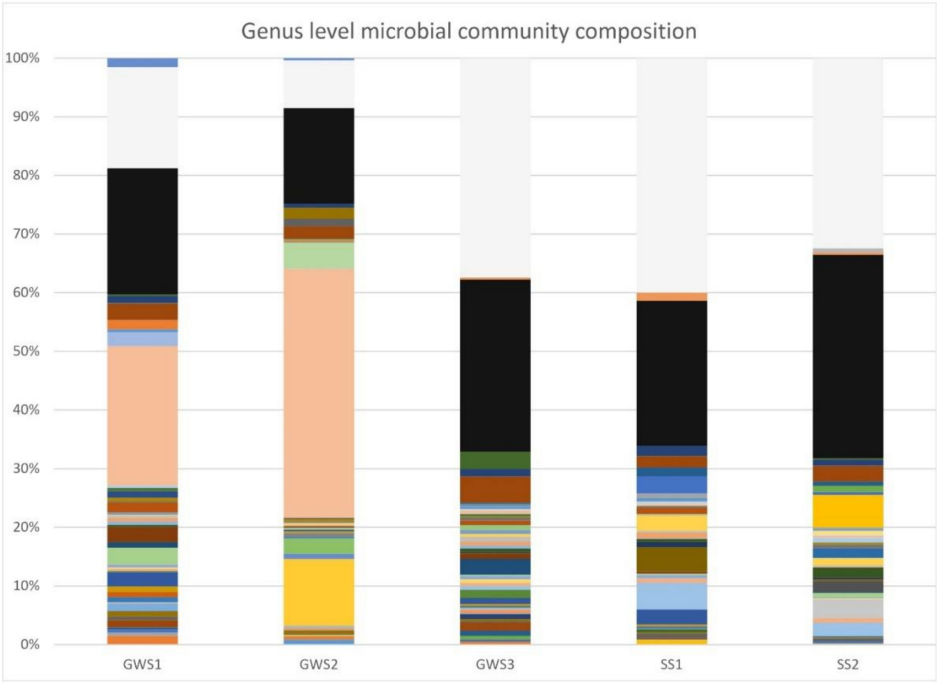

Figure 7. Genus level microbial community composition in samples collected from groundwater and soil: Unclassified bacterial genera are reported in light grey. Taxa with relative abundance below 0.5% are reported in black. The remaining colours indicate identified bacterial genera.

In order to analyze and assess if some hydrological aspects of the low-permeability system could be revealed via the use of autochthonous microorganisms, we focused our attention on those bacterial species for which the presence in groundwater and soil samples could give an indication of local-scale specific processes.

Some of the species detected in groundwater and soil samples are reported in Table 2. The hydraulic interconnection between the topsoil and groundwater is witnessed by the presence of several species in GWS samples linked to aerobic soil environments (e.g., *Pseudomonas frederiksbergensis* [49]): some of them were also found in the analyzed soil samples (e.g., *Pedobacter insulae* [50] and *Ensifer adhaerens* [51]). Nitrate and nitrite reducer bacteria, such as *Ensifer adhaerens* [52], *Devosia glacialis* [53], and *Afipia massiliensis* [54], were detected both in soil and groundwater.

Interestingly, together with soil- and rhizo-bacteria, human pathogens belonging to the genus *Legionella* (*L. pneumophila* and *L. feeleii*) were discovered in some groundwater samples. These microorganisms are well known as responsible for acute human respiratory diseases (Pontiac fever or Legionnaires's disease; [55,56]). Their presence is, thus, of utmost importance since it testifies the possibility that *Legionella* cells can be transported in depth in a clayey saturated medium.

Table 2. Physiological and biochemical characteristics of some of the species found in groundwater and soil samples after the 16S rRNA gene partial sequencing. (− negative; + positive).

Taxonomy	Aerobic	Facultative Anaerobic	Halophilic/Halotolerant	Nitrate Reduction	Pathogen	Samples	Citations
Acinetobacter oleivorans	+	−	−	−	−	GWS1-2-3	[57]
Afipia massiliensis	+	−	−	+	−	GWS1-2	[54]
Deinococcus caeni	+	−	+	−	−	GWS1-2-3	[58]
Devosia glacialis	+	−	−	+	−	GWS1-2-3; SS1	[53]
Ensifer adhaerens	+	−	−	+	−	GWS1-2-3; SS1-2	[52]
Halomonas taeanensis	+	−	+	+	−	SS2	[59]
Halomonas ventosae	+	−	+	+	−	SS2	[60]
Janthinobacterium agaricidamnosum	+	−	−	−	−	GWS1-3; SS1	[61]
Legionella feeleii	+	−	−	−	+	GWS3; SS2	[62]
Legionella nautarum	+	−	−	+	+	GWS3	[63]
Legionella pneumophila	+	−	−	−	+	GWS3	[64]
Pedobacter insulae	+	−	−	−	−	GWS1-2-3; SS1	[50]
Pseudomonas frederiksbergensis	+	−	−	+	−	GWS1-2-3	[49]
Pseudomonas otitidis	+	−	+	−	+	GWS2	[65]
Pseudomonas psychrophila	+	−	+	+	−	GWS1-2-3; SS2	[66]
Pseudomonas xanthomarina	+	−	+	+	−	GWS2	[67]
Sphingomonas yunnanensis	+	−	−	+	−	GWS1-2-3; SS1-2	[39]
Staphylococcus warneri	+	+	+	−	+	GWS2-3	[44]
Stenotrophomonas chelatiphaga	+	−	−	−	−	GWS1-2; SS1	[43]
Streptomyces vinaceusdrappus	+	−	+	+	−	GWS1-2-3; SS1-2	[68]
Streptomyces xinghaiensis	+	−	+	−	−	GWS1-2-3; SS1-2	[69]
Thiohalobacter thiocyanaticus	+	−	+	−	−	SS2	[70]

4. Discussion and Conclusions

During the observation period, the hydraulic head measurements, compared with local precipitations, suggested rapid water percolation from the ground surface to the saturated zone. The mixing between lower-salinity fresh-infiltration waters and higher-salinity groundwater during recharge was further confirmed through the EC vertical profiles reconstructed in P1 and P2, which clearly showed the existence of a halocline.

The percolation of fresh-infiltration waters was also a driver for the transport of microorganisms from the topsoil to the groundwater, as demonstrated by the presence of soil and rhizosphere bacterial species detected in GWS samples. The migration of cells within the clayey unsaturated medium is in agreement with the hypothesis made by Remelli et al. [25] that revealed how, at the study site, both the effective porosity and the permeability of the upper medium were increased by arthropods such as Poduromorpha, Oribatida, Coleoptera, and Hymenoptera because of their ability to create macropore (mm in dimension) networks. However, since arthropods can increase porosity and permeability in several tens of centimeters below ground and the groundwater surface was some meters deep during the observation period, we believe that other features/processes, such as drying cracks and/or rock weathering, could increase porosity and pore size within a thicker subsurface horizon.

The presence of soil- and rhizo-bacteria in groundwater samples taken at different depths further suggests that the pore network within the saturated zone should be partially but diffusely characterized by pore size greater than a few μm (>bacterial cells dimension). This result, obtained at the basin scale, is in agreement with the findings obtained by several authors at a laboratory scale when characterizing the pore diameters in clay-rich media. The porosity of clay minerals is related to the presence of broken edges on the surface of the clay particles, irregularities and voids created by the overlap of the structural packages, and voids in the interlayer sites. Pore size can vary from micropores (<0.002 μm diameter) to mesopores (0.002–0.05 μm diameter). Aggregation of clay particles forms pores >0.1 μm (macropores). The pore size depends on the intrinsic properties of the clay minerals, such as layer charge and exchangeable cation [71]. The greatest effects on porosity are due to clay minerals with a greater surface area: therefore smaller size (such as illite and smectites) and expandability (smectites). In particular, clays containing mixed layers illite-smectite (or montmorillonite) show various types of pore structures, with sizes from 0.003 μm, characteristic of montmorillonite (due to the overlapping of elementary unit cells), to 0.02–0.1 μm for the stacking of structural units (illite and montmorillonite) [72]. Therefore, micropores/fine mesopores occurring in our soils are related to the abundance of illite-montmorillonite mixed layers in the clayey portion. In swelling clay minerals, the size of the exchangeable cation has an important effect on the surface area and, therefore, on the volume of available pores. In the case of Ca^{2+} cations, as in our case, the contribution of the pore volume on the total volume is in the order of 45–50% [71]. Moreover, the porosity of clay soils is influenced not only by the content and type of clay minerals but also by the water regime and the presence of organic matter [73]. When a swelling mineral such as montmorillonite comes into contact with water, its volume increase is instantaneous [74]. It can drastically influence and change the soil porosity and permeability. The bacteria, in turn, can interact with the clay minerals and can alter their features (layer charge, cation exchange capacity, and exchangeable cations), modifying their swelling properties [75]. The iron reduction induced by bacteria can decrease the specific surface area of smectite by about 30% and of montmorillonite by almost 50% (depending on the interlayer cation), inducing a loss of clay swelling; the interparticle association assumes a more compact fabric. Furthermore, the activity of organic matter intercalated in the interlayer of the smectite structure has a strong catalytic effect on the smectite-to-illite reaction which can occur at room temperature, 1 atmosphere, and in a very short time and is less effective at alkaline pH ([75] and references therein). Bacteria can also promote the adhesion of the clay platelets to their cells favoring the aggregate formation, and their organic secretion penetrates the surrounding clay pores and modifies the clay shrinkage/swelling behavior [76].

On the whole, the coexistence of micro-, meso-, and macropores leads to a nonuniform path within the clayey medium, and the migration of bacterial cells could be concentrated in some

sub-volumes [77–79]. As a consequence, different degrees of retention can be identified at the core scale, therefore emphasizing the importance of studying such phenomena at the basin scale.

In a wide context, the transport of bacterial cells from the topsoil to the groundwater through a clay-rich horizon opens two opposing scenarios. Firstly, some bacterial species detected in both soil and groundwater are denitrifying or nitrate-reducing microorganisms. From a broader perspective, the "permeability" of clay-rich media could allow the transport of these kinds of microorganisms from the topsoil to the groundwater also in confined or semi-confined aquifers and, thus, could enhance denitrification and/or nitrate-reduction processes within the underlying saturated zone. These findings could be of the utmost importance when studying the evolution of nitrate contamination over space and time in those areas where agricultural, industrial, and civil activities have significantly increased the levels of reactive nitrogen (N) in water bodies [80,81]. In fact, in many cases, N input sources (both organic and synthetic fertilizers) exceed crops' N requirements and fertilization plans seldom consider mineralization rates and factors regulating N dynamics in agricultural land [82–84]. As a result, nitrogen surplus is often observed, with a high impact on ecosystems, including groundwater pollution and eutrophication [85–87]. On the other hand, the same findings lead to the awareness that groundwater vulnerability of confined or semi-confined aquifers against contamination (both chemical and microbiological) could be higher than expected. In this specific context, the retrieval of DNA sequences of known human pathogens, such as the *Legionella* species, draw serious concerns and, in a broader perspective, sets the stage for further analyses aimed at 1) specifically evaluating the transport dynamics of these microorganisms through the soil and 2) assessing their viability over time and space in order to prevent water-related infectious diseases.

Author Contributions: Conceptualization, E.P., A.B., A.M.S., and F.C.; formal analysis, P.R.; investigation, P.R., M.R., and A.Q.; supervision, E.P., A.B., A.M.S., and F.C.; validation, P.R.; visualization, P.R.; writing—original draft, P.R., E.P., and A.B.; writing—review and editing, P.R., E.P., A.B., E.S.-M., A.C., A.M.S., and F.C. All authors have read and agreed to the published version of the manuscript.

Funding: This research received no external funding.

Acknowledgments: This work has benefited from the equipment and framework of the COMP-HUB Initiative, funded by the "Departments of Excellence" program of the Italian Ministry for Education, University, and Research (MIUR, 2018-2022). We are grateful to the reviewers for their constructive comments and valuable suggestions.

Conflicts of Interest: The authors declare no conflict of interest.

References

1. Tufenkji, N.; Emelko, M.B. Fate and transport of microbial contaminants in groundwater. In *Encyclopedia of Environmental Health*; Nriagu, J.O., Ed.; Elsevier: Amsterdam, The Netherlands, 2011; pp. 715–726.
2. Bucci, A.; Petrella, E.; Celico, F.; Naclerio, G. Use of molecular approaches in hydrogeological studies: The case of carbonate aquifers in southern Italy. *Hydrogeol. J.* **2017**, *25*, 1017–1031. [CrossRef]
3. Mills, A.L.; Herman, J.S.; Hornberger, G.M.; Dejesus, T.H. Effect of solution ionic-strength and iron coatings on mineral grains on the sorption of bacterial-cells to quartz sand. *Appl. Environ. Microbiol.* **1994**, *60*, 3300–3306. [CrossRef] [PubMed]
4. Mccaulou, D.R.; Bales, R.C.; Arnold, R.G. Effect of temperature-controlled motility on transport of bacteria and microspheres through saturated sediment. *Water Resour. Res.* **1995**, *31*, 271–280. [CrossRef]
5. Hendry, M.J.; Lawrence, J.R.; Maloszewski, P. Effects of velocity on the transport of two bacteria through saturated sand. *Ground Water* **1999**, *37*, 103–112. [CrossRef]
6. Yee, N.; Fein, J.B.; Daughney, C.J. Experimental study of the pH, ionic strength, and reversibility behavior of bacteria-mineral adsorption. *Geochim. Cosmochim. Acta* **2000**, *64*, 609–617. [CrossRef]
7. Dong, H.L.; Onstott, T.C.; Deflaun, M.F.; Fuller, M.E.; Scheibe, T.D.; Streger, S.H.; Rothmel, R.K.; Mailloux, B.J. Relative dominance of physical versus chemical effects on the transport of adhesion-deficient bacteria in intact cores from South Oyster, Virginia. *Environ. Sci. Technol.* **2002**, *36*, 891–900. [CrossRef]
8. Bradford, S.A.; Šimůnek, J.; Walker, S.L. Transport and straining of *E. coli* O157: H7 in saturated porous media. *Water Resour. Res.* **2006**, *42*. [CrossRef]

9. Chen, G.X.; Walker, S.L. Role of solution chemistry and ion valence on the adhesion kinetics of groundwater and marine bacteria. *Langmuir* **2007**, *23*, 7162–7169. [CrossRef]
10. Ochiai, N.; Kraft, E.L.; Selker, J.S. Methods for colloid transport visualization in pore networks. *Water Resour. Res.* **2006**, *42*. [CrossRef]
11. Streit, W.R.; Schmitz, R.A. Metagenomics—The key to the uncultured microbes. *Curr. Opin. Microbiol.* **2004**, *7*, 492–498. [CrossRef]
12. Kucharzyk, K.H.; Rectanus, H.V.; Bartling, C.M.; Rosansky, S.; Minard-Smith, A.; Mullins, L.A.; Neil, K. Use of omic tools to assess methyl tert-butyl ether (MTBE) degradation in groundwater. *J. Hazard. Mater.* **2019**, *378*, 120618. [CrossRef] [PubMed]
13. Mosaddeghi, M.R.; Mahboubi, A.A.; Zandsalimi, S.; Unc, A. Influence of organic waste type and soil structure on the bacterial filtration rates in unsaturated intact soil columns. *J. Environ. Manag.* **2009**, *90*, 730–739. [CrossRef] [PubMed]
14. Naclerio, G.; Fardella, G.; Marzullo, G.; Celico, F. Filtration of *Bacillus subtilis* and *Bacillus cereus* spores in a pyroclastic topsoil, carbonate Apennines, southern Italy. *Colloids Surf. B Biointerfaces* **2009**, *70*, 25–28. [CrossRef] [PubMed]
15. Safadoust, A.; Mahboubi, A.A.; Mosaddeghi, M.R.; Gharabaghi, B.; Voroney, P.; Unc, A.; Khodakaramian, G. Significance of physical weathering of two-texturally different soils for the saturated transport of *Escherichia coli* and bromide. *J. Environ. Manag.* **2012**, *107*, 147–158. [CrossRef]
16. Moradi, A.; Mosaddeghi, M.R.; Chavoshi, E.; Safadoust, A.; Soleimani, M. Effect of Crude Oil-Induced Water Repellency on Transport of *Escherichia coli* and Bromide Through Repacked and Physically-Weathered Soil Columns. *Environ. Pollut.* **2019**, *255*, 113230. [CrossRef]
17. Boschetti, T.; Falasca, A.; Bucci, A.; De Felice, V.; Naclerio, G.; Celico, F. Influence of soil on groundwater geochemistry in a carbonate aquifer, southern Italy. *Int. J. Speleol.* **2014**, *43*, 79–94. [CrossRef]
18. Bucci, A.; Allocca, V.; Naclerio, G.; Capobianco, G.; Divino, F.; Fiorillo, F.; Celico, F. Winter survival of microbial contaminants in soil: An *in situ* verification. *J. Environ. Sci.* **2015**, *27*, 131–138. [CrossRef]
19. Rizzo, P.; Bucci, A.; Sanangelantoni, A.M.; Iacumin, P.; Celico, F. Coupled Microbiological–Isotopic Approach for Studying Hydrodynamics in Deep Reservoirs: The Case of the Val d'Agri Oilfield (Southern Italy). *Water* **2020**, *12*, 1483. [CrossRef]
20. Bucci, A.; Petrella, E.; Naclerio, G.; Gambatese, S.; Celico, F. Bacterial migration through low-permeability fault zones in compartmentalised aquifer systems: A case study in Southern Italy. *Int. J. Speleol.* **2014**, *43*, 273–281. [CrossRef]
21. Bucci, A.; Petrella, E.; Naclerio, G.; Allocca, V.; Celico, F. Microorganisms as contaminants and natural tracers: A 10-year research in some carbonate aquifers (southern Italy). *Environ. Earth Sci.* **2015**, *74*, 173–184. [CrossRef]
22. Bucci, A.; Naclerio, G.; Allocca, V.; Celico, P.; Celico, F. Potential use of microbial community investigations to analyze hydrothermal systems behaviour: The case of Ischia island, southern Italy. *Hydrol. Process.* **2011**, *25*, 1866–1873. [CrossRef]
23. Hernandez-Diaz, R.; Petrella, E.; Bucci, A.; Naclerio, G.; Feo, A.; Sferra, G.; Chelli, A.; Zanini, A.; Gonzales-Hernandez, P.; Celico, F. Integrating hydrogeological and microbiological data and modelling to characterize the hydraulic features and behavior of coastal carbonate aquifers: A case in Western Cuba. *Water* **2019**, *11*, 1989. [CrossRef]
24. Vescovi, P.; Andreozzi, M.; De Nardo, M.T.; Lasagna, S.; Martelli, L.; Rio, D.; Tellini, C.; Vernia, L. Note illustrative della carta geologica d'Italia alla scala 1:50,000, foglio 216, Borgo Val di Taro. In *Presidenza del Consigio dei Ministri, Servizio Geologico d'Italia, Regione Emilia-Romagna*; S.El.Ca. SRLS.El.Ca. SRL: Florence, Italy, 2002.
25. Remelli, S.; Petrella, E.; Chelli, A.; Conti, F.D.; Lozano Fondon, C.; Celico, F.; Francese, R.; Menta, C. Hydrodynamic and soil biodiversity characterization in an active landslide. *Water* **2019**, *11*, 1882. [CrossRef]
26. Frouz, J. Use of soil dwelling Diptera (Insecta, Diptera) as bioindicators: A review of ecological requirements and response to disturbance. *Agric. Ecosyst. Environ.* **1999**, *74*, 167–186. [CrossRef]
27. Edwards, C.A. The ecology of Symphyla. *Entomol. Exp. Appl.* **1958**, *1*, 308–319. [CrossRef]
28. Menta, C.; Leoni, A.; Gardi, C.; Conti, F. Are grasslands important habitats for soil microarthropod conservation? *Biodivers. Conserv.* **2011**, *20*, 1073–1087. [CrossRef]

29. Geoportale. Base Map: Technical Regional Map 1:5000, Emilia-Romagna Region 1998 (ed.). Available online: https://geoportale.regione.emilia-romagna (accessed on 23 June 2020).
30. Morin, R.H.; Carleton, G.B.; Poirier, S. Fractured-aquifer hydrogeology from geophysical logs; the passaic formation, New Jersey. *Ground Water* **1997**, *35*, 328–338. [CrossRef]
31. Cook, P.G.; Love, A.J.; Dighton, J.C. Inferring ground water flow in fractured rock from dissolved radon. *Ground Water* **1999**, *37*, 606–610. [CrossRef]
32. Aquino, D.; Petrella, E.; Florio, M.; Celico, P.; Celico, F. Complex hydraulic interactions between compartmentalized carbonate aquifers and heterogeneous siliciclastic successions: A case study in southern Italy. *Hydrol. Process.* **2015**, *29*, 4252–4263. [CrossRef]
33. Milani, C.; Hevia, A.; Foroni, E.; Duranti, S.; Turroni, F.; Lugli, G.A.; Sanchez, B.; Martín, R.; Gueimonde, M.; Van Sinderen, D.; et al. Assessing the fecal microbiota: An optimised ion torrent 16S rRNA gene-based analysis protocol. *PLoS ONE* **2013**, *8*, e68739. [CrossRef]
34. Caporaso, J.G.; Kuczynski, J.; Stombaugh, J.; Bittinger, K.; Bushman, F.D.; Costello, E.K.; Fierer, N.; Gonzalez Peña, A.; Goodrich, J.K.; Gordon, J.I.; et al. QIIME allows analysis of high-throughput community sequencing data. *Nat. Methods* **2010**, *7*, 335–336. [CrossRef] [PubMed]
35. Callahan, B.J.; McMurdie, P.J.; Rosen, M.J.; Han, A.W.; Johnson, A.J.; Holmes, S.P. DADA2: High-resolution sample inference from Illumina amplicon data. *Nat. Methods* **2016**, *13*, 581–583. [CrossRef] [PubMed]
36. Bokulich, N.A.; Kaehler, B.D.; Rideout, J.R.; Dillon, M.; Bolyen, E.; Knight, R.; Huttley, G.A.; Caporaso, J.G. Optimizing taxonomic classification of marker-gene amplicon sequences with QIIME 2's q2-feature-classifier plugin. *Microbiome* **2018**, *6*, 90. [CrossRef] [PubMed]
37. Quast, C.; Pruesse, E.; Yilmaz, P.; Gerken, J.; Schweer, T.; Yarza, P.; Peplies, J.; Glöckner, F.O. The SILVA ribosomal RNA gene database project: Improved data processing and web-based tools. *Nucleic Acids Res.* **2012**, *41*, D590–D596. [CrossRef] [PubMed]
38. Stackebrandt, E.; Koch, C.; Gvozdiak, O.; Schumann, P. Taxonomic Dissection of the Genus *Micrococcus*: *Kocuria* gen. nov., *Nesterenkonia* gen. nov., *Kytococcus* gen. nov., *Dermacoccus* gen. nov., and *Micrococcus* Cohn 1872 gen. emend. *Int. J. Syst. Bacteriol.* **1995**, *45*, 682–692. [CrossRef]
39. Zhang, Y.Q.; Chen, Y.G.; Li, W.J.; Tian, X.P.; Xu, L.H.; Jiang, C.L. *Sphingomonas yunnanensis* sp. nov., a novel Gram-negative bacterium from a contaminated plate. *Int. J. Syst. Evol. Microbiol.* **2005**, *55*, 2361–2364. [CrossRef]
40. Baldani, J.I.; Rouws, L.; Cruz, L.M.; Olivares, F.L.; Schmid, M.; Hartmann, A. The family *Oxalobacteraceae*. In *The Prokaryotes*; Rosenberg, E., DeLong, E.F., Lory, S., Stackebrandt, E., Thompson, F., Eds.; Springer: Berlin/Heidelberg, Germany, 2014; pp. 919–974.
41. Bernardet, J.F.; Bowman, J.P. The genus *Flavobacterium*. In *The Prokaryotes*; Dworkin, M., Falkow, S., Rosenberg, E., Schleifer, K.H., Stackebrandt, E., Eds.; Springer: New York, NY, USA, 2006; pp. 481–531.
42. Berge, O.; Heulin, T.; Achouak, W.; Richard, C.; Bally, R.; Balandreau, J. *Rahnella aquatilis*, a nitrogen-fixing enteric bacterium associated with the rhizosphere of wheat and maize. *Can. J. Microbiol.* **1991**, *37*, 195–203. [CrossRef]
43. Kaparullina, E.; Doronina, N.; Chistyakova, T.; Trotsenko, Y. *Stenotrophomonas chelatiphaga* sp. nov., a new aerobic EDTA-degrading bacterium. *Syst. Appl. Microbiol.* **2009**, *32*, 157–162. [CrossRef]
44. Kloos, W.E.; Schleifer, K.H. Isolation and characterization of staphylococci from human skin II. descriptions of four new species: *Staphylococcus warneri*, *Staphylococcus capitis*, *Staphylococcus hominis*, and *Staphylococcus simulans1*. *Int. J. Syst. Evol. Microbiol.* **1975**, *25*, 62–79. [CrossRef]
45. Higashioka, Y.; Kojima, H.; Watanabe, M.; Fukui, M. *Desulfatitalea tepidiphila* gen. nov., sp. nov., a sulfate-reducing bacterium isolated from tidal flat sediment. *Int. J. Syst. Evol. Microbiol.* **2013**, *63*, 761–765. [CrossRef]
46. Fauque, G.D. Ecology of sulfate-reducing bacteria. In *Sulfate-Reducing Bacteria*; Barton, L.L., Ed.; Springer: Boston, MA, USA, 1995; Volume 8, pp. 217–241.
47. Kojima, H.; Shinohara, A.; Fukui, M. *Sulfurifustis variabilis* gen. nov., sp nov., a sulfur oxidizer isolated from a lake, and proposal of *Acidiferrobacteraceae* fam. nov and *Acidiferrobacterales* ord. nov. *Int. J. Syst. Evol. Microbiol.* **2015**, *65*, 3709–3713. [CrossRef] [PubMed]
48. Kao, P.M.; Tung, M.C.; Hsu, B.M.; Chiu, Y.C.; She, C.Y.; Shen, S.M.; Huang, Y.L.; Huang, W.C. Identification and quantitative detection of *Legionella* spp. in various aquatic environments by real-time PCR assay. *Environ. Sci. Pollut. Res. Int.* **2013**, *20*, 6128–6137. [CrossRef] [PubMed]

49. Andersen, S.M.; Johnsen, K.; Sorensen, J.; Nielsen, P.; Jacobsen, C.S. *Pseudomonas frederiksbergensis* sp. nov., isolated from soil at a coal gasification site. *Int. J. Syst. Evol. Microbiol.* **2000**, *50*, 1957–1964. [CrossRef] [PubMed]
50. Yoon, J.H.; Kang, S.J.; Oh, H.W.; Oh, T.K. *Pedobacter insulae* sp. nov., isolated from soil. *Int. J. Syst. Evol. Microbiol.* **2007**, *57*, 1999–2003. [CrossRef]
51. Rogel, M.A.; Hernandez-Lucas, I.; Kuykendall, L.D.; Balkwill, D.L.; Martinez-Romero, E. Nitrogen-fixing nodules with *Ensifer adhaerens* harboring *Rhizobium tropici* symbiotic plasmids. *Appl. Environ. Microbiol.* **2001**, *67*, 3264–3268. [CrossRef]
52. Casida, L.E. *Ensifer adhaerens* gen. nov., sp. nov.: A bacterial predator of bacteria in soil. *Int. J. Syst. Bacteriol.* **1982**, *32*, 339–345. [CrossRef]
53. Zhang, D.C.; Redzic, M.; Liu, H.C.; Zhou, Y.G.; Schinner, F.; Margesin, R. *Devosia psychrophile* sp. nov. and *Devosia glacialis* sp. nov., from alpine glacier cryoconite, and an emended description of the genus *Devosia*. *Int. J. Syst. Evol. Microbiol.* **2012**, *62*, 710–715. [CrossRef]
54. La Scola, B.; Mallet, M.N.; Grimont, P.A.D.; Raoult, D. Description of *Afipia birgiae* sp. nov. and *Afipia massiliensis* sp. nov. and recognition of *Afipia felis* genospecies A. *Int. J. Syst. Evol. Microbiol.* **2002**, *52*, 1773–1782.
55. Newton, H.J.; Ang, D.K.Y.; Van Driel, I.R.; Hartland, E. Molecular pathogenesis of infections caused by *Legionella pneumophila*. *Clin. Microbiol. Rev.* **2010**, *23*, 274–298. [CrossRef]
56. Wang, C.; Chuai, X.; Liang, M. *Legionella feeleii*: Pneumonia or Pontiac fever? Bacterial virulence traits and host immune response. *Med. Microbiol. Immunol.* **2019**, *208*, 25–32. [CrossRef]
57. Kang, Y.S.; Jung, J.; Jeon, C.O.; Park, W. *Acinetobacter oleivorans* sp. nov. is capable of adhering to and growing on diesel-oil. *J. Microbiol.* **2011**, *49*, 29–34. [CrossRef] [PubMed]
58. Im, W.T.; Jung, H.M.; Ten, L.N.; Kim, M.K.; Bora, N.; Goodfellow, M.; Lim, S.; Jung, J.; Lee, S.T. *Deinococcus aquaticus* sp. nov., isolated from fresh water, and *Deinococcus caeni* sp. nov., isolated from activated sludge. *Int. J. Syst. Evol. Microbiol.* **2008**, *58*, 2348–2353. [CrossRef] [PubMed]
59. Lee, J.C.; Jeon, C.O.; Lim, J.M.; Lee, S.M.; Lee, J.M.; Song, S.M.; Park, D.J.; Li, W.J.; Kim, C.J. *Halomonas taeanensis* sp. nov., a novel moderately halophilic bacterium isolated from a solar saltern in Korea. *Int. J. Syst. Evol. Microbiol.* **2005**, *55*, 2027–2032. [CrossRef] [PubMed]
60. Martínez-Cánovas, M.J.; Quesada, E.; Llamas, I.; Bejar, V. *Halomonas ventosae* sp. nov., a moderately halophilic, denitrifying, exopolysaccharide-producing bacterium. *Int. J. Syst. Evol. Microbiol.* **2004**, *54*, 733–737. [CrossRef] [PubMed]
61. Lincoln, S.P.; Fermor, T.R.; Tindall, B.J. *Janthinobacterium agaricidamnosum* sp. nov., a soft rot pathogen of *Agaricus bisporus*. *Int. J. Syst. Evol. Microbiol.* **1999**, *49*, 1577–1589. [CrossRef] [PubMed]
62. Herwaldt, L.A.; Gorman, G.W.; McGrath, T.; Toma, S.; Brake, B.; Hightower, A.W.; Jones, J.; Reingold, A.L.; Boxer, P.A.; Tang, P.W. A new *Legionella* species, *Legionella feeleii* species nova, causes Pontiac fever in an automobile plant. *Ann. Intern. Med.* **1984**, *100*, 333–338. [CrossRef]
63. Dennis, P.J.; Brenner, D.J.; Thacker, W.L.; Wait, R.; Vesey, G.; Steigerwalt, A.G.; Benson, R.F. Five new *Legionella* species isolated from water. *Int. J. Syst. Evol. Microbiol.* **1993**, *43*, 329–337. [CrossRef]
64. Orrison, L.H.; Cherry, W.B.; Fliermans, C.B.; Dees, S.B.; McDougal, L.K.; Dodd, D.J. Characteristics of environmental isolates of *Legionella pneumophila*. *Appl. Environ. Microbiol.* **1981**, *42*, 109–115. [CrossRef]
65. Clark, L.L.; Dajcs, J.J.; McLean, C.H.; Bartell, J.G.; Stroman, D.W. *Pseudomonas otitidis* sp. nov., isolated from patients with otic infections. *Int. J. Syst. Evol. Microbiol.* **2006**, *56*, 709–714. [CrossRef]
66. Yumoto, I.; Kusano, T.; Shingyo, T.; Nodasaka, Y.; Matsuyama, H.; Okuyama, H. Assignment of *Pseudomonas* sp. strain E-3 to *Pseudomonas psychrophila* sp. nov., a new facultatively psychrophilic bacterium. *Extremophiles* **2001**, *5*, 343–349. [CrossRef]
67. Romanenko, L.A.; Uchino, M.; Falsen, E.; Lysenko, A.M.; Zhukova, N.V.; Mikhailov, V.V. *Pseudomonas xanthomarina* sp. nov., a novel bacterium isolated from marine ascidian. *J. Gen. Appl. Microbiol.* **2005**, *51*, 65–71. [CrossRef]
68. Yandigeri, M.S.; Malviya, N.; Solanki, M.K.; Shrivastava, P.; Sivakumar, G. Chitinolytic *Streptomyces vinaceusdrappus* S5MW2 isolated from Chilika lake, India enhances plant growth and biocontrol efficacy through chitin supplementation against *Rhizoctonia solani*. *World J. Microbiol. Biotechnol.* **2015**, *31*, 1217–1225. [CrossRef]

69. Zhao, X.Q.; Li, W.J.; Jiao, W.C.; Li, Y.; Yuan, W.J.; Zhang, Y.Q.; Klenk, H.P.; Suh, J.W.; Bai, F.W. *Streptomyces xinghaiensis* sp. nov., isolated from marine sediment. *Int. J. Syst. Evol. Microbiol.* **2009**, *59*, 2870–2874. [CrossRef]
70. Sorokin, D.Y.; Kovaleva, O.L.; Tourova, T.P.; Muyzer, G. *Thiohalobacter thiocyanaticus* gen. nov., sp. nov., a moderately halophilic, sulfur-oxidizing gammaproteobacterium from hypersaline lakes, that utilizes thiocyanate. *Int. J. Syst. Evol. Microbiol.* **2010**, *60*, 444–450. [CrossRef]
71. Rutherford, D.W.; Chiou, C.T.; Eberl, D.D. Effects of exchanged cation on the microporosity of montmorillonite. *Clays Clay Miner.* **1997**, *45*, 534–543. [CrossRef]
72. Kuila, U.; Prasad, M. Specific surface area and pore-size distribution in clays and shales. *Geophys. Prospect.* **2013**, *61*, 341–362. [CrossRef]
73. Zaffar, M.; Lu, S.-G. Pore size distribution of clayey soils and its correlation with soil organic matter. *Pedosphere* **2015**, *25*, 240–249. [CrossRef]
74. Aksu, I.; Bazilevskaya, E.; Karpyn, Z.T. Swelling of clay minerals in unconsolidated porous media and its impact on permeability. *GeoResJ* **2015**, *7*, 1–13. [CrossRef]
75. Mueller, B. Experimental interactions between clay minerals and bacteria: A review. *Pedosphere* **2015**, *25*, 799–810. [CrossRef]
76. Alimova, A.; Katz, A.; Steiner, N.; Rudolph, E.; Wei, H.; Steiner, J.C.; Gottlieb, P. Bacteria-clay interaction: Structural changes in smactite induced during biofilm formation. *Clays Clay Miner.* **2009**, *57*, 205–212. [CrossRef]
77. Dexter, A.R. Heterogeneity of unsaturated, gravitational flow of water through beds of large particles. *Water Resour. Res.* **1993**, *29*, 1859–1862. [CrossRef]
78. Wildenschild, D.; Jensen, K.H.; Villholth, K.; Illangasekare, T.H. A laboratory analysis of the effect of macropores on solute transport. *Ground Water* **1994**, *32*, 381–389. [CrossRef]
79. McMurry, S.W.; Coyne, M.S.; Perfect, E. Fecal coliforms transport through intact soil blocks amended with poultry manure. *J. Environ. Qual.* **1998**, *27*, 86–92. [CrossRef]
80. Galloway, J.N.; Townsend, A.R.; Erisman, J.W.; Bekunda, M.; Cai, Z.; Freney, J.R.; Martinelli, L.A.; Seizinger, S.P.; Sutton, M.A. Transformation of the Nitrogen cycle: Recent trends, questions and potential solutions. *Science* **2008**, *320*, 889–892. [CrossRef]
81. Overeem, I.; Kettner, A.J.; Syvitski, J.P.M. 9.40 impacts of humans on river fluxes and morphology. In *Treatise on Geomorphology*; Shroder, J.F., Wohl, E., Eds.; Academic Press: Cambridge, MA, USA, 2013; pp. 828–842.
82. Sutton, M.; Howard, C.; Erisman, J.W.; Billen, G.; Bleeker, A.; Grennfelt, P.; Van Grinsven, H.; Grizzetti, B. *The European Nitrogen Assessment*; Cambridge University Press: Cambridge, UK, 2011.
83. Barakata, M.; Cheviron, B.; Angulo-Jaramillo, R. Influence of the irrigation technique and strategies on the nitrogen cycle and budget: A review. *Agric. Water Manag.* **2016**, *178*, 225–238. [CrossRef]
84. Racchetti, E.; Salmaso, F.; Pinardi, M.; Quadroni, S.; Soana, E.; Sacchi, E.; Severini, E.; Celico, F.; Viaroli, P.; Bartoli, M. Flood irrigation increases river-groundwater interactions and diffuse nitrate pollution in agricultural watersheds. *Water* **2019**, *11*, 2304. [CrossRef]
85. Van Grinsven, H.J.M.; Ward, M.H.; Benjamin, N.; De Kok, T.M. Does the evidence about health risks associated with nitrate ingestion warrant an increase of the nitrate standard for drinking water? *Environ. Health* **2006**, *5*, 26. [CrossRef]
86. Rivett, M.O.; Buss, S.R.; Morgan, P.; Smith, J.W.N.; Bemment, C.D. Nitrate attenuation in groundwater: A review of biogeochemical controlling processes. *Water Res.* **2008**, *42*, 4215–4232. [CrossRef]
87. Howarth, R.; Chan, F.; Conley, D.J.; Garnier, J.; Doney, S.C.; Marino, R.; Billen, G. Coupled biogeochemical cycles: Eutrophication and hypoxia in temperate estuaries and coastal marine ecosystems. *Front. Ecol. Environ.* **2011**, *9*, 18–26. [CrossRef]

applied sciences

MDPI

Article

Hydrogeological Behaviour and Geochemical Features of Waters in Evaporite-Bearing Low-Permeability Successions: A Case Study in Southern Sicily, Italy

Pietro Rizzo [1], Chiara Cappadonia [2,*], Edoardo Rotigliano [2], Paola Iacumin [1], Anna Maria Sanangelantoni [1], Giulia Zerbini [1] and Fulvio Celico [1]

[1] Department of Chemistry, Life Sciences and Environmental Sustainability, University of Parma, Parco Area delle Scienze 157/A, 43124 Parma, Italy; pietro.rizzo@unipr.it (P.R.); paola.iacumin@unipr.it (P.I.); annamaria.sanangelantoni@unipr.it (A.M.S.); giulia.zerbini@studenti.unipr.it (G.Z.); fulvio.celico@unipr.it (F.C.)

[2] Department of Earth and Marine Sciences, University of Palermo, Via Archirafi 22, 90123 Palermo, Italy; edoardo.rotigliano@unipa.it

* Correspondence: chiara.cappadonia@unipa.it; Tel.: +39-091-2386-4664

Received: 4 September 2020; Accepted: 17 November 2020; Published: 18 November 2020

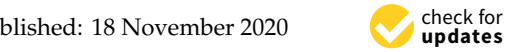

Featured Application: The research suggests an approach for refining the guidelines to be used in studying heterogeneous media and planning optimal monitoring networks and protocols for several anthropogenic purposes (e.g., environmental monitoring of landfills or contaminated sites managing).

Abstract: Knowledge about the hydrogeological behaviour of heterogeneous low-permeability media is an important tool when designing anthropogenic works (e.g., landfills) that could potentially have negative impacts on the environment and on people's health. The knowledge about the biogeochemical processes in these media could prevent "false positives" when studying groundwater quality and possible contamination caused by anthropogenic activities. In this research, we firstly refined knowledge about the groundwater flow field at a representative site where the groundwater flows within an evaporite-bearing low-permeability succession. Hydraulic measurements and tritium analyses demonstrated the coexistence of relatively brief to very prolonged groundwater pathways. The groundwater is recharged by local precipitation, as demonstrated by stable isotopes investigations. However, relatively deep groundwater is clearly linked to very high tritium content rainwater precipitated during the 1950s and 1960s. The deuterium content of some groundwater samples showed unusual values, explained by the interactions between the groundwater and certain gases (H_2S and CH_4), the presences of which are linked to sulfate-reducing bacteria and methanogenic archaea detected within the saturated medium through biomolecular investigations in the shallow organic reach clayey deposits. In a wider, methodological context, the present study demonstrates that interdisciplinary approaches provide better knowledge about the behaviour of heterogeneous low-permeability media and the meaning of each data type.

Keywords: conceptual model; evaporites; bacterial community; stable isotopes; tritium; Southern Italy

1. Introduction

The Mediterranean region was affected by a pervasive "salinity crisis" during the Messinian, when it was progressively restricted and partially isolated from the Atlantic Ocean by a combination

of tectonic and glacio-eustatic processes [1–4] that resulted in the deposition of large volumes of evaporitic sediments [5,6]. The Messinian Sicilian Basins are very important geologic systems for analysing these evaporite successions, in view of their lateral variations and subsequent deformation [7]. Their syn-tectonic evolution is in fact fundamental to reconstructing the timing and geometry of the propagating thrust belt [8,9]. In particular, progressive filling of sub-basins led to the formation of aquifer systems characterised by the coexistence of very low permeability clay successions and evaporitic lenses/horizons [10]. From a hydrochemical point of view, both low- and high-salinity groundwaters may be found associated with the mineralogical features described above.

Several hydrogeological and geochemical studies have been carried out in such settings. Some of these studies provided preliminary characterisations through the analysis of single sampling campaigns [11–13], whereas others investigated in greater detail the hydrogeological behaviour and the hydrochemical evolution over time based on more prolonged and multidisciplinary approaches [14–16]. Worldwide, a variety of conceptual models have been proposed for groundwater circulation in evaporite deposits. In some systems, the hydrogeology and hydrochemistry of the evaporitic aquifers are significantly influenced by deep ascending regional fluids [17–20]; conversely, at other sites, the hydrogeology and hydrochemistry of the studied system are influenced by the mixing of saline groundwater (flowing through evaporitic rocks) with more diluted waters flowing through nearby porous aquifers [21], with the possible influence of surface waters [22,23] or peat layers [24].

The main objective of this study was to refine knowledge about the hydrogeological behaviour of such systems. Because of the expected complexity, the study was carried out by merging hydraulic head measurements, isotopic analyses, and microbial community investigations, as to acquire a broad spectrum of complementary hydraulic and biogeochemical information.

The hydraulic head measurements were carried out to analyse the groundwater flow field from a three-dimensional perspective and investigate the existence of possible vertical flow components influencing the groundwater pathways and residence times.

The isotopic analyses were conducted to refine knowledge about the groundwater origins (stable isotopes of oxygen and deuterium) and residence times (tritium). Isotopes, together with chemical features, are among the major groundwater tracers traditionally and widely employed in hydrogeological studies (e.g., [25–29]).

The microbial community investigations were performed to analyse the isotopic signatures of the groundwater from a biogeochemical perspective, as to avoid incorrect interpretations of geochemical data. Microbial communities are influenced by the physicochemical features of the environment in which they live and are excellent investigative tools in several hydrogeological scenarios. The efficacy of using microorganisms for specific hydrogeological purposes has been verified in several settings that are partially comparable with that addressed in this study, such as karstified media (e.g., [30,31]), low-permeability media (e.g., [32,33]), and high-salinity groundwaters (e.g., [34]).

The usefulness and the efficacy of a coupled isotopic-microbiological approach has been verified in other complex hydrogeological settings (e.g., [35]), taking into consideration how microorganisms migrate in the subsurface (e.g., [36]).

Taking into consideration the key items highlighted in previous papers, this study was devoted mainly to examining in depth the role of certain hydraulic heterogeneities in influencing the groundwater flow field, as well as the role of microbial communities in influencing the isotopic signature of groundwater. Based on this goal, and according to the successful results of former studies performed at the same scale in similar setting [14–16], this first step of the research was carried out within a relatively narrow experimental site (in the order of 1 km^2). In fact, minimising the extension of the study site at this stage, allowed to minimise the distance between investigation boreholes and wells, and maximise the opportunity to understand the heterogeneity degree of the studied system from the geological, hydrogeological and biogeochemical points of view.

2. Study Area

The study area is located in south-western Sicily, between the small towns of Siculiana and Montallegro (Figure 1). It geologically corresponds (Figure 2a; [37]) to the south to southeast-vergent Sicilian Fold and Thrust Belt (FTB, [38]) bordered by the Gela thrust front and Kabilian-Calabrian thrust front. The FTB is an element of the collisional complex of Sicily, which also includes a late Pliocene-Quaternary foredeep (Gela foredeep), onlapping the frontal sector of the thrust belt in the southern part of the island, its offshore area, and the Pelagian-Iblean foreland with its African crust. In particular, the southern and central parts of the FTB (Figure 2b), are characterised by the outcropping of the most complete evaporitic succession of the "Gessoso-Solfifera" formation of the Messinian age [39].

The evaporitic deposits (Figure 3) mainly consist of limestone, gypsum, salt, and numerous intercalations of clays, marls, and carbonates. Gypsum strata are composed of various kinds of selenite (branching, banded, and massive) and detrital gypsum layers alternating with marl and carbonate. The Messinian units overlie diatomitic laminites (Tripoli formation [Fm.]: TRP) and clay deposits of late Tortonian to Early Messinian age, and the succession is overlain by Pliocene marly calcilutites (Trubi Fm.: TRB). The whole sequence [41] is locally overlain by middle–upper Pliocene marly clays (Monte Narbone Fm.: NRB). Sandy clays and arenites (Montallegro Fm.: MNT), clays breccias (BRC), and turbiditic calcarenites (Agrigento Fm.: GRG) are the more recent Pleistocene units.

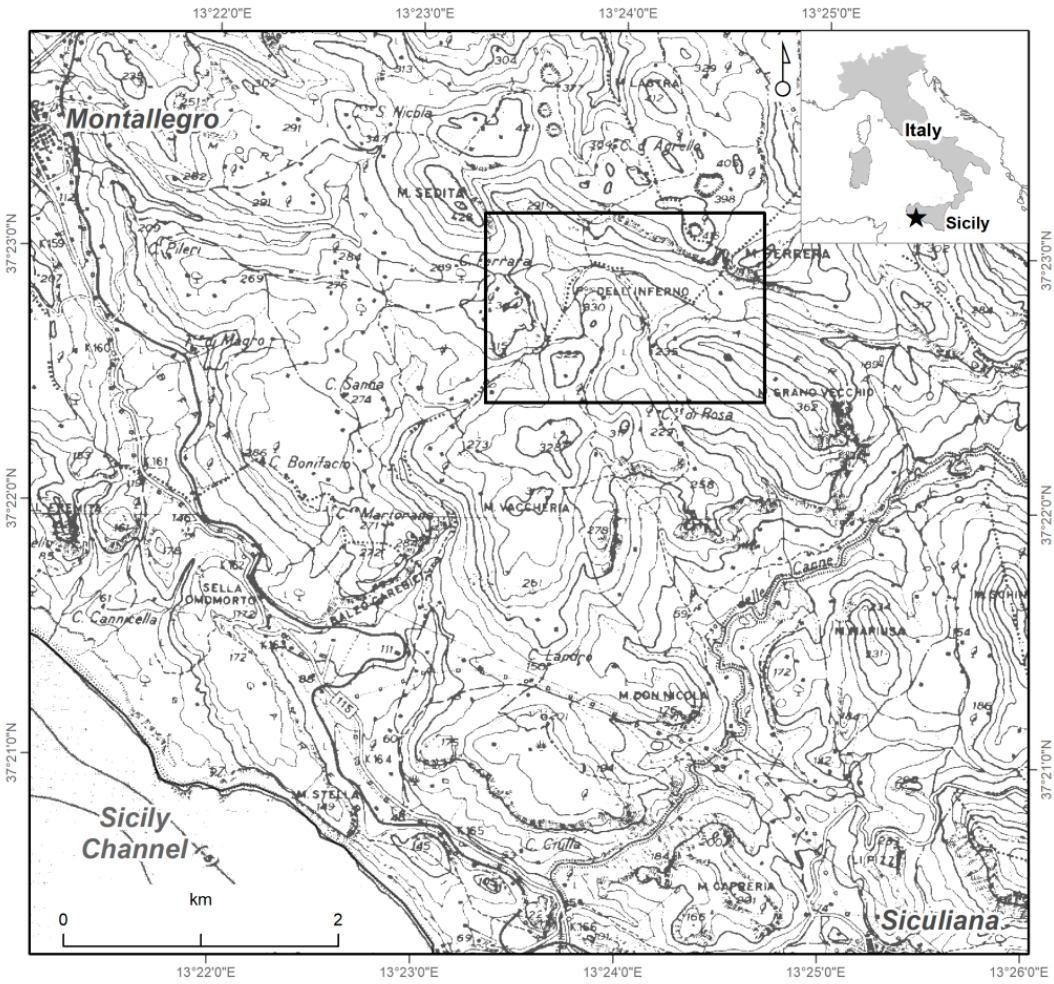

Figure 1. Geographic setting and general map of the study area.

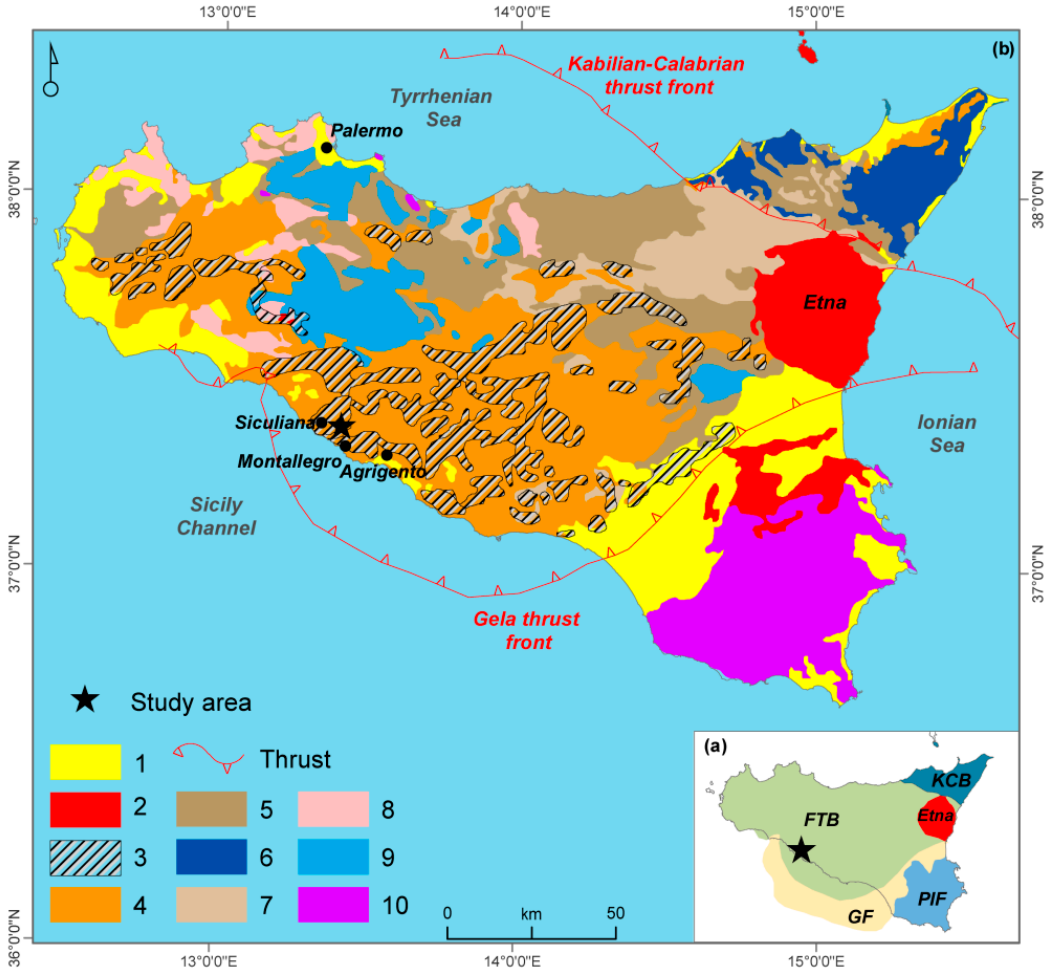

Figure 2. (**a**) Mt. Etna edifice and main elements of the collisional complex of Sicily: Kabylian-Calabrian thrust basement—KCB; fold and thrust belt—FTB; Gela foredeep—GF; Pelagian-Iblean foreland—PIF; (**b**) structural map of Sicily (modified from [40]) highlighting the spatial distribution of the evaporite outcrops in Sicily (after [39]): (1) Plio-Pleistocene cover, (2) volcanics, (3) evaporites (Messinian), (4) upper Miocene-lower Pliocene deformed foreland deposits, (5) upper Oligocene-lower Miocene deformed foreland deposits, (6) Kabilian-Calabrian crystalline units, (7) Sicilide units, (8) Meso-Cenozoic carbonate platform deformed units (Sicilian-Maghrebian shallow-water units), (9) Meso-Cenozoic slope-to-deep-basin deformed units (Sicilian-Maghrebian deep-water units), and (10) Meso-Cenozoic carbonate platform not-deformed units (Sicilian-Maghrebian foreland).

In greater detail, a first and a second sedimentary cycle [42] are distinguished in the Messinian evaporites, which are separated by an angular unconformity. The first cycle comprises [43]: carbonate deposits (Calcare di Base Fm.: BEC), massive selenite (Cattolica Fm.: CTL), and a salt unit (Clastic Ca-sulfates, Mg and K salts, and halite unit: SLT). The younger second cycle is mainly characterised by thin gypsum layers (balatino and selenite: GPQ) and marls layers (upper evaporites, Pasquasia Fm.: GPQ) levels interbedded with detrital mud, silt, sandstones, and conglomerates overlain by siliciclastic sediments (mainly silty clays; Arenazzolo Fm.: RNZ), characterised by marked organic matter levels.

The complexity of the geological setting of the area is increased to be a consequence of the Plio-Pleistocene tectonic phases that generated the fold and thrust belts and high-angle faults with subsequent lateral contacts between the Messinian gypsum units and the older clayey deposits. In addition, the wide distribution of soluble rocks in this sector of Sicily is responsible for intense karstic processes, producing a great variety of either epigeous and hypogeous landforms [41].

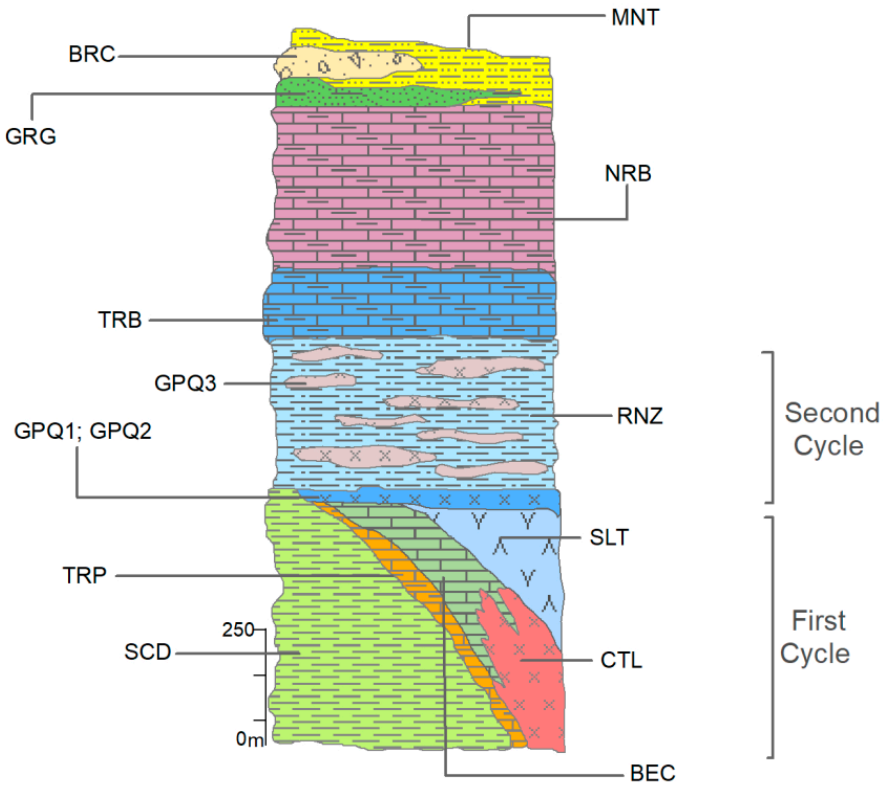

Figure 3. Schematic stratigraphic sequence of the evaporites in south-western Sicily (after [44]): clayey deposits (SCD—Tortonian-middle Serravallian); Messinian evaporites—first cycle: white diatomitic marls, Tripoli Fm. (TRP-Messinian); carbonate breccias and clastic gypsum, Calcare di Base Fm. (BEC—Messinian); massive selenite, Cattolica Fm. (CTL—Messinian); clastic Ca-sulfates, Mg- and K-salts, and halite unit, forming a salt unit (SLT—Messinian); second cycle: gypsum-arenites and limestones and carbonate arenites, Pasquasia Fm. (GPQ1; GPQ2—Messinian); gypsum (balatino and selenite) and marls, Pasquasia Fm. (GPQ3–Messinian); Siliciclastic sediments rich in organic matter, Arenazzolo Fm. (RNZ–Messinian); marly calcilutites, Trubi Fm. (TRB—Early Pliocene); marls, marly clays, sandy clays, Monte Narbone Fm. (NRB—middle–upper Pliocene); yellow sands and lagoonal sandy-clays, Montallegro Fm. (MNT—lower Pleistocene); turbiditic calcarenites, Agrigento Fm. (GRG—lower Pleistocene); clay breccias (BRC—lower Pleistocene).

From a morpho-structural standpoint, the landscape is characterised by a system of gentle anticlines and synclines extending parallel to the NW-SE trend of the FTB and large blocks of evaporitic rocks encircled by clayey deposits, with frequent relief inversion produced by differential erosion phenomena [39]. The folded relief is also intersected by perpendicular faults connecting different parts of the evaporites bodies and/or clayey deposits. The area is characterised by a series of slightly sloped fluvial terraces, frequently cut in their upper parts by long gullies and V-shaped valleys. Karst processes have affected gypsum areas, resulting in a great variety of surface landforms, such as poljes, karren, and gypsum bubbles. On the clayey slopes, morphogenetic processes produced landforms such as shallow landslides, rills, and gullies [45].

Following the above-mentioned general geological setting, in the study area, the Mio-Pliocene deposits consisting of an evaporite series and pre-evaporite strata are involved in a wide range of fold structures on a NNW-SSE axis and are capped by weakly deformed Pleistocene deposits and Quaternary terrains. The shapes of the structures are irregular fashion because of the different stratigraphic thicknesses of the evaporitic rocks, which were also controlled by active thrust and fold structures at the time of deposition [7] and by the significant competence contrasts between various formations described in Figure 3, such as coarse-grained gypsum, muds, silty clays, and silts. In general, the evaporitic deposits of the second cycle (gypsum and marls; GPQ1; GPQ2 and GPQ3) locally overlie

the massive selenites of the CTL (first cycle) and the SCD with an erosional unconformity, and are in turn overlain by the silty clays of the RNZ.

To reconstruct the local geology, the stratigraphic logs of 18 geognostic boreholes and 22 piezometers were taken into consideration, and a geological map (Figure 4) was constructed, which is marked by the outcropping of several components of the whole succession. Based on the available stratigraphic data, two interpretative profiles extending E–W and N–S were also drawn (Figure 5).

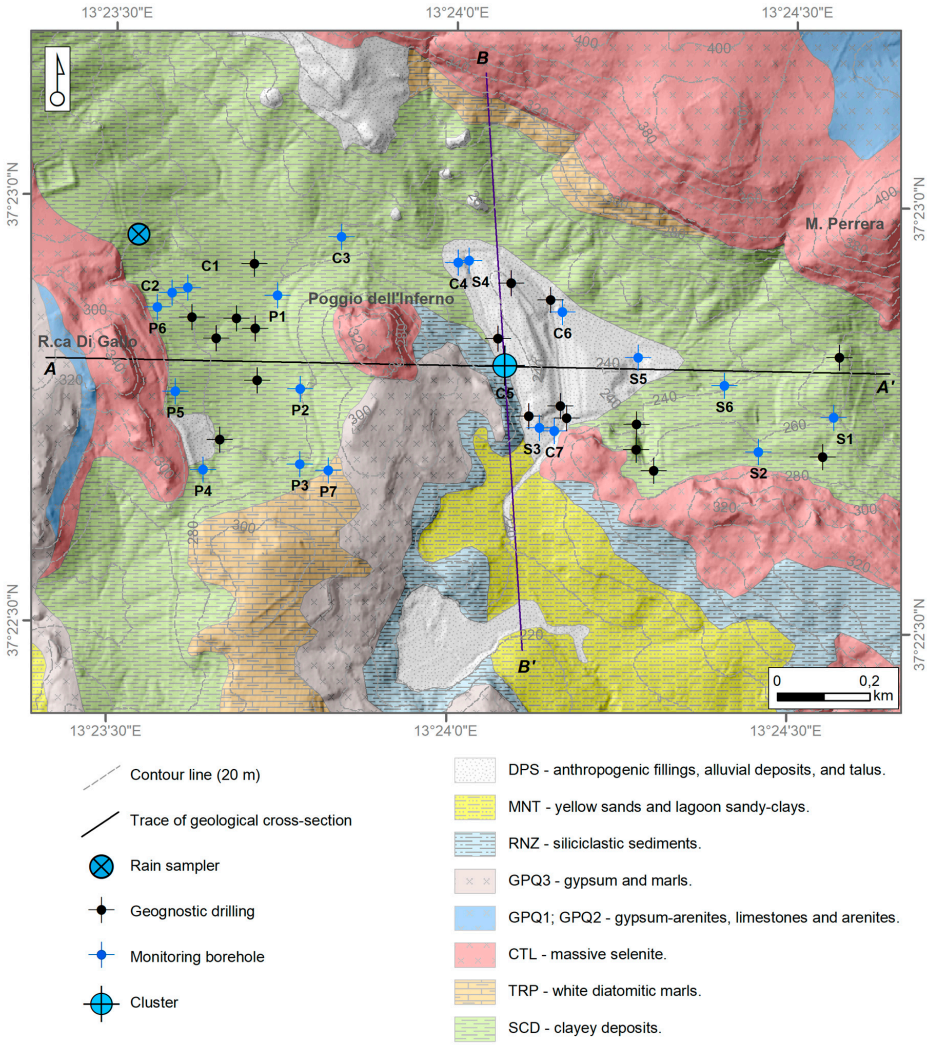

Figure 4. Geological map of the study area and location of the geognostic and monitoring boreholes.

The two profiles depict the general expected setting of the area, with a folded regular sequence marked by first cycle (CTL) gypsum layers overlaying the diatomites (TRP) levels or directly in contact on the Tortonian clayey deposits (SCD). The second cycle evaporitic layers (GPQ1, GPQ2, GPQ3, and RNZ) cover in sequence the CTL only along the north-south profile, and elsewhere directly overlie the SCD. At the base, the whole area is characterised by the continuous thick Tortonian clayey layer (SCD). In the southern flank of the anticline, a thick sandy/sandy-clayey (MNT) layer outcrops, covering the RNZ. In the central sector of the study area, along the main drainage surficial line, the evaporitic terrains are covered by a large patch of mainly alluvial quaternary deposits and characterised by high organic matter content.

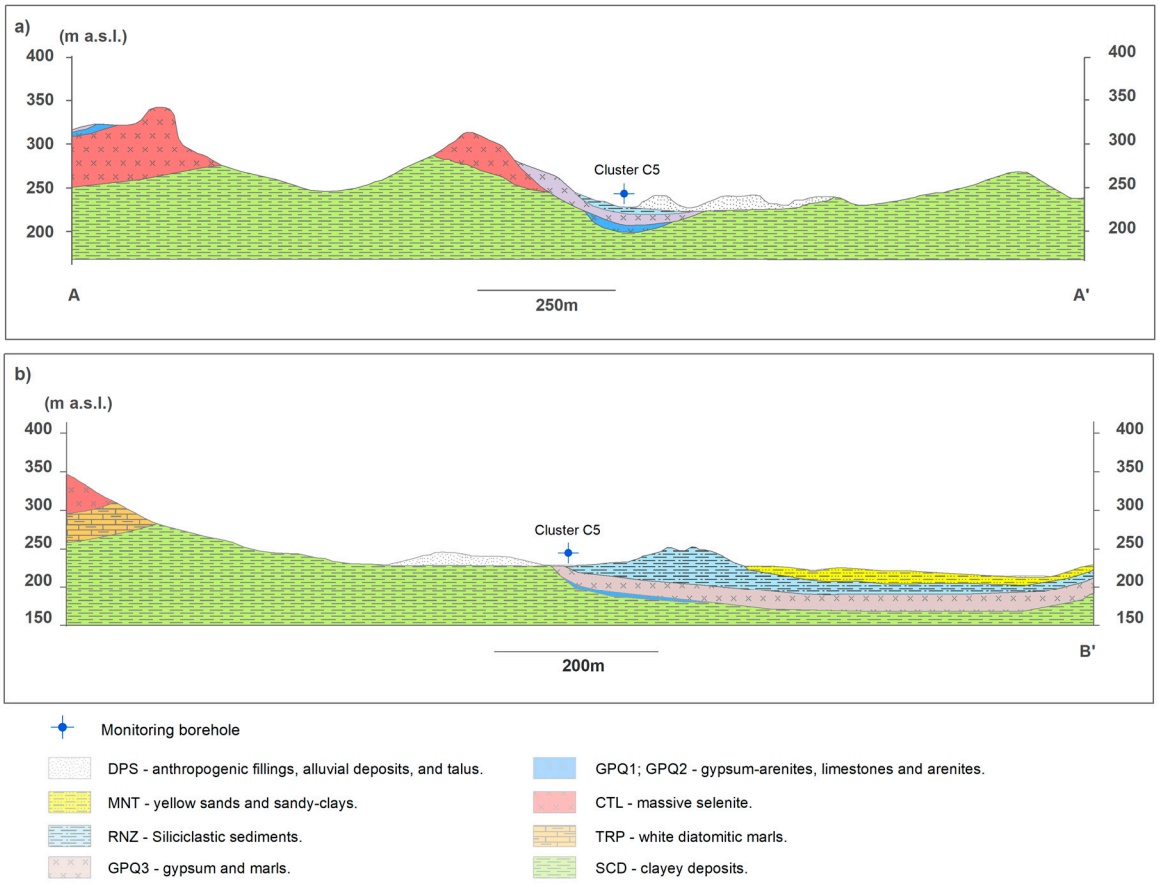

Figure 5. Geological cross-sections (see Figure 4 for traces).

3. Materials and Methods

An interdisciplinary approach was employed in order to analyse the groundwater flow field and the hydrogeological behavior of the studied system from a three-dimensional perspective. The possible influence of vertical flow on groundwater pathways and residence times was explored by merging hydrogeological and isotopic investigations. Microbial community analyses were conducted to investigate the isotopic signature of the groundwater from a biogeochemical perspective, to ensure that the results of the isotopic analyses were correctly interpreted, with emphasis on the deuterium content.

Graphic images were obtained using QGIS, Adobe Illustrator and Microsoft Excel.

3.1. Hydrogeological Investigations

From May 2011 to November 2019, the hydraulic head at the piezometers was measured on a weekly to monthly basis using a water level meter to reconstruct the groundwater flow net and its evolution over time. To specifically investigate the vertical zonation of the hydraulic head and the isotopic/microbiological features within the heterogeneous medium, one multilevel groundwater monitoring system (cluster type) was drilled in August 2019: the C5 cluster (Figure 6), which included three piezometers screened at different depths (C5a, C5b, and C5c). The C5 cluster was drilled close to a former and abandoned piezometer (30 m deep and fully screened), in which the sampled groundwater was characterised by high tritium content (36.5 tritium units [T.U.]), to also deeply investigate the origin of this apparent anomaly. The other piezometers ranged in depth between 15 and 40 m, depending on the local depth of the groundwater head.

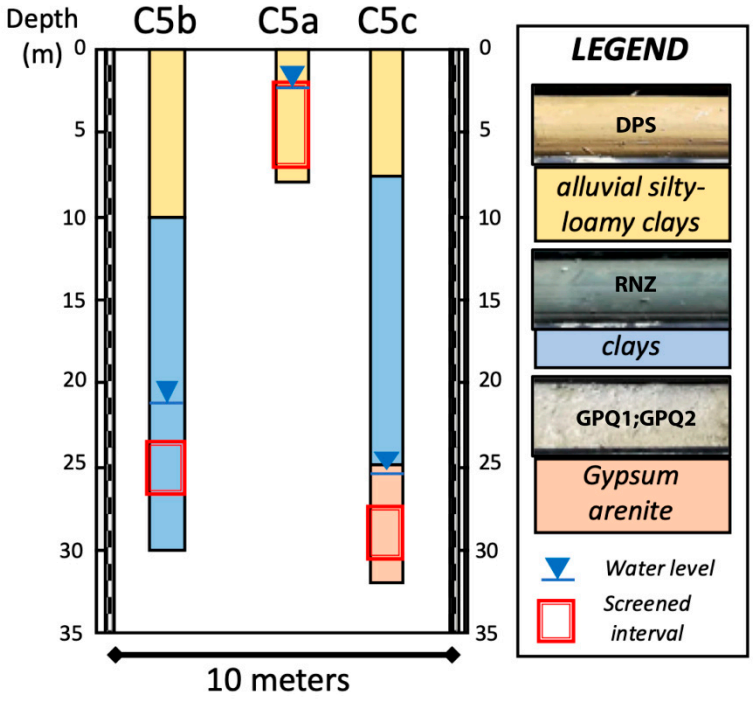

Figure 6. Cluster C5: stratigraphy, screened intervals, and water levels in December 2019. DPS-anthropogenic fillings, alluvial deposits, and talus (Quaternary); RNZ-siliciclastic sediments with high organic matter content, Arenazzolo Fm. (Messinian); GPQ1 and GPQ2-gypsum-arenites and limestones and carbonate arenites, Pasquasia Fm. (Messinian).

3.2. Isotopic Investigations

Groundwater samples for stable isotope ($\delta^{18/16}O$ and $\delta^{2/1}H$) and tritium (^3H) analyses were collected four times (January, June, September and December 2019), together with the hydraulic head measurements. During the same observation period, rainwater samples for $\delta(^{18/16}O)$, $\delta(^{2/1}H)$ and tritium analyses were collected monthly (depending on the amount of precipitation) from one rain sampler installed at the test site (Figure 4). The rainfall was collected using ten-liter polyethylene bottles containing about 300 mL of Vaseline oil to prevent evaporation. Oil contamination was carefully avoided by syringing the water samples out of the bottles. All the samples were transported to the laboratory in a refrigerated box.

Stable isotope analyses were carried out at the Isotope Geochemistry Laboratory of the University of Parma, Italy, using a water equilibrator at 18 °C equipped with a Finnigan Delta XP spectrometer. For oxygen isotope determination, 5 cm^3 of water was equilibrated with pure CO_2, whereas for hydrogen isotopes, 5 cm^3 of water was equilibrated with pure H_2 (platinum wire was used as a catalyser of gas-liquid water equilibration). The isotope ratio is expressed as:

$$^{A/B}\delta_{i/RF} = \frac{^{A/B}R_i}{^{A/B}R_{RF}} - 1 = \left[\left(\frac{^{A/B}R_i}{^{A/B}R_{RF}} - 1\right)10^3\right]‰ \quad (1)$$

where A is ^{18}O or ^2H, B is ^{16}O or ^1H, R is the ratio of the isotopic abundances, i the sample of interest, ‰ = 10^{-3}, and RF is the primary international standard of reference (in our case VSMOW-SLAP). The analyses of ^3H were carried out at the Isotope Geochemistry Laboratory of the University of Trieste, Italy. Following other authors (e.g., [46]), the samples followed the procedure of the preventive electrolytic enrichment of tritium was applied to the samples to decrease measurement errors. In this process, the 250 g of the water sample was expected to be reduced to 20 g by electrolysis.

The analyses for the determination of the tritium activity were carried out according to the procedures provided by the International Atomic Energy Agency [47].

The analytical prediction uncertainty was ±0.1‰ for $\delta^{18}O$, ±1‰ for $\delta^{2}H$, and ±0.5 T.U. for ^{3}H.

3.3. Microbiological Analyses: 16S Ribosomal RNA Gene Next Generation Sequencing (NGS)

The microbiological survey was carried out in December 2019 on samples from the multilevel piezometers C5a-c to refine knowledge about the bacterial community in the groundwater. This survey was limited to cluster C5 because it was carried out to investigate the possible influence of microbial activity on some isotopic features, with emphasis on deuterium content in the C5 groundwater.

Water samples (1 L) were filtered through sterile mixed esters of cellulose filters (S-Pak™ membrane filters, 47 mm diameter, 0.22 µm pore size, Millipore Corporation, Billerica, MA, USA) within 24 h after collection. Bacterial DNA extraction from the sample filters was performed using the commercial kit FastDNA SPIN Kit for soil and the FastPrep®Instrument. Once the DNA extraction was complete, the quantity and integrity of the DNA were evaluated by electrophoresis in 0.8% agarose gel, containing 1 µg/mL of Gel-Red™, in the running buffer TAE 1X (40 mM tris base, 20 mM acetic acid, and 1 mM EDTA pH 8), and amplification reactions were performed by polymerase chain reaction (PCR). The 16S rDNA profiles of the bacterial communities in the samples were obtained by NGS technologies at the Genprobio Srl Laboratory (Parma, Italy). Partial 16S rRNA gene sequences were obtained from the extracted DNA by PCR, using the primer pair Probio_Uni and/Probio_Rev, which targets the V3 region of the bacterial 16S rRNA gene sequence [48], and the primer pair ArchV46 for archaeal 16S rRNA [49]. Amplifications were carried out using a Verity Thermocycler (Applied Biosystems Foster City, CA, USA), and PCR products were purified by the magnetic purification using Agencourt AMPure XP DNA Purification Beads (Beckman Coulter Genomics GmbH, Bernried, Germany) to remove primer dimers. Amplicon checks were carried out as previously described [48]. Sequencing was performed using an Illumina MiSeq sequencer with MiSeq Reagent Kit v3 chemicals. The fastq files were processed using a custom script based on the QIIME software suite [50]. Quality control retained sequences with lengths between 140 and 400 bp and mean sequence quality scores >20, whereas sequences with homopolymers >7 bp and mismatched primers were omitted. To calculate downstream diversity measures, operational taxonomic units (OTUs) were defined at 100% sequence homology using DADA2 [51]; OTUs not encompassing at least two sequences of the same sample were removed. All reads were classified to the lowest possible taxonomic rank using QIIME2 [50,52] and a reference dataset from the SILVA database v132 [53]

4. Results and Discussion

4.1. Hydrogeological Features

The hydraulic head fluctuated over the year from tens of centimeters to several meters, depending on the area. A recession period was typically observed from late spring to early autumn, whereas recharge was typically observed from early autumn to spring (Figure 7). Overall, the head measurements suggested relatively slow recharge, according to the low bulk permeability of the studied system, which does not favor rapid percolation of fresh-infiltration waters within the unsaturated zone and corresponding short-term fluctuations of the groundwater surface. The low bulk permeability of the studied medium is in agreement with the findings of other authors who performed pumping tests in similar Messinian successions in Southern Italy (transmissivity on the order of 10^{-5} m^2/s; [14,16]).

Based on the hydrogeological monitoring and survey results, the general groundwater flow scheme in the area was reconstructed (Figure 8a). The groundwater flows from the highlands towards the topographic depressions, with the hydraulic gradient ranging from ~30% to ~3%, respectively. The lowest head was consistently measured within the eastern depression, in the area of piezometers S3–S5, and no significant modifications of the groundwater flow net were observed over time, during the observation period. Therefore, all the piezometers used to analyse the isotopic signature from a hydrogeological perspective maintained the same hydraulic relationships throughout the year.

This finding implies that all the results discussed in the isotopic section were not influenced at all by modifications of the groundwater flow field.

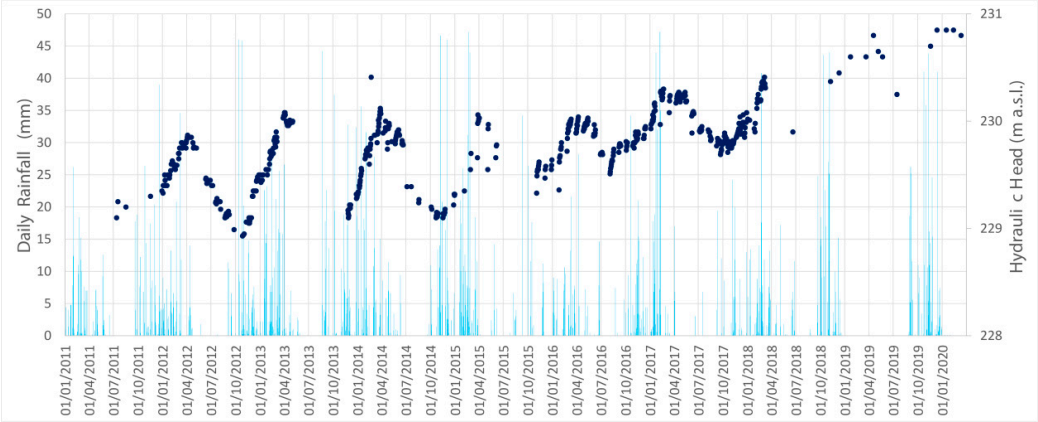

Figure 7. Hydraulic head variations in piezometer S4 (blue dots) vs. daily rainfall (light blue bars). Dates are given in day/month/year format.

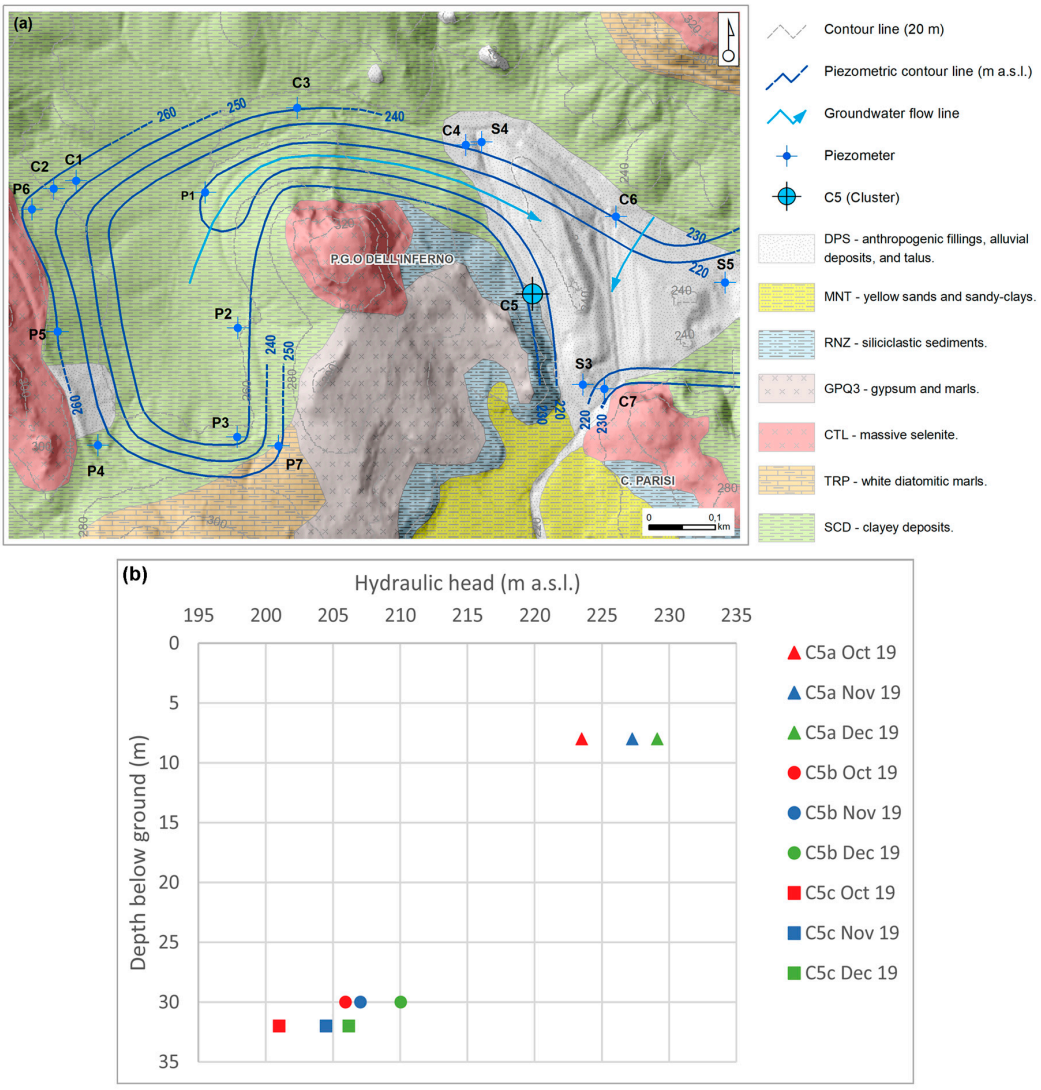

Figure 8. (**a**) Hydrogeological map of the study area (December 2019); (**b**) relationship between the hydraulic head and the depth below ground observed at the C5 cluster.

In light of the sedimentological features and common lateral inhomogeneity of the evaporitic layers (Figure 3), simple expected hydrogeological and hydrochemical behaviors are difficult to define for the sequence that outcrops at the key site of the C5 cluster. In fact, the RNZ layer, which overlies the second cycle gypsum evaporitic bodies, is composed of a very chaotic sandy-clayey deposits, including dispersed gypsum blocks; consequently, a moderate primary permeability is expected, despite the high clay content. In addition, the first cycle evaporitic layers and the basal Tortonian clays are expected to be characterised by high and low permeability, respectively, whereas the role of the second cycle gypsum bodies, which are to be classified as permeable on a small scale, could be strongly controlled, overall, by the lack of lateral continuity, resulting in very slow hydraulic circuits.

As observed at the C5 cluster, the hydraulic head significantly varied with depth (Figure 8b). In greater detail, it progressively decreased with increasing depth, showing the highest head in the shallow system and the lowest one into the piezometer C5c, screened within a gypsum horizon. The head zonation was confirmed based on the seasonal groundwater oscillation, with coherent hydraulic heads shifts, consistent with the fact that the analysed medium behaves as a continuum at the observation scale of the present study. This finding is also in agreement with the expectation for saturated heterogeneous media comparable with the studied media. In these media, if a lower geological formation has a higher hydraulic conductivity than the overlying layer, it acts as the major conduit of flow [54]. The highest head in C5a was compatible with the phreatic surface reconstructed within the whole studied area, the morphology of which reflects the local topography (Figure 8a), as expected in such low-permeability systems.

4.2. Hydrogen and Oxygen Isotopes

Waters from all the piezometers P, S, and C shown in Figure 8a were sampled for $\delta^{18/16}O$ and $\delta^{2/1}H$ measurements. The values of the analysed samples ranged from −37.0‰ to 2.2‰ for hydrogen and from −6.8‰ to −0.2‰ for oxygen. Three different main groups could be identified: Group A (P1, P2, P3 and S6) exhibited the highest $\delta^{2/1}H$ and $\delta^{18/16}O$ values in the intervals from −5.2‰ to 2.2‰ and from −1.1‰ to −0.2‰, respectively; Group B (wells P4, P5, P7, S1, S2, S3, and S5) had intermediate values in the ranges from −16.0‰ to −10.6‰ for $\delta^{2/1}H$, and from −3.4‰ to −2.4‰ for $\delta^{18/16}O$; Group C (wells P6, S4, C1, C3, and C4) included the lowest $\delta^{2/1}H$ and $\delta^{18/16}O$ values, from −26.3‰ to −20.5‰ and from −5.5‰ to −4.2‰, respectively (Figure 9). For all the piezometers, the isotopic values did not change in the different sampling periods, with the exception of C2, C6 and C7, which showed swings across groups B and C (C2: $\delta^{2/1}H$ = −22.9‰ to −8.4‰ and $\delta^{18/16}O$ = −4.6‰ to −2.0‰; C6: $\delta^{2/1}H$ = −25.0‰ to −9.8‰ and $\delta^{18/16}O$ = −5.1‰ to −2.3‰; C7: $\delta^{2/1}H$ = −37.0‰ to −24.1‰ and $\delta^{18/16}O$ = −6.8‰ to −5.0‰). The groundwater samples collected in the C5 cluster exhibited a very unusual distribution. In the $\delta^{2/1}H$ vs. $\delta^{18/16}O$ diagram shown in Figure 9, their $\delta^{2/1}H$ values are distributed vertically ranging from about −23.5 to −8.5‰ (see below for more details).

Regarding the affinity of the sampled groundwaters, all groups plotted along the local meteoric water lines available in the scientific literature [55–62], being consistent with those of rainwater collected in the study area during the observation period; this finding suggests a meteoric origin for the analysed waters (Figure 9), with no influence of ascending fluids coming from deep reservoirs, the isotopic signature of which are notably different from those of actual precipitations [35].

The $\delta^{2/1}H$ and $\delta^{18/16}O$ values are correlated with the depth of the phreatic surface (Figure 10). The piezometers showing the deepest phreatic surface (>25 m below ground, m b.g.) belong to Group A; Group B includes phreatic surface at 23.5 to 17 m b.g.; Group C may be divided into two different sub-groups: one with a depth lower than 6 m b.g., and another one with a level ranging from 14.5 to 17 m b.g. Wells C5b and C5c are excluded because their water levels are representative of the hydraulic head measured at different depths below ground and is not referable to the local phreatic surface (coinciding with the water level measured in C5a).

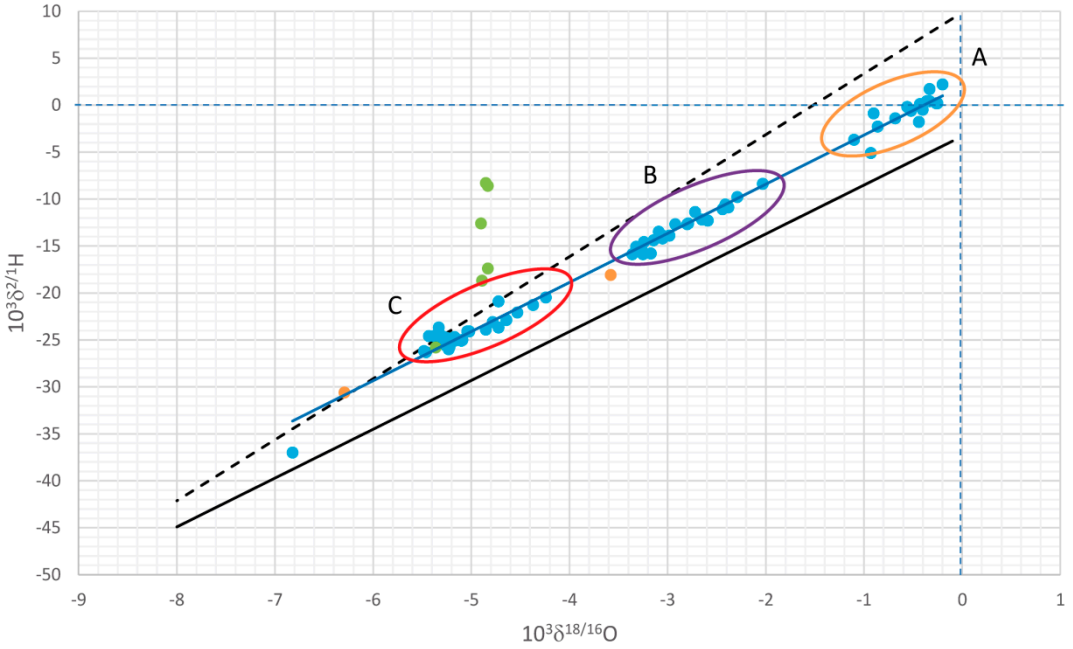

Figure 9. Relations between 10^3 $\delta^{2/1}$H and 10^3 $\delta^{18/16}$O for the investigated waters (blue dots). Groups A, B, and C are encircled in ochre, purple, and red, respectively. The green dots represent C5a-c waters. The orange dots indicate the rainwater samples analysed during this study. The solid black and the dashed black lines are representative of the meteoric water lines available in Sicily (with emphasis on [62] and [56], respectively). The blue line is the linear interpolation of the groundwater isotopic data.

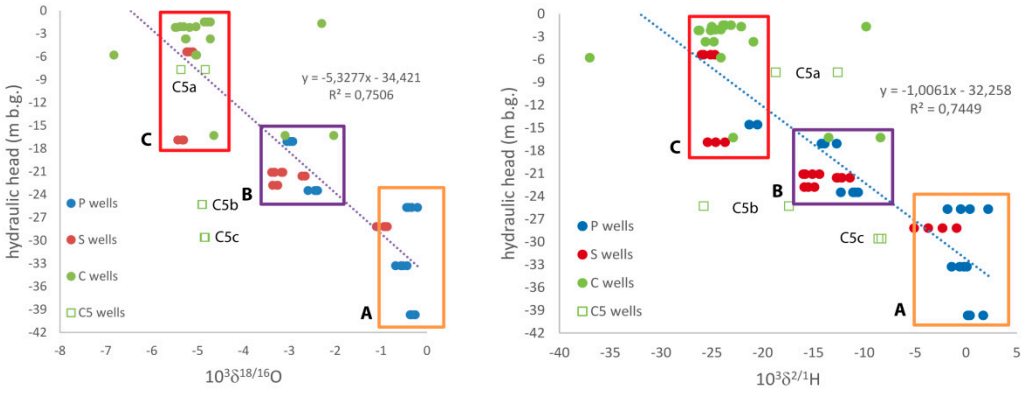

Figure 10. Relations between the hydraulic head and 10^3 $\delta^{2/1}$H and 10^3 $\delta^{18/16}$O for the investigated waters. Waters from the C5 cluster are not considered in the regressions.

Regarding tritium, the rainwater samples had high ^{3}H contents (6.2 to 10.8 T.U.), whereas the groundwater samples showed a wide range of tritium contents (Figure 11). Taking into consideration the tritium content detected in local rainwater during the observation period, as well as data already available for Southern Italy (e.g., 4.5 T.U. in [63]; 5.0 T.U. in [16]), three groundwater types have been detected at the study site: (i) groundwater related to rapid and/or short pathways within the aquifer system (4 to 10 T.U.), (ii) groundwater related to longer and/or prolonged pathways, with higher mean-residence times (<4 T.U.), (iii) groundwater related to very prolonged pathways (>10 T.U., corresponding to at least 300 T.U. at the beginning of 1960s), the recharge of which, according to findings in other sites in Italy [64], is linked mainly to rainwater precipitated during the 1950s and 1960s, when tritium was spiked in the atmosphere by nuclear weapons testing [65], reaching up to several thousand T.U. in rainwater (e.g., [66]).

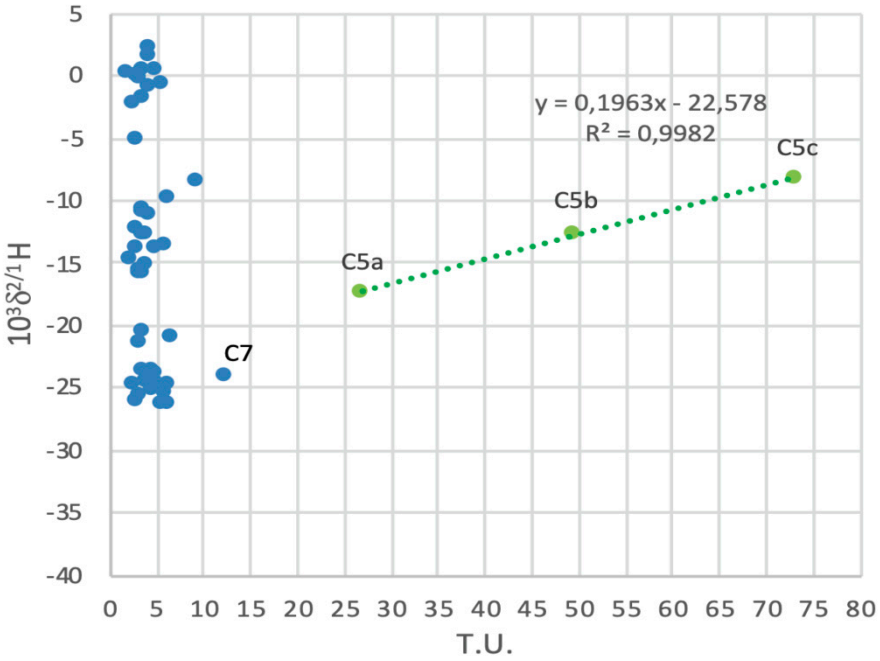

Figure 11. Relation between 10^3 $\delta^{2/1}$H and T.U. in the investigated waters. Waters from the C5 wells exhibit a significant 10^3 $\delta^{2/1}$H vs. T.U. correlation.

Figure 11 reports the relation between 10^3 $\delta^{2/1}$H and T.U. The evident and strongly significant correlation (R^2 = 0.998, and null hypothesis $H_{o(slope=0)}$ < 0.001) for the data of the C5 cluster is an intriguing problem. Different explanations for this interesting correlation are proposed below.

4.3. Next-Generation Sequencing Results

The microbial community of groundwater sampled in the C5 cluster was analysed to explore the possible influence of microbial activity (H_2S and CH_4 production) on the unusual deuterium content detected in C5-waters. The 16S rRNA gene sequences of both bacteria and archaea identified in this study have been deposited in the National Center for Biotechnology Information (NCBI) Sequence Read Archive under the accession number PRJNA631131. Based on analysis of the sequences obtained from the C5 cluster with NGS technologies, the broad diversity of the microbial community in terms of relative abundance of bacterial genera has been highlighted (Table 1).

Regarding the main aim of the present study, the analyses showed a bacterial community characterised by aerobic and anaerobic/facultative anaerobic genera. Many of these genera are common in bacterial communities found in salty groundwater and marine environments. Halophilic bacteria can be considered moderate halophiles or extreme halophiles based on the concentration of salts present in water and soils (e.g., *Alcanivorax* [67] and *Marinomonas* [68] in Table 2); in contrast, halotolerant bacteria, despite growing better without NaCl, can tolerate high quantities of salt [69] (e.g., *Arcobacter* [70] and *Pseudomonas* [71] in Table 2). In addition, some of the bacterial genera can exploit sulfate reduction (*Desulfatiglans* [72], *Desulfovibrio* [73], and *Shewanella* [74] in Table 2) as a metabolic pathway. Sulfate reduction is a form of anaerobic respiration, typical of sulfate-reducing bacteria (SRB) or sulfur-reducing bacteria, and as such typically occurs in anoxic environments and leads to the production of hydrogen sulfide (H_2S); however, some studies have found that this process can also occur in the presence of oxygen [71,75].

Table 1. Bacterial genera detected in groundwater samples collected in C5a-c (relative abundance >0.7%).

Taxonomy	C5a	C5b	C5c
Aeromonas	2.13%	0.14%	0.07%
Alcanivorax	0.72%	0.95%	0.46%
Arcobacter	1.67%	0.13%	1.12%
Candidatus Nitrotoga	0.00%	0.74%	0.33%
Idiomarina	0.20%	0.08%	0.84%
Limnobacter	1.57%	0.00%	2.18%
Magnetospira	0.18%	0.73%	0.31%
Marinobacter	0.11%	0.36%	0.98%
Marinobacterium	0.05%	0.00%	1.29%
Marinomonas	1.23%	0.00%	0.30%
Nitrosomonas	0.00%	3.43%	0.64%
Nitrospina	0.06%	1.91%	0.36%
Oceanobacter	0.12%	3.82%	0.46%
Parvibaculum	0.28%	0.42%	1.19%
Pseudohongiella	0.85%	2.72%	0.85%
Pseudomonas	58.95%	52.18%	47.22%
Rehaibacterium	0.17%	7.38%	2.29%
Rheinheimera	2.50%	0.00%	0.55%
Roseovarius	0.04%	0.78%	0.30%
Shewanella	7.39%	0.07%	0.72%
Sphingobium	1.60%	0.00%	1.06%
Sphingomonas	0.92%	0.11%	0.44%
Thiobacillus	0.00%	0.19%	1.34%
Vibrio	0.00%	0.03%	5.77%

Table 2. Metabolic characteristics of selected bacterial genera detected in groundwater samples collected in C5a–c.

Taxonomy	Aerobic	Facultative Aerobic	Anaerobic	Facultative Anaerobic	Halophilic/ Halotolerant	Sulfate Reduction
Alcanivorax	+				+	
Arcobacter		+	+		+	
Desulfatiglans		+	+		+	+
Desulfovibrio		+	+		+	+
Marinobacter		+			+	
Marinomonas	+				+	
Oceanobacter	+				+	
Pseudomonas	+	+			+	
Shewanella	+			+	+	+
Vibrio	+			+	+	

Regarding the archaeal component, the most abundant genus found in the analysed groundwater samples (C5a-c) was *Candidatus Nitrosopumilus* [76] (Table 3). This genus is typically found in marine environments where ammonia can be oxidised to nitrite. Moreover, halophilic genera were identified, such as *Halococcus* [77] (Table 3), a genus capable of living in the presence of very high concentrations of NaCl (up to 4.5 M NaCl). Methanogenic genera, such as *Methanobacterium* [78], *Methanimicrococcus* [79], and *Methanolobus* [80] were also found (Table 3). Methanogenesis is a strictly anaerobic metabolic pathway that leads to the formation of methane, and s performed only by methanogenic archaea.

Thus, the biomolecular investigations demonstrated that C5-groundwaters are characterised by bacterial (*Desulfatiglans*, *Desulfovibrio*, and *Shewanella*) and archaeal (*Methanobacterium*, *Methanimicrococcus*, and *Methanolobus*) genera able to produce H_2S and CH_4, respectively, therefore suggesting that microbial activity is a factor of utmost importance to be taken into consideration when analysing the isotopic signature of local groundwater.

Table 3. Metabolic characteristics of selected archaeal genera detected in groundwater samples collected in C5a-c.

Taxonomy	Aerobic	Anaerobic	Halophilic/ Halotolerant	Methanogenesis	Sulfate Reduction	Ammonia Oxidizing
Candidatus Nitrocosmicus	+		+			+
Candidatus Nitrosoarchaeum	+		+			+
Candidatus Nitrosopumilus	+		+			+
Halococcus	+		+			
Halogranum	+		+		+	
Methanimicrococcus		+	+	+		
Methanobacterium		+	+	+		
Methanolobus		+	+	+		
Methanothermobacter		+	+	+	+	

5. Hydrogeological Model

Geological, hydrogeological, isotopic and biomolecular investigations allowed characterisation of the hydrogeological functioning of the studied heterogeneous low-permeability system, as well as refinement of knowledge about the residence time of groundwater within such systems.

As expected, taking into consideration previous studies in similar geologic settings [16], the studied system is characterised by vertical and discontinuous heterogeneity [81], caused by various factors such as (i) the coexistence of different geological formations, (ii) their folded regular sequence, and (iii) the fractured (karstified) evaporitic intrastrata/lenses that locally increase the bulk permeability of the low-permeability system. In contrast with other heterogeneous systems, no fault zones influence fluid flow, neither enhancing [82–84] nor partially or totally impeding it [85–87].

When the hydrogeological system is analysed at the basin scale, the whole system can be depicted as a continuous medium, and the groundwater flow net is a smoothed replica of the local topography. Groundwater flow clearly occurs from the highlands towards the topographic depressions.

The vertical heterogeneity of the system causes the hydraulic head to significantly vary with depth. Close to the C5a-c cluster, the hydraulic head decreases with increasing depth, with the lowest head into the karstified gypsum layer (C5c). This head distribution agrees with that observed by Petrella et al. [16] within the peninsular Southern Italy, where the more transmissive and discontinuous localised media drain the surrounding lower permeability rocks up-gradient (lower hydraulic head), whereas they are characterised by higher head down-gradient and feed the surrounding lower permeability media (Figure 12). Because the vertical heterogeneity is discontinuous, it is unable to provide a continuous solution within the stratigraphic sequence over an extended area. Therefore, in contrast with other systems characterised by vertical heterogeneity, from the hydraulic point of view [64,88–90], no perched aquifers overlie deeper ones, and a unique saturated zone can be assumed.

Overall, the heterogeneous distribution of lower- and higher-permeability rocks within the studied system, as well as the groundwater flow field described above (Figure 12), cause the mean residence time of groundwater to not necessarily be in agreement with the only groundwater flow net depicted in Figure 8. The coexistence of slower and faster flow velocities and the existence of vertical flow, cause a sort of patchwork distribution of tritium content, with higher levels detected at depths extending into evaporitic interstrata/lenses, linked mainly to rainwater precipitated during the 1950s and 1960s, when tritium was spiked in the atmosphere by nuclear weapons testing.

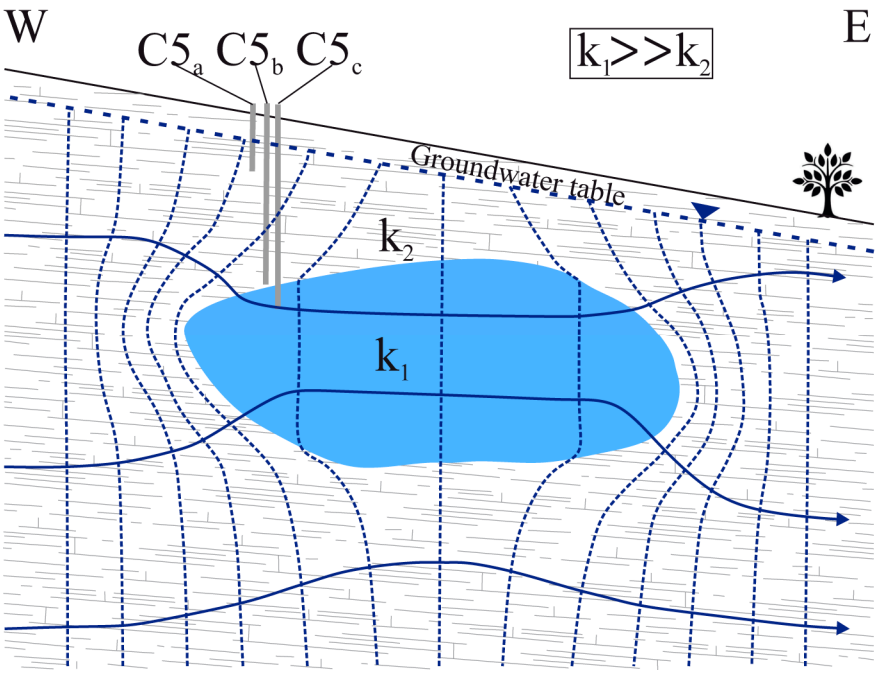

Figure 12. Conceptual hydrogeological sketch of heterogeneous media characterised by evaporite-bearing successions. The blue lens is a discontinuous evaporitic layer immersed in a clay sequence (grey). Blue dashed lines are the equipotential lines. Blue arrows are the groundwater flow lines. The C5a-c cluster is also shown. The symbols K1 and K2 are the hydraulic conductivities of the evaporitic lens and clay sequence, respectively.

The stable isotopes confirmed the local origin of the groundwater. However, as indicated above, the isotopic features of the samples coming from C5a-c cluster are unusual for groundwaters, and may be due to the phenomena discussed hereafter. Based on data reported by [91] for partitioning between liquid and gaseous water and by Galley et al. [92] for gaseous water and H_2S gas, the following approximate value for the fractionation factor of H_2O liquid vs. H_2S gas at 21 °C is obtained:

$$^{2/1}\alpha_{H_2O-\,H_2S} = \frac{^{2/1}\delta_{H_2O+1}}{^{2/1}\delta_{H_2S+1}} = 2.587 \text{ at } 21\,^{\circ}C \quad (2)$$

However, based on the data reported by Horibe and Craig [93], for H_2O liquid vs. CH_4 gas, the value:

$$^{2/1}\alpha_{H_2O-\,CH_4} = \frac{^{2/1}\delta_{H_2O+1}}{^{2/1}\delta_{CH_4S+1}} = 1.283 \text{ at } 21\,^{\circ}C \quad (3)$$

Thus, liquid water is strongly enriched in heavy isotopes with respect to H_2S and CH_4. Based on the presence of sulfate-reducing bacteria and methanogenic archaea in the analysed C5-waters, we suggest two possible explanations for the high hydrogen isotope values: (1) interaction of water with gaseous H_2S and/or CH_4 coming from the surrounding environment, and (2) generation of H_2S and CH_4 by reduction of oxidised sulfur and carbon species involving the H component of the water (Equations (4) and (5)) [94,95]:

$$SO_4^{2-} + 2CH_2O \rightarrow HS^- + 2HCO_3^- + H^{\mp} \quad (4)$$

$$4H_2 + HCO_3^- + H^+ \rightarrow CH_4 + 3H_2O \quad (5)$$

Here, we consider the case of continuous seepage of H_2S gas and/or CH_4 gas through groundwater with the exchange of hydrogen isotopes between the gases and water. At the highest $\delta^{2/1}H = -8.3‰$ (C5c), using Equations (2) and (3), we obtain:

$$^{2/1}\delta_{H_2S} = \frac{1}{^{2/1}\alpha_{H_2O-\ H_2S}}\left(^{2/1}\delta_{H_2O} + 1\right) - 1 = \frac{1}{2.587}\left(-0.0085 + 1\right) - 1 = -617‰$$

and

$$^{2/1}\delta_{CH_4} = \frac{1}{^{2/1}\alpha_{H_2O-\ CH_4}}\left(^{2/1}\delta_{H_2O} + 1\right) - 1 = \frac{1}{1.283}\left(-0.0085 + 1\right) - 1 = -227‰.$$

At least for CH_4, the $^{2/1}\delta$ values are, for example, in the range of the values characterising the gases related to oil fields worldwide [96].

Next, we consider a closed system under strongly reducing conditions in which H_2S and/or CH_4 are produced by reduction at the expense of S of sulfate and/or of C of carbonate species in solution and of H of the water molecules (d n_{H_2S} = −d n_{H_2O}). How much H_2S and/or CH_4 are generated to produce the hydrogen isotope variation observed in the investigated groundwater (i.e., $^{2/1}\delta_{H_{tot}}$ from −23.5‰ to −8.3‰)? We consider $^{2/1}\delta$ in the water at the beginning of reduction (in our case, $^{2/1}\delta_{H_{tot}} = {}^{2/1}\delta_{H_2O,o}$ = −23.5 ‰, where the subscript, *o*, indicates the initial condition) and at a defined stage of reduction ($^{2/1}\delta_{H_2O}$ = −8.3‰) as well as the value of $^{2/1}\alpha_{H_2O-\ H_2S}$ (liquid water and gaseous hydrogen sulfide). The following equation is easily derived from the isotope balance.

$$n_{H_{(tot)}}\ ^{2/1}\delta_{Htot} \cong n_{H(H_2O)}\ ^{2/1}\delta_{H_2O} + n_{H(H_2S)}\ ^{2/1}\delta_{H_2S}:$$

$$\frac{n_{H(H_2S)}}{n_{Htot}} = \frac{n_{H_2S}}{n_{H_2O,o}} = \frac{\left(^{2/1}\delta_{Htot} - {}^{2/1}\delta_{H_2O}\right)}{\left(\frac{^{2/1}\delta_{H_2O}+1}{^{2/1}\alpha_{H_2Olq\ -\ H_2Sgas}} - 1 - {}^{2/1}\delta_{H_2O}\right)}\ \frac{(-0.0235 + 0.0085)}{\left(\frac{-0.0085+1}{2.587} - 1 + 0.0085\right)} = 0.024,$$

where $n_{H(H_2S)}$ and n_{Htot} indicate the number of moles of H in H_2S and the total number of moles of H in H_2O at the beginning of the process, respectively. This equation may be used to estimate the molar ratio $n_{H_2S}/n_{H_2O,o}$ when is $^{2/1}\delta_{H_2O}$ = −8.5‰. For $n_{H_2O,o}$ = 100, we obtain n_{H_2S} = 100 ∗ 0.024 = 2.4 (moles). Although this calculation is only a rough approximation, it indicates that the formation of a few moles of H_2S is sufficient to greatly increase the delta values of hydrogen of the groundwater.

Similarly, we write:

$$\frac{n_{H(CH_4)}}{n_{Htot}} = \frac{2\ n_{CH4}}{n_{H2O,o}} = \frac{\left(^{2/1}\delta_{Htot} - {}^{2/1}\delta_{H_2O}\right)}{\left(\frac{^{2/1}\delta_{H_2O}+1}{^{2/1}\alpha_{H_2O-\ CH_4}} - 1 - {}^{2/1}\delta_{H_2O}\right)}\ \frac{(-0.0235 + 0.0085)}{\left(\frac{-0.0085+1}{1.283} - 1 + 0.0085\right)} = 0.064$$

In this case, for $n_{H2O,o}$ = 100, we obtain n_{CH4} = 0.5 ∗ 100 ∗ 0.0636 = 3.2 (moles). Thus, a few moles per cent of CH_4 formed is sufficient to greatly increase the hydrogen delta values of the groundwater.

It is noteworthy that whereas CH_4 gas is only slightly soluble, H_2S gas is strongly soluble in water. The weight ratio total S(II-) as H_2S to total C(IV-) as CH_4 is about 122 ± 3 in pure water at the temperature of 21 °C for partial pressure of these gases ranging from 10^{-4} to 3 atm, according to the PHREEQC speciation program [97]; moreover, salinity does not greatly change this result. Already at about 3–4 mg/L of total H_2S, the waters typically smell; thus, the absence of a bad smell would indicate that H_2S is absent or present in only a small amount that supports a prevalent long-term role of methane seepage or the relevant role of methane generation.

As described in a previous paragraph, there is an evident correlation between $\delta^{2/1}$H and T.U. Two different explanations can be proposed for this behavior:

(1) The chemical component carrying ^{3}H may also be the cause of increasing $\delta^{2/1}$H. This carrier could be methane formed by degradation of organic matter in an environment where tritium may reach high values, such as sediments rich in organic matter that acquired a high tritium concentration at the time of atomic weapon experiments. For instance, Eyrolle et al. [98] reported high tritium concentrations in the organic portion of the sediments from the Loire River in Western France.

These findings "demonstrate that tritium from global atmospheric fallout stored in a sedimentary reservoir for decades as organically bound forms". However, the presence of a modern organic substance in deep sediments is impossible in undisturbed settings.

(2) The chemical component carrying ^{3}H may be different from that of increasing $\delta^{2/1}H$. Thus, the two processes are separate but correlated. The enrichment in ^{2}H is caused by exchange with methane, whereas the enrichment in ^{3}H is attributed to more or less prolonged groundwater pathways. In this scenario, the deepest investigated groundwater (higher ^{3}H content in C5c) is characterised by a longer residence time and a major link to rainwater precipitated during the 1950s and 1960s. At the same time, a heterogeneous distribution of organic matter and methanogenic archaea within the saturated medium could lead to (i) different amounts of methane and (ii) a more or less prolonged interaction between the gas and groundwater at different depths. Moreover, considering the decrease of hydraulic head with depth and the downward groundwater flow component, the C5a groundwater type (characterised by relatively low $\delta^{2/1}H$ and ^{3}H values) may progressively dilute the deepest C5c groundwater type, thus causing a mixing between two waters with extreme $\delta^{2/1}H$ and ^{3}H values, namely C5a and C5c.

With the currently available data, we cannot choose between these hypotheses, but the second one seems the most reasonable. Further research is planned to be carried out to refine knowledge about this issue, including the possibility of finding a similar phenomenon in other portions of the heterogeneous medium.

6. Concluding Remarks

The in-depth analysis carried out at the study site made it possible to refine knowledge about the hydrogeological behavior of evaporite-bearing low-permeability successions at a representative site. In more details:

- Hydrogeological investigations and isotopic analyses demonstrated the coexistence of relatively brief to very prolonged groundwater pathways, but everywhere recharged by local precipitation;
- The deuterium content of some samples showed unusual values for groundwater; however, the coupled isotopic-biomolecular approach allowed to demonstrate that these unusual values are due to the interactions between the groundwater and certain gases (H_2S and CH_4), the presences of which are linked to sulfate-reducing bacteria and methanogenic archaea;
- At this stage of the research, these unusual isotopic content was detected in only one sampling sub-area (C5-cluster); nevertheless, this discrepancy between C5-groundwaters and those sampled in the other available wells is not surprising when taking into consideration the (hydro)geological heterogeneity of the investigated system, as well as the results obtained in a similar setting from the biogeochemical points of view [14–16]; in this previous case, a "patchwork" of geochemical and microbiological sub-environments was detected within the whole heterogeneous system, therefore demonstrating the coexistence of different microbial communities (with different microbial activity) also at a metric or decametric scale.

Taking into consideration the interesting results obtained at this stage concerning the heterogeneous distribution of biogeochemical processes, and the importance of moving from speculations to statements concerning the role of H_2S/CH_4 in influencing the local anomaly in deuterium content, a second step of the research is in progress. During this new phase, the study area will be significantly expanded, and the actual data set will be integrated also with measures of gas concentration and their isotopes, organic carbon percentage in both sediments and groundwater.

In a wider, and methodological context, the present study further demonstrates the importance of interdisciplinary approaches when studying such complex hydrogeological systems. An interdisciplinary approach combining well-established investigation methods (in this case, hydrogeological, isotopic and biomolecular methods), allows refinement of knowledge about the hydrogeological features and behavior of heterogeneous media characterised by evaporite-bearing

successions, and can help ensure correct interpretation of the meaning of each data type, avoiding misunderstandings and misinterpretations. Thus, this work can be used to refine the guidelines used to study heterogeneous media through purpose-designed interdisciplinary approaches and plan optimal monitoring networks and protocols for several anthropogenic purposes (e.g., environmental monitoring of landfills or contaminated sites).

Author Contributions: Conceptualisation, P.R., C.C., P.I., E.R., A.M.S., F.C.; methodology, P.R., C.C., P.I., E.R., A.M.S., F.C.; investigation, P.R., C.C., G.Z.; data curation, P.R., C.C., G.Z.; writing—original draft preparation, P.R., C.C.; writing—review and editing, P.R., C.C., P.I., E.R., A.M.S., F.C.; visualisation, P.R., C.C., G.Z.; supervision, P.I., E.R., A.M.S., F.C.; project administration, F.C. and E.R.; funding acquisition, F.C. and E.R. All authors have read and agreed to the published version of the manuscript.

Funding: This research was funded by Catanzaro Costruzioni S.r.l. (Heads of Funds: E. Rotigliano, F. Celico).

Acknowledgments: We warmly acknowledge Fabio Catanzaro, Salvatore Accardo and Rosario Varsalona and Giampiero Venturelli for useful discussions. The authors would like to thank anonymous reviewers for their fruitful comments. This work has benefited from the equipment and framework of the COMP-HUB Initiative, funded by the 'Departments of Excellence' program of the Italian Ministry for Education, University and Research (MIUR, 2018–2022).

Conflicts of Interest: The authors declare no conflict of interest.

References

1. Hsu, K.J.; Ryan, W.B.F.; Cita, M.B. Late miocene desiccation of the Mediterranean. *Nature* **1973**, *242*, 240–244. [CrossRef]
2. Krijgsman, W.; Hilgen, F.J.; Raffi, I.; Sierro, F.J.; Wilson, D.S. Chronology, causes and progression of the Messinian salinity crisis. *Nature* **1999**, *400*, 652–655. [CrossRef]
3. Vidal, L.; Bickert, T.; Wefer, G.; Rohl, U. Late Miocene stable isotope stratigraphy of SE Atlantic ODP Site 1085: Relation to Messinian events. *Mar. Geol.* **2002**, *180*, 71–85. [CrossRef]
4. Duggen, S.; Hoernie, K.; van Den Bogaard, V.; Rqpke, L.; Morgan, J.P. Deep roots of the Messinian salinity crisis. *Nature* **2003**, *422*, 602–606. [CrossRef]
5. Selli, R., II. Messiniano Mayer-Eymar. Proposta di un neostratotipo (The Messinian Mayer-Eymar. A proposal for a neostratotype). *G. Geol.* **1960**, *28*, 1–33.
6. Hsü, K.; Montadert, L.; Bernoulli, D.; Cita, M.B.; Erickson, A.; Garrison, R.E.; Kidd, R.B.; Melieres, F.; Muller, C.; Wright, R. History of the Mediterranean salinity crisis. *Nature* **1977**, *267*, 399–403. [CrossRef]
7. Butler, R.W.H.; Maniscalco, R.; Sturiale, G.; Grasso, M. Stratigraphic variations control deformation patterns in evaporite basins: Messinian examples, onshore and offshore Sicily (Italy). *J. Geol. Soc. Lond.* **2015**, *172*, 113–124. [CrossRef]
8. Balestra, M.; Corrado, S.; Aldega, L.; Gasparo Morticelli, M.; Sulli, A.; Rudkiewicz, J.L.; Sassi, W. Thermal and structural modeling of the Scillato wedge-top basin source-to-sink system: Insights into the Sicilian fold-and-thrust belt evolution (Italy). *Geol. Soc. Am. Bull.* **2019**, *131*, 1763–1782. [CrossRef]
9. Gasparo Morticelli, M.; Valenti, V.; Catalano, R.; Sulli, A.; Agate, M.; Avellone, G.; Gugliotta, C. Deep controls on foreland basin system evolution along the sicilian fold and thrust belt. *Bull. Soc. Géol. Fr.* **2015**, *186*, 273–290. [CrossRef]
10. Conti, A.; Sacchi, E.; Chiarle, M.; Martinelli, G.; Zuppi, G.M. Geochemistry of the formation waters in the Po plain (Northern Italy): An overview. *Appl. Geochem.* **2000**, *15*, 51–65. [CrossRef]
11. Pingue, L.; Marrone, G. Su alcune acque mineralizzate della provincia di Avellino (Some insight on a mineralized water in the Avellino province). *Econ. Irp.* **1972**, *1*, 5–16.
12. Di Nocera, S.; Imperato, M.; Matano, F.; Stanzione, D.; Valentino, G.M. Caratteri geologici ed idrogeologici della valle di Ansanto (Irpinia Centrale, Appennino Campano-Lucano) (Geological and hydrogeological features of the Ansanto Valley (Irpinia, Campano-Lucano Appenine). *Boll. Soc. Geol. Ital.* **1999**, *118*, 395–406.
13. Ortolani, F.; De Gennaro, M.; Ferreri, M.; Ghiara, M.R.; Stanzione, D.; Zenone, F. Prospettive geotermiche dell'Irpinia centrale (Appennino Meridionale): Studio geologico-strutturale e geochimica (Geothermal perspectives of the central Irpinia (Southern Appenine): Geological, structural ande geochemical studies). *Boll. Soc. Geol. Ital.* **1981**, *100*, 139–159.

14. Celico, F.; Capuano, P.; De Felice, V.; Naclerio, G. Hypersaline groundwater genesis assessment through a multidisciplinary approach: The case of Pozzo del Sale spring (southern Italy). *Hydrogeol. J.* **2008**, *16*, 1441–1451. [CrossRef]
15. Boschetti, T.; De Felice, V.; Celico, F. The Pozzo del Sale waters (Irpinia, Southern Apennines, Italy): Chemical—Isotope salt effects and paleoenvironmental implications for Late Messinian evaporates. *Aquat. Geochem.* **2013**, *19*, 303–322. [CrossRef]
16. Petrella, E.; Bucci, A.; Ogata, K.; Zanini, A.; Naclerio, G.; Chelli, A.; Francese, R.; Boschetti, T.; Pittalis, D.; Celico, F. Hydrodynamics in evaporate-bearing fine-grained successions investigated through an interdisciplinary approach: A test study in Southern Italy. *Geofluids* **2018**. [CrossRef]
17. Eastoe, C.J.; Long, A.; Knauth, P. Stable chlorine isotopes in the Palo Duro Basin, Texas: Evidence for preservation of Permian evaporate brines. *Geochim. Cosmochim. Acta* **1999**, *63*, 1375–1382. [CrossRef]
18. Andreo, B.; Gil-Márquez, J.M.; Mudarra, M.; Linares, L.; Carrasco, F. Hypothesis on the hydrogeological context of wetland areas and springs related to evaporitic karst aquifers (Málaga, Córdoba and Jaén provinces, Southern Spain). *Environ. Earth Sci.* **2016**, *75*, 759. [CrossRef]
19. Gil-Màrquez, J.M.; Barberà, J.A.; Andreo, B.; Mudarra, M. Hydrological and geochemical processes constraining groundwater salinity in wetland areas related to evaporitic (karst) systems. A case study from Southern Spain. *J. Hydrol.* **2017**, *544*, 538–554. [CrossRef]
20. Lyu, M.; Pang, A.; Yin, L.; Zhang, J.; Huang, T.; Yang, S.; Li, Z.; Wang, X.; Gulbostan, T. The control of groundwater flow systems and geochemical processes on groundwater chemistry: A case study in Wushenzhao Basin, NW China. *Water* **2019**, *11*, 790. [CrossRef]
21. Acero, P.; Auqué, L.F.; Galve, J.P.; Gutiérrez, F.; Carbonel, D.; Gimeno, M.J.; Yechieli, Y.; Asta, M.P.; Gómez, J.B. Evaluation of geochemical and hydrogeological processes by geochemical modeling in an area affected by evaporate karstification. *J. Hydrol.* **2015**, *529*, 1874–1889. [CrossRef]
22. Chiesi, M.; de Waele, J.; Forti, P. Origin and evolution of a salty gypsum/anhydrite karst spring: The case of Poiano (Northern Apennines, Italy). *Hydrogeol. J.* **2010**, *18*, 1111–1124. [CrossRef]
23. Zhu, S.; Zhang, F.; Zhang, Z.; Kung, H.; Yushanjiang, A. Hydrogen and oxygen isotope composition and water quality evaluation for different water bodies in the Ebinur Lake watershed, Northwestern China. *Water* **2019**, *11*, 2067. [CrossRef]
24. Porowski, A.; Porowska, D.; Halas, S. Identification of sulfate sources and biogeochemical processes in an aquifer affected by peatland: Insights from monitoring the isotopic composition of groundwater sulfate in Kampinos National Park, Poland. *Water* **2019**, *11*, 1388. [CrossRef]
25. Petrella, E.; Celico, F. Mixing of water in a carbonate aquifer, southern Italy, analysed through stable isotope investigations. *Int. J. Speleol.* **2013**, *42*, 25–33. [CrossRef]
26. Walker, D.; Parkin, G.; Gowing, J.; Haile, A.T. Development of a Hydrogeological Conceptual Model for Shallow Aquifers in the Data Scarce Upper Blue Nile Basin. *Hydrology* **2019**, *6*, 43. [CrossRef]
27. Duckett, K.A.; Langman, J.B.; Bush, J.H.; Brooks, E.S.; Dunlap, P.; Welker, J.M. Isotopic Discrimination of Aquifer Recharge Sources, Subsystem Connectivity and Flow Patterns in the South Fork Palouse River Basin, Idaho and Washington, USA. *Hydrology* **2019**, *6*, 15. [CrossRef]
28. Eissa, M.A. Application of Multi-Isotopes and Geochemical Modeling for Delineating Recharge and Salinization Sources in Dahab Basin Aquifers (South Sinai, Egypt). *Hydrology* **2018**, *5*, 41. [CrossRef]
29. Clauer, N.; Techer, I.; Chaudhuri, S. Geochemical Tracing of Potential Hydraulic Connections between Groundwater and Run-Off Water in Northeastern Kansas, USA. *Hydrology* **2017**, *4*, 56. [CrossRef]
30. Bucci, A.; Petrella, E.; Naclerio, G.; Allocca, V.; Celico, F. Microorganisms as contaminants and natural tracers: A 10-year research in some carbonate aquifers (southern Italy). *Environ. Earth Sci.* **2015**, *74*, 173–184. [CrossRef]
31. Bucci, A.; Petrella, E.; Celico, F.; Hynds, P.D.; Naclerio, G. The use of molecular approaches in hydrogeological studies: Carbonate aquifers in Southern Italy. *Hydrogeol. J.* **2017**, *25*, 1017–1031. [CrossRef]
32. Bucci, A.; Petrella, E.; Naclerio, G.; Gambatese, S.; Celico, F. Bacterial migration through low-permeability fault zones in compartmentalised aquifer systems: A case study in Southern Italy. *Int. J. Speleol.* **2014**, *43*, 273–281. [CrossRef]
33. Rizzo, P.; Petrella, E.; Bucci, A.; Salvioli Mariani, E.; Chelli, A.; Sanangelantoni, A.M.; Raimondo, M.; Quagliarini, A.; Celico, F. Studying hydraulic interconnections in low-permeability media by using bacterial communities as natural tracers. *Water* **2020**, *12*, 1795. [CrossRef]

34. Bucci, A.; Naclerio, G.; Allocca, V.; Celico, P.; Celico, F. Potential use of microbial community investigations to analyze hydrothermal systems behaviour: The case of Ischia island, southern Italy. *Hydrol. Process.* **2011**, *25*, 1866–1873. [CrossRef]
35. Rizzo, P.; Bucci, A.; Sanangelantoni, A.M.; Iacumin, P.; Celico, F. Coupled Microbiological–Isotopic Approach for Studying Hydrodynamics in Deep Reservoirs: The Case of the Val d'Agri Oilfield (Southern Italy). *Water* **2020**, *12*, 1483. [CrossRef]
36. Naclerio, G.; Fardella, G.; Marzullo, G.; Celico, F. Filtration of Bacillus subtilis and Bacillus cereus spores in a pyroclastic topsoil, carbonate Apennines, southern Italy. *Colloids Surf. B Biointerfaces* **2009**, *70*, 25–28. [CrossRef] [PubMed]
37. Gugliotta, C.; Gasparo Morticelli, M.; Avellone, G.; Agate, M.; Barchi, M.R.; Albanese, C.; Valenti, V.; Catalano, R. Middle Miocene—Early Pliocene wedge-top basins of North-Western Sicily (Italy). Constraints for the tectonic evolution of a "non-conventional" thrust belt, affected by transpression. *J. Geol. Soc. Lond.* **2014**, *171*, 211–226. [CrossRef]
38. Avellone, G.; Barchi, M.R.; Catalano, R.; Gasparo Morticelli, M.; Sulli, A. Interference between shallow and deep-seated structures in the sicilian fold and thrust belt, Italy. *J. Geol. Soc. Lond.* **2010**, *167*, 109–126. [CrossRef]
39. de Waele, J.; Piccini, L.; Columbu, A.; Madonia, G.; Vattano, M.; Calligaris, C.; D'Angeli, I.; Parise, M.; Chiesi, M.; Sivelli, M.; et al. Evaporite karst in Italy: A review. *Int. J. Speleol.* **2017**, *46*, 137–168. [CrossRef]
40. Caracausi, A.; Sulli, A. Outgassing of mantle volatiles in compressional tectonic regime away from volcanism: The role of continental delamination. *Geochem. Geophys.* **2019**, *20*, 2007–2020. [CrossRef]
41. Di Maggio, C.; Madonia, G.; Parise, M.; Vattano, M. Karst of Sicily and its conservation. *J. Cave Karst Stud.* **2012**, *74*, 157–172. [CrossRef]
42. Decima, D.; Wezel, F.C. Late Miocene evaporites of the central Sicilian Basin, Italy. *Initial Rep. Deep Sea Drill. Proj.* **1973**, *13*, 1234–1241.
43. Roveri, M.; Schreiber, B.C.; Iaccarino, S.M.; Vitale, F.P.; Lugli, S.; Caruso, A.; Lucchi, F.R. Clastic vs. primary precipitated evaporites in the messinian sicilian basins. *Ateneo Parm. Acta Nat.* **2006**, *42*, 125–199.
44. Decima, A.; Bommarito, S.; La Rosa, N.; Aiello, R. *Foglio 636—Agrigento. Carta Geologica d'Italia Alla Scala 1:50.000*; Servizio Geologico d'Italia, Istituto Superiore per la Protezione e la Ricerca Ambientale (ISPRA): Roma, Italy, 1972.
45. Cappadonia, C.; Coratza, P.; Agnesi, V.; Soldati, M. Malta and Sicily joined by geoheritage enhancement and geotourism within the framework of land management and development. *Swiss J. Geosci.* **2018**, *8*, 253. [CrossRef]
46. Abiye, T.; Shaduka, I. Radioactive Seepage through Groundwater Flow from the Uranium Mines, Namibia. *Hydrology* **2017**, *4*, 11. [CrossRef]
47. International Atomic Energy Agency. *Water and Environment News*; IAEA: Vienna, Austria, 1998.
48. Milani, C.; Hevia, A.; Foroni, E.; Duranti, S.; Turroni, F.; Lugli, G.A.; Sanchez, B.; Martín, R.; Gueimonde, M.; van Sinderen, D.; et al. Assessing the Fecal Microbiota: An Optimized Ion Torrent 16S rRNA Gene-Based Analysis Protocol. *PLoS ONE* **2013**, *8*, e68739. [CrossRef]
49. Fischer, M.A.; Güllert, S.; Neulinger, S.C.; Streit, W.R.; Schmitz, R.A. Evaluation of 16S rRNA gene primer pairs for monitoring microbial community structures showed high reproducibility within and low comparability between datasets generated with multiple archaeal and bacterial primer pairs. *Front. Microbiol.* **2016**, *7*, 1297. [CrossRef]
50. Caporaso, J.G.; Kuczynski, J.; Stombaugh, J.; Bittinger, K.; Bushman, F.D.; Costello, E.K.; Fierer, N.; Gonzalez Peña, A.; Goodrich, J.K.; Gordon, J.I.; et al. QIIME allows analysis of high-throughput community sequencing data. *Nat. Methods* **2010**, *7*, 335–336. [CrossRef]
51. Callahan, B.J.; McMurdie, P.J.; Rosen, M.J.; Han, A.W.; Johnson, A.J.; Holmes, S.P. DADA2: High-resolution sample inference from Illumina amplicon data. *Nat. Methods* **2016**, *13*, 581–583. [CrossRef]
52. Bokulich, N.A.; Kaehler, B.D.; Rideout, J.R.; Dillon, M.; Bolyen, E.; Knight, R.; Huttley, G.A.; Caporaso, G.J. Optimizing taxonomic classification of marker-gene amplicon sequences with QIIME 2's q2-feature-classifier plugin. *Microbiome* **2018**, *6*, 90. [CrossRef]
53. Quast, C.; Pruesse, E.; Yilmaz, P.; Gerken, J.; Schweer, T.; Yarza, P.; Peplies, J.; Glöckner, F.O. The SILVA ribosomal RNA gene database project: Improved data processing and web-based tools. *Nucleic Acids Res.* **2012**, *41*, 590–596. [CrossRef] [PubMed]

54. Freeze, R.A.; Witherspoon, P.A. Theoretical analysis of regional groundwater flow: 2. Effect of water-table configuration and subsurface permeability variation. *Water Resour. Res.* **1967**, *3*, 623–634. [CrossRef]
55. Grassa, F.; Favara, R.; Valenza, M. Moisture source in the Hyblean Mountains region (South-Eastern Sicily, Italy): Evidence from stable isotopes signature. *Appl. Geochem.* **2006**, *21*, 2082–2095. [CrossRef]
56. Liotta, M.; Favara, R.; Valenza, M. Isotopic composition of the precipitations in the Central Mediterranean: Origin marks and orographic precipitation effects. *J. Geophys. Res.* **2006**, *111*, D19302. [CrossRef]
57. Liotta, M.; Brusca, L.; Grassa, F.; Inguaggiato, S.; Longo, M.; Madonia, P. Geochemistry of rainfall at Stromboli volcano (Aeolian Islands): Isotopic composition and plume-rain interaction. *Geochem. Geophys. Geosyst.* **2006**, *7*, Q07006. [CrossRef]
58. Liotta, M.; Bellissimo, S.; Favara, R.; Valenza, M. Isotopic composition of single rain events in the Central Mediterranean. *J. Geophys. Res.* **2008**, *113*, D16304. [CrossRef]
59. Fontana, M.; Grassa, F.; Cusimano, G.; Favara, R.; Hauser, S.; Scaletta, R. Geochemistry and potential use of groundwater in the Rocca Busambra area (Sicily, Italy). *Environ. Geol.* **2009**, *57*, 885–898. [CrossRef]
60. Liotta, M.; Grassa, F.; D'Alessandro, W.; Favara, R.; Gagliano, E.; Candela, A.; Pisciotta, C.; Scaletta, R. Isotopic composition of precipitation and groundwater in Sicily, Italy. *Appl. Geochem.* **2013**, *34*, 199–206. [CrossRef]
61. Madonia, P.; D'Aleo, R.; Di Maggio, C.; Favara, R.; Hartwig, A. The use of shallow dripwater as an isotopic marker of seepage in karst areas: A comparison between Western Sicily (Italy) and the Harz Mountains (Germany). *Appl. Geochem.* **2013**, *34*, 231–239. [CrossRef]
62. Giustini, F.; Brilli, M.; Patera, A. Mapping oxygen stable isotopes of precipitation in Italy. *J. Hydrol. Reg. Stud.* **2016**, *8*, 162–181. [CrossRef]
63. Petrella, E.; Celico, F. Heterogeneous aquitard properties in sedimentary successions in the Apennine chain: Case studies in southern Italy. *Hydrol. Process.* **2009**, *23*, 3365–3371. [CrossRef]
64. Segadelli, S.; Vescovi, P.; Ogata, K.; Chelli, A.; Zanini, A.; Boschetti, T.; Petrella, E.; Toscani, L.; Gargini, A.; Celico, F. A conceptual hydrogeological model of ophiolitic aquifers (serpentinized peridodite): The test example of Mt. Prinzera (northern Italy). *Hydrol. Process.* **2017**, *31*, 1058–1073. [CrossRef]
65. Morgenstern, U.; Stewart, M.K.; Stenger, R. Dating of streamwater using tritium in a post nuclear bomb pulse world: Continuous variation of mean transit time with streamflow. *Hydrol. Earth Syst. Sci.* **2010**, *14*, 2289–2301. [CrossRef]
66. Harms, P.A.; Visser, A.; Moran, J.E.; Esser, B.K. Distribution of tritium in precipitation and surface water in California. *J. Hydrol.* **2016**, *534*, 63–72. [CrossRef]
67. Fernández-Martínez, J.; Pujalte, M.J.; García-Martínez, J.; Mata, M.; Garay, E.; Rodríguez-Valera, F. Description of *Alcanivorax venustensis* sp. nov. and reclassification of *Fundibacter jadensis* DSM 12178T (Bruns and Berthe-Corti 1999) as *Alcanivorax jadensis* comb. nov., members of the emended genus *Alcanivorax*. *Int. J. Syst. Evol. Micr.* **2003**, *53*, 331–338. [CrossRef]
68. Espinosa, E.; Marco-Noales, E.; Gomez, D.; Lucas-Elío, P.; Ordax, M.; Garcías-Bonet, N.; Sanchez-Amat, A. Taxonomic study of Marinomonas strains isolated from the seagrass *Posidonia oceanica*, with descriptions of *Marinomonas balearica* sp. nov. and *Marinomonas pollencensis* sp. nov. *Int. J. Syst. Evol. Microbiol.* **2010**, *60*, 93–98. [CrossRef]
69. Rodriguez-Valera, F.; Ruiz-Berraquero, F.; Ramos-Cormenzana, A. Characteristics of the heterotrophic bacterial populations in hypersaline environments of different salt concentrations. *Microb. Ecol.* **1981**, *7*, 235–243. [CrossRef]
70. Pati, A.; Gronow, S.; Lapidus, A.; Copeland, A.; Del Rio, T.G.; Nolan, M.; Chertkov, O. Complete genome sequence of Arcobacter nitrofigilis type strain (CIT). *Stand. Genom. Sci.* **2010**, *2*, 300. [CrossRef]
71. Rosenberg, A. *Pseudomonas halodurans* sp. nov., a halotolerant bacterium. *Arch. Microbiol.* **1983**, *136*, 117–123. [CrossRef]
72. Suzuki, D.; Li, Z.; Zhang, C.; Katayama, A. Reclassification of *Desulfobacterium anilini* as *Desulfatglans anilini* comb. Nov. within *Desulfatiglans* gen. nov., and description of a 4-chlorophenol-degrading sulfate-reducing bacterium, *Desulfatiglans parachlorophenolica* sp. nov. *Int. J. Syst. Evol. Microbiol.* **2014**, *64*, 3081–3086. [CrossRef]

73. Sigalevich, P.; Baev, M.V.; Teske, A.; Cohen, Y. Sulfate reduction and possible aerobic metabolism of the sulfate-reducing bacterium *Desulfovibrio oxyclinae* in a chemostat coculture with *Marinobacter* sp. strain MB under exposure to increasing oxygen concentrations. *Appl. Environ. Microbiol.* **2000**, *66*, 5013–5018. [CrossRef] [PubMed]
74. Burns, J.L.; DiChristina, T.J. Anaerobic respiration of elemental sulfur and thiosulfate by *Shewanella oneidensis* MR-1 requires psrA, a homolog of the phsA gene of *Salmonella enterica* serovar typhimurium LT2. *Appl. Environ. Microbiol.* **2009**, *75*, 5209–5217. [CrossRef] [PubMed]
75. Jørgensen, B.B.; Bak, F. Pathways and microbiology of thiosulfate transformations and sulfate reduction in a marine sediment (Kattegat, Denmark). *Appl. Environ. Microbiol.* **1991**, *57*, 847–856. [CrossRef] [PubMed]
76. Könneke, M.; Bernhard, A.E.; José, R.; Walker, C.B.; Waterbury, J.B.; Stahl, D.A. Isolation of an autotrophic ammonia-oxidizing marine archaeon. *Nature* **2005**, *437*, 543–546. [CrossRef] [PubMed]
77. Schoop, G. *Halococcus litoralis*, ein obligat halophiler Farbstoffbildner. *Dtsch Tierarztl Wochenschr* **1935**, *43*, 817–820.
78. Boone, D.R. Methanobacterium. In *Bergey's Manual of Systematics of Archaea and Bacteria*; Wiley: Hoboken, NJ, USA, 2015; pp. 1–8.
79. Sprenger, W.W.; van Belzen, M.C.; Rosenberg, J.; Hackstein, J.H.; Keltjens, J.T. *Methanomicrococcus blatticola* gen. nov., sp. nov., a methanol-and methylamine-reducing methanogen from the hindgut of the cockroach *Periplaneta americana*. *Int. J. Syst. Evol. Microbiol.* **2000**, *50*, 1989–1999. [CrossRef]
80. Holt, J.G.; Krieg, N.R.; Sneath, P.H.A.; Staley, J.T. *Bergey's Manual of Determinative Bacteriology*; William and Wilkins Company: Baltimore, MD, USA, 1994; p. 724.
81. Freeze, R.A.; Cherry, J.A. *Groundwater*; Prentice-Hall: Englewood Cliffs, NJ, USA, 1979; p. 604. ISBN 978-01-3365-312-0.
82. Drogue, C. Structure de certains aquifers karstiques d'apres les resultants de traveaux de forage. *CR Acad. Sci. Paris* **1974**, *278*, 2621–2624.
83. Prtoljan, B.; Kapelj, S.; Dukaric, F.; Vlahovic, I.; Mrinjek, E. Hydrochemical and isotopic evidences for definition of tectonically controlled catchment areas of the Konovle area spring (SE Dalmatia, Croatia). *J. Geochem. Explor.* **2012**, *112*, 285–296. [CrossRef]
84. La Vigna, F.; Mazza, R.; Capelli, G. Detecting the flow relationships between deep and shallow aquifers in an exploited groundwater system, using long-term monitoring data and quantitative hydrogeology: The Acque Albule basin case (Rome, Italy). *Hydrol. Process.* **2013**, *27*, 3159–3173. [CrossRef]
85. Agosta, F.; Prasad, M.; Aydin, A. Physical properties of carbonate fault rocks, Fucino basin (Central Italy): Implications for fault seal in platform carbonates. *Geofluids* **2007**, *7*, 19–32. [CrossRef]
86. Petrella, E.; Aquino, D.; Fiorillo, F.; Celico, F. The effect of low-permeability fault zones on groundwater flow in a compartmentalized system. Experimental evidence from a carbonate aquifer (Southern Italy). *Hydrol. Process.* **2015**, *29*, 1577–1587. [CrossRef]
87. Hernandez-Diaz, R.; Petrella, E.; Bucci, A.; Naclerio, G.; Feo, A.; Sferra, G.; Chelli, A.; Zanini, A.; Gonzales-Hernandez, P.; Celico, F. Integrating hydrogeological and microbiological data and modelling to characterize the hydraulic features and behavior of coastal carbonate aquifers: A case in Western Cuba. *Water* **2019**, *11*, 1989. [CrossRef]
88. Mangin, A. Contribution à L'étude Hydrodynamique des Aquiferes Karstiques. Ph.D. Thesis, University de Dijon, Dijon, France, 1975.
89. Mangin, A. Karst hydrogeology. In *Groundwater Ecology*; Gibert, J., Danielopol, D.L., Stanford, J.A., Eds.; Academic Press: San Diego, CA, USA, 1994; pp. 43–67.
90. Segadelli, S.; Vescovi, P.; Chelli, A.; Petrella, E.; De Nardo, M.T.; Gargini, A.; Celico, F. Hydrogeological mapping of heterogeneous, multi-layered ophiolitic aquifers: The test example of Mt. Prinzera (northern Apennines, Italy). *J. Maps* **2017**, *13*, 737–746. [CrossRef]
91. Horita, J.; Wesolowski, D.J. Liquid-vapor fractionation of oxygen and hydrogen isotopes of water from the freezing to the critical temperature. *Geochim. Cosmochim. Acta* **1994**, *58*, 3425–3437. [CrossRef]
92. Galley, M.R.; Miller, A.I.; Atherly, J.F.; Mohn, M. GS process-physical properties: Chalk River, Ontario, Canada, Atomic Energy of Canada Limited, AECL-4225. In *Environmental Isotopes in Hydrogeology*; Clark, I., Fritz, P., Eds.; Lewis Publisher: Boca Reton, FL, USA, 1972.
93. Horibe, Y.; Craig, H. D/H fractionation in the system methane-hydrogen-water. *Geochim. Cosmochim. Acta* **1995**, *59*, 5209–5217. [CrossRef]

94. Meister, P.; Liu, B.; Ferdelman, T.G.; Jørgensen, B.B.; Khalili, A. Control of sulphate and methane distributions in marine sediments by organic matter reactivity. *Geochim. Cosmochim. Acta* **2013**, *104*, 183–193. [CrossRef]
95. Peketi, A.; Mazumdar, A.; Spk, P. Influence of dual sulfate reduction pathways on pore-fluid chemistry and occurrences of methane hydrate in sediment cores (IODP-353) off Mahanadi basin, Bay of Bengal. *Geochem. J.* **2020**, *54*, 1–11. [CrossRef]
96. Liu, Q.; Wu, X.; Wang, X.; Jin, Z.; Zhu, D.; Meng, Q.; Huang, S.; Liu, J.; Fu, Q. Carbon and hydrogen isotopes of methane, ethane, and propane: A review of genetic identification of natural gas. *Earth-Sci. Rev.* **2019**, *190*, 247–272. [CrossRef]
97. Parkhurst, D.L.; Appelo, C.A.J. Description of Input and Examples for PHREEQC Version 3-A Computer Program for Speciation, Batch-Reaction, One-Dimensional Transport, and Inverse Geochemical Calculations. In *Geological Survey Techniques and Methods*; U.S. Department of the Interior; U.S. Geological Survey: Denver, CO, USA, 2013; Book 6, Chapter A43. Available online: https://pubs.usgs.gov/tm/06/a43/ (accessed on 1 July 2020).
98. Eyrolle, F.; Copard, Y.; Lepage, H.; Ducros, L.; Morereau, A.; Grosbois, C.; Cossonnet, C.; Gurriaran, R.; Booth, S.; Desmet, M. Evidence for tritium persistence as organically bound forms in river sediments since the past nuclear weapon tests. *Sci. Rep.* **2009**, *9*, 11487. [CrossRef]

2.2. Approfondimento delle conoscenze relative agli approcci di biorisanamento mediante disamina dei processi di attenuazione naturale e selezione di nuovi ceppi microbici degradatori

Rendiconti Lincei. Scienze Fisiche e Naturali
https://doi.org/10.1007/s12210-018-0748-x

FORESEEING GROUNDWATER RESOURCES

Groundwater characterization from an ecological and human perspective: an interdisciplinary approach in the Functional Urban Area of Parma, Italy

Andrea Zanini[1] · Emma Petrella[2] · Anna Maria Sanangelantoni[2] · Letizia Angelo[1] · Beatrice Ventosi[2] · Luca Viani[2] · Pietro Rizzo[2] · Sara Remelli[2] · Marco Bartoli[2] · Rossano Bolpagni[2,3] · Alessandro Chelli[2] · Alessandra Feo[2] · Roberto Francese[2] · Paola Iacumin[2] · Cristina Menta[2] · Erica Racchetti[2] · Enrico Maria Selmo[2] · Maria Giovanna Tanda[1] · Marco Ghirardi[4] · Pietro Boggio[5] · Francesco Pappalardo[5] · Maria Teresa De Nardo[6] · Stefano Segadelli[6] · Fulvio Celico[2]

Received: 23 July 2018 / Accepted: 12 October 2018

Abstract
In the Parma Functional Urban Area, hydro-geo-ecology was investigated through an interdisciplinary approach, with emphasis on the shallow aquifer system. The study pointed out that domestic wells and *fontanili* are both fed by shallow groundwater affected by PCE and nitrate contamination, upgradient of the rural area located north of Parma City. Moreover, *Folsomia candida* tests suggested the possibility that other types of contaminants (not analysed in this study) can affect the shallow groundwater. Nowadays, PCE concentrations in the city centre are slightly higher than the limit set by law. Moreover, PCE aerobic biodegradation can be due to the local microbial community and then an effective natural attenuation can be expected along the groundwater flow pathway. These results suggest a very low risk for human health, linked to the groundwater consumption in the rural area north of Parma City. Conversely, no forecasts can be made at present about the possible impact of low PCE concentrations on the aquatic ecosystem observed at the *fontanili*. Concerning nitrate contamination, the higher concentrations detected in some wells and *fontanili* suggest a high risk for both human health and aquatic ecosystems. In a wider context, thanks to the interdisciplinary approach that combines successfully well-established investigation methods, the present study allows a better knowledge of the hydro-geo-ecological behaviour of groundwater-dependent ecosystems. At the same time, through purpose-designed experimental investigations and simulation models, this approach could be used as a sort of guideline useful in studying such complex environmental systems.

Keywords Groundwater characterization · Alluvial plain · Shallow aquifer system · Interdisciplinary approach · Functional Urban Area

1 Introduction

Within the AMIIGA project (INTERREG Central Europe), the city of Parma (Italy) became a pilot site with a contamination of chlorinated hydrocarbons in the shallow aquifer. To study the evolution of the contamination and to identify

This contribution is the written, peer-reviewed version of a paper presented at the Conference "Foreseeing groundwater resources" held at Accademia Nazionale dei Lincei in Rome on March 22, 2018.

✉ Emma Petrella
emma.petrella@unipr.it

[1] Department of Engineering and Architecture, University of Parma, Parma, Italy

[2] Department of Chemistry, Life Sciences and Environmental Sustainability, University of Parma, Parma, Italy

[3] Institute of Ecosystem Study, National Research Council, Verbania, Italy

[4] Municipality of Parma, Parma, Italy

[5] Emilia Romagna Environmental Protection Agency, Parma, Italy

[6] Emilia Romagna Region, Bologna, Italy

Published online: 30 October 2018

the possible sources, it was necessary to widen the limits of the focus area to a larger territory. In particular, we studied the shallow aquifer at the Functional Urban Area (FUA) scale of Parma (the city plus its commuting zone), sensu EU-Organisation for Economic Co-operation and Development.

The main drinking water and industrial wells pump groundwater from relatively deep aquifers (from fifty to several hundreds of meters below the ground surface). The actual monitoring wells and the main hydrogeological studies focused on these deeper horizons, whereas little information exists concerning the shallow aquifer that is utilized by the local population for domestic and agricultural purposes. Moreover, the shallow groundwater feeds the so-called *risorgive* or *fontanili* that in turn feed a complex system of channels and ditches (Rossetti et al. 2005; Bonaposta et al. 2011). The *risorgive* or *fontanili* are small, semi-artificial, aquatic ecosystems sensu Kløve et al. (2011) that are typical of the Po River Basin, the largest Italian watershed (about 71,000 km^2). Urban and agricultural pressures cause widespread nitrate contamination of the shallow groundwater in the Po plain (e.g. Cinnirella et al. 2005; Bassanino et al. 2011). The same contamination has been detected in most of the *fontanili* (e.g. Rossetti et al. 2005; Laini et al. 2011; Abdelahad et al. 2015).

Therefore, the anthropic pressure on this shallow aquifer can cause a negative impact on (i) human health [directly (drinking water for private uses) or indirectly [water used for irrigation or cattle breeding)] and (ii) peculiar (*fontanili*) groundwater-dependent ecosystems (GDE).

Taking into consideration the environmental scenario, an interdisciplinary work was necessary to have a complete overview of the hydro-geochemical and hydro-ecological processes taking part in a such complex ecosystem.

The main goal of this manuscript is to present the state of the art of this interdisciplinary and holistic research, as well as to show how different disciplines are necessary to analyse the aquatic environment. Therefore, this work is also a sort of guideline related to an effective interdisciplinary approach necessary to characterize groundwater bodies from both the ecological and human perspective.

This work was carried out in synergy between the University of Parma and other public authorities, within a framework agreement devoted to protect and manage both the groundwater and the groundwater-dependent ecosystems. Recently, within the same agreement, some interdisciplinary studies have been carried out in the Apennine chain (Cantonati et al. 2016; Chelli et al. 2016; Segadelli et al. 2017a, b).

2 Study area

In the Po plain sedimentary basin, the sedimentation processes have been marked by transgressive–regressive cycles (e.g. Ricci Lucchi et al. 1992). On the basis of these discontinuities, sediments may be grouped into supersynthems, synthems and minor rank geological bodies (Di Dio 2005). The Quaternary Marine Supersynthem (Upper Pliocene to Lower Pleistocene) consists of sediments of continental shelf, prodelta, delta front and fan-delta resting on Pliocene clays. The bottom of this supersynthem is defined by an evident sub-aerial surface of erosion and/or absence of deposition related to tectonic regional uplifting and tilting of the southern margin of the Po plain sedimentary basin. As documented by seismic lines and stratigraphic data, in the area of interest this supersynthem is up to 1600 m thick. The Emilia–Romagna Supersynthem (Lower Pleistocene, about 800 ky BP to present) consists of alluvial plain and fan deposits and of intra-valley and terrace deposits. This supersynthem is subdivided in two synthems separated by a stratigraphic discontinuity at about 450 ky (Di Dio 2005).

The grain size of the sediments is largely variable (from gravel to silt–clay) and frequently dependent on the eustatic–climatic oscillations at the scale of 20–40 ky. This heterogeneity causes the aquifer system to be made up of several permeable horizons intercalated by low-permeability clays and silts. The present work is focused mainly on the shallow permeable horizon (the upper 30 m below ground) that directly interacts with the urbanized territory of the City of Parma (Fig. 1), including the historical downtown and recent settlements. The area is densely urbanized, with a concentration of residential built-up areas, trading and services. The mean ground elevation is about 55 m above sea level (m asl).

The first information about groundwater contamination at the pilot site (hydrocarbons, MTBE, BTEX) was collected in 2002 during a gas station decommissioning. At the end of the procedure, chemical analysis showed also PCE concentrations in groundwater higher than the legal limits, even in piezometers upgradient with reference to the gas station. During the last few years, the PCE concentration has been up to 24 µg/L (Parma Municipality, unpublished data). At the present state, the sources of this pollution are still unknown. In 2013, a historical analysis, just on the surrounding of the pilot site of the commercial activities, which potentially used PCE, was carried out (not reported here for brevity). However, it did not allowed the identification of the responsibilities. For this reason it was necessary to design and improve the environmental investigations.

A second, but not less important, contamination that was found in the shallow aquifer regarded the nitrates; unfortunately, only a small amount of information was available and essentially related to the *fontanili*. These data show nitrate concentration up to 83 mg/L south of Parma City (Emilia Romagna Region, unpublished data), therefore suggesting a serious contamination and negative impacts on both the human health and the GDEs.

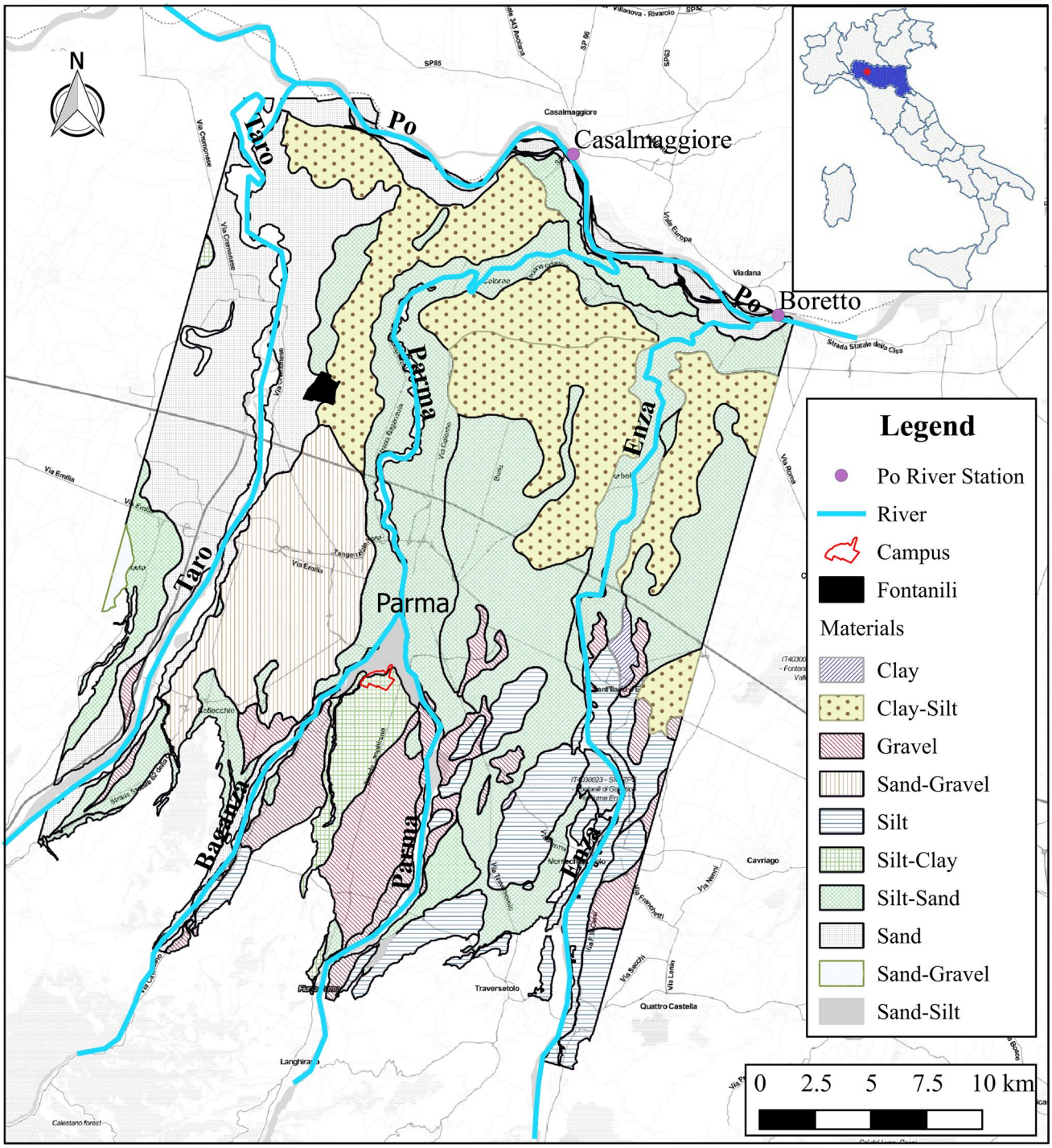

Fig. 1 Schematic map of the study area

3 Materials and methods

3.1 Geological, hydrogeological and geophysical investigations

Nineteen boreholes were drilled within the study area (Fig. 2a), to reconstruct the lithostratigraphic sequence of the shallow alluvial aquifer (Fig. 2b). Two of these boreholes (one cluster made of two wells each) were drilled at the university campus, to analyse possible variations in hydraulic head with depth, due to the vertical heterogeneity of the medium. The cluster is made of one well 27 m deep (P8d; screened from 24 to 27 m below ground) and one well 11 m deep (P8 s; screened from 8 to 11 m below ground). The

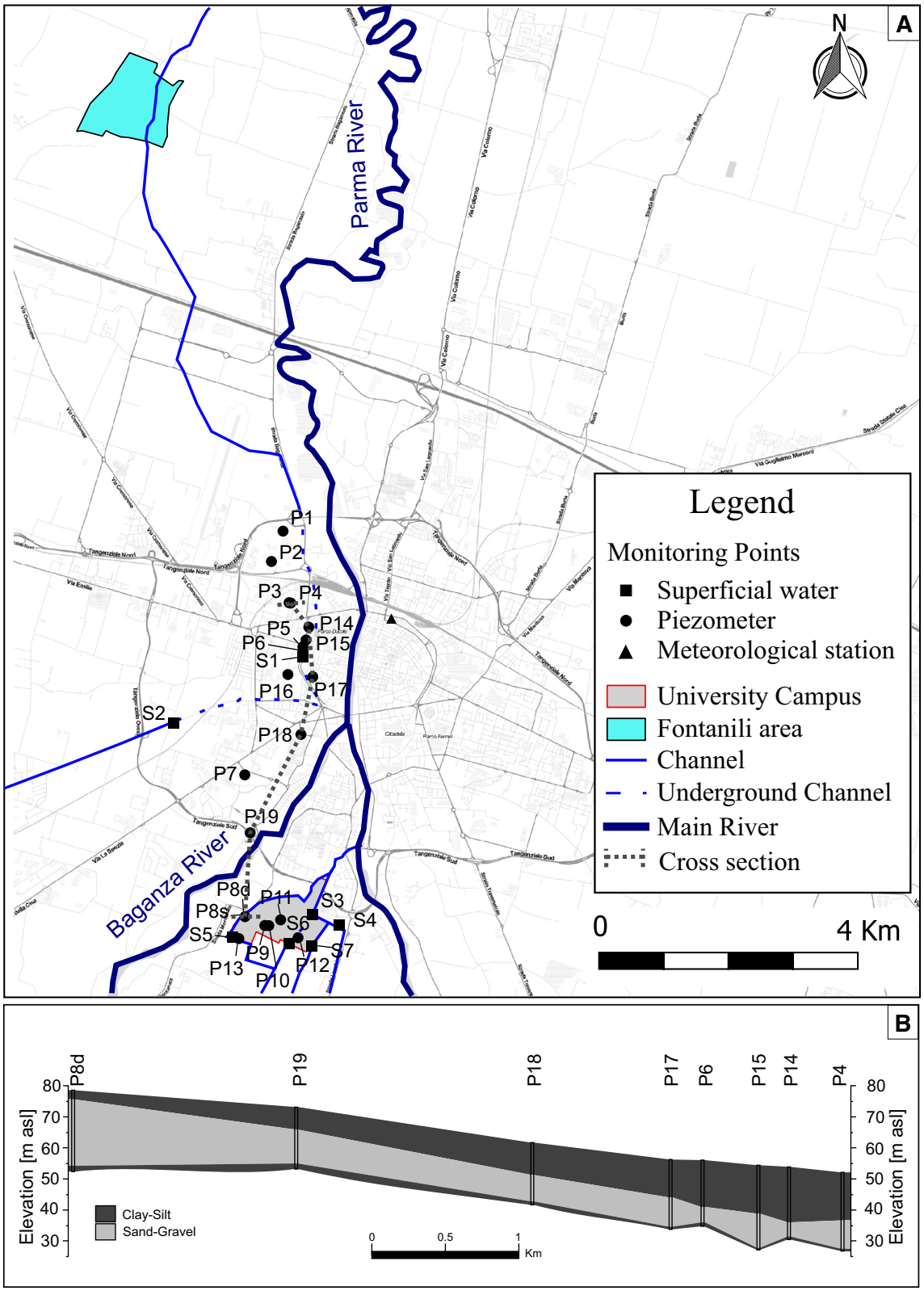

Fig. 2 **a** Location of monitoring points in the study area. **b** Geological cross section

other piezometer was drilled along a transect parallel to the groundwater flow line reconstructed at basin scale (approximately, from south to north), throughout the Parma urban area and passing from a site where the shallow groundwater was polluted by chlorinated solvents. These wells are 25–30 m deep and screened within the coarser-grained sediments (Fig. 2b).

The groundwater head was measured through a water level meter in all the available shallow wells (Fig. 2a) to reconstruct the groundwater flow net at the FUA scale. The hydraulic head was measured on an hourly basis (through pressure transducer with data-logger) in three wells to analyse the relationships between precipitations and groundwater head fluctuations. The precipitations were monitored on an hourly basis at a meteorological station located within the study area.

One pumping test was carried out in P8d. The hydraulic heads were monitored continuously (through pressure transducers with data-logger) in the pumping as well as in some monitoring wells. Three slug tests and five Lefranc tests were carried to calculate the hydraulic conductivity of the coarser and the finer sediments, respectively.

Resistivity data were collected at the university campus using a commercial georesistivimeter, to understand how continuous the confining silty-clay horizon at a scale larger than that of a single borehole was. The measurements were inverted to a true resistivity volume using a finite elements approach on a tetrahedral grid. Inversion was fully 3D and topography was also modelled to account for electrical field distortion due to morphology gradients. This inversion algorithm is well described in the literature (e.g. Cardarelli and Fischanger 2006) and it is generally indicated as the smoothness-constrained approach under Occam assumptions. The misfit between measured and calculated values was lower than 5% for most of the collected data points.

3.2 Isotopic and chemical investigations

The sampling campaigns for chemical, stable isotope ($\delta^{18}O$, $\delta^{2}H$) analyses and metagenomic analyses were carried out from March 2017 to February 2018 every 3 months, approximately. The rainfall at the Parma Campus station was collected on a monthly basis using 10-l polyethylene bottles containing about 300 ml of vaseline oil to prevent the evaporation processes. Oil contamination was carefully avoided by syringing the water samples out of the bottle.

pH measurements were performed in field with multiparametric probe. Alkalinity was determined by Gran titration with HCl. Main anion concentrations were determined by ion chromatography at the Aquatic Ecological Laboratory of the University of Parma, Italy. Samples for cation analysis were acidified at $pH < 3$ with concentrated HNO_3. Global analytical accuracy was evaluated by ionic balance. The main contaminants (hydrocarbons, chlorinated solvents, etc.) were analysed in a certified private laboratory.

Stable isotope analyses ($\delta^{18}O$, $\delta^{2}H$) were carried out at the Isotope Geochemistry Laboratory of the University of Parma, Italy. The analytical prediction uncertainty was better than 0.1‰ for $\delta^{18}O$ and about 1.0‰ for $\delta^{2}H$. The compositions of $\delta^{18}O$ and $\delta^{2}H$ are reported as $10^3 \times \delta^{18}O$ (V-SMOW, Vienna Standard Mean Ocean Water).

3.3 Microbiological and metagenomic investigations

Several studies demonstrated the possibility of using microbial communities as natural tracers of subsurface dynamics (e.g. Naclerio et al. 2009; Celico et al. 2010; Bucci et al. 2017; Farnleitner et al. 2005; Mayer et al. 2016). In this case, microbiological and metagenomic analyses were carried out to verify the existence or not of an autochthonous microbial community able to degrade chlorinated solvents.

Water samples for metagenomic analyses were collected in sterile 1000 ml bottles and transported in a refrigerated box. Filtration processes were completed within 2 h after sampling. The profile of bacterial populations thriving in groundwater partially contaminated by organic chlorinated solvents, of the DNPLs type, was analysed. DNA was extracted from groundwater and NGS 16SrDNA profiling was obtained at the Genprobio Srl Laboratory.

Partial 16S rRNA gene sequences were amplified from extracted DNA Amplifications were carried out and PCR products were purified by the magnetic purification step. Sequencing was performed using an Illumina MiSeqsequencer with MiSeq Reagent Kit v3 chemicals. The fastq files were processed using QIIME (Caporaso et al. 2010). To calculate downstream diversity measures, operational taxonomic units (OTUs) were defined at 97% sequence homology (Edgar 2010). All reads were classified to the lowest possible taxonomic rank using QIIME (Caporaso et al. 2010) and a reference dataset from the SILVA database (Quast et al. 2013). Similarities between samples (beta-diversity) were calculated by Jaccard index using a Dendro-UPGMA program available at http://genomes.urv.es/UPGMA/.

For growth and isolation of the methylotrophic bacteria detected with metagenomic analysis, two selective media were prepared, HYP (Kanamaru et al. 1982) and NMS (https://www.dsmz.de/catalogues/catalogue-microorganisms.html), while TSB medium (tryptic soy broth) was used for the propagation of the bacterial isolates.

Five enrichment cycles were carried out on the two selective culture media HYP and NMS, by adding methanol (1% v/v), as the sole source of carbon, to the single tubes in two parallel enrichment lines. Once the five enrichment cycles have been completed, the bacteria were inoculated on HYP and NMS media solidified with agar. The 25 colonies

isolated by repeated streaks on the selective media were then checked for growth with and without methanol to exclude the presence of autotrophs

As the enzyme methane monoxygenase, possessed by some methylotrophic bacteria, is known to be able to catalyse a fortuitous reaction of dehalogenation on organic halogenate compounds, a dechlorination assay was performed for detecting the chlorine ions released from a halogenated test molecule by the selected bacteria (Song et al. 2004; Bergmann and Sanik 1957).

3.4 *Folsomia candida* tests

Water collected in nine water wells was tested (P3, P5, P6, P14, P15, P16, P17, P18, P19 in Fig. 2a). Water samples for *Folsomia candida* tests were collected in 1000 ml bottles and transported in a refrigerated box to the laboratory. The springtails *F. candida* used in the test were sourced from laboratory cultures at the Parma University, previously synchronized removing the eggs from the culture, and, after the start of hatching, putting in Petri dishes with the breeding substrate. After 10 days, the juveniles were ready for the test to be performed. The experiment considered the springtails' survival. Five replicates for each water sample were prepared adding water to reach 60% of WHC in Petri dishes containing filter papers. Ten specimens from synchronized breeding cultures were transferred into each. 2 mg of pulverized cereal mix was given as food. The Petri dishes were incubated for 14 days in a temperature conditioned room at 20 ± 2 °C. Once a week, the dishes were aerated, the corresponding water was added to reach 60% of WHC, and organisms were fed with 2 mg of cereal mix. At the end of the test, adults were counted under a stereomicroscope after floatation.

Folsomia candida tests were carried out to evaluate the potential groundwater contamination, because this Collembola is an effective bioindicator often used in ecotoxicological studies.

3.5 Plant diversity analysis

Plant diversity was explored at the heads and the first sectors of fed channels (about 50–100 m in length) of five *fontanili* flowing out at the study area, in October 2016 by a whole flora meandering searches exploring the entire habitat under investigation. At each site, the presence of all the visible macrophytes was assessed using an aquascope (i.e. a bucket with a transparent bottom). In addition, several vascular specimens were collected for laboratory identification.

The plant diversity analysis was carried out to characterize the GDEs (*fontanili*) from the biological point of view.

3.6 Numerical flow model

Numerical groundwater modelling is widely used for environmental applications for: (i) investigation of the aquifer properties (e.g. Fienen et al. 2009; Zanini et al. 2017; D'Oria et al. 2018), (ii) prediction of the pollution spread and strength at a site (e.g. Gzyl et al. 2014; Chen et al. 2016), (iii) identification of pollution sources (e.g. Neupauer and Lin 2006; Cupola et al. 2015; Zanini and Woodbury 2016), (iv) design and test of reclamation actions (e.g. Xu et al. 2012) and (v) evaluation of well-capture areas (e.g. Paradis et al. 2007; Chelli et al. 2018; Feo et al. 2018) for developing hydraulic barriers. With the aim of reconstructing the groundwater flow net and the possible effects of groundwater contamination within the rural area, a numerical flow model was implemented at FUA scale. All the computations were performed by MODFLOW 2005 (Harbaugh 2005; Harbaugh et al. 2017). The boundaries of the model are: Po River at north (hydrogeologically downstream), Enza River at east, Taro River at West and the Apennine piedmont south of the Parma town. Concerning the relationships between rivers and shallow groundwater, only the Po River plays an important role as boundary conditions, because it is the only river interacting directly with the shallow aquifer at FUA scale.

The grid frame covers an area of 25×40 km^2. The FUA is represented through a finite difference grid of 200×200 m^2 with 200 rows and 125 columns (25,000 cells per layer). Considering the boundary conditions, only 15,467 cells per layer are active. The active area is about 627 km^2.

The FUA area was represented with two layers: the first one represents the shallow clayey material and the second one the investigated aquifer.

4 Results

4.1 Geological and hydrogeological setting

The reconstruction of the lithostratigraphic sequence takes advantage of the results of stratigraphic and *facies* analysis, using the information from the 14 boreholes drilled within this work. The lithostratigraphic sections allowed the reconstruction of a reliable conceptual model. Beneath the ground surface, the stratigraphic sequence begins with deposits made by silt and clay, whose thickness progressively increases from 1 to 19 m moving northward. Below this horizon, the confined "shallow aquifer" (mainly made of gravels and sands with discontinuous clay lenses) whose thickness is some tens of meters, at least can be found. It is continuous throughout the whole investigated stratigraphic sequence, while it is not detected in the southern end of the FUA where the shallow aquifer is unconfined (Di Dio

2005). Beneath the "shallow aquifer", a continuous bed of fine-grain-sized deposits has been found.

This lithostratigraphic model was further supported by the results of the geophysical investigations. A resistivity profile was extracted from the 3D resistivity volume along the section with higher sensitivity and data were interpretable down to a depth of about 30 m below the surface. The resistivity distribution in depth well shows the presence of a continuous aquifer (300 Ωm, up to 15 m thick at the University Campus), confined between two silty-clay continuous horizons. The upper horizon (50 Ωm) is up to 3 m thick, according to the boreholes stratigraphies, while the lowest one (30 Ωm) is at least 10 m thick.

The hydraulic parameters (transmissivity and storativity) of the shallow aquifer, estimated by means of the pumping test that was carried out at the university campus well field, were 3×10^{-4} m^2/s and 1.9×10^{-4}, respectively. These values are in agreement with the hydraulic conductivity values ($1.0–2.0 \times 10^{-5}$ m/s) calculated through the slug tests performed in the other purpose-drilled boreholes. The hydraulic conductivity (in the order of $10^{-7}/10^{-9}$ m/s) of the finer-grained deposits (aquitards) was calculated by means of Lefranc tests.

On the whole, the shallow groundwater flows from south to north. The groundwater head is not strictly characterized by rapid fluctuations during rainfall events (Fig. 3). This observation is in agreement with the existence of a continuous confining horizon throughout the study area, which does not allow local recharge due to effective infiltration of rainwater and leakage from surface channels. Therefore, the shallow groundwater is recharged upgradient of the urbanized area, where (i) the shallow aquifer crops out, (ii) the rivers are hydraulically linked to the shallow groundwater and (iii) the nearby relieves (Apennines) laterally feed the alluvial aquifer.

The Local Meteoric Water Line (LMWL) was defined using data from 2008 to 2015. The resulting major axis regression line is the following (Fig. 4):

$$\delta^2 H = 7.67\,(\pm 0.07)\,\delta^{18}O + 7.56\,(\pm 0.43) permil.$$

This equation is far from the meteoric water line found by Longinelli and Selmo (2003) for the Northern Italy precipitation (δ^2H = 7.71 δ^{18}O + 9.40). This is not surprising because the thermal features of the perturbations are largely variable in Northern Italy. The annual weighted δ^{18}O mean values of precipitation change largely (from − 10.0 to − 7.6‰, from 2008 to 2015): the average value is − 8.86 ± 0.74 (standard deviation). On the other hand, the Parma, Enza, and Baganza rivers for the period February 2004–August 2006 gave an average value of − 8.79 ‰ (Iacumin et al. 2009), whereas wells of the Parma area gave an average value of − 8.51‰; moreover, recent data on wells in the Parma area give, on

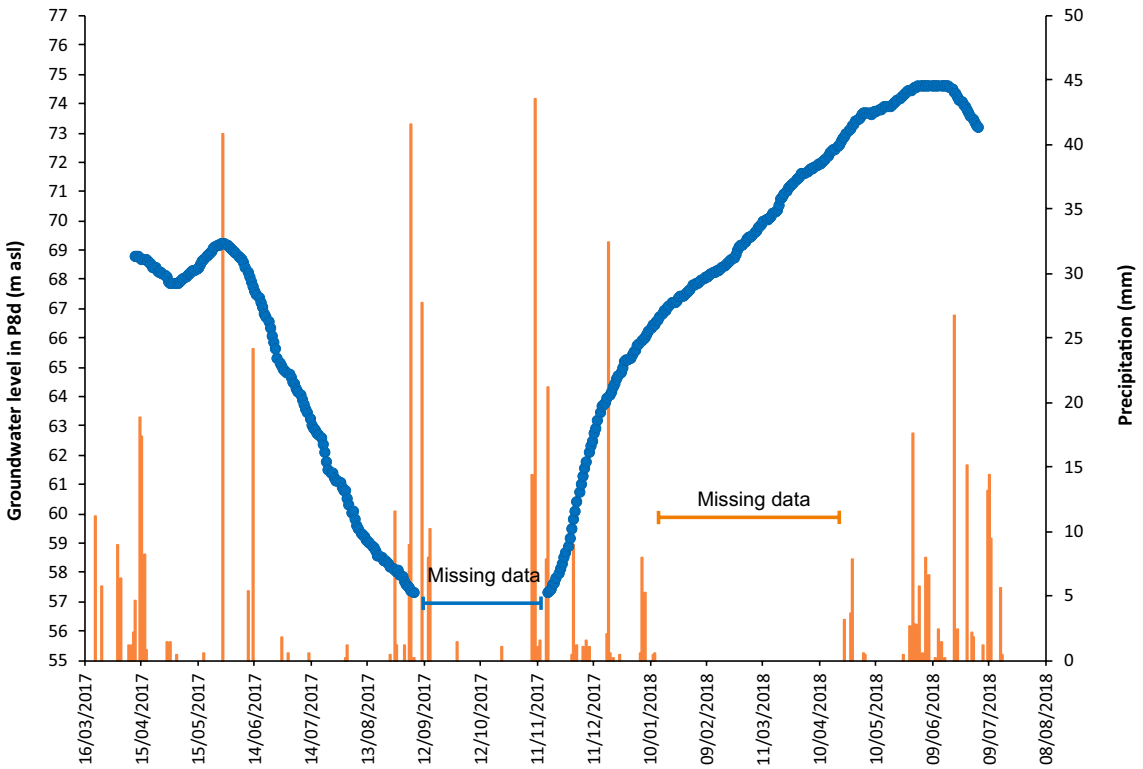

Fig. 3 Groundwater level fluctuations in P8d (dotted line) and daily rainfall in Parma meteorological station (bars)

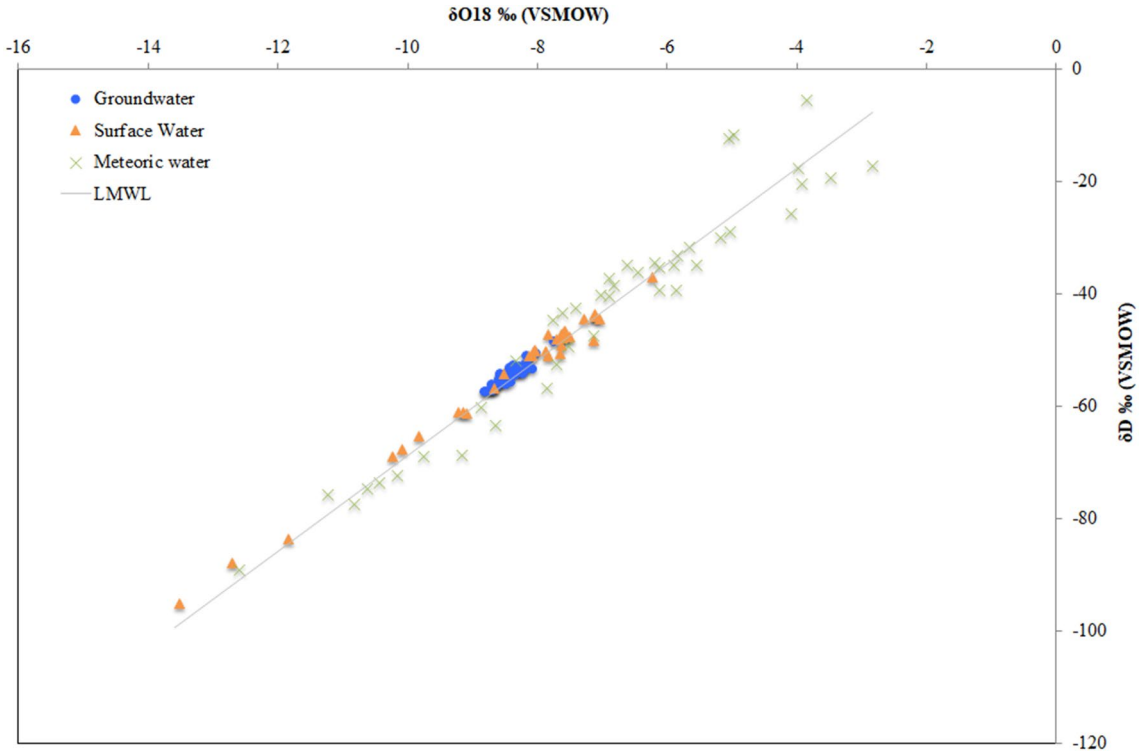

Fig. 4 $\delta^{18}O$ vs $\delta^{2}H$ relationship in rainfall surface and groundwater samples

average, − 8.41‰. Practically, all these values are the same, indicating that rivers and groundwater from the Apennines feed the shallow aquifers within the Parma plain. This data also confirm the finding of the shifted answer of the piezometric fluctuation compared with the local precipitation.

4.2 Groundwater contamination

Nitrate concentrations in groundwater varied over space and time, during the observation period. Concentration was lower in summer and autumn, and rapidly increased in winter. For example, in well P5 the NO_3 concentrations changed from less than 10 mg/L (in July and September 2017; see example in Fig. 5) to 48 mg/L (in December 2017 and February 2018; see example in Fig. 5). Moreover, the concentrations seem to increase northwards, along the groundwater flow lines. For example, in December 2018, concentration in groundwater increased from less than 20 mg/L to up to 30 mg/L from south to north. The exception was the well P5 (located in the city centre) where the highest nitrate concentration was detected (Fig. 5). On the whole, this preliminary investigation suggests the existence of two main nitrate sources. The first source is located in the southern part of the studied FUA and coincides with the agricultural lands in the upper plain, where the shallow aquifer is unconfined. According to observations made worldwide, agricultural lands suffer excess nitrogen application that is not assimilated by crops and, thus, pollutes surface and groundwater (e.g. Hu et al. 2010; Bartoli et al. 2012). In irrigated areas, nitrate is involved in fast transfer towards water bodies (Hu et al. 2010; Sutton et al. 2011; Savci 2012). During the summer period, water of irrigation flows into the surface channels with relatively high nitrate concentration (see for example the sampling campaign made in July 2017; Fig. 5) and migrates easily trough permeable soils, thus creating a major risk of groundwater contamination. Taking also into consideration the transfer time of nitrates in the saturated zone, the easy migration is in agreement with the seasonal variations of nitrate concentrations at the study site. At the same time, the coexistence of high nitrate concentration in surface channels close to the university campus (more than 50 mg/L in S3 in Fig. 5) and the very low concentrations in the local groundwater (less than 10 mg/L in all the piezometers drilled at the Campus area) further supports the absence of hydraulic interaction between surface- and groundwater within the studied portion of the urban plain. The results are in agreement with the finding of groundwater response to precipitation and the isotopic analyses. The second source of nitrates is seepage from the sewer systems in the urban area, according to the highest value detected in piezometer P5.

Chlorinated solvents in concentration higher (PCE up to 15 µg/L) than the legal limits (PCE up to 1.1 µg/L) occurred in groundwater in some observation piezometers. The highest concentrations were detected in a known contaminated

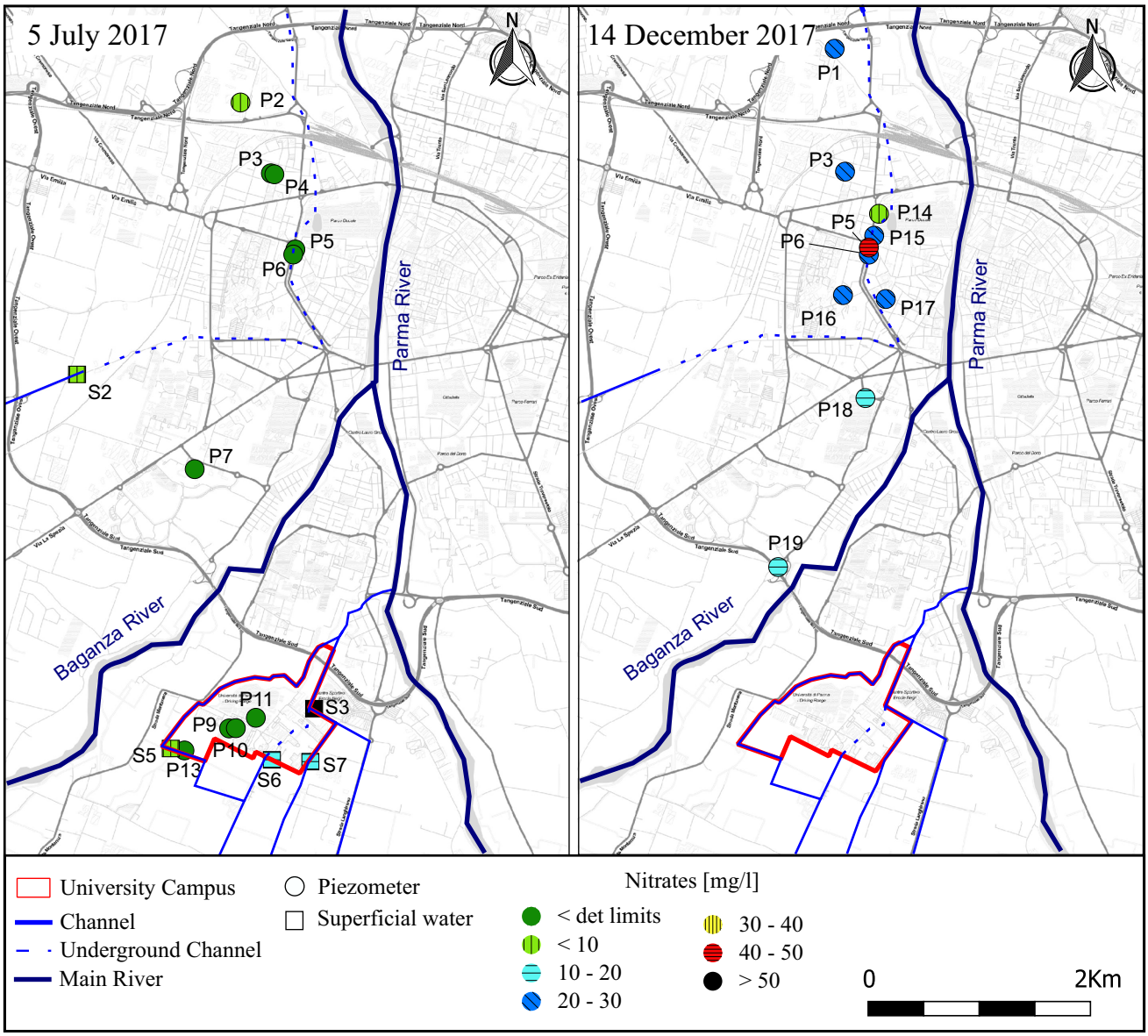

Fig. 5 Nitrate distribution in the shallow groundwater

site of the city centre (e.g. P5 in Fig. 5), as well as downgradient starting from this site (e.g. P3 in Fig. 5). In single observation wells, the PCE concentration varied over time, therefore suggesting possible PCE pools located in the transition zone between the lowest and the highest hydraulic head measured during the observation period. The spatial distribution of PCE suggests the existence of multiple pools, because the highest concentrations cannot be explained as part of a unique plume. At the same time, the rapid decrease of concentration downgradient starting from the most polluted site suggests effective dilution due to dispersion and/or attenuation due to microbial degradation. The latest hypothesis was further investigated through metagenomic analyses (see hereafter).

4.3 Microbial communities

The results obtained with the molecular analyses (community profiling by NGS sequencing) highlighted that the bacterial community present in the groundwater collected in the various piezometers along the groundwater pathway is mainly composed of aerobic bacteria.

Analysis of the samples from the most contaminated piezometers unveiled a community containing a higher percentage of methophiles belonging to different genera (*Methylobacter*, *Methylocella*, *Methylococcus*, *Crenothrix*), all known for being endowed with methane monooxygenase. The presence of these bacterial genera suggested that the most probable pathway of biodegradation of the chlorinated solvents

(e.g. PCE) could be an oxidative (co-metabolic) dehalogenation by means of methane monooxygenase. These bacterial genera were present only in the water from piezometers closer to the focus of PCE contamination (P3, P5 and P6). Bacteria obtained by enrichment, selection and isolation procedures were able to grow with methanol as the sole carbon source. In addition, through the test of the dehalogenase activity, it was shown that some of these isolated bacterial strains have indeed the capacity to dehalogenate chlorinated organic compounds. The isolated strains have been identified as *Proteobacteria* of the *Methylophilaceae* family. Moreover, the samples from wells P5 and P6 contained a number of sequences belonging to the *Rhodoferax* genus known to be a vinyl chloride (VC) utilizing bacterium (Paes et al. 2015) This may indicate a possible reductive pathway in anaerobic niches of the plume leading to incomplete degradation and transport of the contaminant in the aerobic zone where *Rhodoferax* can use it. VC was never found among contaminants.

4.4 *Folsomia candida* tests

The results obtained in this study highlight some differences in *F. candida* survival between water samples. The percentage of surviving specimens comprised between 47% and 83% after 14 days of the test (Fig. 6). P6 and P15 showed the highest percentage of survival with a springtail mortality of 17 and 23%, respectively, followed by P18, showing a mortality of 30%. P3 reported the smallest number of survivors, 47%. P6 and P18 showed the highest variability of results (Fig. 6). However, despite the brief period of the test, P3, P14, P15, P18 and P19 showed eggs and juvenile springtails in the test containers. This suggests that also for water samples where the mortality was higher, the reproduction was not completely inhibited. In a study aimed to evaluate biochar toxicity on *F. candida*, Conti et al. (2018) reported that the reproduction proved to be a more sensitive end point in comparison to survival.

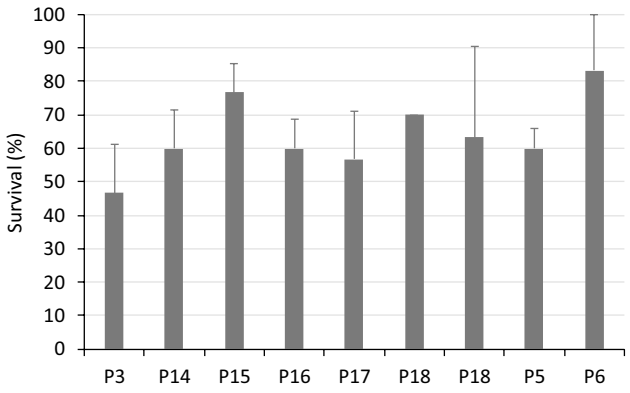

Fig. 6 Survival (in %) of *F. candida* during the test. The error bars correspond to the standard error

On the whole, the results of these tests cannot be completely explained considering only PCE and nitrate contamination, therefore suggesting the possibility of the existence of other types of contaminants not analysed in this study.

4.5 Plant diversity

A total of 38 vascular plants were recorded, with an overall mean number of 21.4 ± 6.7 taxa per site (Table 1). Two additional macroalgal taxa were also recorded: *Chara vulgaris* Linnaeus 1753 and *Nitella mucronata* (A. Braun) F. Miquel 1840 for a total of 40 species were recognized. The most widespread plant taxa, recorded in all the habitats investigated, were amphibian species typical of ecotonal belts (i.e. marginal ecotones): *Lycopus europaeus* L. subsp. *europaeus*, *Lythrum salicaria* L., *Mentha aquatica* L., *Ranunculus repens* L., and *Symphytum officinale* L. subsp. *officinale*. On the contrary, these aquatic species were rather less represented, with exclusively three species present in at least three (*Sparganium erectum* L. subsp. *erectum*) or two sites (*Alisma plantago-aquatica* L. and *Callitriche stagnalis* Scop.), respectively. However, despite the extremely reduced area occupied by *fontanili* (in the order of 300 m^2), a total of 13 hydrophytes were recorded (including the two macroalgae). This is a relevant output compared to data available for the main large lakes of North Italy (up to 370 km^2 for the Garda Lake) that indicate a hydrophyte diversity in the range of 11–26 species (Bolpagni et al. 2013a, 2017).

These data reinforce previous evidences highlighting the pivotal role of GDEs in supporting biodiversity at the local scale, especially in lowlands affected by huge human-driven alterations (Kuglerová et al. 2014; Bolpagni and Laini 2016; Bolpagni et al. 2016). The present results are also in strong agreement with those obtained by Bolpagni et al. (2013b) and Bolpagni and Piotti (2015, 2016) for a series of aquatic habitats placed along the Oglio River, a left tributary of the Po River located about thirty linear kilometres far from the area under analysis. More in detail, the semi-natural lotic habitats in analysis exhibit a relatively high plant diversity in line with that of lentic habitats (6.5 ± 4.2 taxa per site, respectively). This is probably due to the high water level stability of *fontanili*, thanks to their stable underground feeding throughout the year. In fact, this type of water feeding guarantees minimum fluctuations in the hydrometric levels of *fontanili*, as verified by Bolpagni et al. (2013b) for the marginal habitats of the Oglio River. Generally, *fontanili* act actively as refugee for a very rich aquatic and amphibian flora suggesting a key role in local to global strategies for plant conservation (Bolpagni et al. 2018). However, as widely discussed in the present paper, groundwater is largely impacted by multiple stressors that can heavily affect its quality, and cascading the quality of the biocoenoses it sustains. Accordingly, further investigations are needed to better

Table 1 List of the plant species recognized in the five investigated *fontanili*

LF	Species	F1	F2	F3	F4	F5
I rad	*Alisma plantago-aquatica* L.				x	x
G rhiz	*Berula erecta* (Huds.) Coville		x	x	x	x
I rad	*Callitriche stagnalis* Scop.		x	x		
H scap	*Cardamine amara* L. subsp. amara		x	x		x
He	*Carex acutiformis* Ehrh.		x	x		
He	*Carex riparia* Curtis	x	x		x	x
G rhiz	*Eleocharis palustris* (L.) Roem. & Schult.				x	x
I rad	*Elodea canadensis* Michx.					x
G rhiz	*Equisetum ramosissimum* Desf.	x		x	x	x
H scap	*Galium palustre* L. subsp. elongatum (C. Presl) Lange	x	x	x		x
I rad	*Glyceria maxima* (Hartm.) Holmb.					x
I rad	*Groenlandia densa* (L.) Fourr.		x			
G rhiz	*Iris pseudacorus* L.			x	x	x
G rhiz	*Juncus articulatus* L.			x		x
G rhiz	*Juncus subnodulosus* Schrank		x	x		
H scap	*Lycopus europaeus* L. subsp. europaeus	x	x	x	x	x
He	*Lythrum salicaria* L.	x	x	x	x	x
H scap	*Lysimachia nummularia* L.		x	x	x	x
H scap	*Lysimachia vulgaris* L.	x	x	x	x	
H scap	*Mentha aquatica* L.	x	x	x	x	x
H scap	*Myosotis scorpioides* L.		x	x	x	x
I rad	*Myriophyllum spicatum* L.			x		
H scap	*Nasturtium officinale* R. Br.		x	x		
He	*Phragmites australis* (Cav.) Trin. ex Steud. s.l.		x	x	x	x
I rad	*Potamogeton acutifolius* Link		x			
I rad	*Potamogeton crispus* L.			x		
I rad	*Potamogeton friesii* Rupr.		x			
H rept	*Ranunculus repens* L.	x	x	x	x	x
H scap	*Rorippa amphibia* (L.) Besser			x		x
H scap	*Scrophularia auriculata* L.	x		x		x
NP	*Solanum dulcamara* L.			x	x	x
H scap	*Stachys palustris* L.		x	x	x	x
I rad	*Stuckenia pectinata* (L.) Börner			x		
I rad	*Sparganium erectum* L. subsp. erectum			x	x	x
H scap	*Symphytum officinale* L. subsp. officinale	x	x	x	x	x
G rhiz	*Typha latifolia* L.				x	x
H rept	*Veronica beccabunga* L.		x			
H scap	*Veronica anagallis-aquatica* L.	x	x	x		x

For each taxon, we reported the presence/absence datum, and the life form (LF) as follows: *G rhiz* rhizomatous geophyte, *H rept* reptant hemicryptophyte, *H scap* scapose hemicryptophyte, *He* helophyte, *Hy* hydrophyte, *NP* nano-phanerophyte

clarify the interplay between groundwater resurgence and biotic diversity across multiple spatial and temporal scales, especially in lowland human-driven plains.

4.6 Numerical flow model

Since the shallow groundwater flows in confined conditions within the most part of the modelled area, the recharge of the aquifer was represented through a boundary condition at south as the general head boundary. The shallow aquifer at the study area is essentially recharged by rainwater infiltrating within the southern part of the plain, as well as by nearby aquifers belonging to the Apennine Chain, in agreement with findings in other sites (e.g. Aquino et al. 2015; Petrella and Celico 2009) and in agreement with the results of isotopic investigations.

Once the model was completed, it was calibrated at first in steady state using the hydraulic heads monitored

by the Emilia Romagna Environmental Protection Agency (ARPAe; data available at https://www.arpae.it/elenchi_dinamici.asp?tipo=dati_acqua&idlivello=2020).

Taking into account the small amount of information available about the hydraulic features of the shallow aquifer, an estimation of the hydraulic conductivity field was obtained through the software PEST (Doherty and Hunt 2010). In particular, the pilot points procedure was considered. The hydraulic conductivity of the outcropping low-permeability horizon was set to 5×10^{-7} m/s.

The hydraulic conductivity of the aquifer medium (second layer) was estimated through a calibration performed at first in steady state to evaluate a starting solution of the hydraulic conductivities and then in transient conditions using the hydraulic heads measured in the ARPAe wells. Figure 7 shows the location of the pilot points used in the

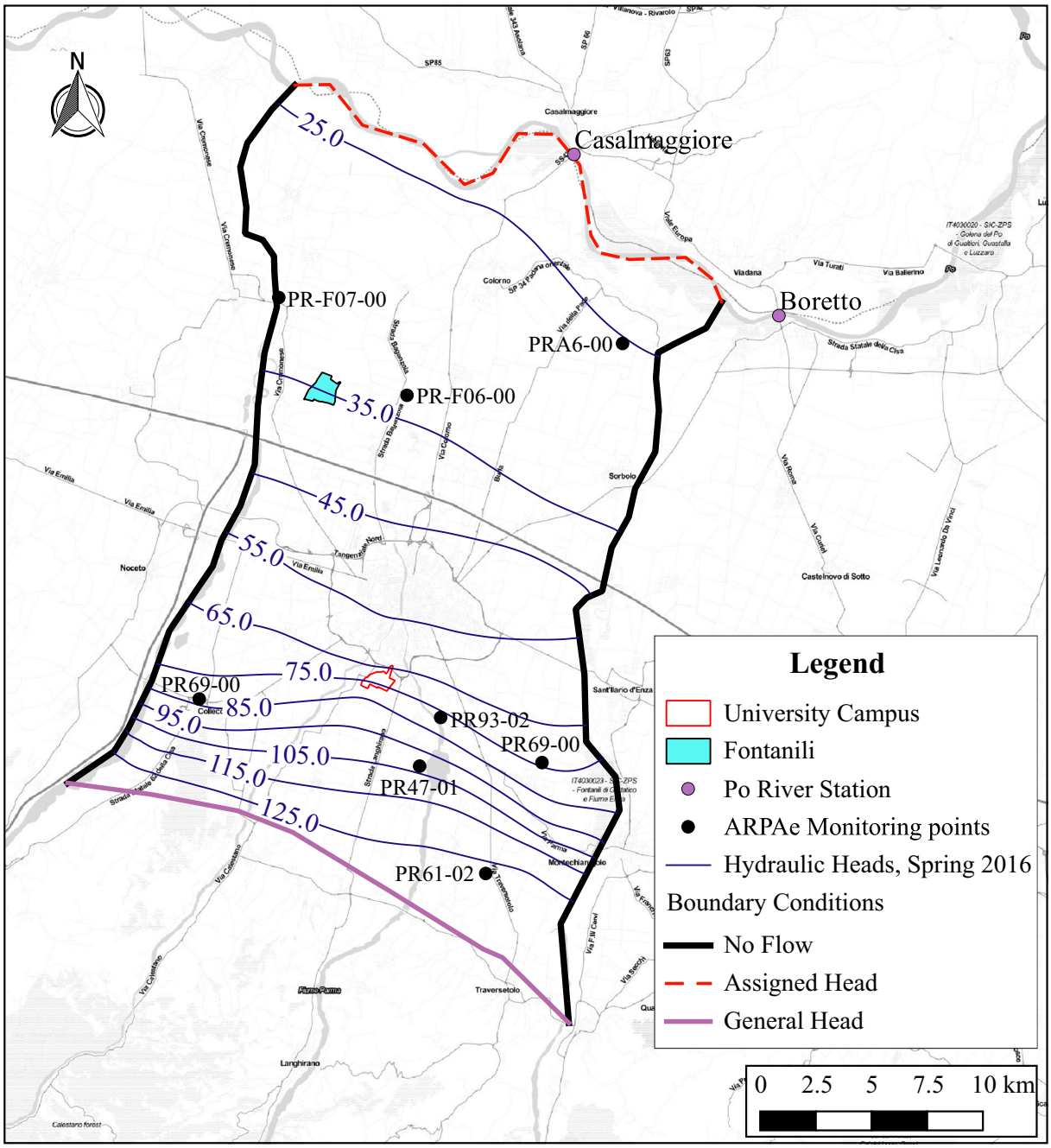

Fig. 7 Modelled groundwater flow net

estimation procedure. An exponential variogram with a small variance (0.2) and a range of 5 km was assumed.

The transient model reproduces 2400 days from April 1, 2010 to October 26, 2016 through 80 stress periods of 30 days each. Stress periods are subdivided into 30 time steps of 1 day. The upstream and downstream boundary conditions (BC) were set up according to observations. In particular, the downstream BC was set up according to the Po River daily level measurement at two monitoring stations (Fig. 7). The upstream boundary condition was set up according to piezometric contour heads. The observations at the monitoring wells showed a seasonal variability. Considering the available data at the ARPAE wells for the period 2010–2016, it was noticed that the average difference between maximum and minimum was about 4 m. The mean estimated level at the upstream boundary conditions was 128 m a.s.l.. For this reason, the upstream boundary condition was set up as a sinusoidal wave with a period of 360 days and a variation of ± 2 m with respect to the average level.

The widely accepted measure of model calibration (Anderson and Woessner 1992) is the normalized root mean square error (nRMSE). If nRMSE is below 10% (ASTM 2006), the model calibration is acceptable.

The following statistics are considered to evaluate the calibration results:

$$\text{Mean error (ME)} : \frac{1}{N}\sum_{i=1}^{N} \mathrm{Hc}_i - \mathrm{Ho}_i,$$

$$\text{Mean absolute error (MAE)} : \frac{1}{N}\sum_{i=1}^{N} \left|\mathrm{Hc}_i - \mathrm{Ho}_i\right|,$$

$$\text{Root mean square error (RMSE)} : \sqrt{\frac{1}{N}\sum_{i=1}^{N} \left(\mathrm{Hc}_i - \mathrm{Ho}_i\right)^2},$$

$$\text{Normalized root mean square error (nRMSE)} : \frac{\sqrt{\frac{1}{N}\sum_{i=1}^{N} \left(\mathrm{Hc}_i - \mathrm{Ho}_i\right)^2}}{H_0\mathrm{MAX} - H_0\mathrm{MIN}},$$

where N è is the number of observations, $\mathrm{Hc_i}$ is the computed hydraulic head level at the monitoring point i, $\mathrm{Ho_i}$ is the observed hydraulic head level, and H_0MAX and $\mathrm{H_0MIN}$ are the maximum and minimum observed hydraulic head.

Figure 8 shows the good agreement between the computed and observed hydraulic heads. Considering the statistics and in particular the nRMSE value, the capability of the numerical model of reproducing the observed values is clear. In this case, 111 observations were used.

Figure 9 shows, as example, the computed and observed hydraulic head levels at the monitoring point PR-F07-00. It is possible to see the good agreement between the computed and observed values and the dependence on the boundary conditions.

5 Parma FUA in a hydro-geo-ecological perspective

The Parma FUA hydro-geo-ecology (sensu Hanckock et al. 2009) was investigated through an interdisciplinary approach, with emphasis on the shallow aquifer system. This approach was carried out because there is an increasing recognition that groundwater is essential not only for human uses (domestic and agricultural, at the study site), but also for many ecological communities. As a matter of fact, when the groundwater flows out or comes close to the ground surface, the contribution of water and nutrients influences both the type and the persistence of aquatic ecosystems. At the same time, groundwater contaminants can have a negative impact on human health, as well as on aquatic communities.

The study pointed out that domestic wells and *fontanili* are both fed by shallow groundwater at least affected by PCE and nitrate contamination, upgradient of the rural area located north of Parma city. Moreover, *Folsomia candida* tests suggested the possibility that other types of contaminants (not analysed in this study) can affect the shallow groundwater.

Nowadays, PCE concentrations in the city centre are slightly higher than the legal limit. Moreover, PCE aerobic biodegradation can be due to the local microbial community and then an effective natural attenuation can be expected along the groundwater flow pathway. These results suggest a very low risk for human health, linked to the groundwater consumption in the rural area north of Parma City. Conversely, no forecasts can be made at present about the possible impact of low PCE concentrations on the aquatic ecosystem observed at the *fontanili*, because no information exists about the effects of a prolonged interaction between low-level chlorinated solvents and local biological species. Concerning nitrate contamination, the higher concentrations detected in some wells and *fontanili* suggest a high risk for both human health and aquatic ecosystems.

Taking into consideration the main findings of this work and the existence of other contamination sources not involved in this preliminary investigation (e.g. a

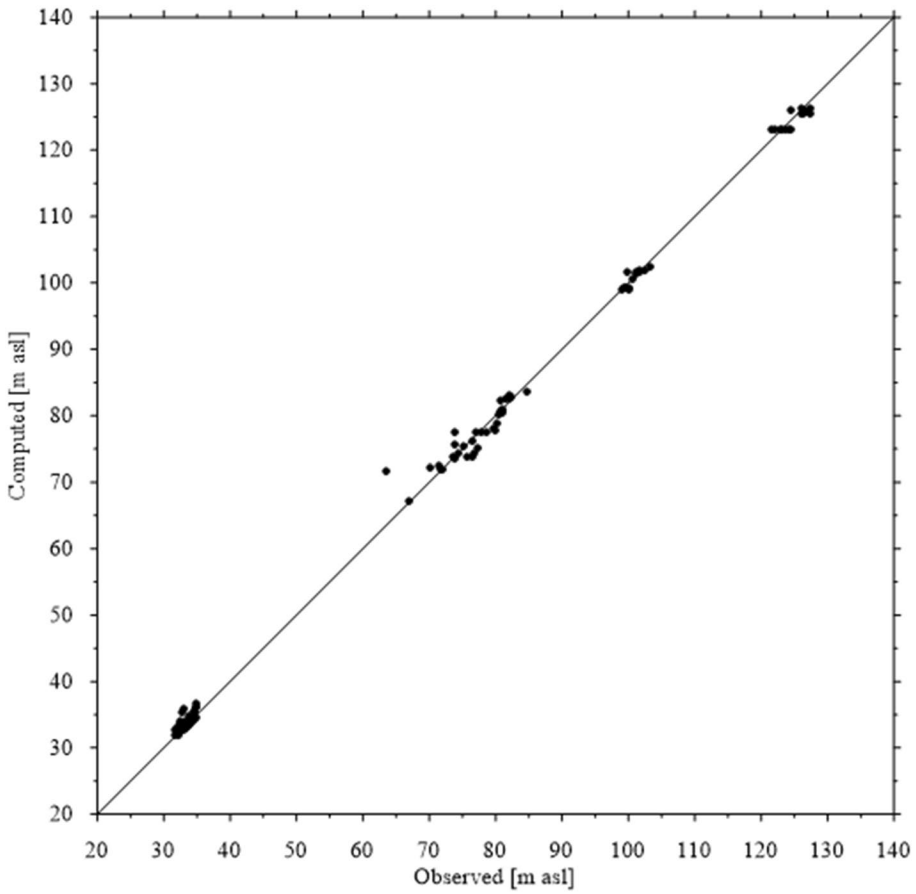

Fig. 8 Computed vs observed hydraulic head levels at PR-F07-00

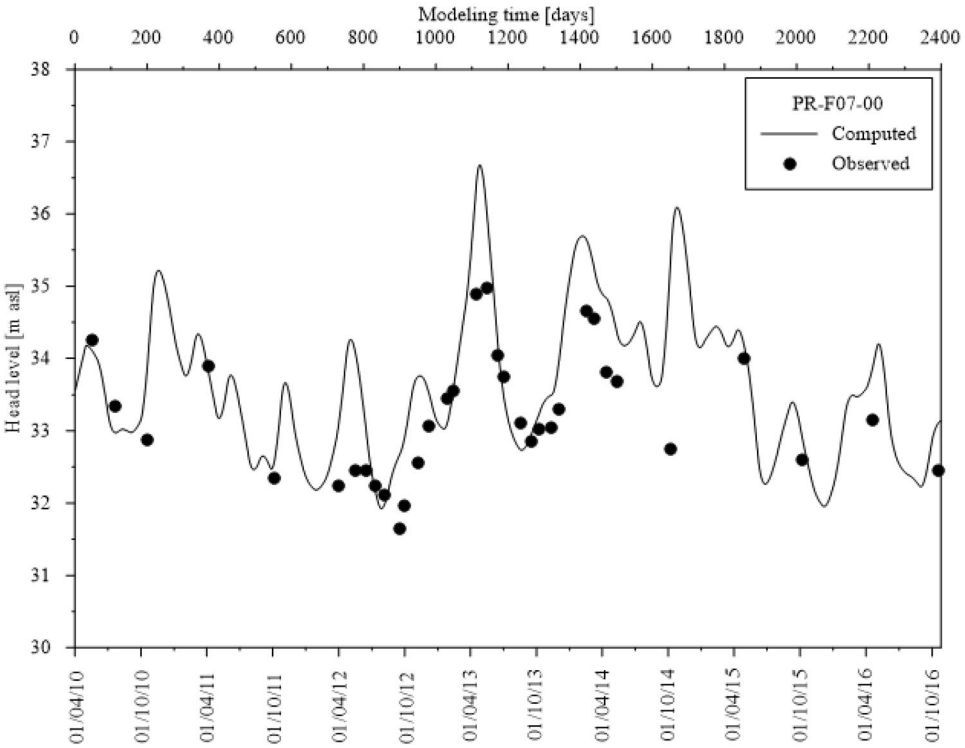

Fig. 9 Observed and modelled hydraulic head levels vs time at PR-F07-00

decommissioned municipal landfill), a long-term hydro-geo-ecological study has been planned. This study will also check possible progressive changes in groundwater temperature due to the increasing number of shallow geothermal boreholes within the FUA. Actually, these boreholes could alter the thermal equilibrium and, thus, make the environment incompatible with the existing biotic species at the *fontanili*. In fact, it is known that the persistence of some organisms in specific aquatic environments is more driven by water temperature than, for example, the hydrochemical features (e.g. Bolpagni and Laini 2016).

In a wider context, thanks to the interdisciplinary approach that combines successfully well-established investigation methods, the present study allows a better knowledge of the hydro-geo-ecological behaviour of GDEs. At the same time, through purpose-designed experimental investigations and simulation models, this approach could be used as a sort of guideline useful in studying such complex environmental systems.

Acknowledgements The research was supported by UE (INTERREG Central Europe) via the AMIIGA Project. The authors would like to thank Prof. Antonio Longinelli and another anonymous reviewer for their fruitful comments.

References

Abdelahad N, Bolpagni R, Lasinio GJ, Vis ML, Amafio C, Laini A, Keil E (2015) Distribution, morphology and ecological niche of *Batrachospermum* and *Sheathia* species (Batrachospermales, Rhodophtyta) in the fontanili of the Po plain (northern Italy). Eur J Phycol 50:318–329

Anderson MP, Woessner WW (1992) Applied Groundwater Modeling: simulation of flow and active transport. Academic press, San Diego

Aquino D, Petrella E, Florio T, Celico P, Celico F (2015) Complex hydraulic interactions between compartmentalized carbonate aquifers and heterogeneous siliciclastic successions: a case study in southern Italy. Hydrol Process 29:4252–4263

ASTM D5880–95 (2006) Standard guide for subsurface flow and transport modelling. ASTM International, West Conshohocken, Pennsylvania

Bartoli M, Racchetti E, Delconte C, Sacchi E, Soana E, Laini A, Longhi D, Viaroli P (2012) Nitrogen balance and fate in a heavily impacted watershed (Oglio River, Northern Italy): in quest of the missing sources and sinks. Biogeosci 9:361–373

Bassanino M, Sacco D, Zavattaro L, Grignani C (2011) Nutrient balance as a sustainability indicator of different agroenvironments in Italy. Ecol Indic 11:715–723

Bergmann JG, Sanik J (1957) Determination of trace amounts of chlorine in naphtha. Anal Chem 29:241–243

Bolpagni R, Laini A (2016) Microhabitat patterns of soft-bodied benthic algae in a lowland river largely fed by groundwater. Fottea 16:244–254

Bolpagni R, Piotti A (2015) Hydro-hygrophilous vegetation diversity and distribution patterns in riverine wetlands in an agricultural landscape: a case study from the Oglio River (Po plain, Northern Italy). Phytocenologia 45(1–2):69–84. https://doi.org/10.1127/0340-269X/2014/0044-0586

Bolpagni R, Piotti A (2016) The importance of being natural in a human-altered riverscape: role of wetland type in supporting habitat heterogeneity and vegetation functional diversity. Aquat Conserv Mar Freshw Ecosyst 26:1168–1883. https://doi.org/10.1002/aqc.2604

Bolpagni R, Bettoni E, Bonomi F, Bresciani M, Caraffini K, Costaraoss S, Giacomazzi F, Monauni C, Montanari P, Mosconi MC, Oggioni A, Pellegrini G, Zampieri C (2013a) Charophytes of Garda lake (Northern Italy): a preliminary assessment of diversity and distribution. J Limnol 72:388–393

Bolpagni R, Bartoli M, Viaroli P (2013b) Species and functional plant diversity in a heavily impacted riverscape: implications for threatened hydro-hygrophilous flora conservation. Limnologica 43(4):230–238

Bolpagni R, Racchetti E, Laini A (2016) Fragmentation and groundwater supply as major drivers of algal and plant diversity and relative cover dynamics along a highly modified lowland river. Sci Total Environ 568:875–884

Bolpagni R, Azzella MM, Agostinelli C, Beghi A, Bettoni E, Brusa G, De Molli C, Formenti R, Galimberti F, Cerabolini BEL (2017) Integrating the Water Framework Directive into the Habitats Directive: analysis of distribution patterns of lacustrine EU habitats in lakes of Lombardy (northern Italy). J Limnol 76(S1):75–83. https://doi.org/10.4081/jlimnol.2016.1627

Bolpagni R, Laini A, Stanzani C, Chiarucci A (2018) Aquatic plant diversity in Italy: distribution, drivers and strategic conservation actions. Front Plant Sci 9:116

Bonaposta D, Segadelli S, De Nardo MT, Alessandrini A, Pezzoli S (2011) Le potenzialità geologiche dei dati storici ambientali: il caso delle sorgenti e dei fontanili in Emilia Romagna. Il Geologo dell'Emilia Romagna, pp 19-34

Bucci A, Petrella E, Celico F, Naclerio G (2017) Use of molecular approaches in hydrogeological studies: the case of carbonate aquifers in southern Italy. Hydrogeol J 25:1017–1031

Cantonati M, Segadelli S, Ogata K, Tran H, Sanders D, Gerecke R, Filippini M, Gargini A, Celico F (2016) A global review on ambient Limestone-Precipitating Springs (LPS): hydrogeological setting, ecology, and conservation. Sci Total Environ 568:624–637

Caporaso JG, Kuczynski J, Stombaugh J, Bittinger K, Bushman FD, Costello EK, Fierer N et al (2010) QIIME allows analysis of high-throughput community sequencing data. Nat Methods 7:335–336

Cardarelli E, Fischanger F (2006) 2D data modelling by electrical resistivity tomography for complex subsurface geology. Geophys Prospect 54:121–133

Celico F, Naclerio G, Bucci A, Nerone V, Capuano P, Carcione M, Allocca V, Celico P (2010) Influence of pyroclastic soil on epikarst formation: a test study in southern Italy. Terra Nova 22:110–115

Chelli A, Segadelli S, Vescovi P, Tellini C (2016) Large-scale geomorphological mapping as a tool to detect structural features: the case of Mt. Prinzera ophiolite rock mass (Northern Apennines, Italy). J Maps 12:770–776

Chelli A, Zanini A, Petrella E, Feo A, Celico F (2018) A multidisciplinary procedure to evaluate and optimize the efficacy of hydraulic barriers in contaminated sites: a case study in Northern Italy. Environ Earth Sci. https://doi.org/10.1007/s12665-018-7420-8

Chen C-S, Tu C-H, Chen S-J, Chen C-C (2016) Simulation of groundwater contaminant transport at a decommissioned landfill site: a case study, Tainan City, Taiwan. Int J Environ Res Public Health 13:467

Cinnirella S, Buttafuoco G, Pirrone N (2005) Stochastic analysis to assess the spatial distribution of groundwater nitrate concentrations in the Po catchment (Italy). Environ Poll 133:569–580

Conti FD, Visioli G, Malcevschi A, Menta C (2018) Safety assessment of gasification biochars using *Folsomia candida* (Collembolan)

ecotoxicological bioassays. Environ Sci Pollut Res Int 25:6668–6679
Cupola F, Tanda MG, Zanini A (2015) Laboratory sandbox validation of pollutant source location methods. Stoch Env Res Risk Assess 29:169–182
D'Oria M, Zanini A, Cupola F (2018) Oscillatory pumping test to estimate aquifer hydraulic parameters in a bayesian geostatistical framework. Math Geosci 50:169–186
Di Dio G (2005) Risorse idropotabili. In: APAT (ed), Note Illustrative della Carta Geologica d'Italia 1:50.000, Foglio 199-Parma Sud. S.EL.CA. Firenze
Doherty JE, Hunt RJ (2010) Approaches to highly parameterized inversion—a guide to using PEST for groundwater-model calibration: US Geological Survey Scientific Investigations Report 5169
Edgar RC (2010) Search and clustering orders of magnitude faster than BLAST. Bioinformatics 26:2460–2461
Farnleitner AH, Wilhartitz I, Ryzinska G, Kirschner AKT, Stadler H, BurtscherMM Hornek R, Szewzyk U et al (2005) Bacterial dynamics in spring water of alpine karst aquifers indicates the presence of stable autochthonous microbial endokarst communities. Environ Microbiol 7:1248–1259
Feo A, Zanini A, Petrella E, Celico F (2018) A Python script to compute isochrones for MODFLOW. Ground Water. https://doi.org/10.1111/gwat.12588
Fienen M, Hunt R, Krabbenhoft D, Clemo T (2009) Obtaining parsimonious hydraulic conductivity fields using head and transport observations: a Bayesian geostatistical parameter estimation approach. Water Resour Res 45:W08405. https://doi.org/10.1029/2008wr007431
Gzyl G, Zanini A, Frączek R, Kura K (2014) Contaminant source and release history identification in groundwater: a multi-step approach. J Contam Hydrol 157:59–72
Hanckock PJ, Randall J, Boulton AJ (2009) Preface: hydrogeoecology, the interdisciplinary study of groundwater dependent ecosystems. Hydrogeol J 17:1–3
Harbaugh AW (2005) MODFLOW-2005, the US Geological Survey modular ground-water model, the ground-water flow process: US Geological Survey Techniques and Methods 6-A16
Harbaugh AW, Langevin CD, Hughes JD, Niswonger RN, Konikow LF (2017) MODFLOW-2005 version 1.12.00, the US Geological Survey modular groundwater model: US Geological Survey software release, 03 February 2017. https://doi.org/10.5066/F7RF5S7G
Hu K, Li Y, Chen W, Chen D, Wei Y, Edis R, Li B, Huang Y, Zhang Y (2010) Modeling nitrate leaching and optimizing water and nitrogen management under irrigated maize in desert oases in Northwestern China. J Environ Qual 39:667–677
Iacumin P, Venturelli G, Selmo E (2009) Isotopic features of rivers and groundwater of the Parma Province (Northern Italy) and their relationships with precipitation. J Geochem Explor 102:56–62
Kanamaru K, Hieda T, Iwamuro Y, Mikami Y, Obi Y, Kisaki T (1982) Isolation and characterization of a *Hyphomicrobium* species and its polysaccharide formation from methanol. Agric Biol Chem 46:2411–2417. https://doi.org/10.1080/00021369.1982.10865468
Kløve B, Ala-aho P, Bertrand G, Boukalova Z, Ertürk A, Goldscheider N, Ilmonen J, Karakaya N, Kupfersberger H, Kvoerner J, Lundberg A, Mileusnić M, Moszczynska A, Muotka T, Preda E, Rossi P, Siergieiev D, Šimek J, Wachniew P, Angheluta V, Widerlund A (2011) Groundwater dependent ecosystems. Part I: hydroecological status and trends. Environ Sci Policy 14:770–781
Kuglerová L, Jansson R, Ågren A, Laudon H, Malm-Renöfält B (2014) Groundwater discharge creates hotspots of riparian plant species richness in a boreal forest stream network. Ecology 95:715–725
Laini A, Bartoli M, Castaldi S, Viaroli P, Capri E, Trevisan M (2011) Greenhouse gases (CO2, CH_4 and N_2O) in lowland springs within an agricultural impacted watershed (Po River Plain, northern Italy). Chem Ecol 27:177–187
Longinelli A, Selmo E (2003) Isotopic composition of precipitation in Italy: a first overall map. J Hydrol 270:75–88
Mayer RE, Bofill-Mas S, Egle L, Reischer GH, Schade M, Fernandez-Cassi X, Fuchs W, Mach RL, Lindner G, Kirschner A, Gaisbauer M, Piringer H, Blaschke AP, Girones R, Zessner M, Sommer R, Farnleitner AH (2016) Occurrence of human-associated Bacteroidetes genetic source tracking markers in raw and treated wastewater of municipal and domestic origin and comparison to standard and alternative indicators of faecal pollution. Water Res 90:265–276
Naclerio G, Fardella G, Marzullo G, Celico F (2009) Filtration of *Bacillus subtilis* and *Bacillus cereus* spores in a pyroclastic topsoil, carbonate Apennines, southern Italy. Colloid Surf B Biointerf 70:25–28
Neupauer RM, Liu R (2006) Identifying sources of a conservative groundwater contaminant using backward probabilities conditioned on measured concentrations. Water Resour Res. https://doi.org/10.1029/2005WR004115
Paes F, Liu X, Mattes TE, Cupples Alison M (2015) Elucidating carbon uptake from vinyl chloride using stable isotope probing and Illumina sequencing. Appl Microbiol Biotechnol 99:7735–7743. https://doi.org/10.1007/s00253-015-6606-1
Paradis D, Martel R, Karanta G, Lefebvre R, Michaud Y, Therrien R, Nastev M (2007) Comparative study of methods for WHPA delineation. Ground Water 45:158–167
Petrella E, Celico F (2009) Heterogeneous aquitard properties in sedimentary successions in the Apennine chain: case studies in southern Italy. Hydrol Process 23:3365–3371
Quast C, Pruesse E, Yilmaz P, Gerken J, Schweer T, Yarza P, Peplies J, Glöckner FO (2013) The SILVA ribosomal RNA gene database project: improved data processing and web-based tools. Nucleic Acids Res. https://doi.org/10.1093/nar/gks1219 **(Database issue: D590-6)**
Ricci Lucchi F, Colalongo ML, Cremonini G, Gasperi G, Iaccarino S, Papani G, Raffi S, Rio D (1992) Evoluzione sedimentaria e paleogeografia nel margine appenninico. In: Cremonini G, Ricci Lucchi F (eds) Guida alla Geologia del Margine Appenninico-Padano, Soc Geol Ita, pp 17–46
Rossetti G, Pieri V, Martens K (2005) Recent ostracods (Crustacea, Ostracoda) found in lowland springs of the provinces of Piacenza and Parma (Northern Italy). Hydrobiologia 542:287–296
Savci S (2012) An agricultural pollutant: chemical fertilizer. Int J Environ Sci Dev 3:73
Segadelli S, Vescovi P, Ogata K, Chelli A, Zanini A, Boschetti T, Petrella E, Toscani L, Gargini A, Celico F (2017a) A conceptual hydrogeological model of ophiolitic aquifers (serpentinized peridotite): the test example of Mt. Prinzera (northern Italy). Hydrol Process 31:1058–1073
Segadelli S, Vescovi P, Chelli A, Petrella E, De Nardo MT, Gargini A, Celico F (2017b) Hydrogeological mapping of heterogeneous and multi-layered ophiolitic aquifers (Mount Prinzera, northern Apennines, Italy). J Maps 13:737–746
Song JS, Lee D, Lee K, Kim C (2004) Genetic organization of the *dhl*A gene encoding 1,2 dichloroethane dechlorinase from *Xanthobacter flavus* UE15. J. Microbiol 42:188–193
Sutton MA, Howard CM, Erisman JW, Billen G, Bleeker A, Grennfelt P, Van Grinsven H, Grizzetti B (2011) The European nitrogen assessment: sources, effects and policy perspectives. Cambridge University Press, Cambridge
Xu Z, Wu Y, Yu F (2012) A three-dimensional flow and transport modelling of an aquifer contaminated by perchloroethylene subject to multi-PRB remediation. Transp Porous Med 91:319. https://doi.org/10.1007/s11242-011-9847-1
Zanini A, Woodbury AD (2016) Contaminant source reconstruction by empirical Bayes and Akaike's Bayesian information criterion. J Contam Hydrol 185–186:74–86

water

MDPI

Article

Coupled Microbiological–Isotopic Approach for Studying Hydrodynamics in Deep Reservoirs: The Case of the Val d'Agri Oilfield (Southern Italy)

Pietro Rizzo [1], Antonio Bucci [2,*], Anna Maria Sanangelantoni [1], Paola Iacumin [1] and Fulvio Celico [1]

[1] Department of Chemistry, Life Sciences and Environmental Sustainability, University of Parma, Parco Area delle Scienze 157/A, 43124 Parma, Italy; pietro.rizzo2@studenti.unipr.it (P.R.); annamaria.sanangelantoni@unipr.it (A.M.S.); paola.iacumin@unipr.it (P.I.); fulvio.celico@unipr.it (F.C.)

[2] Department of Biosciences and Territory, University of Molise, C.da Fonte Lappone, 86090 Pesche, Italy

* Correspondence: antonio.bucci@unimol.it; Tel.: +39-0874-404156

Received: 31 March 2020; Accepted: 20 May 2020; Published: 22 May 2020

Abstract: The studies upstream of the petroleum industry include oil and gas geological exploration and are usually focused on geological, structural, geophysical, and modeling techniques. In this research, the application of a coupled microbiological–isotopic approach was explored to assess its potential as an adequate characterization and monitoring tool of geofluids in oilfield areas, in order to expand and refine the information acquired through more consolidated practices. The test site was selected within the Val d'Agri oilfield, where some natural hydrocarbon springs have been documented since the 19th century in the Tramutola area. Close to these springs, several tens of exploration and production wells were drilled in the first half of the 20th century. The results demonstrated the effectiveness of the proposed approach for the analysis of fluid dynamics in complex systems, such as oilfield areas, and highlighted the capacity of microbial communities to "behave" as "bio-thermometers", that is, as indicators of the different temperatures in various subsurface compartments.

Keywords: hydrocarbon reservoir; groundwater; microbiological investigations; prokaryotes; isotopic investigations; δ^2H and $\delta^{18}O$; southern Italy

1. Introduction

Petroleum reservoirs are discovered in a wide range of geologic settings across the continents [1] and their monitoring is one of the key factors in the management of oil and gas resources [2]. Successful management requires an understanding of the structure of the reservoir, the distribution of fluids within the reservoir, drilling and maintaining wells which can produce fluids from the reservoir, transport and processing of produced fluids, refining and marketing the fluids, safely abandoning the reservoir when it can no longer produce, and mitigating the environmental impact of operations throughout the life cycle of the reservoir [3].

The studies on mineral oil and gas reservoirs are usually focused on geological, structural, and geophysical features, e.g., [4–8]. In this research, we explore, for the first time, the potential application of a coupled microbiological–isotopic approach as a useful tool for the characterization and monitoring of geofluids in oilfield areas, in order to expand and refine the information acquired through more consolidated practices.

The isotopes, and in particular the analysis of the stable isotopes ^{18}O and ^{2}H, allow identifying the origins of groundwater, and their use has long been consolidated in hydrogeological studies, e.g., [9–11].

On the other hand, prokaryotes (domains *Bacteria* and *Archaea*) have developed a high adaptive capacity in the most different habitats on the planet, and they can colonize even the harshest environments. They dominate global biogeochemical cycles, thus regulating ecosystem functions. Bacteria and archaea are ubiquitous in nature and have often been used to monitor water quality, e.g., [12,13], to increase knowledge of the hydrogeological characteristics of aquifer systems, e.g., [14,15], and to evaluate the potential of bioremediation of contaminated sites, e.g., [16–19]. Besides, over the last decades, broad phylogenetic and functional diverse microbial communities of several subsurface oil reservoirs have been described using the newly available molecular techniques, e.g., [20].

It is well known that only a small fraction of naturally occurring microorganisms can be cultivated in laboratory growth conditions. This has hindered, in the past, the full characterization of ecosystems and precluded the understanding of how they work and are regulated. Metagenomics and other "omics" are among the fastest advancing scientific tools at the basis of the recent and unprecedented access to genetic and functional information of entire microbial communities, contributing to knowledge about mechanisms and processes of essential ecosystem services, and to the emergence of innovative applications in many different areas. For instance, the next-generation sequencing (NGS) of 16S rRNA gene is now one of the most widely used applications for the taxonomic and phylogenetic evaluation of microbial community composition, e.g., [21–23], and it has opened the door to a deeper insight of complex environments.

2. Materials and Methods

2.1. Study Area

The Val d'Agri is a Quaternary NW–SE trending intramountain basin located within the southern Apennines thrust belt (southern Italy) (Figure 1), whose formation and evolution were controlled by brittle tectonics. The intense and recent deformation is testified by seismic activity in the last 40 ka, such as the M7 1857 Basilicata earthquake, e.g., [24–26].

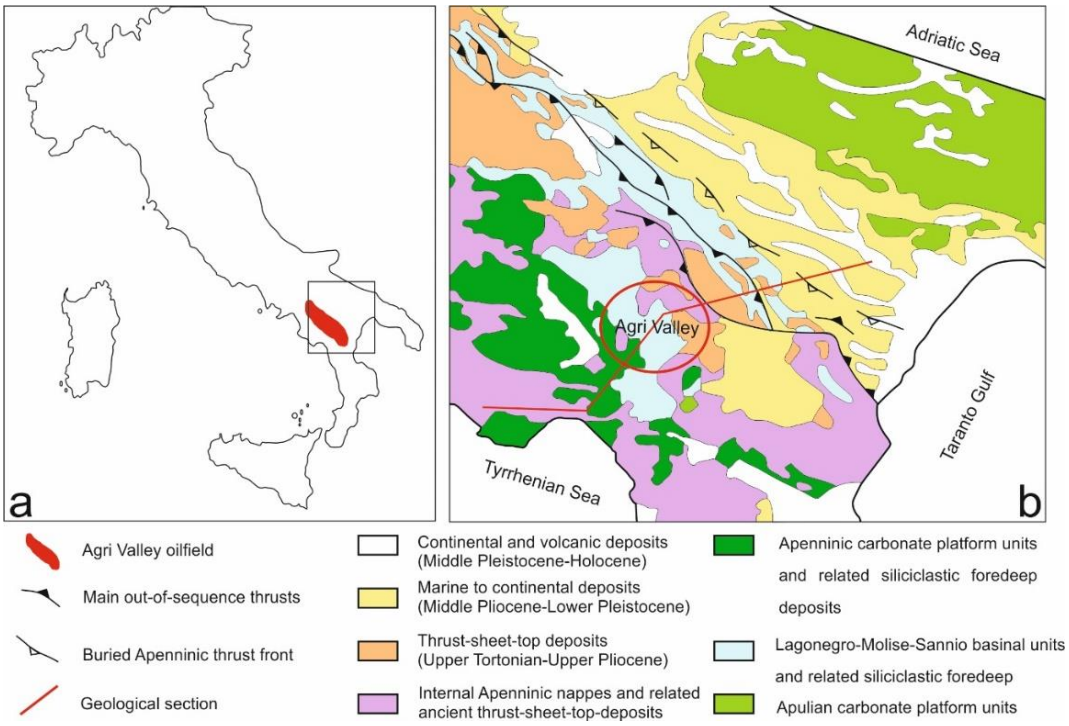

Figure 1. (**a**) Localization of the study area. (**b**) Schematic structural-geological map of the southern Apennines from Patacca et al., 1992, modified [27].

The main Val d'Agri oilfield is hosted in a reservoir made of fractured, low-porosity carbonates belonging to the buried inner Apenninic Platform belt, e.g., [28–30]. Light to medium crude oil and gas are stored in limestone and dolomite (Miocene to Cretaceous age) [31]. The carbonate reservoir lies below the Pliocene siliciclastic foredeep deposits and a thick mélange layer (Figure 2). Hydrocarbons have been extracted since the mid-1900s through several wells at a depth ranging from 1.8 to 3.5 km below sea level.

The Apenninic Platform is about 7000 m thick and characterized by a bottom part made up of evaporites, sandstones, and conglomerates (Triassic age) lying above a crystalline basement. Well data were used to establish the progressive movement of the front of the chain towards the NE during the Pliocene–early Pleistocene.

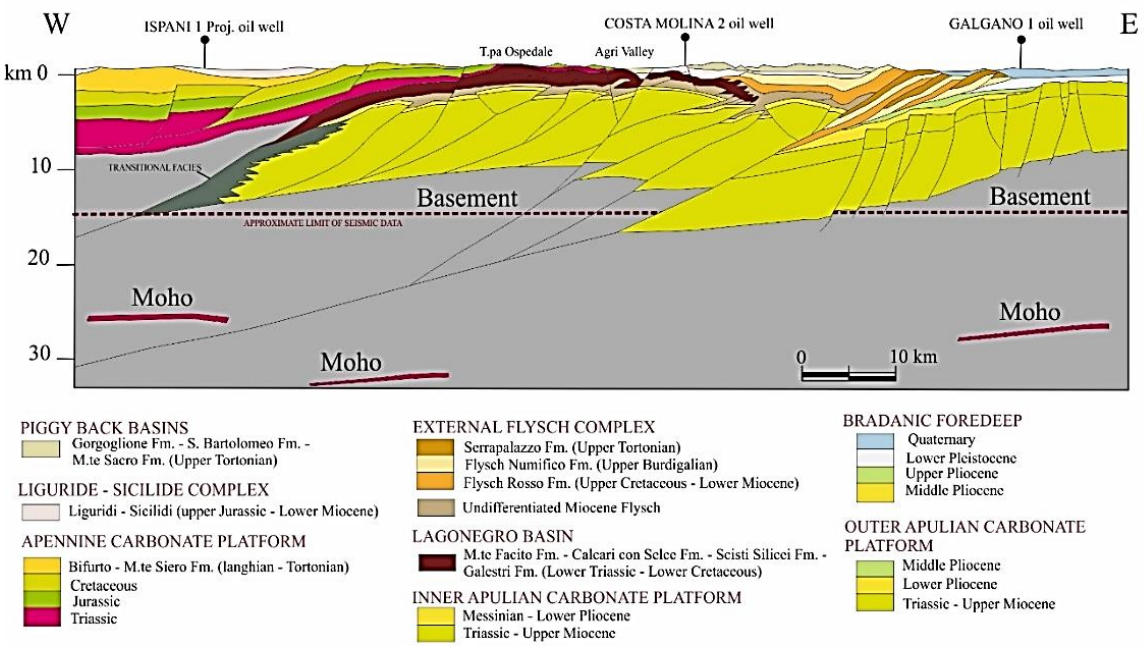

Figure 2. Geological section W–E crossing the Agri Valley from Menardi, Noguera, and Rea 2000, modified [30].

The study area is in Tramutola village. It includes natural hydrocarbon springs whose presence was already known thanks to oral testimonies and several papers published at the end of the 19th century and early 20th century [32]. The hydrocarbon seepages pour in the stream Rio Cavolo, forming oil stains (Figure 3).

From the late nineteenth century onward, research activities led to the discovery of the small and superficial Tramutola oil field exploited by Agip Mineraria in the 1930s and 1940s through 45 exploration and production wells.

These wells intercepted oil and/or gas from a few to several hundreds of meters below the ground (b.g.), e.g., [33]. From one of these wells (P_{art}, artesian well) and the hydrocarbon springs, hydrogen sulfide (H_2S) emissions occur and are immediately recognizable because of the typical smell of "rotten egg" (unpublished data).

The springs S1 and S2, as well as P_{art}, are located along a W–E fault where the Apulian carbonate platform and Rio Cavolo Unit (Oligocene) [34] crop out (Figure 4). The P_{art} stratigraphy can be schematized as follows (from the top to the bottom): Rio Cavolo Unit from 0 to 44 m b.g., Apenninic Platform carbonates from 44 to 136 m b.g., tectonic mélange from 136 to 165 m b.g., Flysch Galestrino Formation from 165 to 352 m b.g., and Scisti Silicei Formation from 352 to 404 m b.g. Oil and gas were detected at a different depth within the Rio Cavolo Unit, Flysch Galestrino, and Scisti Silicei Formations [33].

Figure 3. Hydrocarbon springs S1 (**a**) and S2 (**b**).

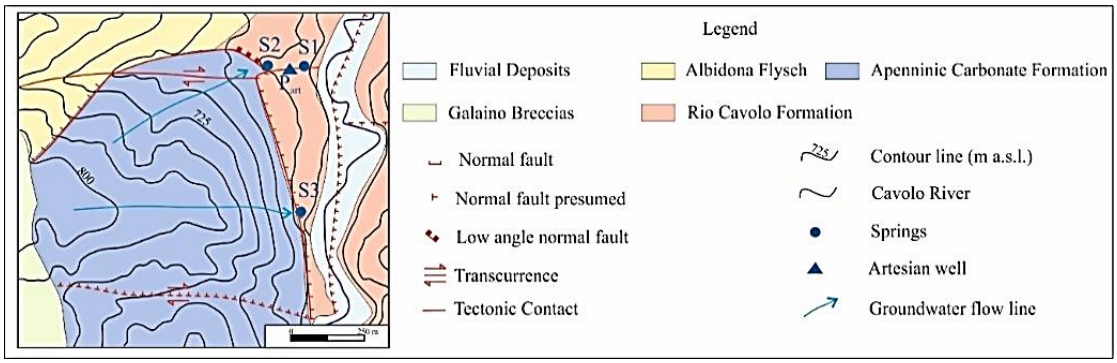

Figure 4. Geological map of the study area; the blue points and the triangle show the location of the investigated springs S1, S2, and S3 and the artesian well P_{art} (the geological sketch is taken from Olita 2018, modified [33]).

The Rio Cavolo Unit is made up of clays, micaceous limestone, and rare marly layers. The tectonic mélange is between (overthrust) the Apennine Platform and the Lagonegrese Units [35]. The Flysch Galestrino Formation (Lower Cretaceous) is made up of clays, marls, and limestone, while the Scisti Silicei Formation (Upper Triassic-Jurassic) is composed of clays, marls, and chert [36,37].

From the hydrogeological point of view, the study site belongs to an area where different hydrogeological series complexes crop out. In more detail, the carbonate rocks belong to the so-called Mesozoic carbonate platform series complexes, whose permeability is very high, due to a well-developed fracture network and the presence of karst conduits [38]. The less permeable sedimentary successions belong to the syn-orogenic turbidite series complexes and both the outer and the inner basins series complexes. The rock masses belonging to these complexes are characterized by a permeability ranging from very low to low, due to a mixed pore-fracture network. However, their hydraulic conductivity can be locally enhanced due to well-developed damage zones associated to fault zones [38]. Along the Cavolo stream and the whole Agri Valley, alluvial sediments crop out. Due to the coexistence of fine and coarse sediments, the hydraulic conductivity of the alluvial complex range between less than 1×10^{-8} and 2×10^{-2} m/s [39].

No detailed studies have been published concerning the hydrogeological behavior of carbonate and siliciclastic media at the study area. However, the same hydrogeological units were deeply investigated and characterized in the wider context of the continental Italian southern Apennines (for siliciclastic low-permeability media, see, for example, Petrella and Celico, 2009 [40]; for high-permeability carbonate

aquifers, see, for example, Petrella and Celico, 2013 [41], De Vita et al. 2012 [42], Allocca et al. 2015 [43], and Fiorillo et al. 2018 and 2019 [44,45]).

As per groundwater geochemistry in the study area, interesting results were obtained by Paternoster et al. 2005 [46]. The springs fed by carbonate aquifers have a Ca–HCO_3 composition, while groundwaters flowing within the siliciclastic sediments have a high amount of As and Cu. However, the concentrations of As and first-row transition elements were usually below the maximum permissible level for drinking water defined by Italian law. The authors link the availability of As, Pb, Cu, Zn, and Fe to the occurrence of iron oxi-hydroxides. Moreover, nitrate concentration seems to be influenced by the use of fertilizers.

2.2. Hydrogeological Investigations

The discharges of the hydrocarbon springs S1 and S2 were measured in low flow (July 2018), in early recharge (October 2018) and in late recharge (March 2019). The flow rate of the P_{art} artesian well was not measurable, but based on some historical data, its order of magnitude is about 30 m^3/h (unpublished data).

2.3. Water Sampling and Analyses

Three sampling campaigns have been carried out in July 2018, October 2018, and March 2019.

Rainwater samples for isotopic analyses were collected monthly in two local rain samplers located at 1047 and 1290 m above sea level (a.s.l.).

The rainfall was collected using ten-liter polyethylene bottles containing about 300 mL of vaseline oil to prevent evaporation processes. Oil contamination was carefully avoided by syringing the water samples out of the bottle.

Groundwater samples for stable isotope ($\delta^{18}O$, $\delta^{2}H$), tritium, and microbiological (Next-Generation Sequencing of 16S rRNA gene) analyses were collected during the discharge measurements at springs S1 and S2, and at the P_{art} well (screened at the well bottom).

The non-hydrocarbon spring S3, fed by the local carbonate aquifer and located at the contact between the high-permeability carbonate rocks and low-permeability siliciclastic successions, was analyzed for its isotopic content and used as a sort of endmember to compare hydrocarbon spring water with groundwater exclusively flowing within a relatively shallow aquifer system.

The localization of the rain samplers, springs, and the artesian well is reported in Table 1.

In addition, a water sample was also collected from the deep reservoir and analyzed to compare its isotopic signature and microbial community with those retrieved in the spring and P_{art} groundwaters.

Electrical conductivity, temperature, and pH measurements were performed *in situ* with portable equipment (Hanna Instruments 9829).

All samples were stored in a refrigerated box and transported to the laboratory.

Stable isotope analyses ($\delta^{18}O$, $\delta^{2}H$) were carried out at the Isotope Geochemistry Laboratory of the University of Parma (Italy), using a Delta Plus mass spectrometer (Thermo Fisher Scientific, Waltham, Massachusetts, USA) coupled to an automatic HDO device preparation system. The technique consists of bringing the liquid sample into an isotopic equilibrium, at a controlled temperature of 18 °C, with a pure gas (CO_2 in the case of oxygen and H_2 in the case of hydrogen). The isotopic equilibrium, in the case of hydrogen, would be reached very slowly, and platinum catalysts are used to accelerate the reaction. For the oxygen isotope determination, 5 cm^3 of water was equilibrated with pure CO_2, while for hydrogen isotopes, 5 cm^3 of water was equilibrated with pure H_2 (platinum wire was used as a catalyzer of gas–liquid water equilibration). Equilibration times were 3 h for hydrogen and 8 h for oxygen. The isotope ratio is expressed as

$$ {}^{A/B}\delta_{i/RF} = \frac{{}^{A/B}R_i}{{}^{A/B}R_{VSMOW-SLAP}} - 1 = \left[\left(\frac{{}^{A/B}R_i}{{}^{A/B}R_{VSMOW-SLAP}} - 1\right) 10^3\right]‰ \quad (1) $$

where "A" is 18 or 2, "B" is 16 or 1, "R" is the ratio of the isotopic abundances, "i" is the sample of interest, and ‰ = 10^{-3}. Analyses of ^{3}H were carried out at the Isotope Geochemistry Laboratory of Trieste University, Italy. To decrease measurement errors, the samples followed the procedure of the preventive electrolytic enrichment of tritium, where 250 g of the water sample was expected to be reduced, by electrolysis, to 20 g. The analyses for the determination of the tritium activity were carried out according to the procedures provided by *Water and Environment News* No. 3 (1998) [47]. The analytical prediction uncertainty was ± 0.1‰ for $\delta^{18}O$, ± 1‰ for $\delta^{2}H$, and ± 0.5 TU for ^{3}H.

Table 1. The coordinates expressed in Latitude N, Longitude E, and the altitude of the two rain samplers (RWS1 and RWS2), springs, and the artesian well.

Name	Latitude N	Longitude E	Altitude (m a.s.l.)
RWS1	40.3247	15.9897	1047
RWS2	40.3411	16.0003	1290
S1	40.3225	15.7597	636
S2	40.3228	15.7586	643
S3	40.3175	15.7594	643
P_{art}	40.3225	15.7592	643

2.4. Chemical Analyses

During the third sampling campaign in March 2019, water samples were collected from the hydrocarbon springs and the well, P_{art}, to analyze Benzene, Toluene, Ethylbenzene, Xylene (BTEX) and Polycyclic aromatic hydrocarbons (PAHs) contents. Forty milliliter colorless glass vials were used for the BTEX analysis, while 1 L black glass bottles were used for PAH analysis. The analyses were performed at Biochemie Lab S.r.l. following the EPA 5030C 2003 + EPA 8015D 2003 protocol for BTEX and the EPA3510C 1996 + EPA 8270E 2018 protocol for PAH [48–51].

2.5. Microbiological Analyses: 16S Ribosomal RNA Gene Next Generation Sequencing (NGS)

For bacterial community analyses, water samples (4 L) were filtered through sterile mixed esters of cellulose filters (S-Pak™ Membrane Filters, 47 mm diameter, 0.22 µm pore size, Millipore Corporation, Billerica, MA, USA) within 24 h from the collection. Bacterial DNA extraction from filters was performed using the commercial kit FastDNA SPIN Kit for soil and FastPrep®Instrument. After the extraction, DNA integrity and quantity were evaluated by electrophoresis in 0.8% agarose gel containing 1 µg/mL of Gel-RedTM. The bacterial community profiles in the samples were generated by NGS technologies at the Genprobio S.r.l. Laboratory. Partial 16S rRNA gene sequences were obtained from the extracted DNA by polymerase chain reaction (PCR), using the primer pair Probio_Uni and Probio_Rev, targeting the V3 region of the bacterial 16S rRNA gene sequence [52]. Amplifications were carried out using a Verity Thermocycler (Applied Biosystems) and PCR products were purified by the magnetic purification step involving the Agencourt AMPure XP DNA purification beads (Beckman Coulter Genomics GmbH, Bernried, Germany) in order to remove primer dimers. Amplicon checks were carried out as previously described [52]. Sequencing was performed using an Illumina MiSeq sequencer with MiSeq Reagent Kit v3 chemicals. The fastq files were processed using a custom script based on the QIIME software suite [53]. Paired-end read pairs were assembled to reconstruct the complete Probio_Uni/Probio_Rev amplicons. Quality control retained sequences with a length between 140 and 400 bp and mean sequence quality score > 20 while sequences with homopolymers > 7 bp and mismatched primers were omitted. To calculate downstream diversity measures, operational taxonomic units (OTUs) were defined at 100% sequence homology using DADA2 [54]; OTUs not encompassing at least two sequences of the same sample were removed. All reads were classified to the lowest possible taxonomic rank using QIIME2 [53,55] and a reference dataset from the SILVA database v132 [56]. The biodiversity of the samples (alpha-diversity) was calculated with the Shannon index.

3. Results

3.1. Hydrogeological Settings

The discharge of the spring S1 varied slightly over time, showing a slight decrease (1.4 to 1.3 m^3/h) from July to late October (dry period), and an increase (1.3 to 1.7 m^3/h) in March (rainy period), in agreement with the distribution of precipitation in that area. The overall synchronicity between rainy periods and the increase in discharge at S1 clearly suggested active pathways within the feeding aquifer system. Unfortunately, the S2 discharge was not measurable after the winter period, therefore no speculation can be formulated concerning recharge processes.

3.2. Isotope Investigations

Monthly values for local precipitation for the period May 2016–April 2017 give the following regression $^{2}\delta$ on $^{18}\delta$ (LMWL, Local Meteoric Water Line):

$$^{2/1}\delta = [6.48\ (\pm 0.66)\ ^{18/16}\delta + 4.6\ (\pm 5.2)]\ ‰ \quad (2)$$

$$s(yx) = 4.56\ ‰, \quad n = 21 \qquad p(A = 0) = 0.39$$

where "s(yx)" is the standard error of regression and "n" is the number of couples of data, "A" is the intercept of the regression line, and p = probability.

For precipitation in Southern Italy [57], the resulting regression line is

$$^{2/1}\delta = [6.97(\pm 0.10)\ ^{18/16}\delta + 7.32\ (\pm 0.61)]\ ‰ \quad (3)$$

$$s(yx) = 3.75\ ‰, n = 317 \quad p(A = 0) << 0.0001$$

According to Zar [58], equation (2) may be compared with equation (3) both for the slope (B) and the elevation (E). Note that elevation indicates the different vertical position on the graph. A comparison gives the following results: $p(B_{(1)} = B_{(2)}) = 0.39$, $p(E_{(1)} = E_{(2)}) = 0.27$. The null hypotheses H_o: $B_{(1)} = B_{(2)}$ and H_o: $E_{(1)} = E_{(2)}$ cannot be rejected with high probability; thus we assume that the two regressions are not different.

The isotopic data of spring and groundwaters collected in the Tramutola study area are located close to the local meteoric water line (2) suggesting a meteoric origin of the analyzed waters (Figure 5). On the contrary, the samples taken from the deep reservoir are far from the line (Figure 5); actually, they represent fossil waters that also interacted with the carbonate formation at an elevated temperature.

The isotopic composition of spring and groundwater samples did not vary widely over time; isotopic variations were lower than 2u, where "u" is prediction uncertainty for the $\delta^{18}O$ and $\delta^{2}H$ data.

As far as tritium is concerned, all samples showed a relatively high ^{3}H content (4.1 to 9.1 TU), if compared with tritium content in recent rainwaters analyzed in southern Italy (e.g., 4.6 TU [59]; 5.0 TU [10]; 6.2 to 10.8 [unpublished data]) and the wider Adriatic area [60]. The non-hydrocarbon spring, S3, was characterized by the highest tritium value (8.4 to 9.1 TU), in agreement with the rapid pathways within the carbonate aquifer. Moreover, the variation of TU values was lower than 2u, suggesting little interaction with waters having quite different TU values. The hydrocarbon springs S1 and S2 had similar tritium contents (5.6 to 6.9 TU and 6.8 to 7.5 TU, respectively), slightly lower than those characterizing the S3 spring water. As for S1 water, the variation over time was slightly higher than the 2σ error of the ^{3}H analyses, therefore suggesting the mixing of different endmembers, possibly related to longer (lower tritium content) and shorter (higher tritium content) pathways. Taking into consideration the homogeneous stable isotope content over time, both pathways are related to well-mixed groundwater. P_{art} waters showed a more significant variation over time (4.1 to 6.2 TU), further confirming the existence of mixing between different endmembers: (i) one related to rainwater infiltrating relatively far from the observation well and (ii) a second one linked to closer pathways.

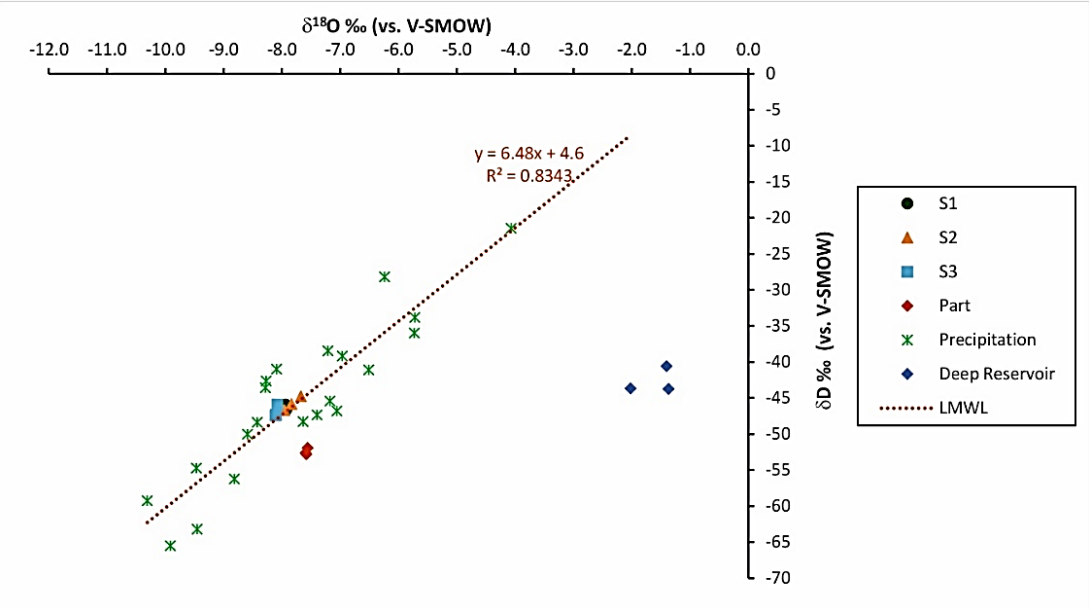

Figure 5. $\delta^{18}O$ versus $\delta^{2}H$ relationship in water samples collected from rainwater samplers, at springs (S1; S2; S3), at the artesian well (P_{art}), and in the deep reservoir. LMWL is the local meteoric water line obtained by local rainwater.

3.3. Chemical Analyses

Chemical analyses were performed on springs S1, S2, and well P_{art}. Samples collected at the spring S3, whose waters are used for drinking purposes, were not considered for BTEX and PAHs determinations. The data revealed detectable PAH such as naphtalene (0.00231 µg/L) in the spring S1, and benzo(b)fluoranthene (0.354 µg/L), benzo(k)fluoranthene (0.0341 µg/L), benzo(g,h,i)perylene (0.199 µg/L), indene (0.101 µg/L), anthracene (0.726 µg/L), phenanthrene (0.465 µg/L), fluoranthene (0.166 µg/L), and benzo(J)fluoranthene (0.0140 µg/L) in the spring S2. BTEX were not detected in either spring. Neither PAH nor BTEX were detected in groundwater sampled from P_{art}.

3.4. Next-Generation Sequencing Results

MiSeq runs produced an average of 61,682 sequences for the samples collected at the springs (S1 and S2) and from the artesian well, P_{art}. An average of 80,061 reads was obtained from the analysis of the deep reservoir bacterial community (Table 2). The 16S rRNA gene sequences generated in this study have been deposited in the NCBI Sequence Read Archive under the accession number PRJNA629324.

The rarefaction analysis (a measure used to estimate the alpha diversity in samples and gauge whether or not sequencing efforts captured the microbial diversity) highlighted a greater microbial diversity in the spring S2 compared to the spring S1, the artesian well, and the deep reservoir (Figure S1).

Table 2. Number of 16S rDNA sequences obtained after NGS analysis for the three sampling campaigns (n.a. is not available).

Sample	Final Read Number		
	Sampling Campaigns		
	19 July 2018	29 October 2018	18 March 2019
S1	73,995	59,369	49,512
S2	93,820	57,630	61,065
P_{art}	n.a.	44,730	53,341
Deep reservoir	101,690	60,563	77,931

Proteobacteria, *Chloroflexi*, and *Bacteroidetes* were the three major phyla in waters from the spring S1 in July 2018 (85.55% of sequences). In October 2018 and March 2019, *Epsilonbacteraeota* were found with the highest percentages (72.25% and 52.48%, respectively) ahead of *Proteobacteria* (25.78% and 20.67%) and *Bacteroidetes* (0.86% and 23.63%).

Spring S2 bacterial communities were dominated by *Proteobacteria* (mean relative abundance 62.86%). *Actinobacteria* occurred at percentages ranging from 3.17% to 22.23%. In addition, *Bacteroidetes* (5.51%), *Acidobacteria* (8.11%), and *Patescibacteria* (4.51%) were among the three most abundant phyla in July 2018, October 2018, and March 2019, respectively.

Microbial communities in groundwater collected from the P_{art} well were mainly characterized by *Proteobacteria* and *Patescibacteria*, with mean relative abundance values of 92.78% and 4.09%, respectively.

The phyla *Proteobacteria*, *Synergistetes*, and *Firmicutes* accounted for, on average, 94.82% of the sequences retrieved from the deep reservoir. Overall, *Proteobacteria* represented the dominant phylum in all the samples collected from July 2018 to March 2019, ranging from 42.65% to 50.88%.

The analysis of the microbial community composition at the family level (Figure 6) revealed, in spring S1, a predominance of *Helicobacteraceae* (47.12%), *Chlorobiaceae* (7.63%), and unclassified microorganisms of the order *Chloroflexales* (6.91%) in July 2018. The top three dominant families were *Sulfurovaceae* (63.38%), *Halothiobacillaceae* (24.75%), and *Thiovulaceae* (8.46%) in October 2018, and *Sulfurovaceae* (31.06%), *Chlorobiaceae* (22.56%), and *Thiovulaceae* (20.61%) in March 2019.

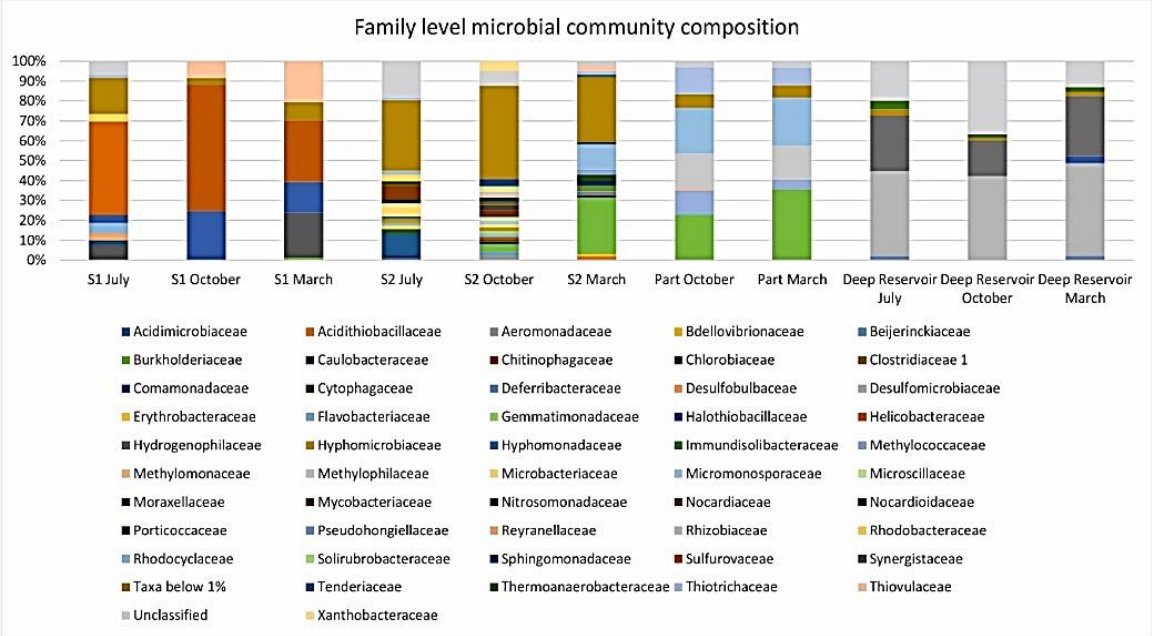

Figure 6. Family level microbial community composition in samples collected from springs, the P_{art} well, and the deep reservoir.

The most abundant families in spring S2 were: *Comamonadaceae* (11.12%), *KCM-B-112* (7.56%), and *Mycobacteriaceae* (7.17%) in July 2018, *Xanthobacteraceae* (4.96%), *Burkholderiaceae* (3.96%), and unclassified microorganisms of the subgroup 6 class of the *Acidobacteria* phylum (3.84%) in October 2018, and *Burkholderiaceae* (28.28%), *Rhodocyclaceae* (12.59%), and *Porticoccaceae* (2.99%) in March 2019.

The bacterial communities of the P_{art} well were mainly characterized by the families *Burkholderiaceae*, *Rhodocyclaceae*, and *Methylophilaceae*, accounting for, on average, 29.16%, 23.49%, and 17.34% of sequences, respectively.

Desulfomicrobiaceae, *Synergistaceae*, and family III of the order *Thermoanaerobacterales* were found at the highest percentages in the deep reservoir, with mean values of 43.97%, 25.49%, and 20.19%, respectively.

At a lower taxonomic level, spring and groundwaters were mostly characterized by genera (Table 3) including aerobic, microaerophilic, facultative anaerobic, and anaerobic species, mainly mesophilic and psychrophilic, such as, *Chelatococcus asaccharovorans* [61], *Vitreoscilla filiformis* [62], *Actinoplanes ferrugineus* [63], *Sphaerotilus natans* [64], *Hydrogenophaga taeniospiralis* [65], and *Sphingomonas yunnanensis* [66].

Many of these genera encompass chemolithotrophic or phototrophic sulfur-oxidizing bacteria (SOB), which derive energy from the oxidation of reduced sulfur compounds, or use sulfide as electron donors for anoxygenic photosynthesis, like the green sulfur bacterium *Chlorobium limicola* [67], playing an important role in the element cycling in the environment. These results are not surprising, especially when considering the hydrogen sulfide emissions from the analyzed well and springs. In fact, the presence of this gas in waters, probably naturally generated in situ from reservoir biomass and sulfate-containing minerals through microbial sulfate reduction and/or thermochemical sulfate reduction, could have represented a driving factor shaping microbial community structure and function.

In the deep reservoir, anaerobic and thermophilic microorganisms belonging to the genera *Acetomicrobium* (e.g., *Acetomicrobium thermoterrenum* [68]), *Desulfomicrobium* (e.g., *Desulfomicrobium thermophilum* [69]), *Thermoanaerobacterium* (e.g., *Thermoanaerobacterium thermosaccharolyticum* [70]), and *Thermoanaerobacter* (e.g., *Thermoanaerobacter ethanolicus* [71]) with optimum growth temperatures in the range of 55–69 °C, were detected. The genus *Acetomicrobium* was found in October 2018 and March 2019 with a mean relative abundance of 13.01%, whereas the genera *Desulfomicrobium*, *Thermoanaerobacterium*, and *Thermoanaerobacter* occurred, on average, at percentages of 43.96%, 18.30%, and 2.07%, respectively.

Table 3. Main bacterial genera identified in the P_{art}, S1, and S2 samples. Growth temperatures of some of the species belonging to the different genera are reported.

Taxonomy	Growth Temperature (°C)	Citations
Actinoplanes	10–35	[63]
Aeromonas	5–25	[72]
Chlorobium	25–30	[67]
Dechloromonas	25	[73]
Flavobacterium	15–30	[74]
Hydrogenophaga	30	[65]
Leptothrix	10–37	[75]
Methylotenera	10–34	[76]
Microvirga	37	[77]
Sphaerotilus	25–40	[64]
Sphingomonas	28	[66]
Sulfuricurvum	25	[78]
Sulfuritalea	10–32	[79]
Sulfurovum	10–40	[80]
Thiovirga	30	[81]
Thiothrix	20–37	[82]

4. Discussion and Conclusions

Both the hydrogeological behavior and the isotopic features of the studied hydrocarbon springs suggest that they are strictly related to active recharge in a local aquifer system, in agreement with findings related to the nearby non-hydrocarbon spring, whose waters are used for drinking purposes. At the same time, the hydrocarbon springs flow out along a fault zone, which enhances fluid flow, allowing the upflow of hydrocarbons and their mixing with the local groundwater, which is reasonably fed by the nearby carbonate aquifer. In detail, this is due to the fault crossing the sequence made

of the Scisti Silicei Formation, Galestri Formation, Tectonic Mélange, Apenninic Carbonate platform, and Rio Cavolo Formation, characterized by oil and gas layers at different depths [33]. The hydraulic behavior of this fault zone is similar to that of faults present in other carbonate aquifers in southern Italy, where the existence of high-permeability damage zones, e.g., [83–85] and/or heterogeneous fault cores, allowing a significant fluid migration, has been revealed in previous research, e.g., [86–93]. In these contexts, bacterial cell filtration typical of low-permeability fine-grained media, e.g., [90,94–97] is limited, and microorganisms can be used effectively as bio-tracers for specific hydrogeological and microbiological purposes, e.g., [97].

The groundwater intercepted by the P_{art} well is also fed by a more prolonged pathway, as demonstrated by the tritium content lower than those detected in the hydrocarbon springs and S3. Taking into consideration the wider geological setting, the artesian well intercepted a relatively deep (compatible with mesophilic and psychrophilic bacteria), but active pathway within the Scisti Silicei aquifer (Figure 7). This aquifer is unconfined upgradient and downgradient with respect to the P_{art} well, where the Scisti Silicei Formation crops out. Differently, it is confined (and locally artesian) where the Scisti Silicei is beneath the low-permeability flysch deposits. This deep groundwater naturally flows eastwards, towards the alluvial aquifer of the Agri Valley.

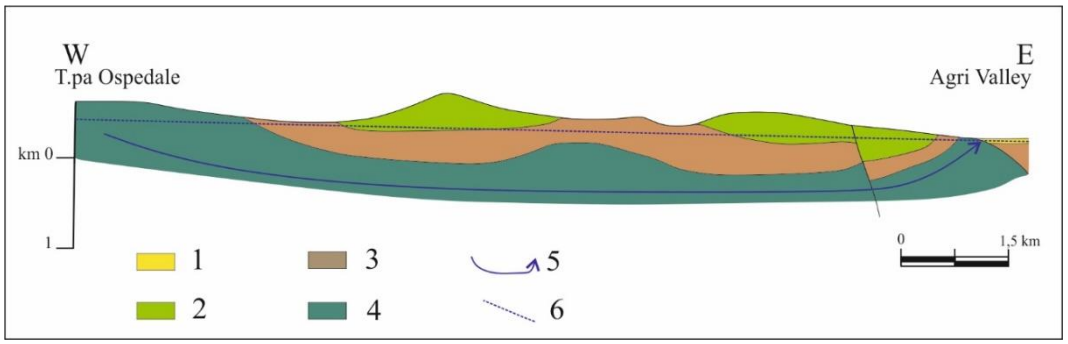

Figure 7. Hydrogeological sketch of the Scisti Silicei aquifer (based on the geological section of Menardi, Noguera, and Rea 2000 [30]). (1) alluvial complex; (2) carbonate complex; (3) low-permeability complex; (4) Scisti Silicei complex; (5) groundwater flow line; (6) hydraulic head.

In the present study, the potential of a coupled microbiological–isotopic approach for monitoring geofluids in hydrocarbon reservoirs and, in detail, the capacity of microbial communities to "behave" as "bio-thermometers", has been assessed for the first time.

When analyzing the communities in the P_{art} waters, collected at about 400 m b.g., and in spring waters, only mesophilic and psychrophilic microorganisms were detected. Differently, in the deep reservoir, thermophilic bacteria thriving at high temperatures, were found. These findings are consistent with geothermal curves and isotherms reported by Candela et al. [98] at the Val d'Agri oilfield (Figure 8), and demonstrate the usefulness of the proposed approach, at least at the study site.

The development and application of molecular biological methods to hydrogeological issues has led to increasing numbers of studies on the microbial communities of aquifer systems over the past few decades, e.g., [90,97]. For example, in the carbonate environments of southern Italy, the potential use of microorganisms as tracers has been examined with reference to the analysis of recharge and flow processes with excellent results, e.g., [90,97]. At the study site, the analysis of bacterial species in spring, groundwater, and deep reservoir samples and isotopic analyses proved to be an effective tool to obtain information on the subsurface dynamics and temperatures (Figure 8). In a broader perspective, the same approach could also be used for the comprehension of more complex phenomena in exploited oil fields.

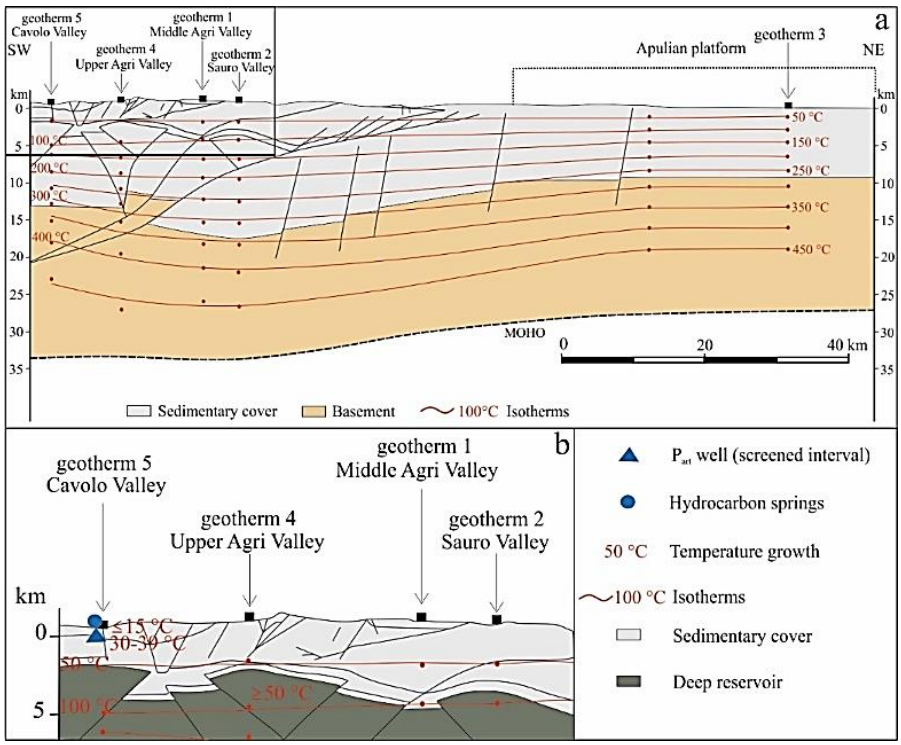

Figure 8. (**a**) Geological cross-section showing isotherms obtained from the interpolation of geothermal profiles through third-degree polynomials. Red dots show temperatures along the geotherm profiles (50 °C steps). (**b**) Detail of Figure 8a. Numbers in red show the growth temperature ranges of psychrophilic, mesophilic, and thermophilic microorganisms. Springs (blue point), the well P_{art} (blue triangle), and the deep reservoir (in grey) are shown (from Candela et al. 2015, modified [98]).

Supplementary Materials: The following material is available online: http://www.mdpi.com/2073-4441/12/5/1483/s1, Figure S1: Rarefaction curves of spring, groundwater, and deep reservoir samples collected in July 2018, October 2018, and March 2019. The alpha diversity plots were obtained by using the Shannon index.

Author Contributions: Conceptualization, A.B., A.M.S. and F.C.; Formal analysis, P.R.; Investigation, P.R.; Supervision, A.B., A.M.S., P.I. and F.C.; Validation, P.R.; Visualization, P.R.; Writing—original draft, P.R. and A.B.; Writing—review & editing, P.R., A.B., A.M.S., P.I. and F.C. All authors have read and agreed to the published version of the manuscript.

Funding: This research received no external funding

Acknowledgments: We warmly acknowledge Dario Avagliano, Francesco Coraggio, Antonella Caputi, and Fabrizio Micucci (ENI S.p.A., Distretto Meridionale) for providing some of the data used in the present work and for useful discussions. This work has benefited from the equipment and framework of the COMP-HUB Initiative, funded by the "Departments of Excellence" program of the Italian Ministry for Education, University and Research (MIUR, 2018–2022). We are grateful to the reviewers for their constructive comments and valuable suggestions.

Conflicts of Interest: There are no conflicts of interest related to this paper.

References

1. Satter, A.; Iqbal, G.M. Oil and gas recovery methods in low permeability and unconventional reservoirs. In *Reservoir Engineering-The Fundamentals, Simulation, and Management of Conventional and Unconventional Recoveries*; Gulf Professional Publishing: Houston, TX, USA, 2016; pp. 353–364.
2. Djuraev, U.; Jufar, S.R.; Vasant, P. A review on conceptual and practical oil and gas reservoir monitoring methods. *J. Petrol. Sci. Eng.* **2017**, *152*, 586–601. [CrossRef]
3. Fanchi, J.R. Introduction to Reservoir Simulation. In *Principles of Applied Reservoir Simulation*, 4th ed.; Gulf Professional Publishing: Houston, TX, USA, 2018; pp. 1–8.

4. Agosta, F.; Alessandroni, M.; Antonellini, M.; Tondi, E.; Giorgioni, M. From fractures to flow: A field-based quantitative analysis of an outcropping carbonate reservoir. *Tectonophysics* **2010**, *490*, 197–213. [CrossRef]
5. Garland, J.; Neilson, J.E.; Laubach, S.E.; Whidden, K.J. Advances in carbonate exploration and reservoir analysis. In *Advances in Carbonate Exploration and Reservoir Analysis*; Garland, J., Neilson, J.E., Laubach, S.E., Whidden, K.J., Eds.; Geological Society of London: London, UK, 2012; Volume 370, pp. 1–15.
6. Lavenu, A.P.C.; Lamarche, J.; Gallois, A.; Gauthier, B.D.M. Tectonic versus diagenetic origin of fractures in a naturally fractured carbonate reservoir analog (Nerthe anticline, southeastern France). *AAPG Bull.* **2013**, *97*, 2207–2232. [CrossRef]
7. Amoroso, O.; Ascione, A.; Mazzoli, S.; Virieux, J.; Zollo, A. Seismic imaging of a fluid storage in the actively extending Apennine mountain belt, southern Italy. *Geophys. Res. Lett.* **2014**, *41*, 3802–3809. [CrossRef]
8. Korneva, I.; Cilona, A.; Tondi, E.; Agosta, F.; Giorgioni, M. Characterisation of the permeability anisotropy of Cretaceous platform carbonates by using 3D fracture modeling: The case study of Agri Valley fault zones (southern Italy). *Ital. J. Geosci.* **2015**, *134*, 396–408. [CrossRef]
9. Guo, X.; Feng, Q.; Liu, W.; Li, Z.; Wen, X.; Si, J.; Xi, H.; Guo, R.; Jia, B. Stable isotopic and geochemical identification of groundwater evolution and recharge sources in the arid Shule River Basin of Northwestern China. *Hydrol. Process.* **2015**, *29*, 4703–4718. [CrossRef]
10. Petrella, E.; Bucci, A.; Ogata, K.; Zanini, A.; Naclerio, G.; Chelli, A.; Francese, R.; Boschetti, T.; Pittalis, D.; Celico, F. Hydrodynamics in Evaporate-Bearing Fine-Grained Successions Investigated through an Interdisciplinary Approach: A Test Study in Southern Italy—Hydrogeological Behaviour of Heterogeneous Low-Permeability Media. *Geofluids* **2018**, *2018*, 5978597. [CrossRef]
11. Zanini, A.; Petrella, E.; Sanangelantoni, A.M.; Angelo, L.; Ventosi, B.; Viani, L.; Rizzo, P.; Remelli, S.; Bartoli, M.; Bolpagni, R.; et al. Groundwater characterisation from an ecological and human perspective: An interdisciplinary approach in the Functional Urban Area of Parma, Italy. *Rend. Fis. Acc. Lincei* **2019**, *30*, 93–108. [CrossRef]
12. Noble, R.T.; Lee, I.M.; Schiff, K.C. Inactivation of indicator micro-organisms from various sources of faecal contamination in seawater and freshwater. *J. Appl. Microbiol.* **2004**, *96*, 464–472. [CrossRef]
13. WHO. *Guidelines for Drinking-Water Quality*, 1st Addendum to, 3rd ed.; World Health Organization: New York, NY, USA, 2006.
14. Harvey, R.W.; George, L.H.; Smith, R.L.; LeBlanc, D.R. Transport of microspheres and indigenous bacteria through a sandy aquifer: Results of natural-and forced-gradient tracer experiments. *Environ. Sci. Technol.* **1989**, *23*, 51–56. [CrossRef]
15. Bucci, A.; Petrella, E.; Celico, F.; Naclerio, G. Use of molecular approaches in hydrogeological studies: The case of carbonate aquifers in southern Italy. *Hydrogeol. J.* **2017**, *25*, 1017–1031. [CrossRef]
16. Chapelle, F.H. Bioremediation of petroleum hydrocarbon-contaminated ground water: The perspectives of history and hydrology. *Groundwater* **1999**, *37*, 122–132. [CrossRef]
17. Samanta, S.K.; Singh, O.V.; Jain, R.K. Polycyclic aromatic hydrocarbons: Environmental pollution and bioremediation. *Trends Biotechnol.* **2002**, *20*, 243–248. [CrossRef]
18. Menendez-Vega, D.; Gallego, J.L.R.; Pelaez, A.I.; de Cordoba, G.F.; Moreno, J.; Muñoz, D.; Sanchez, J. Engineered *in situ* bioremediation of soil and groundwater polluted with weathered hydrocarbons. *Eur. J. Soil Biol.* **2007**, *43*, 310–321. [CrossRef]
19. Xu, X.; Liu, W.; Tian, S.; Wang, W.; Qi, Q.; Jiang, P.; Gao, X.; Li, F.; Li, H.; Yu, H. Petroleum hydrocarbon-degrading bacteria for the remediation of oil pollution under aerobic conditions: A perspective analysis. *Front. Microbiol.* **2018**, *9*, 2885. [CrossRef]
20. Li, X.-X.; Mbadinga, S.M.; Liu, J.-F.; Zhou, L.; Yang, S.-Z.; Gu, J.-D.; Mu, B.-Z. Microbiota and their affiliation with physiochemical characteristics of different subsurface petroleum reservoirs. *Int. Biodeterior. Biodegradation* **2017**, *120*, 170–185. [CrossRef]
21. Streit, W.R.; Schmitz, R.A. Metagenomics–the key to the uncultured microbes. *Curr. Opin. Microbiol.* **2004**, *7*, 492–498. [CrossRef]
22. Chen, L.; Wang, L.-Y.; Liu, S.-J.; Hu, J.-Y.; He, Y.; Zhou, H.-W.; Zhang, X.-H. Profiling of microbial community during *in situ* remediation of volatile sulfide compounds in river sediment with nitrate by high throughput sequencing. *Int. Biodeterior. Biodegrad.* **2013**, *85*, 429–437. [CrossRef]

23. Kucharzyk, K.H.; Rectanus, H.V.; Bartling, C.M.; Rosansky, S.; Minard-Smith, A.; Mullins, L.A.; Neil, K. Use of omic tools to assess methyl *tert*-butyl ether (MTBE) degradation in groundwater. *J. Hazard. Mater.* **2019**, *378*, 120618. [CrossRef]
24. Giano, S.I.; Maschio, L.; Alessio, M.; Ferranti, L.; Improta, S.; Schiattarella, M. Radiocarbon dating of active faulting in the Agri high valley, southern Italy. *J. Geodyn.* **2000**, *29*, 371–386. [CrossRef]
25. D'Addezio, G.; Karner, D.B.; Burrato, P.; Insinga, D.; Maschio, L.; Ferranti, L.; Renne, P.R. Tephrochronology in faulted Middle Pleistocene tephra layer in the Val d'Agri area (Southern Italy). *Ann. Geophys.* **2006**, *49*, 1029–1040.
26. Giocoli, A.; Stabile, T.A.; Adurno, I.; Perrone, A.; Gallipoli, M.R.; Gueguen, E.; Norelli, E.; Piscitelli, S. Geological and geophysical characterisation of the southeastern side of the High Agri Valley (southern Apennines, Italy). *Nat. Hazards Earth Syst. Sci.* **2015**, *15*, 315–323. [CrossRef]
27. Patacca, E.; Scandone, P.; Bellatalla, M.; Perilli, N.; Santini, U. The Numidian-sand event in the Southern Apennines. *Mem. Sci. Geol. Padova* **1992**, *43*, 297–337.
28. Merlini, S.; Mostardini, F. Appennino centro-meridionale: Sezioni geologiche e proposta di modello strutturale. *Mem. Soc. Geol. It.* **1986**, *35*, 177–202.
29. Butler, R.W.H.; Corrado, S.; Mazzoli, S.; De Donatis, M.; Di Bucci, D.; Naso, G.; Scrocca, D.; Nicolai, C.; Zucconi, V. Time and space variability of «thin-skinned» and «thick-skinned» thrust tectonics in the Apennines (Italy). *Rend. Fis. Acc. Lincei* **2000**, *11*, 5–39. [CrossRef]
30. Menardi Noguera, A.; Rea, G. Deep structure of the Campanian–Lucanian arc (southern Apennine, Italy). *Tectonophysics* **2000**, *324*, 239–265. [CrossRef]
31. Wavrek, D.A.; Mosca, F. Compositional grading in the oil column: Advances from a mass balance and quantitative molecular analysis. In *Understanding Petroleum Reservoirs: Towards an Integrated Reservoir Engineering and Geochemical Approach*; Cubitt, J.M., England, W.A., Larter, S.R., Eds.; Geological Society of London: London, UK, 2004; Volume 237, pp. 207–220.
32. Cazzini, F.F. The history of the upstream oil and gas industry in Italy. In *History of the European Oil and Gas Industry*; Craig, J., Gerali, F., MacAulay, F., Sorkhabi, R., Eds.; Geological Society Special Publications: London, UK, 2018; Volume 465, pp. 243–274.
33. Olita, F. Investigation of the natural hydrocarbon manifestations and 3D reconstruction of the reservoir in the Tramutola area (Basilicata). Master's thesis, University of Basilicata, Potenza, Italy, 2019.
34. Scandone, P.; Sgrosso, I. Flysch con Inocerami nella valle del Cavolo presso Tramutola (Lucania). *Boll. Soc. Nat. Napoli* **1964**, *73*, 166–175.
35. Mattioni, L.; Tondi, E.; Shiner, P.; Renda, P.; Vitale, S.; Cello, G. The Argille Varicolori unit in Lucania (Italy): A record of tectonic offscraping and gravity sliding in the Mesozoic-Tertiary Lagonegro Basin, southern Apennines. In *Tectonics of the Western Mediterranean and North Africa*; Moratti, G., Chalouan, A., Eds.; Geological Society of London: London, UK, 2006; Volume 262, pp. 277–288.
36. Scandone, P. Studi di geologia lucana: La serie calcareo-silico-marnosa e i suoi rapporti con l'Appennino calcareo. *Boll. Soc. Nat. Napoli* **1967**, *76*, 1–175.
37. Scandone, P. Studi di geologia lucana: Note illustrative della carta dei terreni della serie calcareo–silico–marnosa. *Boll. Soc. Nat. Napoli* **1972**, *81*, 225–300.
38. De Vita, P.; Allocca, V.; Celico, F.; Fabbrocino, S.; Cesaria, M.; Monacelli, G.; Musilli, I.; Piscopo, V.; Scalise, A.R.; Summa, G.; et al. Hydrogeology of continental Southern Italy. *J. Maps* **2018**, *14*, 230–241.
39. Berserzio, R.; Felletti, F.; Giudici, M.; Miceli, A.; Zembo, I. Aquifer analogues to assist modeling of groundwater flow: The Pleistocene aquifer complex of the Agri Valley (Basilicata). In *Proceedings Italian National Workshop "Developments in Aquifer Sedimentology and Ground Water Flow Studies in Italy*; Ist. Poligrafico e Zecca dello Stato: Roma, Italy, 2007; pp. 51–66.
40. Petrella, E.; Celico, F. Heterogeneous aquitard properties in sedimentary successions in the Apennine chain: Case studies in southern Italy. *Hydrol. Process.* **2009**, *23*, 3365–3371. [CrossRef]
41. Petrella, E.; Celico, F. Mixing of water in a carbonate aquifer, southern Italy, analysed through stable isotope investigations. *Int. J. Speleol.* **2013**, *42*, 25–33. [CrossRef]
42. De Vita, P.; Allocca, V.; Manna, F.; Fabbrocino, S. Coupled decadal variability of the North Atlantic Oscillation, regional rainfall and karst spring discharges in the Campania region (southern Italy). *Hydrol. Earth Sys. Sci.* **2012**, *16*, 1389–1399. [CrossRef]

43. Allocca, V.; De Vita, P.; Manna, F.; Nimmo, J.R. Groundwater recharge assessment at local and episodic scale in a soil mantled perched karst aquifer in southern Italy. *J. Hydrol.* **2015**, *529*, 843–853. [CrossRef]
44. Fiorillo, F.; Esposito, L.; Testa, G.; Ciarcia, S.; Pagnozzi, M. The upwelling water flux feeding springs: Hydrogeological and hydraulic features. *Water* **2018**, *10*, 501. [CrossRef]
45. Fiorillo, F.; Leone, G.; Pagnozzi, M.; Catani, V.; Testa, G.; Esposito, L. The upwelling groundwater flow in the karst area of Grassano-Telese springs (Southern Italy). *Water* **2019**, *11*, 872. [CrossRef]
46. Paternoster, M.; Scarfiglieri, A.; Mongelli, G. Groundwater chemistry in the high Agri Valley (Southern Apennines, Italy). *GeoActa* **2005**, *4*, 25–42.
47. International Atomic Energy Agency. *Water and Environment News*, Issue 3, IAEA: Vienna, Austria, April 1998.
48. U.S. EPA. *Method 3510C (SW-846): Separatory Funnel Liquid-Liquid Extraction*; U.S. Environmental Protection Agency: Washington, DC, USA, 1996.
49. U.S. EPA. *Method 5030C (SW-846): Purge-and-Trap for Aqueous Samples Revision 3*; U.S. Environmental Protection Agency: Washington, DC, USA, 2003.
50. U.S. EPA. *Method 8015D (SW-846): Nonhalogenated Organics Using GC/FID Revision 4*; U.S. Environmental Protection Agency: Washington, DC, USA, 2003.
51. U.S. EPA. *Method 8270E (SW-846): Semivolatile Organic Compounds by Gas Chromatography/Mass Spectrometry (GC/MS)*; U.S. Environmental Protection Agency: Washington, DC, USA, 2018.
52. Milani, C.; Hevia, A.; Foroni, E.; Duranti, S.; Turroni, F.; Lugli, G.A.; Sanchez, B.; Martín, R.; Gueimonde, M.; van Sinderen, D.; et al. Assessing the fecal microbiota: An optimised ion torrent 16S rRNA gene-based analysis protocol. *PLoS ONE* **2013**, *8*, e68739. [CrossRef]
53. Caporaso, J.G.; Kuczynski, J.; Stombaugh, J.; Bittinger, K.; Bushman, F.D.; Costello, E.K.; Fierer, N.; Gonzalez Peña, A.; Goodrich, J.K.; Gordon, J.I.; et al. QIIME allows analysis of high-throughput community sequencing data. *Nat. Methods* **2010**, *7*, 335–336. [CrossRef]
54. Callahan, B.J.; McMurdie, P.J.; Rosen, M.J.; Han, A.W.; Johnson, A.J.; Holmes, S.P. DADA2: High-resolution sample inference from Illumina amplicon data. *Nat. Methods* **2016**, *13*, 581–583. [CrossRef]
55. Bokulich, N.A.; Kaehler, B.D.; Rideout, J.R.; Dillon, M.; Bolyen, E.; Knight, R.; Huttley, G.A.; Caporaso, J.G. Optimising taxonomic classification of marker-gene amplicon sequences with QIIME 2's q2-feature-classifier plugin. *Microbiome* **2018**, *6*, 90. [CrossRef] [PubMed]
56. Quast, C.; Pruesse, E.; Yilmaz, P.; Gerken, J.; Schweer, T.; Yarza, P.; Peplies, J.; Glöckner, F.O. The SILVA ribosomal RNA gene database project: Improved data processing and web-based tools. *Nucleic Acids Res.* **2013**, *41*, D590–D596. [CrossRef] [PubMed]
57. Longinelli, A.; Selmo, E. Isotopic composition of precipitation in Italy: A first overall map. *J. Hydrol.* **2003**, *270*, 75–88.
58. Zar, J.H. *Biostatistical Analysis*, 5th ed.; Prentice Hall, Inc.: Englewood Cliffs, NJ, USA, 2010.
59. Petrella, E.; Naclerio, G.; Falasca, A.; Bucci, A.; Capuano, P.; De Felice, V.; Celico, F. Non-permanent shallow halocline in a fractured carbonate aquifer, southern Italy. *J. Hydrol.* **2009**, *373*, 267–272. [CrossRef]
60. Krajcar Bronić, I.; Barešić, J.; Borković, D.; Sironić, A.; Mikelić, I.L.; Vreča, P. Long-Term Isotope Records of Precipitation in Zagreb, Croatia. *Water* **2020**, *12*, 226. [CrossRef]
61. Auling, G.; Busse, H.-J.; Egli, T.; El-Banna, T.; Stackebrandt, E. Description of the Gram-negative, obligately aerobic, nitrilotriacetate (NTA)-utilizing bacteria as *Chelatobacter heintzii*, gen. nov., sp. nov., and *Chelatococcus asaccharovorans*, gen. nov., sp. nov. *Syst. Appl. Microbiol.* **1993**, *16*, 104–112. [CrossRef]
62. Mahe, Y.F.; Perez, M.J.; Tacheau, C.; Fanchon, C.; Martin, R.; Rousset, F.; Seite, S. A new *Vitreoscilla filiformis* extract grown on spa water-enriched medium activates endogenous cutaneous antioxidant and antimicrobial defenses through a potential Toll-like receptor 2/protein kinase C, zeta transduction pathway. *Clin. Cosmet. Investig Dermatol.* **2013**, *6*, 191–196.
63. Palleroni, N.J. New species of the genus *Actinoplanes, Actinoplanes ferrugineus*. *Int. J. Syst. Evol. Microbiol.* **1979**, *29*, 51–55. [CrossRef]
64. Pellegrin, V.; Juretschko, S.; Wagner, M.; Cottenceau, G. Morphological and biochemical properties of a *Sphaerotilus* sp. isolated from paper mill slimes. *Appl. Environ. Microbiol.* **1999**, *65*, 156–162. [CrossRef]

65. Willems, A.; Busse, J.; Goor, M.; Pot, B.; Falsen, E.; Jantzen, E.; Hoste, B.; Gillis, M.; Kersters, K.; Auling, G.; et al. *Hydrogenophaga*, a new genus of hydrogen-oxidizing bacteria that includes *Hydrogenophaga flava* comb. nov.(formerly *Pseudomonas flava*), *Hydrogenophaga palleronii* (formerly *Pseudomonas palleronii*), *Hydrogenophaga pseudoflava* (formerly *Pseudomonas pseudoflava* and "*Pseudomonas carboxydoflava*"), and *Hydrogenophaga taeniospiralis* (formerly *Pseudomonas taeniospiralis*). *Int. J. Syst. Evol. Microbiol.* **1989**, *39*, 319–333.
66. Zhang, Y.-Q.; Chen, Y.-G.; Li, W.-J.; Tian, X.-P.; Xu, L.-H.; Jiang, C.-L. *Sphingomonas yunnanensis* sp. nov., a novel Gram-negative bacterium from a contaminated plate. *Int. J. Syst. Evol. Microbiol.* **2005**, *55*, 2361–2364. [PubMed]
67. Van Niel, C.B. On the morphology and physiology of the purple and green sulphur bacteria. *Archiv. Mikrobiol.* **1932**, *3*, 1–112. [CrossRef]
68. Rees, G.N.; Patel, B.K.; Grassia, G.S.; Sheehy, A.J. *Anaerobaculum thermoterrenum* gen. nov., sp. nov., a novel, thermophilic bacterium which ferments citrate. *Int. J. Syst. Bacteriol.* **1997**, *47*, 150–154. [CrossRef] [PubMed]
69. Thevenieau, F.; Fardeau, M.L.; Ollivier, B.; Joulian, C.; Baena, S. *Desulfomicrobium thermophilum* sp. nov., a novel thermophilic sulphate-reducing bacterium isolated from a terrestrial hot spring in Colombia. *Extremophiles* **2007**, *11*, 295–303. [CrossRef] [PubMed]
70. Chimtong, S.; Tachaapaikoon, C.; Pason, P.; Kyu, K.L.; Kosugi, A.; Mori, Y.; Ratanakhanokchai, K. Isolation and characterization of endocellulase-free multienzyme complex from newly isolated *Thermoanaerobacterium thermosaccharolyticum* strain NOI-1. *J. Microbiol. Biotechnol.* **2011**, *21*, 284–292. [CrossRef] [PubMed]
71. Wiegel, J.; Ljungdahl, L.G. *Thermoanaerobacter ethanolicus* gen. nov., spec. nov., a new, extreme thermophilic, anaerobic bacterium. *Arch. Microbiol.* **1981**, *128*, 343–348. [CrossRef]
72. Knøchel, S. Growth characteristics of motile *Aeromonas* spp. isolated from different environments. *Int. J. Food Microbiol.* **1990**, *10*, 235–244. [CrossRef]
73. Horn, M.A.; Ihssen, J.; Matthies, C.; Schramm, A.; Acker, G.; Drake, H.L. *Dechloromonas denitrificans* sp. nov., *Flavobacterium denitrificans* sp. nov., *Paenibacillus anaericanus* sp. nov. and *Paenibacillus terrae* strain MH72, N2O-producing bacteria isolated from the gut of the earthworm *Aporrectodea caliginosa*. *Int. J. Syst. Evol. Microbiol.* **2005**, *55*, 1255–1265. [CrossRef]
74. Bernardet, J.-F.; Bowman, J.P. *Flavobacterium*. In *Bergey's Manual of Systematics of Archaea and Bacteria*; Whitman, W.B., Rainey, F., Kämpfer, P., Trujillo, M., Chun, J., DeVos, P., Hedlund, B., Dedysh, S., Eds.; John Wiley & Sons, Inc., in association with Bergey's Manual Trust: Hoboken, NJ, USA, 2015.
75. Spring, S.; Kampfer, P.; Ludwig, W.; Schleifer, K.-H. Polyphasic characterization of the genus *Leptothrix*: New descriptions of *Leptothrix mobilis* sp. nov. and *Leptothrix discophora* sp. nov. nom. rev. and emended description of *Leptothrix cholodnii* emend. *Syst. Appl. Microbiol.* **1996**, *19*, 634–643. [CrossRef]
76. Kalyuzhnaya, M.G.; Bowerman, S.; Lara, J.C.; Lidstrom, M.E.; Chistoserdova, L. *Methylotenera mobilis* gen. nov., sp. nov., an obligately methylamine-utilising bacterium within the family *Methylophilaceae*. *Int. J. Syst. Evol. Microbiol.* **2006**, *56*, 2819–2823. [CrossRef]
77. Zhang, J.; Song, F.; Xin, Y.H.; Zhang, J.; Fang, C. *Microvirga guangxiensis* sp. nov., a novel alphaproteobacterium from soil, and emended description of the genus *Microvirga*. *Int. J. Syst. Evol. Microbiol.* **2009**, *59*, 1997–2001. [CrossRef] [PubMed]
78. Kodama, Y.; Watanabe, K. *Sulfuricurvum kujiense* gen. nov., sp. nov., a facultatively anaerobic, chemolithoautotrophic, sulfur-oxidising bacterium isolated from an underground crude-oil storage cavity. *Int. J. Syst. Evol. Microbiol.* **2004**, *54*, 2297–2300. [CrossRef] [PubMed]
79. Kojima, H.; Fukui, M. *Sulfuritalea hydrogenivorans* gen. nov., sp. nov., a facultative autotroph isolated from a freshwater lake. *Int. J. Syst. Evol. Microbiol.* **2011**, *61*, 1651–1655. [CrossRef] [PubMed]
80. Inagaki, F.; Takai, K.; Nealson, K.H.; Horikoshi, K. *Sulfurovum lithotrophicum* gen. nov., sp. nov., a novel sulfur-oxidising chemolithoautotroph within the ε-Proteobacteria isolated from Okinawa Trough hydrothermal sediments. *Int. J. Syst. Evol. Microbiol.* **2004**, *54*, 1477–1482. [CrossRef]
81. Ito, T.; Sugita, K.; Yumoto, I.; Nodasaka, Y.; Okabe, S. *Thiovirga sulfuroxydans* gen. nov., sp. nov., a chemolithoautotrophic sulfur-oxidising bacterium isolated from a microaerobic waste-water biofilm. *Int. J. Syst. Evol. Microbiol.* **2005**, *55*, 1059–1064. [CrossRef]
82. Aruga, S.; Kamagata, Y.; Kohno, T.; Hanada, S.; Nakamura, K.; Kanagawa, T. Characterisation of filamentous Eikelboom type 021N bacteria and description of *Thiothrix disciformis* sp. nov. and *Thiothrix flexilis* sp. nov. *Int. J. Syst. Evol. Microbiol.* **2002**, *52*, 1309–1316.

83. Storti, F.; Billi, A.; Salvini, F. Particle size distributions in natural carbonate fault rocks: Insights for non-self-similar cataclasis. *Earth Planet. Sci. Lett.* **2003**, *206*, 173–186. [CrossRef]
84. Ferraro, F.; Grieco, D.S.; Agosta, F.; Prosser, G. Space-time evolution of cataclasis in carbonate fault zones. *J. Struct. Geol.* **2018**, *110*, 45–64. [CrossRef]
85. Giuffrida, A.; La Bruna, V.; Castelluccio, P.; Panza, E.; Rustichelli, A.; Tondi, E.; Giorgioni, M.; Agosta, F. Fracture simulation parameters of fractured reservoirs: Analogy with outcropping carbonates of the Inner Apulian Platform, southern Italy. *J. Struct. Geol.* **2019**, *123*, 18–41. [CrossRef]
86. Chiodini, G.; Avino, R.; Brombach, T.; Caliro, S.; Cardellini, C.; De Vita, S.; Frondini, F.; Granirei, D.; Marotta, E.; Ventura, G. Fumarolic and diffuse soil degassing west of Mount Epomeo, Ischia, Italy. *J. Volcanol. Geotherm. Res.* **2004**, *133*, 291–309. [CrossRef]
87. Celico, F.; Petrella, E.; Celico, P. Hydrogeological behaviour of some fault zones in a carbonate aquifer of Southern Italy: An experimentally based model. *Terra Nova* **2006**, *18*, 308–313. [CrossRef]
88. Petrella, E.; Capuano, P.; Carcione, M.; Celico, F. A high-altitude temporary spring in a compartmentalised carbonate aquifer: The role of low-permeability faults and karst conduits. *Hydrol. Process.* **2009**, *23*, 3354–3364. [CrossRef]
89. Bucci, A.; Naclerio, G.; Allocca, V.; Celico, P.; Celico, F. Potential use of microbial community investigations to analyse hydrothermal systems behaviour: The case of Ischia Island, Southern Italy. *Hydrol. Process.* **2011**, *25*, 1866–1873. [CrossRef]
90. Bucci, A.; Petrella, E.; Naclerio, G.; Gambatese, S.; Celico, F. Bacterial migration through low-permeability fault zones in compartmentalised aquifer systems: A case study in Southern Italy. *Int. J. Speleol.* **2014**, *43*, 273–281. [CrossRef]
91. Aquino, D.; Petrella, E.; Florio, M.; Celico, P.; Celico, F. Complex hydraulic interactions between compartmentalised carbonate aquifers and heterogeneous siliciclastic successions: A case study in southern Italy. *Hydrol. Process.* **2015**, *29*, 4252–4263. [CrossRef]
92. Petrella, E.; Aquino, D.; Fiorillo, F.; Celico, F. The effect of low-permeability fault zones on groundwater flow in a compartmentalised system. Experimental evidence from a carbonate aquifer (Southern Italy). *Hydrol. Process.* **2015**, *29*, 1577–1587. [CrossRef]
93. Allocca, V.; Marzano, E.; Tramontano, M.; Celico, F. Environmental impact of cattle grazing on a karst aquifer in the southern Apennines (Italy): Quantification through the grey water footprint. *Ecol. Indic.* **2018**, *93*, 830–837. [CrossRef]
94. Pekdeger, A.; Matthess, G. Factors of bacteria and virus transport in groundwater. *Environ. Geol.* **1983**, *5*, 49–52. [CrossRef]
95. McMurry, S.W.; Coyne, M.S.; Perfect, E. Fecal coliform transport through intact soil blocks amended with poultry manure. *J. Environ. Qual.* **1998**, *27*, 86–92. [CrossRef]
96. Naclerio, G.; Fardella, G.; Marzullo, G.; Celico, F. Filtration of *Bacillus subtilis* and *Bacillus cereus* spores in a pyroclastic topsoil, carbonate Apennines, southern Italy. *Colloids Surf. B Biointerfaces* **2009**, *70*, 25–28. [CrossRef]
97. Bucci, A.; Petrella, E.; Naclerio, G.; Allocca, V.; Celico, F. Microorganisms as contaminants and natural tracers: A 10-year research in some carbonate aquifers (southern Italy). *Environ. Earth Sci.* **2015**, *74*, 173–184. [CrossRef]
98. Candela, S.; Mazzoli, S.; Megna, A.; Santini, S. Finite element modelling of stress field perturbations and interseismic crustal deformation in the Val d'Agri region, southern Apennines, Italy. *Tectonophysics* **2015**, *657*, 245–259. [CrossRef]

water

MDPI

Article

Potential Enhancement of the *In-Situ* Bioremediation of Contaminated Sites through the Isolation and Screening of Bacterial Strains in Natural Hydrocarbon Springs

Pietro Rizzo [1], Matilde Malerba [1], Antonio Bucci [2,*], Anna M. Sanangelantoni [1], Sara Remelli [1] and Fulvio Celico [1]

[1] Department of Chemistry, Life Sciences and Environmental Sustainability, University of Parma, Parco Area delle Scienze 157/A, 43124 Parma, Italy; pietro.rizzo2@studenti.unipr.it (P.R.); matilde.malerba@studenti.unipr.it (M.M.); annamaria.sanangelantoni@unipr.it (A.M.S.); sara.remelli@unipr.it (S.R.); fulvio.celico@unipr.it (F.C.)

[2] Department of Biosciences and Territory, University of Molise, C.da Fonte Lappone, 86090 Pesche, Italy

* Correspondence: antonio.bucci@unimol.it; Tel.: +39-0874-404-156

Received: 5 June 2020; Accepted: 21 July 2020; Published: 23 July 2020

Abstract: Petroleum hydrocarbon contamination (PHC) is an issue of major concern worldwide. These compounds represent the most common environmental pollutants and their cleaning up is mandatory. The main goal of this research was to analyze microbial communities in a site in southern Italy characterized by the presence of hydrocarbons of natural origin by using a multidisciplinary approach based on microbiological, geological and hydrological investigations. Bacterial communities of two springs, the surrounding soils, and groundwater were studied through a combination of molecular and culture-dependent methodologies to explore the biodiversity at the study site, to isolate microorganisms with degradative abilities, and to assess their potential to develop effective strategies to restore the environmental quality. Next-generation sequencing revealed the dominance of species of the *Proteobacteria* phylum but also the presence of other autochthonous hydrocarbon-oxidizing microorganisms affiliated to other phyla (e.g., species of the genera *Flavobacterium* and *Gordonia*). The traditional cultivation-based approach led to the isolation and identification of 11 aerobic hydrocarbon-oxidizing proteobacteria, some of which were able to grow with phenanthrene as the sole carbon source. Seven out of the 11 isolated bacterial strains produced emulsion with diesel fuel (most of them showing emulsifying capacity values greater than 50%) with a high stability after 24 h and, in some cases, after 48 h. These results pave the way for further investigations finalized at (1) exploiting both the degradation ability of the bacterial isolates and/or microbial consortia to remediate hydrocarbon-contaminated sites and (2) the capability to produce molecules with a promoting effect for oil polluted matrices restoration.

Keywords: hydrocarbon springs; groundwater; bioremediation; microbiological-hydrogeological investigations; next-generation sequencing (NGS)

1. Introduction

Hydrocarbon pollution is a widespread phenomenon that affects human health and the environment, including air, water, and soil [1]. Hydrocarbons of petroleum origin, despite being essential energy resources and one of the raw materials needed for different types of industries [2], are classified as priority pollutants [3]. Many of them, such as Polycyclic Aromatic Hydrocarbons

(PAHs), are recalcitrant and highly dangerous, as they can be hemotoxic, carcinogenic and teratogenic [3–7]. Accordingly, over the decades, the awareness to protect the environment has increased, especially now that pollution is recognized as one of the most severe and urgent issues society has to face. The sources of environmental contamination caused by hydrocarbons are different, such as accidents in the transport of fuel by ships and tankers, leaks from underground tanks and service stations, oil extraction and processing operations, release of oily waste generated by industries that use oil in the production of plastics, solvents, pharmaceuticals and cosmetics [8,9]. The cleaning up of these contaminants from the environment is mandatory and can be reached by using physical-chemical or biological strategies [1,10]. Biological approaches have shown several advantages compared to traditional physical-chemical treatments, being more cost effective and allowing for the complete mineralization of the organic pollutant [10,11]. For this reason, bioremediation has been widely studied and is an environmentally friendly technology used for the removal of hydrocarbons in both terrestrial and aquatic ecosystems [12]. The bioremediation of contaminated sites by organic compounds is based on the stimulation of the catabolic activity of microorganisms capable of using polluting organic contaminants as a source of carbon and energy. So far, bioremediation is performed through different practices such as biostimulation (the addition of macro- and/or micronutrients to enhance indigenous biomass growth and pollutant degradation), bioaugmentation (inoculation with pollutant-degrading microorganisms) or combined biostimulation and bioaugmentation [13].

The microbial community in a given ecosystem is crucial for the biodegradation of pollutants to occur [14]. In fact, bacterial adaptation, defined as an evolutionary process in which shifts in the microbial community composition or abundances take place in response to changes in environmental conditions and contaminant content, can improve the biodegradation rate of a chemical.

On the other hand, the existence of a microbial potential does not always lead to in situ biodegradation since many limitations, such as insufficient biomass, utilization of a wide range of substrates, competitive inhibition, or catabolite repression, can all inhibit the process [14].

From this perspective, the analysis and characterization of microorganisms involved in biodegradation processes are of the utmost importance for the ultimate success of bioremediation. Furthermore, it is essential not only to dwell upon microbial communities but also have knowledge on the geological, hydrogeological and geochemical characteristics of the environment in which they live because several other factors may influence their activities [5,15].

The main aim of the present work was to analyze microbial communities in soil, spring and groundwaters from a study site in southern Italy characterized by the presence of hydrocarbons of natural origin, through a combination of culture-dependent and molecular methods. In addition, the comprehension of the geological and hydrogeological features of the aquifer system was fundamental to identify the active circuits that continuously feed the studied soil, springs and groundwaters, all year round, and could influence the composition of the bacterial communities. Some of the bacterial isolates were identified and screened for their ability to grow in the presence of different pollutants and emulsifying capacity, to assess their potential as candidates in biotechnological applications to treat and recover the polluted environmental matrices.

2. Materials and Methods

2.1. Study Area

The study area (Tramutola, Agri Valley, Southern Italy; Figures 1 and S1) is characterized by some natural outcrops of hydrocarbons, whose existence was already known from the end of the 19th century [16]. The Agri Valley is an intramountain valley, with a North-West/South-East orientation, a length of 30 km and an average width of 12 km. This study is focused on a small portion of the valley that includes two springs (S1 and S2) with natural hydrocarbon outcrops close to wells drilled in the early 20th century by the AGIP Company (at present ENI, Milano, Italy) for gas and oil extraction. Among these wells, the artesian well P_{art} was included in this research. The springs S1 and S2 (Figure S2), as well as the P_{art} well, are located along an E-W fault where the Apulian carbonate

platform and Rio Cavolo Unit (Oligocene) [17] crop out (Figure 2). The Rio Cavolo Unit is made up of clays, micaceous limestone and rare marly layers. The P_{art} well (404 m deep) intercepted oil and gas at different depths [18,19].

Different hydrogeological series complexes crop out at the study site [20]: (i) carbonate rocks belonging to the Mesozoic carbonate platform series complexes, characterized by very high permeability due to a well-developed fracture network and karst conduits; (ii) sedimentary rocks belonging to the syn-orogenic turbidite series complexes and the outer and the inner basins' series complexes, characterized by a permeability ranging from very low to low due to a mixed pore-fracture network. Along the Cavolo stream and the whole Agri Valley, heterogeneous alluvial sediments crop out, whose hydraulic conductivity ranges between less than 1×10^{-8} to 2×10^{-2} m/s [21].

The hydrocarbon springs S1 and S2 flow out along a fault zone which enhances fluid upflow and allows the mixing of hydrocarbons and gas (mainly CH_4 and H_2S) [22] with the local groundwater, which is primarily fed by the nearby carbonate aquifer (Figure 2) [19]. The groundwater intercepted by the P_{art} well is fed by a more prolonged pathway in a relatively deep aquifer made of Scisti Silicei (Figure 3) [19]. This deep groundwater naturally flows eastwards, towards the alluvial aquifer of the Agri Valley.

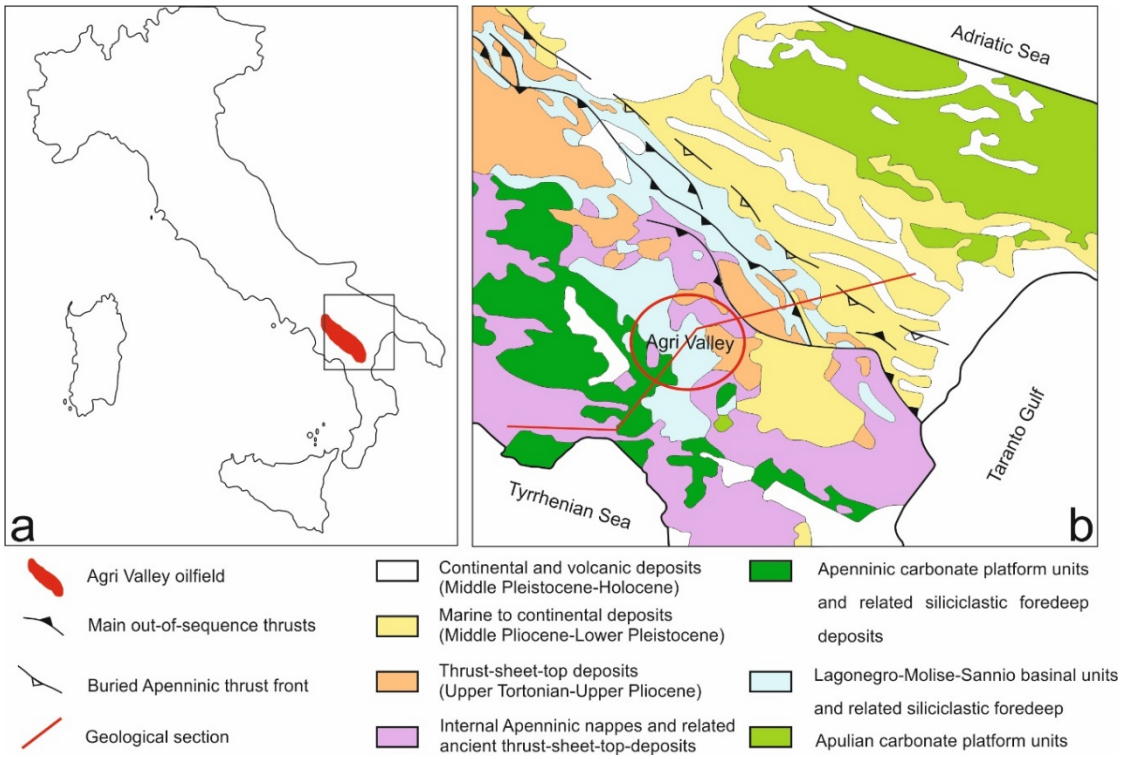

Figure 1. (**a**) Localization of the study area. (**b**) Schematic structural-geological map of the southern Apennines from Patacca et al. [23], modified.

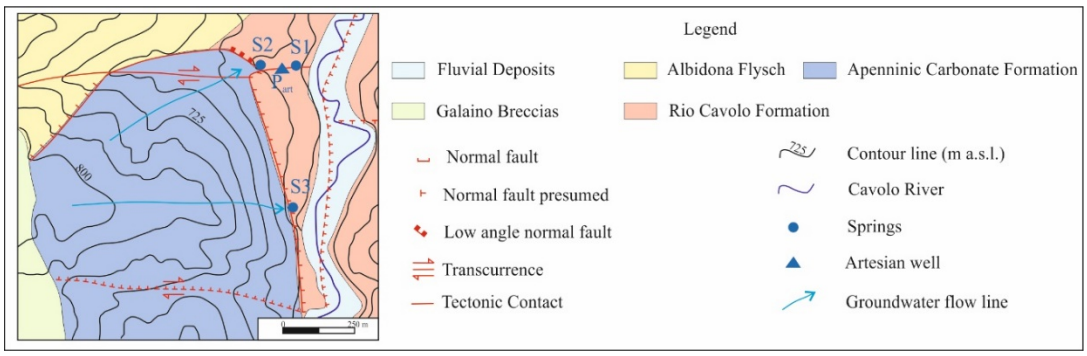

Figure 2. Hydrogeological map of the study area (from Rizzo et al. [19]); the blue points and the triangle show the location of the investigated springs S1 and S2 and the artesian well P_{art} (the geological sketch is taken from Olita [18], modified).

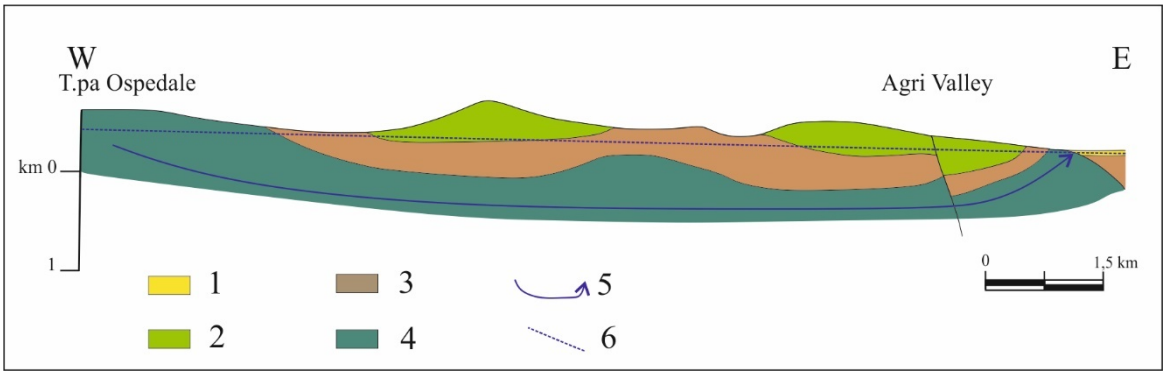

Figure 3. Hydrogeological schetch of the Scisti Silicei aquifer (Rizzo et al. [19]; based on the geological section of Menardi Noguera and Rea [24]): the (1) alluvial complex, (2) carbonate complex, (3) low-permeability complex, (4) Scisti Silicei complex, (5) groundwater flow line, (6) and hydraulic head.

2.2. Hydrogeological and Chemical-Physical Investigations

The discharge of the two springs S1 and S2 was measured in low flow (July 2018), in early recharge (October 2018) and in late recharge (March 2019). Moreover, it was measured hourly during a rainfall event to analyze the time lag between precipitation and springs' recharge increase. The flow rate of the P_{art} artesian well was not measurable but, based on some historical data, its order of magnitude is about 30 m^3/h [19]. In conjunction with discharge measurements and sample collection for chemical and microbiological analyses (March 2019), physico-chemical parameters such as temperature (°C), pH, electrical conductivity (EC µS/cm), redox potential (ORP millivolts) and total dissolved solids (TDS ppm), were measured with the multiparameter HANNA probe (mod. HI9828, HANNA Instruments, Villafranca Padovana, Italy).

Three water and two soil samples were collected to analyze PAHs and benzene, toluene, ethylbenzene, and xylene (BTEX) content. These data were compared with those acquired during sampling campaigns carried out in 2013 (unpublished data). One-liter (L) black glass bottles and 40-milliliter colorless glass vials (filled with water or soil) were used for PAHs and BTEX analyses, respectively. The analyses were performed at Biochemie Lab S.r.l. following the EPA 3510C 1996 + EPA 8270E 2018 protocol for PAHs and the EPA 5030C 2003 + EPA 8015D 2003 protocol for BTEX in water and EPA 3550C 2007 + EPA 8015D 2003 protocol for PAHs and the EPA 5021A 2014 + EPA 8015D 2003 protocol for BETX in soil [25–30].

2.3. Next-Generation Sequencing (NGS) for Bacterial Community Analyses

For bacterial community analyses, spring and groundwater samples (4 L) and two soil samples (0.5 g), collected close to the springs (0.5 m distance), were used. Water samples were filtered through sterile mixed esters of cellulose filters (S-Pak™ Membrane Filters, 47 mm diameter, 0.22 µm pore size,

Millipore Corporation, Billerica, MA, USA) within 24 h from the collection. Bacterial DNA extraction from filters and soils was performed using the commercial kit FastDNA SPIN Kit for soil (MP Biomedicals, LLC, Solon, OH, USA) and FastPrep®Instrument (MP Biomedicals, LLC, Solon, OH, USA). After the extraction, DNA integrity and quantity were evaluated by electrophoresis in 0.8% agarose gel containing 1μg/mL of Gel-RedTM (Biotium, Inc., Fremont, CA, USA). The bacterial community profiles in the samples were generated by next-generation sequencing (NGS) technologies at the Genprobio Srl Laboratory. Partial 16S rRNA gene sequences were obtained from the extracted DNA by polymerase chain reaction (PCR), using the primer pair Probio_Uni and Probio_Rev, targeting the V3 region of the bacterial 16S rRNA gene [31]. Amplifications were carried out using a Veriti Thermal Cycler (Applied Biosystems, Foster City, CA, USA), and PCR products were purified by the magnetic purification step involving the Agencourt AMPure XP DNA purification beads (Beckman Coulter Genomics GmbH, Bernried, Germany) in order to remove primer dimers. Amplicon checks were carried out as previously described [31]. Sequencing was performed using an Illumina MiSeq sequencer (Illumina, Hayward, CA, USA) with MiSeq Reagent Kit v3 chemicals. The fastq files were processed using a custom script based on the QIIME software suite [32]. Paired-end read pairs were assembled to reconstruct the complete Probio_Uni/Probio_Rev amplicons. Quality control retained sequences with a length between 140 and 400 bp and mean sequence quality score > 20, while sequences with homopolymers > 7 bp and mismatched primers were omitted. To calculate downstream diversity measures, operational taxonomic units (OTUs) were defined at 100% sequence homology using DADA2 [33]; OTUs not encompassing at least two sequences of the same sample were removed. All reads were classified to the lowest possible taxonomic rank using QIIME2 [32,34] and a reference dataset from the SILVA database v132 [35]. The biodiversity of the samples (alpha-diversity) was calculated with the Shannon index. Similarities between samples (beta-diversity) were calculated by weighted uniFrac. The range of similarities is calculated between values 0 and 1. Principal Coordinate Analysis (PCoA) representations of beta-diversity were performed using QIIME2. In the PCoA, each dot represented a sample that is distributed in tridimensional space according to its own bacterial composition.

2.4. Enrichment and Isolation of Bacteria with Potential Hydrocarbon Degrading Ability

To isolate hydrocarbon-oxidizing bacteria, 1-mL aliquots of water from springs S1 and S2 and P_{art} well, and 5 g of soils collected close to the springs (0.5 m distance), were inoculated in sterile test tubes containing peptone water. Then, 1 mL of the suspensions was inoculated in 5 mL of liquid Bushnell-Haas (BH) medium ($MgSO_4$-0.2 g/L; $CaCl_2$-0.02 g/L; KH_2PO_4-1.0 g/L; K_2HPO_4-1.0 g/L; NH_4NO_3-1.0 g/L; $FeCl_3$-0.05 g/L) [36]. Diesel fuel was added at a concentration of 2% as the only carbon source, to select the hydrocarbon degrading bacteria. Cultures were, then, incubated at 28 °C for seven days with agitation. The enrichment step was repeated for seven cycles. From the fourth enrichment cycle, 100-μL aliquots of the cultures were spread on Bushnell-Haas (BH) agar medium supplemented with diesel fuel as a carbon source. Diesel fuel was supplied by diffusion through a soaked paper disk (9-mm diameter).

The colonies grown on the plates were repeatedly streaked over the entire surface of fresh BH agar medium supplemented with diesel fuel and, finally, on TSA (Tryptone Soy Agar) plates to be sure to obtain pure cultures.

2.5. Identification of the Bacterial Strains Isolated from Spring, Groundwater and Soil Samples

After the enrichment, the isolated bacterial strains were analyzed by Amplified Ribosomal DNA Restriction Analysis (ARDRA) with the restriction endonuclease HaeIII, to group them on the basis of the restriction profiles. One representative strain for each ARDRA haplotype was selected for the 16S rDNA gene partial sequencing at BMR Genomics srl in Padua (Italy). The obtained sequences were then compared with those stored in the GenBank database at the NCBI (National Center for Biotechnology Information) by using the BLAST (Basic Local Alignment Search Tool) program (http://www.ncbi.nlm.nih.gov/blast). The partial 16S rDNA gene sequences were deposited in GenBank under the accession numbers MT703034 to MT703044.

2.6. Growth Response of Bacterial Isolates in the Presence of Different Hydrocarbons as the Sole Carbon Source

The potential degradation ability of some bacterial strains has been evaluated in BH agar medium containing different hydrocarbons (Naphthalene, Phenanthrene, Pristane and Hexadecane) as the sole carbon source. Naphthalene and Phenanthrene occur, at room temperature, in the solid state as granules; after spreading the individual bacterial strains onto the medium surface, the granules were added directly to the surface of the medium. The Pristane and the Hexadecane occur, at room temperature, in the liquid state and were delivered by diffusion from a soaked paper disk placed in the center of the plate. The plates were incubated at 30 °C for 4 weeks, monitoring the growth every week.

2.7. Determination of the Emulsifying Capacity and Emulsion Index

The assay used to determine the emulsifying capacity (EC%) and the emulsion index (E) is a re-adaptation of the method previously described by Mohebali et al. [37]; 2 mL of pure cultures of the isolated strains, grown in BH medium at 28 °C with agitation until the optical density (OD) at the wavelength of 600 nm reached 1.0 (OD measured with a Cary 50 UV-Vis spectrophotometer, VARIAN INC, Palo Alto, CA, USA), were transferred to test tubes and diesel fuel (0.2 mL) was added; the test tubes were vigorously shaken for 30 s and left standing for 10 min. The samples showing an emulsion over the liquid were selected and, once the emulsion was stabilized, more diesel fuel (0.2 mL) was added; the procedure was repeated until a distinct and clear fraction of non-emulsified diesel fuel was observed on the surface of the emulsion.

The emulsifying capacity (EC%) was calculated using the following formula:

$$\mathrm{EC} = \frac{\text{total diesel volume}}{\text{initial aqueous phase volume}} \times 100$$

The emulsion index (E) was calculated after the test for the emulsifying capacity; the variation of the emulsion thickness was measured after 24 (E_{24}) and 48 (E_{48}) h with the following formula:

$$\mathrm{E} = 100 \times \frac{\text{emulsion thickness at } t_x}{\text{emulsion thickness at } t_0}$$

where t_x is the time in which the measurement was taken (e.g., t_{24}, t_{48}) and t_0 is the test start time.

3. Results

3.1. Hydrogeological and Physico-Chemical Features

The flow rate of both hydrocarbon springs S1 and S2 slightly varied overtime during the observation period (1.3 to 1.7 m^3/h at spring S1; 1.0 to 1.2 m^3/h at spring S2), suggesting an active groundwater pathway. The spring regime, further analyzed through hourly measurements during a rainfall event (about 11 mm in a few tens of hours), demonstrated a very rapid and synchronous response of spring S1 (2.5 to 3.6 m^3/h) and spring S2 (2.0 to 2.5 m^3/h) to precipitation.

The main physico-chemical features of hydrocarbon springs and P_{art} well are synthesized in Table 1. The temperature ranged from 13.9 to 15.7 °C in spring waters, while it varied between 27.5 and 27.8 °C in P_{art} waters. The pH was constantly close to neutrality. Redox potential was slightly negative. The electrical conductivity was higher and more variable in P_{art}-water (1444 to 2433 μS/cm) than in springs waters (460 to 507 μS/cm).

Table 1. Physico-chemical features of spring- and groundwaters.

Sample	Date	Temperature	pH	Redox Potential	Electrical Conductivity
ID	dd/mm/yyyy	°C		mV	μS/cm
P_{art}	19/07/2018	27.8	6.8	−26.0	1444
P_{art}	29/10/2018	27.6	6.8	−30.0	2433
P_{art}	18/03/2019	27.5	6.8	−7.5	2432
S1	19/07/2018	15.6	6.9	−60.0	507
S1	29/10/2018	15.6	6.8	−51.8	494
S1	18/03/2019	15.7	6.9	−33.4	494
S2	19/07/2018	14.3	6.9	−20.0	460
S2	29/10/2018	15.6	6.9	−15.0	467
S2	18/03/2019	13.9	6.9	−4.0	493

3.2. Chemical Analyses of Spring, Groundwater and Soil Samples

Chemical analyses revealed detectable PAHs and no BTEX in both springs S1 and S2 (Table 2). Neither PAHs nor BTEX were detected in groundwater sampled from the P_{art} artesian well. These results agree with those obtained by ENI in 2013 (unpublished data).

Table 2. Results of chemical analyses of spring- and groundwater samples.

Parameter	Spring S1	Spring S2	P_{art} Well
Unit	μg/L	μg/L	μg/L
Benzene	<0.1	<0.1	<0.1
Ethylbenzene	<1.0	<1.0	<1.0
p-Xylene	<1.0	<1.0	<1.0
Styrene	<1.0	<1.0	<1.0
Toluene	<1.0	<1.0	<1.0
Benzo(a)anthracene	<0.002	<0.002	<0.002
Benzo(a)pyrene	<0.002	<0.002	<0.002
Benzo(b)fluoranthene	<0.002	0.354	<0.002
Benzo(k)fluoranthene	<0.002	0.0341	<0.002
Benzo(g,h,i)perylene	<0.002	0.199	<0.002
Chrysene	<0.002	<0.002	<0.002
Dibenzo(a,h)anthracene	<0.002	<0.002	<0.002
Indene(1,2,3-c,d)pyrene	<0.002	0.101	<0.002
Pyrene	<0.002	<0.002	<0.002
Acenaphthene	<0.002	<0.002	<0.002
Acenaphthylene	<0.002	<0.002	<0.002
Anthracene	<0.005	0.726	<0.005
Naphthalene	0.00231	<0.002	<0.002
Phenanthrene	<0.002	0.465	<0.002
Fluoranthene	<0.005	0.166	<0.005
Fluorene	<0.005	<0.005	<0.005
Benzo(J)fluoranthene	<0.001	0.0140	<0.001
Dibenzo(a,e)pyrene	<0.001	<0.001	<0.001
Dibenzo(a,l)pyrene	<0.001	<0.001	<0.001
Dibenzo(a,i)pyrene	<0.001	<0.001	<0.001
Dibenzo(a,h)pyrene	<0.001	<0.001	<0.001
Σ PAHs	<0.002	0.689	<0.002

Consistent with the results obtained in spring water samples, several PAHs were detected in soils collected close to both the investigated springs. Higher concentrations were found close to spring S2 (Table 3).

Table 3. Results of chemical analyses of soil samples.

Parameter	Soil S1	Soil S2
Unit	mg/kg	mg/kg
Benzene	<0.01	<0.01
Etilbenzene	<0.05	<0.05
Toluene	<0.05	<0.05
Xylenes	<0.05	<0.05
o-Xylene	<0.05	<0.05
p,m-Xylenes	<0.05	<0.05
Benzo(a)anthracene	0.16	0.95
Benzo(a)pyrene	<0.01	<0.01
Benzo(b)fluoranthene	<0.05	3.93
Benzo(g,h,i)perylene	0.28	1.45
Benzo(k)fluoranthene	<0.05	0.58
Chrysene	0.21	1.23
Dibenzo(a,e)pyrene	<0.01	<0.01
Dibenzo(a,h)anthracene	<0.01	0.34
Dibenzo(a,h)pyrene	<0.01	<0.01
Dibenzo(a,i)pyrene	<0.01	<0.01
Dibenzo(a,l)pyrene	<0.01	0.10
Indene(1,2,3-c,d)pyrene	0.05	0.19
Pyrene	<0.05	0.61
Σ PAHs	<1.0	8.25

3.3. 16S Ribosomal RNA Gene Next-Generation Sequencing (NGS)

MiSeq runs produced 294,432 final reads (Table 4). The 16S rRNA gene sequences generated in this study have been deposited in the NCBI Sequence Read Archive under the accession numbers PRJNA629324 and PRJNA636951. The rarefaction analysis, a measure used to estimate the alpha diversity in samples and gauge whether or not sequencing efforts captured the microbial diversity, showed a relatively higher biodiversity in soil samples and spring S2-water (Shannon index values ranging from 7.59 to 8.88) compared to spring S1-water and P_{art}-groundwater (index values of 3.40 and 4.32, respectively; Figure S3). Principal Coordinate Analysis (PCoA) based on weighted uniFrac index revealed a clear separation of soil, spring, and groundwater samples and highlighted marked differences between the S1 spring water microbial community and all the others (Figure 4).

The NGS results allowed us to obtain detailed information about the composition of microbial communities in spring water, groundwater and soil samples.

Table 4. Number of 16S rDNA sequences obtained after next-generation sequencing (NGS) analysis for spring water, groundwater and soil samples.

Sample	Final Read Number
S1 Water	49,512
S1 Soil	61,621
S2 Water	61,065
S2 Soil	68,893
P_{art} Water	53,341

The phylum *Proteobacteria* was dominant in most of the analyzed samples, reaching relative abundance values of up to 93.60% (sample P_{art}) (Figure 5). Other phyla abundantly represented were *Epsilonbacteraeota* in the spring water sample S1 (52.48%), and *Actinobacteria*, found in the two soil samples at percentages of 16.38% and 22.20%.

In line with the PCoA results, significant differences between the two spring water microbial communities were detectable already at this level. In fact, *Epsilonbacteraeota*, *Bacteroidetes*, and *Proteobacteria* were the three major phyla in water from the spring S1 with relative abundance values of 52.48%, 23.63%, and 20.67%, respectively, whereas *Proteobacteria* dominated in S2 spring water (78.63%) followed by *Patescibacteria* (4.51%) and *Actinobacteria* (3.17%).

At a lower taxonomic level (Figure 6), the genus *Hydrogenophaga*, affiliated to the phylum *Proteobacteria*, was found at higher percentages in P_{art} (34.09%) and S2 water samples (15.17%). *Hydrogenophaga* and some other bacterial genera retrieved in the samples, such as *Flavobacterium*, *Gordonia*, *Sulfuritalea*, and *Rhodoferax*, are known to include microorganisms able to oxidize hydrocarbons [38–43].

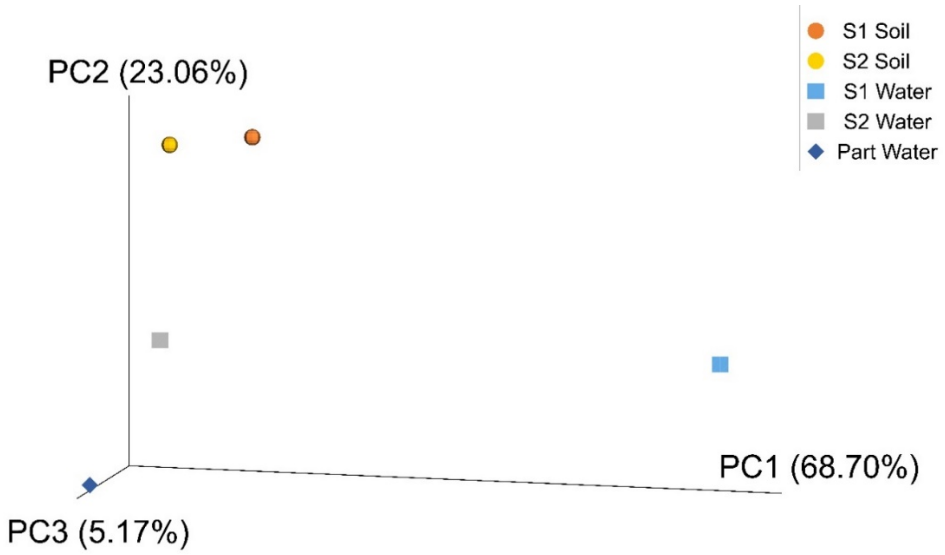

Figure 4. Principal Coordinate Analysis (PCoA). The plot was generated using a weighted uniFrac distance matrix. Soil, spring water, and groundwater samples are shown.

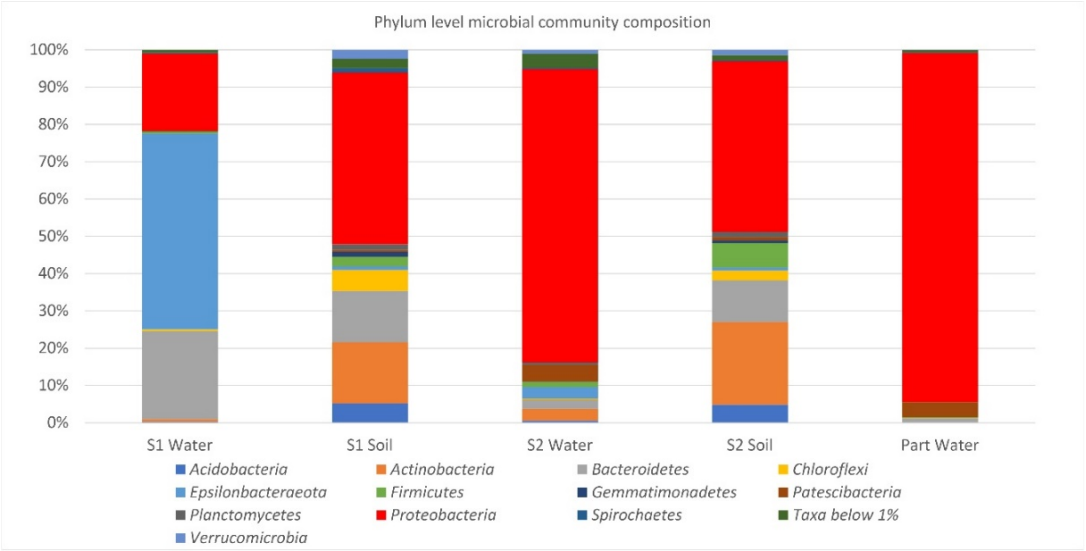

Figure 5. Phylum level microbial community composition in spring water, Part well, and soil samples.

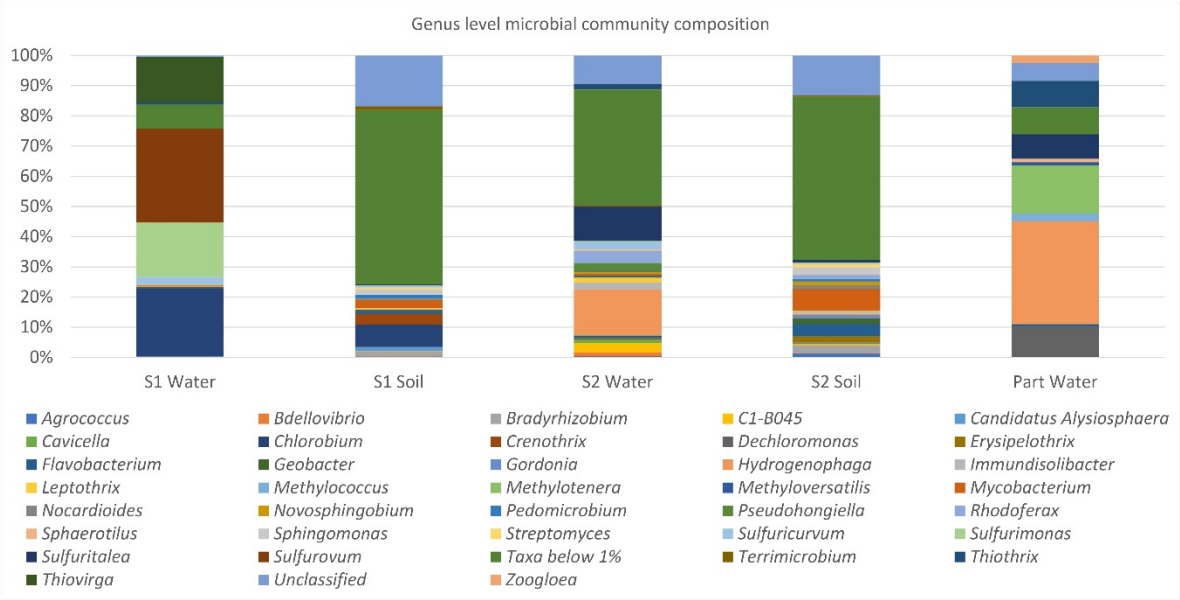

Figure 6. Genus level microbial community composition in spring water, P_{art} well, and soil samples.

3.4. Isolation and Identification of Bacterial Strains

Following the seven enrichment cycles on BH medium with diesel fuel as the only carbon source, 26 bacterial strains with different colony morphology were isolated from springs S1 and S2, P_{art} artesian well and soils.

An identification number from 1 to 26 was assigned to each strain. The 26 bacterial isolates were subjected to ARDRA analysis that allowed us to group them based on electrophoretic profiles. ARDRA analysis was also performed on five strains (1C–5C) obtained from S1 and S2 spring waters in previous experiments carried out at the study site (unpublished data). Seventeen bacterial isolates, representing all the ARDRA haplotypes, were chosen for 16S rRNA gene partial sequencing. Eleven bacterial strains were identified (Table 5), while the remaining isolates could not be rendered perfectly axenic in isolation procedures and, therefore, the sequencing failed. Some of the 16S rRNA gene sequences showed an identity < 97% with those stored in the GenBank database, suggesting that the bacterial isolates could be representatives of novel genera or species (Table 5).

Table 5. Results of 16S rRNA gene partial sequencing of bacterial strains isolated from spring water, groundwater and soil samples.

Strain	Sequence Accession Number	Most Closely Related Organism (Accession Number)	Identity (%)
3C	MT703034	*Achromobacter spanius* strain LMG 5911 (NR_025686)	97.80
1C	MT703035	*Pseudomonas protegens* strain CHA0 (NR_114749)	99.78
3	MT703036	*Dyella japonica* strain NBRC 102414 (NR_114075)	90.69
4	MT703037	*Pseudomonas protegens* strain CHA0 (NR_114749)	98.42
7	MT703038	*Cupriavidus metallidurans* CH34 (NR_074704)	98.16
8	MT703039	*Pseudomonas protegens* strain CHA0 (NR_114749)	98.19
10	MT703040	*Stenotrophomonas maltophilia* strain ATCC 13637 (NR_112030)	99.19
15	MT703041	*Stenotrophomonas tumulicola* strain T5916-2-1b (NR_148818)	90.86
16	MT703042	*Stenotrophomonas maltophilia* strain ATCC 13637 (NR_112030)	86.38
18	MT703043	*Dyella terrae strain* JS14-6 (NR_044540)	92.50
20	MT703044	*Dyella terrae strain* JS14-6 (NR_044540)	91.00

3.5. Growth Test

Five bacterial strains (1C, 2C, 3C, 4C and 5C), isolated in a previous experiment from S1 and S2 spring waters, and identified by sequencing of partial 16S rDNA together with the new isolates, were subjected to growth tests with four different recalcitrant hydrocarbons, naphthalene, phenanthrene, pristane and hexadecane (Table 6). These isolates were identified as *Achromobacter* sp. (3C) and *Pseudomonas* sp. (1C, 2C, 4C and 5C).

Table 6. Growth test results after 4 weeks (bacterial growth: +slight; ++moderate; +++high).

Isolate	Naphthalene	Phenanthrene	Pristane	Hexadecane
1C	+	+	+	++
2C	+	+++	+++	++
3C	+	++	++	++
4C	+	+++	++	++
5C	+	+	+	++

As shown in Table 6, some of the *Pseudomonas* sp. isolates (2C and 4C) have returned the best results when supplementing phenanthrene and pristane as the only carbon sources. All the isolates gave equivalent results for the growth on medium containing naphthalene and hexadecane.

3.6. Determination of the Emulsifying Capacity and Emulsion Index

The 11 identified strains were tested for emulsion capacity. Moreover, one strain of *Escherichia coli* and one of *Bacillus subtilis* were used as controls (Table 7).

Table 7. Emulsifying capacity results (EC%) (- absence; + presence).

Strain	EC	EC%
Proteobacteria bacterium strain 3	-	0
Pseudomonas sp. strain 4	+	60
Cupriavidus sp. strain 7	-	0
Pseudomonas sp. strain 8	+	60
Stenotrophomonas sp. strain 10	-	0
Proteobacteria bacterium strain 15	-	0
Proteobacteria bacterium strain 16	+	30
Proteobacteria bacterium strain 18	+	60
Proteobacteria bacterium strain 20	+	60
Pseudomonas sp. strain 1C	+	40
Achromobacter sp. strain 3C	+	50
Escherichia coli (negative control)	-	0
Bacillus subtilis (positive control)	+	50

Seven out of the 11 bacterial strains produced emulsion with diesel fuel, most of which with an EC% greater than 50%. As shown in Figure 7, the stability of the emulsions (E%) after 24 (t24) and 48 h (t48) was higher for *Pseudomonas* sp. strain 8 and *Proteobacteria* bacterium strain 18. After 24 and 48 h, a decrease of 17% and 20%, and 15% and 23%, was observed for the strains 8 and 18, respectively. The emulsion of the *Proteobacteria* bacterium strain 16 was much less stable with a difference from t_0 to t_{24} of 70% and exhausted after 48 h.

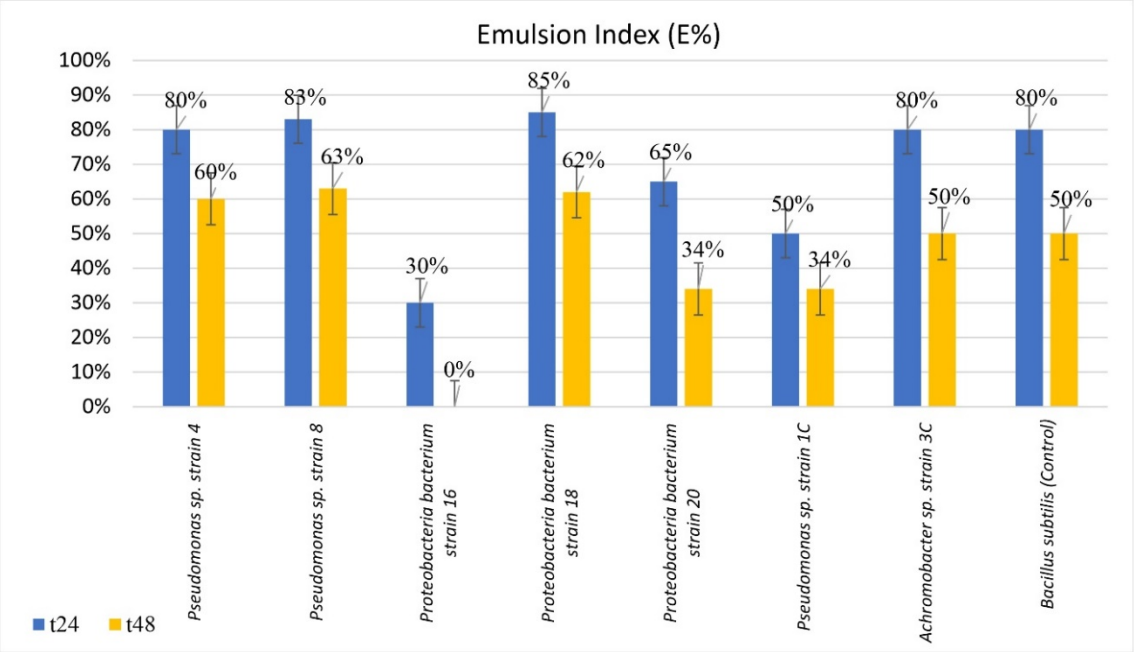

Figure 7. Histogram with emulsion index results (E%) of the strains that showed emulsifying capacity, respectively, at time t_{24} and t_{48}. The error used in the histogram is "the standard error".

4. Discussion and Conclusions

Petroleum hydrocarbon contamination is an issue of major concern worldwide. These compounds represent the most common environmental pollutants and their presence is destructive to the ecosystem and economic and human health [44]. The clean-up of hydrocarbon-contaminated sites is expensive and time consuming; however, bioremediation is a cost-effective and environmentally safe approach for petroleum hydrocarbon contamination (PHC) removal [44]. This technology involves the use of living organisms such as microbes and/or plants to reduce/degrade, eliminate and transform contaminants present in soils, sediments and water and has gained wider acceptance in recent years for all its potential [45]. In fact, although oil pollution is difficult to treat, indigenous bacteria can ultimately degrade or metabolize most petroleum hydrocarbons encountered in the environment because of their energetic and carbon needs for growth and reproduction, as well as the requirement to relieve physiological stress caused by their presence [46–48]. Accordingly, petroleum hydrocarbon-degrading bacteria, which have evolved as a result of existing in close proximity to naturally occurring petroleum hydrocarbons in the environment, represent suitable candidates for the treatment of oil polluted sites and to achieve the best purification effect [49–51].

An understanding of the temporal and spatial structures, functions, interactions, and population dynamics of microbial communities is critical for biotechnological development, environmental protection, and human health [52] so much that several methods have been employed to reveal microbial community composition, function and responses to environmental changes, in various environments and different contexts [53–60]. The main goal of this research was to analyze microbial communities in a site in southern Italy characterized by the presence of hydrocarbons of natural origin, by using a multidisciplinary approach based on microbiological, geological and hydrogeological investigations.

In detail, bacterial communities of two springs (S1 and S2), the surrounding soils, and groundwater (P_{art} well) were studied through a combination of molecular and culture-dependent methodologies to explore the biodiversity at the study site, to isolate microorganisms with degradative abilities and to assess their potential to develop effective strategies to restore the environmental quality.

The two hydrocarbon springs S1 and S2 are linked to the recharge in a local aquifer system and distributed along a fault zone that favors the rise of fluids and hydrocarbons within the shallow low-

permeability media. This hydrogeological behavior of the fault zone is not surprising when analyzing the possible roles (conduit, barrier, combined conduit-barrier systems) that these zones can play from the hydraulic point of view, depending on the relative percentage of fault core and damage zone [61–67]. In many aquifer systems worldwide, comparable with the studied one, both structural and hydrogeological approaches demonstrated the possible migration of fluids within fault zones acting as high- or low-flow discontinuities [68–74]. This evidence was further confirmed by the presence of H_2S at spring S1.

Chemical analyses of hydrocarbons highlighted the existence of several and different PAHs, such as Naphthalene, Benzo(b)fluoranthene, Benzo(k)fluoranthene, Benzo(g,h,i)perylene, Indene(1,2,3-c,d)pyrene, Chrysene, Anthracene, Phenanthrene, Fluoranthene, Benzo(j)fluoranthene, Dibenzo(a,h)anthracene, Pyrene and Dibenzo(a,l)pyrene in spring waters and soils. Generally, polycyclic aromatic hydrocarbons are chemicals with various structures and varied toxicity, stable, persistent in the environment, and resistant to degradation [75,76]. Chemically, they are comprised of two or more benzene rings bonded in linear, cluster, or angular arrangements [75]. The increase in the number of fused rings leads to higher hydrophobicity and recalcitrance to microbial degradation [77]. The continuous interaction with hydrocarbons could have influenced the bacterial communities of the two springs and the soils, naturally selecting some strains capable to biodegrade these pollutants.

The NGS results allowed us to obtain detailed information about the composition of microbial communities and revealed the dominance of species belonging to the phylum *Proteobacteria*. In this very large phylum of Gram-negative organisms, the majority of the formally described genera of hydrocarbon-degrading bacteria is included [78]; thus, it is likely that the continuous outflow of oil over time led to a stable and highly specialized microbiota, particularly adapted to grow and thrive in those environmental conditions. However, in addition to *Proteobacteria*, it was possible to also detect other autochthonous hydrocarbon-oxidizing bacteria affiliated to other phyla (e.g., species of the genera *Flavobacterium* and *Gordonia*), strengthening the assumption that natural exposure to pollutants can have impacted the structure and function of microbial populations. As expected, a higher biodiversity was found in soils compared to the aquatic ecosystems, generally lacking inputs of fresh, easily available organic carbon. In addition, beta-diversity analysis revealed a clear separation of soil, spring water, and groundwater samples and highlighted marked differences between S1 spring water microbial community and all the others. Although it is not surprising to find diverse microbial communities in different habitats due to their peculiar physico-chemical properties, it is likely that the observed results for the two springs reflect the influence of specific hydrogeological and other environmental factors that, on a local scale, shape bacterial community composition. As a matter of fact, P_{art}-groundwater is fed by a deep confined aquifer. Differently, the springs S1 and S2 are fed by a common groundwater coming from the nearby carbonate aquifer, mixed with different fluids (rising along a fault zone) in different proportions. This is clearly demonstrated by differences in some physico-chemical features (Table 1) and hydrocarbon concentrations (Table 2), and are further supported when taking into consideration the different mean residence time of spring waters, determined through tritium analyses (S1 = 5.6 to 6.9 tritium unit (TU), S2 = 6.8 to 7.5 TU; the spring fed by the only carbonate aquifer = 8.4 to 9.1 TU in Rizzo et al. [19]). These results are also in agreement with findings in other hydrogeological settings, where differences in microbial communities were clearly explained through the differences in (i) the aquifer type, (ii) the mixing between shallow groundwater and ascending fluids, (iii) the mixing between waters characterized by different salinity [53].

The traditional cultivation-based approach, performed by applying a selective pressure with diesel fuel supplementations, led to the isolation and identification of 11 aerobic hydrocarbon-oxidizing proteobacteria. Most of the bacteria isolated and identified belong, or are related, to genera or species known for their degradation abilities of polycyclic aromatic hydrocarbons [79–85]. The results are in line with those obtained by chemical analyses, which showed higher concentrations of these compounds at the investigated site. It is interesting to note that microorganisms of the genera *Hydrogenophaga*, *Sulfuritalea* and *Sulfurovum*, whose abundant presence was revealed by DNA-based

analyses, have not been isolated after the enrichment procedures. This "paradox" can be explained by the theory of the "Great Plate Count Anomaly" [86], which refers to the observation that only a small fraction (0.01–1%) of the microorganisms present in the environment can be cultivated in the laboratory. Despite this, the cultivation procedures led to the isolation of bacterial strains showing low values of 16S rRNA gene sequence identity with known species, contributing to get insights into the hidden microbial diversity of the analyzed ecosystem.

Some of the isolates were found to be able to grow better when phenanthrene was supplied as the sole carbon source compared to other simpler aliphatic and aromatic hydrocarbons. Subsequently, their emulsifying capacity was assessed and the emulsion index was calculated. Seven out of the 11 isolated bacterial strains produced emulsion with diesel fuel (most of them showing EC values greater than 50%) with high stability after 24 h and, in some cases, after 48 h. The tests have clearly demonstrated the capability of some strains to increase hydrocarbon bioavailability, most likely through the production of biosurfactants. These compounds are naturally derived surfactants produced from biological entities (especially microorganisms), which can be utilized as a cost-effective and eco-friendly mean to enhance bioremediation of oil components, including PAHs, in the natural environment. Fungi, bacteria, and yeasts belonging to different species and strains are known for producing biosurfactants of a diverse variety of molecular structures. Amongst the bacteria domain, the genera of *Pseudomonas*, *Bacillus*, and *Acinetobacter* dominate the literature space as excellent producers of biosurfactants [87]. For example, *Bacillus subtilis* is known for its ability to enhance diesel solubility [88] and to improve its degradation by producing surfactin, a lipoprotein-type biosurfactant [89].

In the late 1960s, biosurfactants attracted attention as hydrocarbon-dissolving agents as potential replacements for synthetic surfactants (usually toxic, hardly degraded by microorganism, and causing damage to the environment) especially in the food, pharmaceutical, and oil industries [90]. Bioemulsifiers get accumulated at the interphase between the two immiscible phases by which they can reduce the surface tension, thereby increasing the solubility and emulsification of the immiscible phases. Accordingly, these compounds may convert insoluble substrate into soluble substrates, increasing their bioavailability and making them usable by the microorganisms [91].

In conclusion, the data collected in this study pave the way for further investigations finalized at exploiting both (i) the degradation ability of the bacterial isolates and/or microbial consortia to remediate hydrocarbon-contaminated sites through strategies like biostimulation or bioaugmentation, and (ii) the capability to produce molecules with a good promoting effect for the restoration of oil polluted matrices. In addition, the isolation of strains showing a 16S rRNA gene sequence identity < 97% with those available in the genetic sequence database, constitutes a significant result and represents a further exciting challenge to fully unravel the existing biodiversity at the study site and expand the current knowledge on biodegradation processes, also through the description and characterization of novel bacterial species.

Supplementary Materials: The following are available online at www.mdpi.com/2073-4441/12/8/2090/s1, Figure S1: Geological section W-E crossing the Agri Valley, Figure S2: Hydrocarbon springs S1 and S2, Figure S3: Rarefaction curves of spring water, groundwater, and soil samples collected at the study site.

Author Contributions: Conceptualization, A.B., A.M.S., and F.C.; formal analysis, P.R.; investigation, P.R., M.M., S.R.; supervision, A.B., A.M.S., and F.C.; validation, P.R.; visualization, P.R.; writing—original draft, P.R., and A.B.; writing—review & editing, P.R., A.B., A.M.S., and F.C. All authors have read and agreed to the published version of the manuscript.

Funding: This research received no external funding.

Acknowledgments: We warmly acknowledge Dario Avagliano, Francesco Coraggio, Antonella Caputi, and Fabrizio Micucci (ENI S.p.A., Distretto Meridionale) for providing some of the data used in the present work and for useful discussions. This work has benefited from the equipment and framework of the COMP-HUB Initiative, funded by the 'Departments of Excellence' program of the Italian Ministry for Education, University and Research (MIUR, 2018–2022). We are grateful to the reviewers for their constructive comments and valuable suggestions.

Conflicts of Interest: There are no conflicts of interest related to this paper.

References

1. Espinoza-Tofalos, A.; Daghio, M.; Palma, E.; Aulenta, F.; Franzetti, A. Structure and functions of hydrocarbon-degrading microbial communities in bioelectrochemical systems. *Water* **2020**, *12*, 343.
2. Varjani, S.J.; Upasani, V.N. Biodegradation of petroleum hydrocarbons by oleophilic strain of *Pseudomonas aeruginosa* NCIM 5514. *Bioresour. Technol.* **2016**, *222*, 195–201.
3. Costa, A.S.; Romão, L.P.C.; Araújo, B.R.; Lucas, S.C.O.; Maciel, S.T.A.; Wisniewski, A., Jr.; Alexandre, M.D.R. Environmental strategies to remove volatile aromatic fractions (BTEX) from petroleum industry wastewater using biomass. *Bioresour. Technol.* **2012**, *105*, 31–39.
4. Zhang, Z.; Hou, Z.; Yang, C.; Ma, C.; Tao, F.; Xu, P. Degradation of n-alkanes and polycyclic aromatic hydrocarbons in petroleum by a newly isolated *Pseudomonas aeruginosa* DQ8. *Bioresour. Technol*. **2011**, *102*, 4111–4116.
5. Chandra, S.; Sharma, R.; Singh, K.; Sharma, A. Application of bioremediation technology in the environment contaminated with petroleum hydrocarbon. *Ann. Microbiol.* **2013**, *63*, 417–431.
6. Souza, E.C.; Vessoni-Penna, T.C.; de Souza Oliveira, R.P. Biosurfactant-enhanced hydrocarbon bioremediation: An overview. *Int. Biodeter. Biodegr.* **2014**, *89*, 88–94.
7. Meckenstock, R.U.; Boll, M.; Mouttaki, H.; Koelschbach, J.S.; Tarouco, P.C.; Weyrauch, P.; Himmelberg, A.M. Anaerobic degradation of benzene and polycyclic aromatic hydrocarbons. *J. Mol. Microbiol. Biotechnol.* **2016**, *26*, 92–118.
8. Chaudhary, D.K.; Kim, J. New insights into bioremediation strategies for oil-contaminated soil in cold environments. *Int. Biodeter. Biodegr.* **2019**, *142*, 58–72.
9. Alberti, L.; Lombi, S.; Zanini, A. Identifying sources of chlorinated aliphatic hydrocarbons in a residential area in Italy using the integral pumping test method. *Hydrogeol. J.* **2011**, *19*, 1253–1267.
10. Varjani, S.J. Microbial degradation of petroleum hydrocarbons. *Bioresour. Technol.* **2017**, *223*, 277–286.
11. Daghio, M.; Aulenta, F.; Vaiopoulou, E.; Franzetti, A.; Arends, J.B.A.; Sherry, A.; Suárez-Suárez, A.; Head, I.M.; Bestetti, G.; Rabaey, K. Electrobioremediation of oil spills. *Water Res.* **2017**, *114*, 351–370.
12. Abbasian, F.; Lockington, R.; Mallavarapu, M.; Naidu, R. A comprehensive review of aliphatic hydrocarbon biodegradation by bacteria. *Appl. Biochem. Biotechnol.* **2015**, *176*, 670–699.
13. Bosco, F.; Casale, A.; Chiampo, F.; Godio, A. Removal of diesel oil in soil microcosms and implication for geophysical monitoring. *Water* **2019**, *11*, 1661.
14. Balaban, N.; Yankelzon, I.; Adar, E.; Gelman, F.; Ronen, Z.; Bernstein, A. The spatial distribution of the microbial community in a contaminated aquitard below an industrial zone. *Water* **2019**, *11*, 2128.
15. Varjani, S.J.; Thaker, M.B.; Upasani, V.N. Optimisation of growth conditions of native hydrocarbon utilizing bacterial consortium "HUBC" obtained from petroleum pollutant contaminated sites. *Indian J. Appl. Res.* **2014**, *4*, 474–476.
16. Cazzini, F.F. The history of the upstream oil and gas industry in Italy. In *History of the European Oil and Gas Industry*; Craig, J., Gerali, F., MacAulay, F., Sorkhabi, R., Eds.; Geological Society Special Publications: London, UK, 2018; Volume 465, pp. 243–274.
17. Scandone, P.; Sgrosso, I. Flysch con Inocerami nella valle del Cavolo presso Tramutola (Lucania). *Boll. Soc. Nat. Napoli* **1964**, *73*, 166–175.
18. Olita, F. Investigation of the Natural Hydrocarbon Manifestations and 3D Reconstruction of the Reservoir in the Tramutola Area (Basilicata). Master's Thesis, University of Basilicata, Potenza, Italy, 2019.
19. Rizzo, P.; Bucci, A.; Sanangelantoni, A.M.; Iacumin, P.; Celico, F. Coupled microbiological-isotopic approach for studying hydrodynamics in deep reservoirs: The case of the Val d'Agri oilfiled (southern Italy). *Water* **2020**, *12*, 1483.
20. De Vita, P.; Allocca, V.; Celico, F.; Fabbrocino, S.; Cesaria, M.; Monacelli, G.; Musilli, I.; Piscopo, V.; Scalise, A.R.; Summa, G.; et al. Hydrogeology of continental Southern Italy. *J. Maps* **2018**, *14*, 230–241.
21. Berserzio, R.; Felletti, F.; Giudici, M.; Miceli, A.; Zembo, I. Aquifer analogues to assist modeling of groundwater flow: The Pleistocene aquifer complex of the Agri Valley (Basilicata). *Mem. Descr. Carta Geol. d'It*. **2007**, *LXXVI*, 51–66.
22. Azienda Generale Italiana Petroli, Ricerche petrolifere (AGIP) (Roma, Italy). *Cantiere di Tramutola, Sondaggio N. 2. in Italian, 1939*; Unpublished.

23. Patacca, E.; Scandone, P.; Bellatalla, M.; Perilli, N.; Santini, U. The Numidian-sand event in the Southern Apennines. *Mem. Sci. Geol. Padova* **1992**, *43*, 297–337.
24. Menardi Noguera, A.; Rea, G. Deep structure of the Campanian–Lucanian arc (southern Apennine, Italy). *Tectonophysics* **2000**, *324*, 239–265.
25. U.S. EPA. *Method 3510C (SW-846): Separatory Funnel Liquid-Liquid Extraction*; U.S. Environmental Protection Agency: Washington, DC, USA, 1996.
26. U.S. EPA. *Method 5030C (SW-846): Purge-and-Trap for Aqueous Samples Revision 3*; U.S. Environmental Protection Agency: Washington, DC, USA, 2003.
27. U.S. EPA. *Method 8015D (SW-846): Nonhalogenated Organics Using GC/FID Revision 4*; U.S. Environmental Protection Agency: Washington, DC, USA, 2003.
28. U.S. EPA. *Method 3550C (SW-846): Ultrasonic Extraction*; U.S. Environmental Protection Agency: Washington, DC, USA, 2007.
29. U.S. EPA. *Method 5021A (SW-846): Volatile Organic Compounds (VOCs) in Various Sample Matrices Using Equilibrium Headspace Analysis*; U.S. Environmental Protection Agency: Washington, DC, USA, 2014.
30. U.S. EPA. *Method 8270E (SW-846) Semivolatile Organic Compounds by Gas Chromatography/Mass Spectrometry (GC/MS)*; U.S. Environmental Protection Agency: Washington, DC, USA, 2018.
31. Milani, C.; Hevia, A.; Foroni, E.; Duranti, S.; Turroni, F.; Lugli, G.A.; Margolles, A. Assessing the fecal microbiota: An optimized ion torrent 16S rRNA gene-based analysis protocol. *PLoS ONE* **2013**, *8*, e68739.
32. Caporaso, J.G.; Kuczynski, J.; Stombaugh, J.; Bittinger, K.; Bushman, F.D.; Costello, E.K.; Huttley, G.A. QIIME allows analysis of high-throughput community sequencing data. *Nat. Methods* **2010**, *7*, 335.
33. Callahan, B.J.; McMurdie, P.J.; Rosen, M.J.; Han, A.W.; Johnson, A.J.; Holmes, S.P. DADA2: High-resolution sample inference from Illumina amplicon data. *Nat. Methods* **2016**, *13*, 581–583.
34. Bokulich, N.A.; Kaehler, B.D.; Rideout, J.R.; Dillon, M.; Bolyen, E.; Knight, R.; Caporaso, J.G. Optimizing taxonomic classification of marker-gene amplicon sequences with QIIME 2's q2-feature-classifier plugin. *Microbiome* **2018**, *6*, 90.
35. Quast, C.; Pruesse, E.; Yilmaz, P.; Gerken, J.; Schweer, T.; Yarza, P.; Glöckner, F.O. The SILVA ribosomal RNA gene database project: Improved data processing and web-based tools. *Nucleic Acids Res.* **2012**, *41*, D590–D596.
36. Bushnell, L.D.; Haas, H.F. The utilization of certain hydrocarbons by microorganisms. *J. Bacteriol.* **1941**, *41*, 653–673.
37. Mohebali, G.; Ball, A.; Kaytash, A.; Rasekh, B. Stabilization of water/gas oil emulsions by desulfurizing cells of *Gordonia alkanivorans* RIPI90A. *Microbiology* **2007**, *153*, 1573–1581.
38. Magic-Knezev, A.; Wullings, B.; Van der Kooij, D. *Polaromonas* and *Hydrogenophaga* species are the predominant bacteria cultured from granular activated carbon filters in water treatment. *J. Appl. Microbiol.* **2009**, *107*, 1457–1467.
39. Aburto, A.; Peimbert, M. Degradation of a benzene–toluene mixture by hydrocarbon-adapted bacterial communities. *Ann. Microbiol.* **2011**, *61*, 553–562.
40. Rahman, K.S.M.; Thahira-Rahman, J.; Lakshmanaperumalsamy, P.; Banat, I.M. Towards efficient crude oil degradation by a mixed bacterial consortium. *Bioresour. Technol.* **2002**, *85*, 257–261.
41. Hemalatha, S.; Veeramanikandan, P. Characterization of aromatic hydrocarbon degrading bacteria from petroleum contaminated sites. *J. Environ. Prot.* **2011**, *2*, 243–254.
42. Franzetti, A.; Caredda, P.; Ruggeri, C.; La Colla, P.; Tamburini, E.; Papacchini, M.; Bestetti, G. Potential applications of surface active compounds by *Gordonia sp.* strain BS29 in soil remediation technologies. *Chemosphere* **2009**, *75*, 801–807.
43. Sperfeld, M.; Diekert, G.; Studenik, S. Anaerobic aromatic compound degradation in *Sulfuritalea hydrogenivorans* sk43H. *FEMS Microbiol. Ecol.* **2018**, *95*, fiy199.
44. Truskewycz, A.; Gundry, T.D.; Khudur, L.S.; Kolobaric, A.; Taha, M.; Aburto-Medina, A.; Ball, A.S.; Shahsavari, E. Petroleum hydrocarbon contamination in terrestrial ecosystems-fate and microbial responses. *Molecules* **2019**, *24*, 3400.
45. Dhir, B. Bioremediation technologies for the removal of pollutants. In *Advances in Environmental Biotechnology*; Kumar, R., Sharma, A., Ahluwalia, S., Eds.; Springer: Singapore, 2017.
46. Hazen, T.C.; Dubinsky, E.A.; DeSantis, T.Z.; Andersen, G.L.; Piceno, Y.M.; Singh, N.; Stringfellow, W.T. Deep-sea oil plume enriches indigenous oil-degrading bacteria. *Science* **2010**, *330*, 204–208.

47. Kleindienst, S.; Paul, J.H.; Joye, S.B. Using dispersants after oil spills: Impacts on the composition and activity of microbial communities. *Nat. Rev. Microbiol.* **2015**, *13*, 388–396.
48. Xu, X.; Liu, W.; Tian, S.; Wang, W.; Qi, Q.; Jiang, P.; Gao, X.; Li, F.; Li, H.; Yu, H. Petroleum hydrocarbon-degrading bacteria for the remediation of oil pollution under aerobic conditions: A perspective analysis. *Front. Microbiol.* **2018**, *9*, 2885.
49. Margesin, R.; Labbé, D.; Schinner, F.; Greer, C.W.; Whyte, L.G. Characterization of hydrocarbon-degrading microbial populations in contaminated and pristine alpine soils. *Appl. Environ. Microbiol.* **2003**, *69*, 3085–3092.
50. Ron, E.Z.; Rosenberg, E. Enhanced bioremediation of oil spills in the sea. *Curr. Opin. Biotechnol.* **2014**, *27*, 191–194.
51. Lea-Smith, D.J.; Biller, S.J.; Davey, M.P.; Cotton, C.A.; Sepulveda, B.M.P.; Turchyn, A.V.; Howe, C.J. Contribution of cyanobacterial alkane production to the ocean hydrocarbon cycle. *Proc. Natl. Acad. Sci. USA* **2015**, *112*, 13591–13596.
52. Bucci, A.; Petrella, E.; Celico, F.; Naclerio, G. Use of molecular approaches in hydrogeological studies: The case of carbonate aquifers in southern Italy. *Hydrogeol. J.* **2017**, *25*, 1017–1031.
53. Bucci, A.; Naclerio, G.; Allocca, V.; Celico, P.; Celico, F. Potential use of microbial community investigations to analyse hydrothermal systems behaviour: The case of Ischia Island, Southern Italy. *Hydrol. Process.* **2011**, *25*, 1866–1873.
54. Bucci, A.; Petrella, E.; Naclerio, G.; Gambatese, S.; Celico, F. Bacterial migration through low-permeability fault zones in compartmentalised aquifer systems: A case study in Southern Italy. *Int. J. Speleol.* **2014**, *43*, 273–281.
55. Bucci, A.; Allocca, V.; Naclerio, G.; Capobianco, G.; Divino, F.; Fiorillo, F.; Celico, F. Winter survival of microbial contaminants in soil: An *in situ* verification. *J. Environ. Sci.* **2015**, *27*, 131–138.
56. Bucci, A.; Petrella, E.; Naclerio, G.; Allocca, V.; Celico, F. Microorganisms as contaminants and natural tracers: A 10-year research in some carbonate aquifers (southern Italy). *Environ. Earth Sci.* **2015**, *74*, 173–184.
57. Crescenzo, R.; Mazzoli, A.; Cancelliere, R.; Bucci, A.; Naclerio, G.; Baccigalupi, L.; Cutting, S.M.; Ricca, E.; Iossa, S. Beneficial effects of carotenoid-producing cells of *Bacillus indicus* HU16 in a rat model of diet-induced metabolic syndrome. *Benef. Microbes* **2017**, *8*, 823–831.
58. Di Luccia, B.; Mazzoli, A.; Cancelliere, R.; Crescenzo, R.; Ferrandino, I.; Monaco, A.; Bucci, A.; Naclerio, G.; Iossa, S.; Ricca, E.; et al. *Lactobacillus gasseri* SF1183 protects the intestinal epithelium and prevents colitis symptoms *in vivo*. *J. Func. Foods* **2018**, *42*, 195–202.
59. Petrella, E.; Bucci, A.; Ogata, K.; Zanini, A.; Naclerio, G.; Chelli, A.; Francese, R.; Boschetti, T.; Pittalis, D.; Celico, F. Hydrodynamics in evaporate-bearing fine-grained successions investigated through an interdisciplinary approach: A test study in Southern Italy. *Geofluids* **2018**, *2018*, 15; Article ID 5978597.
60. Pietrangelo, L.; Bucci, A.; Maiuro, L.; Bulgarelli, D.; Naclerio, G. Unraveling the composition of the root-associated bacterial microbiota of *Phragmites australis* and *Typha latifolia*. *Front. Microbiol.* **2018**, *9*, 1650.
61. Celico, P. *Prospezioni Idrogeologiche*; Liguori Ed.: Napoli, Italy, 1986.
62. Antonellini, M.; Aydin, A. Effect of faulting on fluid flow in por- ous sandstones: Petrophysical proper-ties. *Am. Assoc. Petrol. Geol. Bull.* **1994**, *78*, 355–377.
63. Newman, J.; Mitra, G. Fluid- influenced deformation and recrystalli- zation of dolomite at low temperatures along a natural fault zone, Mountain City window, Tennessee. *Geol. Soc. Am. Bull.* **1994**, *106*, 1267–1280.
64. Goddard, J.V.; Evans, J.P. Chemical changes and fluid-rock inter- action in faults of crystalline thrust sheets, northwestern Wyoming, USA. *J. Struct. Geol.* **1995**, *17*, 533–547.
65. Caine, J.S.; Evans, J.P.; Forster, C.B. Fault zone architecture and per- meability structure. *Geology* **1996**, *24*, 1025–1028.
66. Bense, V.F.; Van den Berg, E.H.; Van Balen, R.T. Deformation mecha- nisms and hydraulic properties of fault zones in unconsolidated sediments; the Roer Valley Rift System, The Nether- lands. *Hydrogeol. J.* **2003**, *11*, 319–332.
67. Fairley, J.P.; Hinds, J.J. Field observation of fluid circulation patterns in a normal fault system. *Geophys. Res. Lett.* **2004**, *31*, 1–4.
68. Celico, F.; Petrella, E.; Celico, P. Hydrogeological behaviour of some fault zones in a carbonate aquifer of Southern Italy: An experimentally based model. *Terra Nova* **2006**, *18*, 308–313.

69. Agosta, F.; Alessandroni, M.; Antonellini, M.; Tondi, E.; Giorgioni, M. From fractures to flow: A field-based quantitative analysis of an outcropping carbonate reservoir. *Tectonophysics* **2010**, *490*, 197–213.
70. Aquino, D.; Petrella, E.; Florio, T.; Celico, P.; Celico, F. Complex hydraulic interactions between compartmentalized carbonate aquifers and heterogeneous siliciclastic successions: A case study in southern Italy. *Hydrol. Process*. **2015**, *29*, 4252–4263.
71. Petrella, E.; Aquino, D.; Fiorillo, F.; Celico, F. The effect of low-permeability fault zones on groundwater flow in a compartmentalized system. Experimental evidence from a carbonate aquifer (Southern Italy). *Hydrol. Process*. **2015**, *29*, 1577–1587.
72. Giuffrida, A.; La Bruna, V.; Castelluccio, P.; Panza, E.; Rustichelli, A.; Tondi, E.; Giorgini, M.; Agosta, F. Fracture simulation parameters of fractured reservoirs: Analogy with outcropping carbonates of the Inner Apulian Platform, southern Italy. *J. Struct. Geol.* **2019**, *123*, 18–41.
73. Hernandez-Diaz, R.; Petrella, E.; Bucci, A.; Naclerio, G.; Feo, A.; Sferra, G.; Chelli, A.; Zanini, A.; Gonzales-Hernandez, P.; Celico, F. Integrating hydrogeological and microbiological data and modelling to characterize the hydraulic features and behavior of coastal carbonate aquifers: A case in Western Cuba. *Water* **2019**, *11*, 1989.
74. Ferraro, F.; Agosta, F.; Prasad, M.; Vinciguerra, S.; Violay, M.; Giorgioni, M. Pore space properties in carbonate fauklt rocks of peninsular Italy. *J. Struct. Geol.* **2020**, *130*, 103913.
75. Abdel-Shafy, H.I.; Mansour, M.S.M. A review on polycyclic aromatic hydrocarbons: Source, environmental impact, effect on human health and remediation. *Egypt. J. Pet.* **2016**, *25*, 107–123.
76. Martirani-Von Abercron, S.-M.; Pacheco, D.; Benito-Santano, P.; Marín, P.; Marqués, S. Polycyclic aromatic hydrocarbon-induced changes in bacterial community structure under anoxic nitrate reducing conditions. *Front. Microbiol.* **2016**, *7*, 1775.
77. Wang, W.; Wang, L.; Shao, Z. Polycyclic aromatic hydrocarbon (PAH) degradation pathways of the obligate marine PAH degrader *Cycloclasticus* sp. Strain P1. *Appl. Environ. Microbiol.* **2018**, *84*, e01261-18.
78. Prince, R.C.; Gramain, A.; McGenity, T.J. Prokaryotic Hydrocarbon Degraders. In *Handbook of Hydrocarbon and Lipid Microbiology*; Timmis, K.N., Eds.; Springer: Berlin/Heidelberg, Germany, 2010.
79. Jahin, H.S.; Gaber, S.E.; Ewida, A.Y.I. Biodegradation of phenanthrene by native bacterial strains isolated from River Nile water in Egypt. *Nat. Sci. J.* **2014**, *12*, 1–8.
80. Farjadfard, S.; Borghei, S.M.; Hassani, A.H.; Yakhchali, B.; Ardjmand, M.; Zeinali, M. Efficient biodegradation of naphthalene by a newly characterized indigenous *Achromobacter sp.* FBHYA2 isolated from Tehran Oil Refinery Complex. *Water Sci. Technol.* **2012**, *66*, 594–602.
81. Gracioso, L.H.; Vieira, P.B.; Baltazar, M.P.; Avanzi, I.R.; Karolski, B.; Nascimento, C.A.; Perpetuo, E.A. Removal of phenolic compounds from raw industrial wastewater by *Achromobacter sp.* isolated from a hydrocarbon-contaminated area. *Water Environ. J.* **2019**, *33*, 40–50.
82. Espinoza Tofalos, A.; Daghio, M.; González, M.; Papacchini, M.; Franzetti, A.; Seeger, M. Toluene degradation by *Cupriavidus metallidurans* CH34 in nitrate-reducing conditions and in Bioelectrochemical Systems. *FEMS Microbiol. Lett.* **2018**, *365*, fny119.
83. Qu, Y.; Shen, E.; Ma, Q.; Zhang, Z.; Liu, Z.; Shen, W.; Zhou, J. Biodegradation of indole by a newly isolated *Cupriavidus sp.* SHE. *J. Environ. Sci.* **2015**, *34*, 126–132.
84. Juhasz, A.L.; Stanley, G.A.; Britz, M.L. Microbial degradation and detoxification of high molecular weight polycyclic aromatic hydrocarbons by *Stenotrophomonas maltophilia* strain VUN 10,003. *Lett. Appl. Microbiol.* **2000**, *30*, 396–401.
85. Gao, S.; Seo, J.S.; Wang, J.; Keum, Y.S.; Li, J.; Li, Q.X. Multiple degradation pathways of phenanthrene by *Stenotrophomonas maltophilia* C6. *Int. Biodeter. Biodegr.* **2013**, *79*, 98–104.
86. Harwani, D. The great plate count anomaly and the unculturable bacteria. *Microbiology* **2013**, *2*, 350–351.
87. Fenibo, E.O.; Ijoma, G.N.; Selvarajan, R.; Chikere, C.B. Microbial surfactants: The next generation multifunctional biomolecules for applications in the petroleum industry and its associated environmental remediation. *Microorganisms* **2019**, *7*, 581.
88. Mnif, I.; Ellouze-Chaabouni, S.; Ghribi, D. Economic production of *Bacillus subtilis* SPB1 biosurfactant using local agro-industrial wastes and its application in enhancing solubility of diesel. *J. Chem. Technol. Biotechnol.* **2013**, *88*, 779–787.
89. Whang, L.M.; Liu, P.W.G.; Ma, C.C.; Cheng, S.S. Application of biosurfactants, rhamnolipid, and surfactin, for enhanced biodegradation of diesel-contaminated water and soil. *J. Hazard. Mater.* **2008**, *151*, 155–163.

90. Sáenz-Marta, C.I.; Ballinas-Casarrubias M de Lourdes Rivera-Chavira, B.E.; Nevárez-Moorillón, G.V. Biosurfactants as Useful Tools in Bioremediation. In *Advances in Bioremediation of Wastewater and Polluted Soil*; Naofumi, S., Ed.; IntechOpen: London, UK, 2015; Volume 5.
91. Peele, K.A.; Ch, V.R.; Kodali, V.P. Emulsifying activity of a biosurfactant produced by a marine bacterium. *3 Biotech* **2016**, *6*, 177.

3. Considerazioni di Sintesi

Gli elementi di conoscenza acquisiti nel corso del Dottorato hanno permesso di affinare e di comprovare la robustezza di approcci idrogeologico-metagenomici per la messa a punto di modelli di flusso e per l'ottimizzazione di soluzioni di bonifica in siti contaminati.

Più in dettaglio, la componente più squisitamente idrogeologica è stata sviluppata in seno a mezzi geologici a bassa permeabilità, la cui presenza e le cui caratteristiche influenzano in modo determinante, non solo la propagazione nel sottosuolo di eventuali contaminanti idroveicolati, ma anche la progettazione di efficaci interventi di bonifica. In merito a quest'ultimo aspetto, l'attenzione è stata focalizzata anche sull'incidenza del fenomeno del *well clogging* sull'efficienza delle barriere idrauliche, sulla selezione di isolati ambientali in grado di migliorare ulteriormente l'efficacia di approcci incentrati sul biorisanamento in chiave microbica e sullo studio del fenomeno dell'attenuazione naturale.

Gli studi svolti hanno evidenziato come, in fase di caratterizzazione di un sito contaminato, per la corretta realizzazione di un sistema di bonifica che sia efficiente ed efficace, vada approfondita la caratterizzazione degli eventuali mezzi a bassa permeabilità (*aquitard o aquiclude*), non solo attraverso tecniche comuni in ambito idrogeologico (come ad esempio *test* su campioni o prove di assorbimento in foro, che indagano volumi limitati del mezzo), ma anche attraverso lo studio del trasporto in sospensione o in soluzione di traccianti naturali (microbici e/o chimico-isotopici, rispettivamente) in grado di restituire il modello di funzionamento del mezzo alla scala di sito. Tale integrazione dell'approccio di caratterizzazione dei mezzi a bassa permeabilità risulta tanto più importante quanto maggiore è il grado di eterogeneità (nota o attesa) dell'*aquitard*.

Nell'ambito del Dottorato, questo aspetto è stato affrontato in due siti sperimentali, al fine di testare l'efficacia dei traccianti microbici (sito ubicato in Val di Taro, Parma) e dei traccianti isotopici (sito ubicato in Sicilia Sud-Occidentale Agrigento). In entrambi i casi, le prove di permeabilità (Lefranc) hanno restituito valori di conducibilità idraulica estremamente bassi (dell'ordine di $1 \times 10^{-9} – 1 \times 10^{-8}$ m/s), propri di un *aquiclude*.

Per quanto riguarda il sito sperimentale ubicato nell'Appennino parmense, l'utilizzo delle comunità microbiche, a dispetto dei risultati delle prove di caratterizzazione idraulica, ha consentito di accertare che:

- la percolazione delle acque di infiltrazione efficace nel mezzo insaturo non è trascurabile ed è tale da trasportare cellule di microrganismi dal suolo al sottostante mezzo saturo, come dimostrato dalla presenza di specie batteriche tipiche del suolo e della rizosfera rilevate nei campioni di acque sotterranee (Tab. 3.1);

Tabella 3.1 Alcune specie trovate nei campioni di acqua di falda e suolo in seguito al sequenziamento del 16S rRNA [40]; le citazioni riportate in tabella fanno riferimento alla bibliografia dell'articolo

Taxonomy	Aerobic	Facultative anaerobic	Halophilic/ Halotolerant	Nitrate reduction	Pathogen	Samples	Citations
Acinetobacter oleivorans	+	−	−	−	−	GWS1-2-3	[57]
Afipia massiliensis	+	−	−	+	−	GWS1-2	[54]
Deinococcus caeni	+	−	+	−	−	GWS1-2-3	[58]
Devosia glacialis	+	−	−	+	−	GWS1-2-3; SS1	[53]
Ensifer adhaerens	+	−	−	+	−	GWS1-2-3; SS1-2	[52]
Halomonas taeanensis	+	−	+	+	−	SS2	[59]
Halomonas ventosae	+	−	+	+	−	SS2	[60]
Janthinobacterium agaricidamnosum	+	−	−	−	−	GWS1-3; SS1	[61]
Legionella feeleii	+	−	−	−	+	GWS3; SS2	[62]
Legionella nautarum	+	−	−	+	+	GWS3	[63]
Legionella pneumophila	+	−	−	−	+	GWS3	[64]
Pedobacter insulae	+	−	−	−	−	GWS1-2-3; SS1	[50]
Pseudomonas frederiksbergensis	+	−	−	+	−	GWS1-2-3	[49]
Pseudomonas otitidis	+	−	+	−	+	GWS2	[65]
Pseudomonas psychrophila	+	−	+	+	−	GWS1-2-3; SS2	[66]
Pseudomonas xanthomarina	+	−	+	+	−	GWS2	[67]
Sphingomonas yunnanensis	+	−	−	+	−	GWS1-2-3; SS1-2	[39]
Staphylococcus warneri	+	+	+	−	+	GWS2-3	[44]
Stenotrophomonas chelatiphaga	+	−	−	−	−	GWS1-2; SS1	[43]
Streptomyces vinaceusdrappus	+	−	+	+	−	GWS1-2-3; SS1-2	[68]
Streptomyces xinghaiensis	+	−	+	−	−	GWS1-2-3; SS1-2	[69]
Thiohalobacter thiocyanaticus	+	−	+	−	−	SS2	[70]

- al contempo, la presenza delle suddette cellule microbiche in campioni prelevati a profondità diverse (fino a circa 40 metri dal piano campagna), testimonia che il progressivo decremento del carico idraulico accertato lungo la verticale, mediante un *cluster* di piezometri, induce un flusso con componente verticale discendente, tale da consentire il trasporto delle cellule a profondità via via maggiori;
- la discrepanza emersa tra i risultati delle prove di caratterizzazione idraulica del mezzo (a scala da microscopica e macroscopica) e quelli ottenuti dalla disamina delle comunità microbiche (a scala megascopica) attesta che sussiste una sorta di "volume elementare rappresentativo" al di sotto del quale un mezzo a bassa permeabilità può apparire "impermeabile" (*aquitard integrity* così elevata da poter parlare di *aquiclude*) e al di sopra del quale sussiste una rete di vuoti intercomunicanti che, per quanto rada, consente una migrazione non trascurabile di fluidi e di potenziali contaminanti idroveicolati (*aquitard integrity* relativamente bassa).

Per quanto riguarda il sito sperimentale ubicato in Sicilia, l'utilizzo dei traccianti isotopici ($\delta^{18}O$, $\delta^{2}H$, ^{3}H) ha contribuito ad accertare che:

- la migrazione dei fluidi non è circoscritta ad un rado e discontinuo insieme di interstrati evaporitici inglobati all'interno di una successione prevalentemente argillosa, ma interessa in modo pervasivo l'intero mezzo a bassa permeabilità (Fig.3.1), come testimoniato dalla coerenza tra il contenuto isotopico ($\delta^{18}O$, $\delta^{2}H$) delle acque sotterranee e quello delle precipitazioni locali (Fig. 3.2);

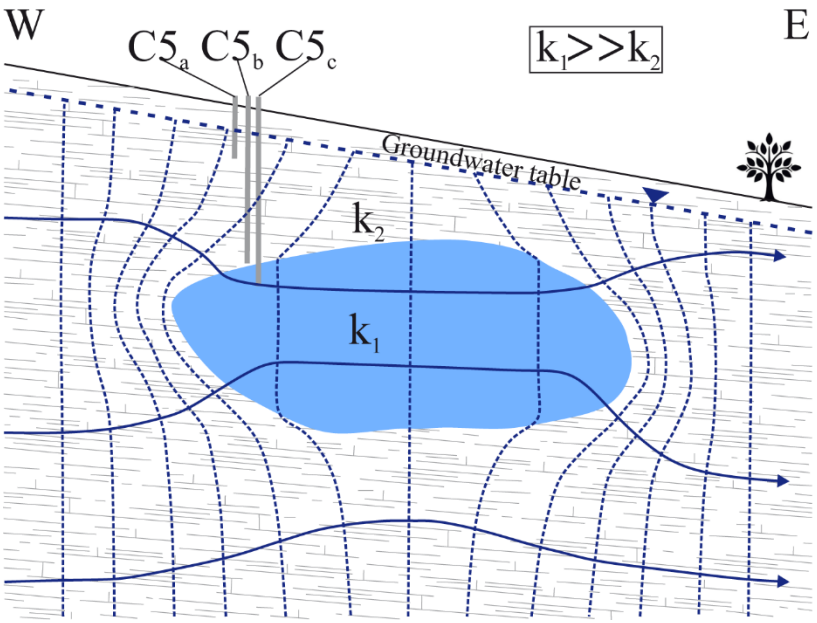

Figura 3.1 Schema idrogeologico concettuale di mezzi eterogenei caratterizzati da successioni evaporitiche. La lente blu è uno strato evaporitico discontinuo immerso in una successione argillosa (grigia). Le linee tratteggiate blu sono le linee equipotenziali. Le frecce blu sono le linee di flusso delle acque di falda. Viene mostrato anche il cluster C5a-c. I simboli K1 e K2 sono rispettivamente le conduttività idrauliche della lente evaporitica e della successione di argillosa [41].

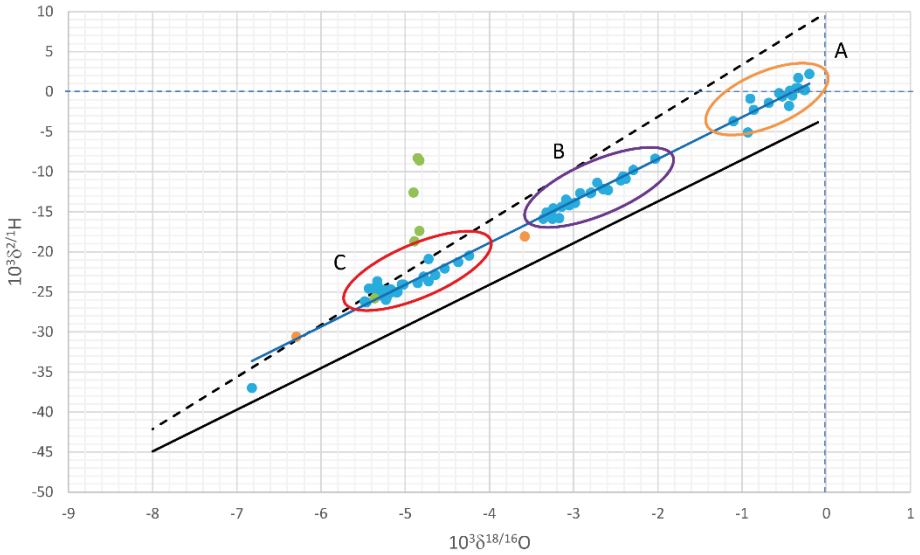

Figura 3.2 Relazioni tra 10^3 $\delta^{2/1}H$ e 10^3 $\delta^{18/16}O$ per le acque investigate (punti blu). I gruppi A, B e C sono circondati rispettivamente da ocra, viola e rosso. I punti verdi rappresentano le acque C5a-c. I punti arancioni indicano i campioni di acqua piovana analizzati durante questo studio. Le linee nere continue e quelle nere tratteggiate sono rappresentative delle linee d'acqua meteoriche disponibili in Sicilia. La linea blu è l'interpolazione lineare dei dati isotopici delle acque sotterranee [41].

- tuttavia, il deflusso all'interno della componente a bassa permeabilità induce velocità di migrazione molto basse (ma non trascurabili o nulle; *aquitard integrity* relativamente bassa), testimoniate da contenuti di trizio che tendono alla non rilevabilità (tempi di residenza medi dell'ordine delle diverse decine di anni) o tendono verso le svariate decine di unità trizio, queste ultime riconducibili all'infiltrazione di piogge degli anni '50-'60, caratterizzate da elevati contenuti dell'isotopo radioattivo dell'idrogeno, in virtù dei ripetuti *test* nucleari dell'epoca (Fig. 3.3).

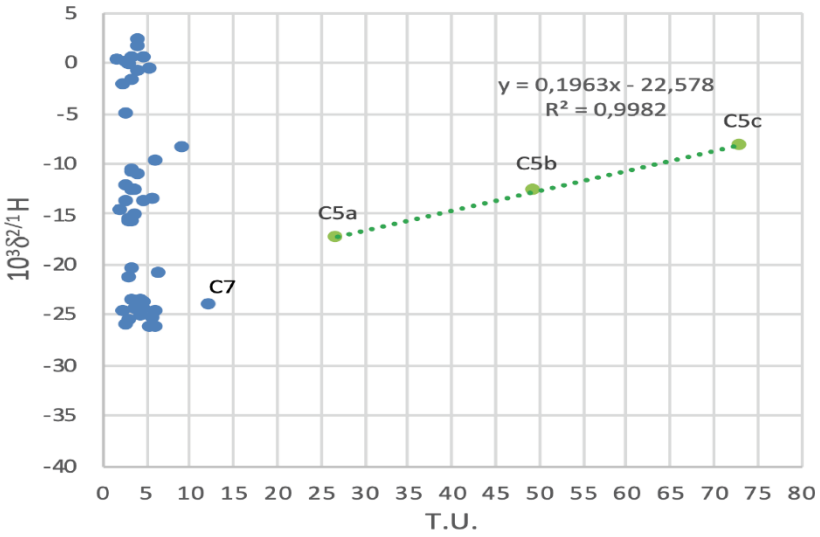

Figura 3.3 Relazione tra 10^3 $\delta^{2/1}H$ e T.U. nelle acque investigate [41].

In merito all'approfondimento sull'ottimizzazione di sistemi di bonifica in siti contaminati, gli studi hanno evidenziato come la componente microbica presente negli acquiferi saturi possa

influenzare positivamente o negativamente la gestione di tali interventi. In tal senso le analisi metagenomiche, utilizzate per la caratterizzazione delle comunità microbiche, sono state la base fondamentale (i) per lo sviluppo degli approfondimenti mirati alla ricerca di nuovi ceppi microbici da sfruttare in chiave biorisanamento, (ii) per esaminare un fenomeno di attenuazione naturale e (iii) per verificare l'impatto complessivo delle comunità microbiche sulla perdita di efficienza di sistemi di barrieramento idraulico.

Per quanto riguarda la selezione di nuovi ceppi microbici potenzialmente utilizzabili in chiave biorisanamento, è stato selezionato un sito in Val d'Agri (Potenza) in cui sono presenti delle sorgenti caratterizzate dalla presenza naturale di idrocarburi. In questo sito, le indagini idrogeologiche ed isotopiche, la caratterizzazione delle comunità microbiche e l'isolamento e la caratterizzazione di ceppi microbici di interesse, hanno contribuito ad accertare che:

- le due sorgenti caratterizzate dalla presenza di idrocarburi fanno parte di un sistema idrogeologico attivo e vengono alimentate da un acquifero carbonatico locale che alimenta anche una terza sorgente (priva di idrocarburi) captata per scopi potabili (Fig. 3.4);

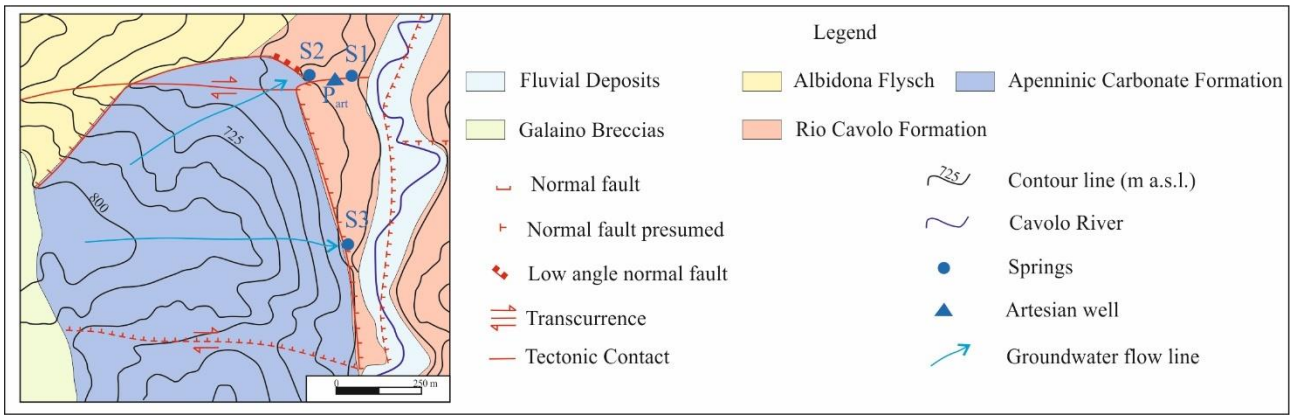

Figura 2.4 Carta idrogeologica dell'area di studio; i punti blu e il triangolo indicano l'ubicazione delle sorgenti indagate S1 e S2 e del pozzo artesiano P_{art} [44].

- al contempo queste due sorgenti affiorano lungo una zona di faglia che consente un flusso ascendente di idrocarburi e la miscelazione di questi con le acque sotterranee provenienti dal suddetto acquifero carbonatico (Fig.3.4);
- le sorgenti caratterizzate dalla presenza naturale di idrocarburi rappresentano un interessante "serbatoio" di ceppi microbici utilizzabili per potenziali approcci di biorisanamento, come emerso dall'isolamento e la caratterizzazione di alcuni di essi (Tab. 3.2);

Tabella 3.2 Risultati del sequenziamento del 16S rRNA di ceppi batterici isolate dai campioni di acqua delle sorgenti, della falda e del suolo [44].

Strain	Sequence Accession Number	Most Closely Related Organism (Accession Number)	Identity (%)
3C	MT703034	*Achromobacter spanius* strain LMG 5911 (NR_025686)	97.80
1C	MT703035	*Pseudomonas protegens* strain CHA0 (NR_114749)	99.78
3	MT703036	*Dyella japonica* strain NBRC 102414 (NR_114075)	90.69
4	MT703037	*Pseudomonas protegens* strain CHA0 (NR_114749)	98.42
7	MT703038	*Cupriavidus metallidurans* CH34 (NR_074704)	98.16
8	MT703039	*Pseudomonas protegens* strain CHA0 (NR_114749)	98.19
10	MT703040	*Stenotrophomonas maltophilia* strain ATCC 13637 (NR_112030)	99.19
15	MT703041	*Stenotrophomonas tumulicola* strain T5916-2-1b (NR_148818)	90.86
16	MT703042	*Stenotrophomonas maltophilia* strain ATCC 13637 (NR_112030)	86.38
18	MT703043	*Dyella terrae strain* JS14-6 (NR_044540)	92.50
20	MT703044	*Dyella terrae strain* JS14-6 (NR_044540)	91.00

- l'isolamento ha portato all'identificazione di nuovi ceppi aerobi in grado di ossidare idrocarburi, la maggior parte dei quali riconducibili a specie note per la loro capacità di degradare IPA; inoltre, molti di questi sono stati in grado di produrre biosurfattanti, sostanze in grado di aumentare la biodisponibilità di idrocarburi e favorirne la degradazione (Tab. 3.3);

Tabella 3.3 Risultati della capacità emulsionante (EC%) (- assenza; + presenza) [44].

Strain	EC	EC%
Proteobacteria bacterium strain 3	-	0
Pseudomonas sp. strain 4	+	60
Cupriavidus sp. strain 7	-	0
Pseudomonas sp. strain 8	+	60
Stenotrophomonas sp. strain 10	-	0
Proteobacteria bacterium strain 15	-	0
Proteobacteria bacterium strain 16	+	30
Proteobacteria bacterium strain 18	+	60
Proteobacteria bacterium strain 20	+	60
Pseudomonas sp. strain 1C	+	40
Achromobacter sp. strain 3C	+	50
Escherichia coli (negative control)	-	0
Bacillus subtilis (positive control)	+	50

- partendo da questi ceppi sarà possibile sviluppare consorzi microbici utilizzabili per il biorisanamento di siti antropicamente contaminati, da affiancare in parallelo a tecnologie già in uso come i sistemi *pump & treat*.

Per quanto riguarda lo studio del fenomeno dell'attenuazione naturale è stato individuato un sito urbano contaminato da solventi clorurati (Parma) in cui le analisi metagenomiche, affiancate ad un approccio colturale, hanno contribuito ad accertare che:

- la comunità microbica riscontrata nei punti di monitoraggio più contaminati è costituita prevalentemente da ceppi aerobi legati ad alcuni generi batterici in grado di compiere la metano monoosigenasi come via metabolica per la degradazione di solventi clorurati;

- dai *test* svolti in laboratorio è emerso come alcuni dei ceppi isolati (aerobi) sono in grado di compiere dealogenazione di composti organici clorurati;
- tali risultati hanno permesso di ipotizzare la presenza di una degradazione cometabolica, che coinvolge ceppi aerobi (generalmente poco studiati per la degradazione di solventi clorurati) e ceppi anaerobi individuati in porzioni più anossiche dell'acquifero.

Per quanto riguarda l'approfondimento dell'influenza delle comunità microbiche sulla progressiva perdita di efficienza idraulica dei pozzi-barriera (eseguito in due siti industriali contaminati con caratteristiche idrogeologiche e chimiche in parte dissimili), le correlazioni tra le indagini idrogeologiche, la caratterizzazione delle comunità microbiche, l'isolamento di ceppi microbici di interesse, le analisi con il microscopio ottico ed elettronico a scansione ambientale, le analisi con diffrattometro a raggi X e le video ispezioni, hanno consentito di accertare che:

- l'efficienza idraulica dei pozzi-barriera in siti contaminati è fortemente influenzata dallo sviluppo di *biofilm* e, più in generale, dall'azione di cellule microbiche;
- in entrambi i siti, il *clogging* è causato principalmente dalla presenza di batteri ferrossidanti e filamentosi (aerobi) capaci di produrre *biofilm*;
- le differenti tipologie di contaminazione presenti nei due siti e i differenti assetti idrogeologici non sono apparsi quali fattori discriminanti nella formazione del *clogging*, né nella selezione delle comunità microbiche responsabili della produzione di *biofilm*, a differenza delle caratteristiche chimico-fisiche delle acque di falda, con particolare riferimento alla concentrazione di O_2 disciolto;
- per preservare l'efficienza di un sistema di barrieramento idraulico e per progettare interventi di biorisanamento efficaci (e sostenibili) non si può trascurare la componente biologica della falda, in quanto alcune soluzioni di biorisanamento che prevedono l'ossigenazione del mezzo saturo potrebbero in parallelo incrementare la proliferazione di ceppi produttori di *biofilm*, inducendo *clogging* e perdita di efficienza dei pozzi-barriera.

In estrema sintesi, le attività di ricerca sviluppate nel corso del Dottorato hanno dimostrato che gli approcci interdisciplinari (ed, in particolare, quello idrogeologico-metagenomico) sono estremamente utili ed efficaci per la corretta comprensione del ruolo idrogeologico svolto da mezzi a bassa permeabilità, anche in aree antropizzate e/o in siti contaminati s.s. Inoltre, il medesimo approccio si è rivelato estremamente efficace nell'ottica di massimizzare ed ottimizzare interventi di biorisanamento accoppiati a sistemi di barrieramento idraulico, attraverso (i) la corretta gestione di processi di attenuazione naturale legati all'attività di comunità microbiche autoctone, (ii) la mirata selezione (all'interno di sistemi idrogeologici attivi) di nuovi ceppi microbici degradatori e (iii) la futura messa a punto di soluzioni in grado di minimizzare lo sviluppo del *well clogging* nei pozzi-barriera.

Tutto quanto sopra sintetizzato dimostra altresì l'innovatività dell'approccio utilizzato in questa sede. Innovatività che deriva, non solo dall'approfondita analisi sinergica di diversi aspetti abiotici e biotici di sistemi idrogeologici complessi (con particolare riferimento ai temi oggetto della presente Tesi), ma soprattutto dal modo in cui tale analisi è stata condotta. In questo specifico caso, infatti, è stata sviluppata una ricerca "ibrida" attraverso la contestuale formazione di una figura di Idrogeologo che fosse in grado (i) di acquisire, utilizzare e sintetizzare saperi tradizionalmente appannaggio di aree e di settori disciplinari distinti, e quindi (ii) di affrontare e risolvere alcuni problemi complessi

con un livello di ottimizzazione del disegno sperimentale maggiore di quello ottenibile dall'insieme di specialisti monodisciplinari.

4. Bibliografia

Il seguente elenco fa esclusivo riferimento alle citazioni bibliografiche riportate nei paragrafi 1 e 2 del presente elaborato.

1. European Environmental Agency, (2011). Progress in management of contaminated sites. https://www.eea.europa.eu/data-and-maps/indicators/progress-in-management-of-contaminated-sites-3/assessment (permalink last version IND-10-en)
2. Espinoza-Tofalos, A., Daghio, M., Palma, E., Aulenta, F., & Franzetti, A. Structure and functions of hydrocarbon-degrading microbial communities in bioelectrochemical systems. *Water* 2020, 12, 343. https://doi.org/10.3390/w12020343
3. Lerner, D. N., Kueper, B. H., Wealthall, G. P., Smith, J. W. N., & Leharne, S. A. (2003). An illustrated handbook of DNAPL transport and fate in the subsurface. *Environment Agency*, Bristol, UK
4. Al-Mansouri, F. A. A., & Alam, M. A. (2008). Sources of Hydrocarbon Leaks & Spills in Upstream Oil Industries-Its Potential Reasons & Preventive Measures. In SPE International Conference on Health, Safety, and Environment in Oil and Gas Exploration and Production. *SPE*. https://doi.org/10.2118/111725-MS
5. Alberti, L., Lombi, S., & Zanini, A. (2011). Identifying sources of chlorinated aliphatic hydrocarbons in a residential area in Italy using the integral pumping test method. *Hydrogeol. J.*, 19, 6, 1253–1267. https://doi.org/10.1007/s10040-011-0742-1
6. Hadley, P. W., & Newell, C. (2014). The new potential for understanding groundwater contaminant transport. *Groundwater*, 52, 2, 174-186. https://doi.org/10.1111/gwat.12135
7. Tomlinson, D. W., Rivett, M. O., Wealthall, G. P., & Sweeney, R. E. (2017). Understanding complex LNAPL sites: Illustrated handbook of LNAPL transport and fate in the subsurface. *J. Environ. Manage.*, 204, 748-756. https://doi.org/10.1016/j.jenvman.2017.08.015
8. Chaudhary, D.K., & Kim, J. (2019). New insights into bioremediation strategies for oil-contaminated soil in cold environments. *Int. Biodeter. Biodegr.*, 142, 58–72. https://doi.org/10.1016/j.ibiod.2019.05.001
9. Deshpande, S., Shiau, B. J., Wade, D., Sabatini, D. A., & Harwell, J. H. (1999). Surfactant selection for enhancing ex situ soil washing. *Water Res.*, 33, 2, 351-360 https://doi.org/10.1016/S0043-1354(98)00234-6
10. Zhou, Q., Sun, F., & Liu, R. (2005). Joint chemical flushing of soils contaminated with petroleum hydrocarbons. *Environ. Int.*, 31, 6, 835-839 https://doi.org/10.1016/j.envint.2005.05.039
11. Albergaria, J. T., Maria da Conceição, M., & Delerue-Matos, C. (2012). Remediation of sandy soils contaminated with hydrocarbons and halogenated hydrocarbons by soil vapour extraction. *J. Environ. Manage.*, 104, 195-201. https://doi.org/10.1016/j.jenvman.2012.03.033
12. Zhuo, C., Hu, S., Yang, Y., & Ran, Y. (2020). Effects of the structures and micropores of sedimentary organic matter on the oxidative degradation of benzo (a) pyrene by $Na_2S_2O_8$. *Water Res.*, 174, 115635. https://doi.org/10.1016/j.watres.2020.115635
13. Johnson, R. L., Johnson, P. C., McWhorter, D. B., Hinchee, R. E., & Goodman, I. (1993). An overview of in situ air sparging. *Ground Water Monit. Remediat.*, 13, 4, 127-135. https://doi.org/10.1111/j.1745-6592.1993.tb00456.x

14. Mao, J., Luo, Y., Teng, Y., e Li, Z. (2012). Bioremediation of polycyclic aromatic hydrocarbon contaminated soil by a bacterial consortium and associated microbial community changes. *Int. Biodeter. Biodegr*, 70, 141–147. https://doi.org/10.1016/j.ibiod.2012.03.002
15. Singh, D., & Fulekar, M. H. (2010). Benzene bioremediation using cow dung microflora in two phase partitioning bioreactor. *J. Hazard. Mater.*, 175, 1-3, 336-343. https://doi.org/10.1016/j.jhazmat.2009.10.008
16. Marin, J. A., Hernandez, T., & Garcia, C. (2005). Bioremediation of oil refinery sludge by landfarming in semiarid conditions: Influence on soil microbial activity. *Environ. Res.*, 98, 2, 185-195. https://doi.org/10.1016/j.envres.2004.06.005
17. Benyahia, F., & Embaby, A. S. (2016). Bioremediation of crude oil contaminated desert soil: effect of biostimulation, bioaugmentation and bioavailability in biopile treatment systems. *Int. J. Environ. Res. Public Health*, 13, 2, 219. https://doi.org/10.3390/ijerph13020219
18. Eslami, E., & Joodat, S. H. S. (2018). Bioremediation of oil and heavy metal contaminated soil in construction sites: a case study of using bioventing-biosparging and phytoextraction techniques. arXiv:1806.03717
19. Ottosen, C. B., Murray, A. M., Broholm, M. M., & Bjerg, P. L. (2018). In situ quantification of degradation is needed for reliable risk assessments and site-specific monitored natural attenuation. *Environ. Sci. Technol*., 53, 1, 1–3. https://doi.org/10.1021/acs.est.8b06630
20. Roy, A., Dutta, A., Pal, S., Gupta, A., Sarkar, J., Chatterjee, A., ... & Kazy, S. K. (2018). Biostimulation and bioaugmentation of native microbial community accelerated bioremediation of oil refinery sludge. *Bioresour. Technol*, 253, 22-32.
21. Truex, M. J., Johnson, C. D., Becker, D. J., Lee, M. H., & Nimmons, M. J. (2015). Performance Assessment for Pump-and-Treat Closure or Transition (No. PNNL-24696). Pacific Northwest National Lab.(PNNL), Richland, WA (USA). DOI: 10.2172/1224519
22. Celico, P. (1986). Prospezioni idrogeologiche. *Liguori Ed., Napoli*. Vol.1, 164.
23. Benedek, T., Táncsics, A., Szabó, I., Farkas, M., Szoboszlay, S., Fábián, K., ... & Kriszt, B. (2016). Polyphasic analysis of an Azoarcus-Leptothrix-dominated bacterial biofilm developed on stainless steel surface in a gasoline-contaminated hypoxic groundwater. *Environ. Sci. Pollut. Res*., 23, 9, 9019-9035. https://doi.org/10.1007/s11356-016-6128-0
24. Macfarlane, P. A., Doveton, J. H., Feldman, H. R., Butler, J. J., Combes, J. M., & Collins, D. R. (1994). Aquifer/aquitard units of the Dakota aquifer system in Kansas; methods of delineation and sedimentary architecture effects on ground-water flow and flow properties. *J. Sediment. Res.*, 64, 4b, 464-480. https://doi.org/10.1306/D4267FE6-2B26-11D7-8648000102C1865D
25. Meyer, J. R., Parker, B. L., Arnaud, E., & Runkel, A. C. (2016). Combining high resolution vertical gradients and sequence stratigraphy to delineate hydrogeologic units for a contaminated sedimentary rock aquifer system. *J. Hydrol.*, 534, 505-523. https://doi.org/10.1016/j.jhydrol.2016.01.015
26. Cherry, J. A., Parker, B. L., Bradbury, K. R., Eaton, T. T., Gotkowitz, M. G., Hart, D. J., & Borchardt, M. A. (2004). Role of aquitards in the protection of aquifers from contamination: a "state of the science" report. *AWWA Research Foundation, Denver, CO*.
27. Eaton, T. T., & Bradbury, K. R. (2003). Hydraulic transience and the role of bedding fractures in a bedrock aquitard, southeastern Wisconsin, USA. *Geophys. Res. Lett*, 30, 18. https://doi.org/10.1029/2003GL017913
28. Eaton, T. T. (2006). On the importance of geological heterogeneity for flow simulation. *Sediment. Geol*, 184, 3-4, 187-201. https://doi.org/10.1016/j.sedgeo.2005.11.002

29. Fjordbøge, A. S., Janniche, G. S., Jørgensen, T. H., Grosen, B., Wealthall, G., Christensen, A. G., ... & Broholm, M. M. (2017). Integrity of clay till aquitards to DNAPL migration: Assessment using current and emerging characterization tools. *Ground Water Monit. Remediat*., 37, 3, 45-61. https://doi.org/10.1111/gwmr.12217
30. Filippini, M., Parker, B. L., Dinelli, E., Wanner, P., Chapman, S. W., & Gargini, A. (2020). Assessing aquitard integrity in a complex aquifer–aquitard system contaminated by chlorinated hydrocarbons. *Water Res.*, 171, 115388. https://doi.org/10.1016/j.watres.2019.115388
31. Bredehoeft, J.D., C.E. Neuzil, and P.C.D. Milly. 1983. Regional flow in the Dakota aquifer: a case study of the role of confining layers. *U.S. Geological Survey Water Supply*, Paper 2237.
32. Nativ, R., O. Dahan, I. Nissim, E. Adar, & M.A. Geyh. (1995). Questions pertaining to isotopic and hydrochemical evidence of fracture-controlled water flow and solute transport in a chalk aquitard. *IAHS* Publication No.232: Wallingford, England: IAHS: 317-327
33. Pucci Jr, A. A. (1998). Hydrogeochemical processes and facies in confining units of the Atlantic Coastal Plain in New Jersey. *Ground Water*, 36, 4, 635-644.
34. Pucci Jr, A. A. (1999). Sulfate transport in a Coastal Plain confining unit, New Jersey, USA. *Hydrogeol. J.*, 7, 3, 251-263. https://doi.org/10.1007/s100400050199
35. Stimson, J., Frape, S., Drimmie, R., & Rudolph, D. (2001). Isotopic and geochemical evidence of regional-scale anisotropy and interconnectivity of an alluvial fan system, Cochabamba Valley, Bolivia. *Appl. Geochemistry*, 16, 9-10, 1097-1114. https://doi.org/10.1016/S0883-2927(01)00019-1
36. Patriarche, D., Ledoux, E., Simon-Coinçon, R., Michelot, J. L., & Cabrera, J. (2004). Characterization and modeling of diffusion process for mass transport through the Tournemire argillites (Aveyron, France). *Appl. Clay Sci.*, 26, 1-4, 109-122. https://doi.org/10.1016/j.clay.2003.10.005
37. Hart, D. J., Bradbury, K. R., & Feinstein, D. T. (2006). The vertical hydraulic conductivity of an aquitard at two spatial scales. *Groundwater*, 44, 2, 201-211. https://doi.org/10.1111/j.1745-6584.2005.00125.x
38. Eaton, T. T., Anderson, M. P., & Bradbury, K. R. (2007). Fracture control of ground water flow and water chemistry in a rock aquitard. *Groundwater*, 45, 5, 601-615. https://doi.org/10.1111/j.1745-6584.2007.00335.x
39. Prinzhofer, A., Girard, J. P., Buschaert, S., Huiban, Y., & Noirez, S. (2009). Chemical and isotopic characterization of hydrocarbon gas traces in porewater of very low permeability rocks: The example of the Callovo-Oxfordian argillites of the eastern part of the Paris Basin. *Chem. Geol.*, 260, 3-4, 269-277. https://doi.org/10.1016/j.chemgeo.2008.12.021
40. Rizzo, P., Petrella, E., Bucci, A., Salvioli-Mariani, E., Chelli, A., Sanangelantoni, A. M., Raimondo, M, Quagliarini, A.,& Celico, F. (2020a). Studying Hydraulic Interconnections in Low-Permeability Media by Using Bacterial Communities as Natural Tracers. *Water*, 12, 6, 1795. https://doi.org/10.3390/w12061795
41. Rizzo, P., Cappadonia, C., Rotigliano, E., Iacumin, P., Sanangelantoni, A.M., Zerbini, G., & Celico, F. (2020b) Hydrogeological Behaviour and Geochemical Features of Waters in Evaporite-Bearing Low-Permeability Successions: A Case Study in Southern Sicily, Italy. https://doi.org/10.3390/app10228177
42. Zanini, A., Petrella, E., Sanangelantoni A.M., Angelo, L., Ventosi, B., Viani, L., Rizzo, P., Remelli, S., Bartoli, M., Bolpagni, R., Chelli, A., Feo, A., Francese, R., Iacumin, P., Menta, C., Racchetti, E., Selmo, E.M., Tanda, M.G., Ghirardi, M., Boggio, P., Pappalardo, F., De Nardo, M.T., Segadelli, S., & Celico, F. (2019). Groundwater characterization from an

ecological and human perspective: an interdisciplinary approach in the Functional Urban Area of Parma, Italy. Rendiconti Lincei. Scienze Fisiche e Naturali, 30, 1, 93-108. https://doi.org/10.1007/s12210-018-0748-x

43. Rizzo, P., Bucci, A., Sanangelantoni, A. M., Iacumin, P., & Celico, F. (2020c). Coupled Microbiological–Isotopic Approach for Studying Hydrodynamics in Deep Reservoirs: The Case of the Val d'Agri Oilfield (Southern Italy). *Water*, 12, 5, 1483. https://doi.org/10.3390/w12051483
44. Rizzo, P., Malerba, M., Bucci, A., Sanangelantoni, A. M., Remelli, S., & Celico, F. (2020d). Potential Enhancement of the In-Situ Bioremediation of Contaminated Sites through the Isolation and Screening of Bacterial Strains in Natural Hydrocarbon Springs. *Water*, 12, 8, 2090. https://doi.org/10.3390/w12082090

5. Ringraziamenti

Desidero ringraziare il Prof. Fulvio Celico e la Prof.ssa Anna Maria Sanangelantoni per tutta la disponibilità, i consigli, la pazienza e l'aiuto che mi hanno dato durante questo percorso lungo tre anni, andando ben oltre il loro ruolo di Tutor. La professionalità, la passione per il vostro lavoro e l'umanità che mi avete dimostrato sono state e saranno sicuramente un caposaldo nella mia vita lavorativa e privata.

Un abbraccio alla mia famiglia, grazie alla quale ho avuto la possibilità di raggiungere questo traguardo.

A Beatrice, se oggi sto scrivendo questi ringraziamenti è anche merito tuo. Tre anni fa sei stata la persona che mi ha spinto ad intraprendere questo percorso che ha in parte rivoluzionato i progetti di vita di entrambi. Potrei scrivere qualunque cosa, ma non sarebbe mai sufficiente ad esprimere quanto io ti sia grato per il tuo sostegno, perciò lascerò a te l'interpretazione di tutti i possibili significati racchiusi in questa semplice parola… Grazie!